Implications of the Zero Lower Bound

A thesis submitted in fulfilment of the requirements for the degree of

Doctor of Philosophy

Presented by

Michaela Haderer

Faculty of Arts and Social Sciences

School of Economics

University of Sydney

2023

Disclaimers

Originality Statement

This is to certify that to the best of my knowledge, the content of this thesis is my own work. This thesis has not been submitted for any degree or other purposes.

I certify that the intellectual content of this thesis is the product of my own work and that all the assistance received in preparing this thesis and sources have been acknowledged.

Michaela Haderer

Authorship Attribution Statement

A joint paper covering material from Chapter 1 to 3 of this thesis is published as

Haderer, Michaela, 2022. "An Estimated DSGE Model of the Euro Area with Expectations about the Timing and Nature of Liftoff from the Lower Bound," Working Papers 2022-05, University of Sydney, School of Economics.

I designed the study, analyzed the data, and wrote the drafts of the Manuscript.

Michaela Haderer

Abstract

This thesis examines the effectiveness of forward guidance in the euro area using a structural New-Keynesian model at the zero lower bound (ZLB). To incorporate forward guidance, I implement a ZLB constraint into a medium-scale Dynamic Stochastic General Equilibrium (DSGE) model that treats a sequence of expected durations of the ZLB as free parameters in estimation. The sequence of expected durations is informed by survey data to produce well-identified estimates that align with macroeconomic data and the underlying model structure. Results indicate that these expected durations play a key role in explaining model dynamics when interest rates are fixed at the ZLB. Further, through the use of a sunspot solution strategy to accommodate different expected liftoff regimes, I quantify how much the effectiveness of forward guidance depends not just on the expected duration of the ZLB regime, but also on expectations regarding the behavior of monetary policy in the liftoff regime. Finally, I propose a time-series approach to address the extreme data outliers during the Covid-19 pandemic. This approach builds on the emerging literature on estimating Covid-19 outliers in VAR models to the setting of estimating structural DSGE models and allows for an assessment of monetary policy during the pandemic period.

Acknowledgements

I would like to express my deepest gratitude to my thesis supervisors, James Morley and Christopher Gibbs, for their invaluable guidance, support, and encouragement throughout my PhD journey. Their expertise, patience, and mentorship have been instrumental in shaping my research, writing, and professional development.

I am particularly grateful to James for adapting to the challenges of the pandemic by making himself available for Zoom meetings, even though we were unable to meet in person for a substantial part of my candidacy.

Likewise, I am grateful to Chris for his invaluable insights and thoughtful feedback, which have greatly enriched my research and honed my analytical skills. His guidance has been instrumental in helping me navigate the intricate landscape of my research questions and hypotheses.

I am indebted to the faculty, staff, and students at the School of Economics at the University of Sydney for creating a vibrant academic community that has fostered my intellectual curiosity, interdisciplinary collaborations, and personal growth. I am particularly grateful to Mariano Kulish, Aarti Singh, Luke Hartigan and James Graham for their support and intellectual exchange. Their feedback, constructive criticism, and insightful discussions have challenged me to think deeply about my research and have improved the quality of my work. I would also like to thank my PhD program coordinators, Rebecca Edwards and Kadir Atalay, for their support, organization, and management throughout my candidacy. I am also grateful to the departmental administrative staff for supporting my academic activities and providing assistance with various administrative tasks.

I would like to acknowledge the funding agencies and organizations that have supported my research, including the DBH Scholarship and the FASS International Postgraduate Research Tuition Fee Scholarship. Their financial support has been instrumental in enabling me to carry out my research work.

I would like to express my deepest appreciation to my family and friends for their emotional support and understanding.

I would also like to thank my parents for their endless love, support, and guidance throughout my life. Their unwavering belief in me, unconditional support, and encouragement have been the cornerstone of my academic success. Despite the challenges of the past few years, they have always been a constant source of support, even from afar. Lastly, I would like to express my profound gratitude to my partner, Fabian, for his unwavering love, support, and encouragement during my doctoral journey. His patience, understanding, and belief in me have been instrumental in helping me navigate graduate school. I am deeply thankful for his decision to move to the other side of the world with me.

Contents

List of Figures

List of Tables

Introductory Chapter

Over the past few decades, the euro area has been subjected to significant economic turmoil. It has experienced the Great Financial Crisis, the Sovereign Debt Crisis, zero fixed interest rates, and the Covid-19 pandemic over a period of 20 years. It might even be argued that unconventional times have become the new norm in recent years.

This thesis investigates the transmission of monetary policy during the latter part of these unconventional times, particularly when nominal interest rates have been constrained by the Zero Lower Bound (ZLB). During times when conventional policy options are limited at the ZLB, unconventional policies such as forward guidance can become a powerful monetary policy tool to influence interest rate expectations.

Chapter I uses a structural DSGE model to assess the effectiveness of forward guidance and introduces a new measure of expected durations at the ZLB derived from the ECB's Survey of Professional Forecasters (SPF) and investigates their role in monetary policy transmission dynamics. To my knowledge, this is the first study to integrate SPF data for the euro area into a DSGE model in order to estimate the expected durations of the ZLB.

Chapters II and III present two applications that build upon this model. These include a comparison of active and passive monetary policy regimes and a time-series approach to managing data outliers during the Covid-19 pandemic. Overall, this thesis contributes to the literature on unconventional monetary policy by examining the effectiveness of forward guidance and the transmission of monetary policy during fixed interest rate periods in the euro area.

Chapter I: Estimating a DSGE model for the Euro Area with Forward Guidance at the Zero Lower Bound

This chapter examines the effectiveness of forward guidance in the euro area by estimating the expected durations of the zero lower bound (hereafter: ZLB) in a structural DSGE model from 2004-Q3 to 2019-Q4. Following Kulish and Pagan (2017) and Kulish, Morley, and Robinson (2017), I incorporate a regime change into the well-known DSGE model of Smets and Wouters (2007, 2003). In the model, monetary policy changes between a conventional policy regime in the form of a Taylor-type rule and an unconventional fixed-rate policy regime at the ZLB. Despite including the ZLB for a substantial part of the sample period, the structural parameters are consistent with those found in the previous literature. This indicates that the model is robust to changes in policy regimes, an essential feature of any structural macroeconometric model that aims to address the Lucas Critique.

An important feature of the Kulish, Morley, and Robinson (2017) approach is that it treats a sequence of expected durations of the ZLB as free parameters in estimation. Due to the fact that the model selects the duration sequence that best fits the data, these estimated durations may exceed the underlying policy constraint that follows a Taylor-type rule. Consequently, the model accommodates unconventional monetary policy in the form of forward guidance to set expectations to go *lower for longer*. Expanding the information set of the model, I construct a new measure of expected durations that is derived from SPF data. To my knowledge, this is the first study to incorporate SPF data for the euro area into a DSGE model in order to estimate the expected duration of the ZLB. By using subjective expectations about the future path of the policy rate as an informative prior, this measure assists in identifying the estimated sequence of expected durations of the ZLB that are reflected in macroeconomic data and model structure.

To identify the impacts of forward guidance on the model, I decompose the expected duration estimates according to their source as in Jones, Kulish, and Rees (2022b). Considering that the estimated durations can exceed the actual policy constraint, they may be at least partially the result of deliberate monetary policy. Based on this decomposition, forward guidance to go *lower for longer* appears to have become increasingly important from 2018 onwards.

Chapter II: Assessing the Effectiveness of Forward Guidance under Different Assumptions about the Nature of Liftoff

The second chapter of the thesis examines the effectiveness of forward guidance regarding agents' expectations about the liftoff regime from the lower bound.

To investigate this, the chapter compares two different liftoff regimes, the benchmark case of active monetary policy and a passive monetary policy regime based on historical examples for instance from the pre-Volcker era in the United States (e.g., Clarida, Gali, and Gertler, 2000) allowing the latter to be considered a policy option.

To accommodate passive monetary policy after liftoff and examine forward guidance in the presence of expectations about the liftoff regime, a sunspot solution is employed. Based on a Bayesian model comparison, the sunspot solution with a passive liftoff regime is marginally preferred to the benchmark solution with an active liftoff regime.

Moreover, as established in the first chapter of the thesis, the response to structural shocks can be counterintuitive when the policy rate is fixed for a certain period of time, even if a model can accommodate a policy change at the ZLB. The results presented in this chapter suggest that a sunspot model with a passive liftoff regime mitigates some of these puzzles and counterintuitive findings. Moreover, the results further support the notion that expectations regarding liftoff contribute to the relatively muted effects of forward guidance, particularly on inflation.

Chapter III: A Time-Series Approach to Estimating DSGE Models with Covid-19 Data

In the third chapter, I propose a time-series approach to address the challenge of large data outliers observed during the Covid-19 pandemic. However, the Covid-19 pandemic has triggered the largest contractionary shock to the euro area since its establishment, surpassing the impacts of both the Great Financial Crisis and the Sovereign Debt Crisis. The Covid-19 contraction was caused by supply and demand constraints such as revised private consumption decisions, lockdowns, and social health measures, rather than structural issues, adding complexity to a structural model estimation.

The chapter aims to extend the existing literature on estimating Covid-19 outliers in VAR models (e.g., Lenza and Primiceri, 2022, Carriero, Clark, Marcellino, and Mertens, 2021, Schorfheide and Song, 2021) to structural DSGE models. Covid-19 data exhibit extreme volatility along with low persistence, posing challenges for the estimation of DSGE models, as it can distort structural parameter estimates. My approach builds on Lenza and Primiceri (2022)'s methodology for VAR models and makes three adjustments to the standard estimation process without modifying the structural equations of the model. Specifically, I introduce a time-varying innovation-covariance matrix to capture the extreme heteroskedasticity in the shock variances, an ARMA(1,1) correction for the persistent effects of the total factor productivity shock innovations during the pandemic, and a measurement correction for consumption data in the Kalman filter.

The proposed estimation approach enables an assessment of monetary policy during the Covid-19 pandemic. In the euro area, conventional monetary policy was severely constrained when the Covid-19 shock hit the economy, with interest rates fixed at the zero lower bound (ZLB). Even so, I demonstrate that the stance of monetary policy was expansionary despite the inability to lower the policy rate below zero.

The incorporation of Covid-19 data produces robust parameter estimates compared to the pre-Covid-19 sample but implies somewhat longer forward guidance durations in recent years. By using this approach, DSGE models can be estimated with data that include extreme outliers, allowing the pandemic period to be included in future research with such models.

Chapter 1

Estimating a DSGE model for the Euro Area with Forward Guidance at the Zero Lower Bound

Abstract

In this chapter, I examine the effectiveness of forward guidance in the euro area using a structural New-Keynesian model at the zero lower bound (ZLB). To accommodate forward guidance, the medium-scale DSGE model treats a sequence of expected durations at the ZLB as free parameters in estimation. As an informative prior to the sequence of expected durations, I propose a new measure constructed from survey expectations, which generates well-defined estimates consistent with macroeconomic data and the model's structure. The empirical findings support the use of the structural model with fixed-interest periods considering relatively stable parameter estimates for the euro area. In order to determine the impacts of forward guidance on the model, I filter the expected duration estimates based on their source. Based on this decomposition, forward guidance to go *lower for longer* appears to have become increasingly important from 2018 onwards.

1.1 Introduction

In recent years, several central banks, including the US Federal Reserve, the Bank of England, and the European Central Bank (ECB), have lowered interest rates to near-zero levels; something that previously seemed to be only a remote possibility rather than an actual policy option. With conventional policy options becoming increasingly limited, unconventional tools such as quantitative easing, central bank lending operations, and forward guidance have become more prevalent. Focusing on the latter, forward guidance refers to credible announcements by the central bank aiming to influence agents' expectations about the future path of the policy rate. In forward-looking models where the expected path of the policy rate determines the current stance of monetary policy, forward guidance provides an additional transmission channel for monetary policy.

In this chapter, I examine the effectiveness of forward guidance in the euro area using the medium-scale DSGE model of Smets and Wouters (2007) (hereafter SW-07). The sample period from 2004-Q3 to 2019-Q4 includes a zero lower bound (hereafter: ZLB) period where the policy rate was fixed at zero. To address this regime change, in the model, monetary policy changes between a conventional policy regime in the form of a Taylor-type rule and an unconventional fixed-rate policy regime at the ZLB. Forward guidance is introduced by modeling agents' expectations about the future path of the policy rate, or in other words by a sequence of estimated expected durations of the lower bound. When policy rates are pegged at a fixed value, this sequence of expected durations introduces an additional channel for monetary policy transmission in the model. To improve the identification of this sequence, subjective information from the ECB's SPF is included in the estimation process.

Incorporating subjective information about agents' expectations of the future path of the policy rate into a standard DSGE model, allows me to **(i)** estimate the expected durations of the ZLB based on an informative prior rather than theoretical assumption; **(ii)** show that the model remains structural at the ZLB; **(iii)** analyze the non-linear model dynamics and implications at the ZLB dependent on the length and existence of the ZLB constraint; and **(iv)** identify the role and importance of unconventional monetary policy in the form of forward guidance in the euro area.

The modeling of unconventional monetary policy at the ZLB presents a new challenge to researchers. Common solution algorithms for linear rational expectation (LRE) models, such as the algorithms by Sims (2002) or Binder and Pesaran (1995, 1997), require monetary policy to fulfill the Taylor (1993) principle. In other words, the central bank must react aggressively enough to inflation changes to trigger adequate real interest rate movements. If they fail to do so and real interest rates fall while inflation rises, the model system has multiple solutions each defined by future inflation expectations. As inflation becomes expectational, the Blanchard and Kahn (1980) conditions are violated since the number of expectational variables exceeds the number of explosive roots in the system.

The issue of indeterminacy has been addressed in multiple ways over the past few decades. Earlier work proposed to solve LRE models at the ZLB via a backward induction method with undetermined coefficients (Eggertsson and Woodford, 2003, Svensson, 2000). According to some papers, including Fernández-Villaverde, Gordon, Guerrón-Quintana, and Rubio-Ramirez (2015), linearized solutions are not optimal for study at the ZLB. However, other papers, such as Jones (2017) and Guerrieri and Iacoviello (2015), disagree. Despite the differences in methodology, the latter propose occasionally-binding-constraint algorithms that provide linear solutions that are acceptable approximations for non-linear models. Furthermore, regime-switching models, such as the Markov-switching approach of Bianchi (2013), allow multiple occurrences of a fixed-interest rate regime, but assume constant durations of the ZLB. The approach I follow is that of Kulish, Morley, and Robinson (2017) (hereafter KMR (2017)), which suggests solving models containing both determinate and indeterminate regimes via backward induction, based on Kulish and Pagan (2017). Using KMR (2017), the sequence of expected durations at the ZLB is treated as free parameters in estimation. Since the model selects the duration sequence that best fits the data, the estimated durations may exceed the underlying policy constraints. Thus, the model accommodates unconventional monetary policy in the form of forward guidance, whereby the central bank influences agents' expectations that the policy rate will be lower for a longer period than implied by the underlying policy rule.

I utilize SPF responses to construct an informative prior for the sequence of expected durations in the euro area. In addition to identifying the estimated expected duration, survey forecasts add subjective information about agents' expectations about the future path of the policy rate to the model's information set. This has been widely discussed in recent literature. Manski (2004) was one of the first to advocate including subjective information to improve expectation formation. Furthermore, Baele et al. (2015) attribute a significant role to survey expectations in regime-switching models with rational expectations. Del Negro and Eusepi (2011) propose a measure for observing inflation expectations to improve the fit of a SW-07-style model in terms of model-implied expectations. More recent, Müller, Christoffel, Mazelis, and Montes-Galdón (2022) use SPF data to assess the effects of forward guidance taking into account earlier work by Campbell, Fisher, Justiniano, and Melosi (2017), but they do not directly consider expected durations. To my knowledge, this is the first study to incorporate SPF data into a DSGE model to estimate the expected duration of the ZLB for the euro area.

The estimation of models at the ZLB challenges standard New-Keynesian theory. In his seminal work Lucas (1976) argued that it is naive to predict structural policy changes from historical data or draw policy advice from large-scale macroeconomic models, because the parameters of the models may not be policy invariant. Due to the fact that agents are essentially forward-looking, backward-looking models are not always appropriate for analyzing structural regime switches. The KMR (2017) solution strategy allows me to test whether the model is indeed structural, finding that despite including the ZLB for a substantial part of the sample period, the structural parameters are consistent with those found in previous literature. This indicates that the model is robust to changes in policy regimes, the primary goal of any structural macroeconometric model seeking to address the Lucas Critique.

Additionally, even if the model can incorporate policy changes, the implications and response to structural shocks, including the underlying microfoundations, can be counterintuitive at the ZLB. Previous research, such as Werning (2011), Cochrane (2017) and Diba and Loisel (2021), has defined some of these properties as *the forward guidance puzzle*, *the paradox of toil*, and *the fiscal multiplier puzzle*. Based on Koop, Pesaran, and Potter (1996), I utilize generalized impulse response functions (GIRFs) analysis to provide insight into the non-linear ZLB dynamics and the linear post-ZLB dynamics.

By using SPF data for the euro area, duration estimates can aid in exploring these non-linearities. In comparison with the KMR (2017) results for the US, duration estimates are considerably longer in the euro area throughout the ZLB period. As the sample period progressed, the expected durations increased and did not indicate an imminent liftoff, which would not occur until mid-2022. However, while the KMR (2017) approach and the SPF data deliver well-identified estimates for the sequence of expected durations, it is not immediately clear from where these durations originate. Considering that the estimated durations can exceed the actual policy constraint, they may be at least partially the result of deliberate monetary policy. Therefore, following Jones, Kulish, and Rees (2022b) and using the occasionally binding constraint algorithm proposed by Jones (2017), I decompose the duration estimates into durations originating from forward guidance policy and durations implied by the underlying constraint. Based on this decomposition, forward guidance becomes increasingly important from 2018 onwards. Unsurprisingly, the model tends to overestimate the expansionary effects of deliberate shocks to the expected duration, a phenomenon referred to in the literature as the forward guidance puzzle (Del Negro, Giannoni, and Patterson, 2012). When the ZLB length increases in this model, the forward guidance puzzle becomes more prominent.

The remainder of this chapter is structured as follows. Section 1.2 summarizes the SW-03, SW-07 model framework for the euro area, including the implementation of the ZLB and yield curve. Section 1.3 presents the solution strategy for the model. The estimation strategy is presented in section 1.4. Section 1.5 summarizes the results and assesses the properties and fit of the model. Section 1.6 explores the non-linearities at the ZLB. Section 1.7 identifies the role of forward guidance in the euro area. Section 1.8 concludes.

1.2 Model

The model follows that for the US economy in SW-07 and also their earlier version for the euro area (SW-03) while incorporating adjustments to the monetary policy rule and the yield curve similar to KMR (2017). All variables are log-linearized around the steady state balanced growth path with deviations from steady state denoted by a hat symbol. In the standard SW-07 framework, households maximize utility by choosing consumption and hours worked over an infinite horizon. Unions differentiate labor over households, which implies some monopoly power over wages. In the goods market, intermediate goods producers operate in monopolistically competitive market while final goods producers operate in a perfectly competitive environment. The model applies Calvo (1983) pricing to account for sticky prices in the goods and labor markets. Final goods producers purchase intermediate goods, transform them, and resell them to households. The technical appendix provides a complete representation of the model, including the sticky and flexible wage economies, as well as all shock processes.

1.2.1 Log-linearized Equations of the SW-07 Model

The demand side of the model can be summarized by an aggregate resource constraint:

$$\hat{y}_t = c_y \hat{c}_t + i_y \hat{i}_t + z_y \hat{z}_t + \varepsilon_t^g \tag{1.1}$$

Aggregate output, $\hat{y}_t$, is determined by consumption, $\hat{c}_t$, investment, $\hat{i}_t$, and capital-utilization costs which are a function of the capital-utilization rate $\hat{z}_t$. The parameter $c_y = 1 - g_y - i_y$ represents the consumption share at steady state in output, where g_y is the steady state exogenous spending-output ratio. The parameter $i_y = (\gamma - 1 + \delta)k_y$ describes the investment-output ratio, where k_y is the steady state capital-output ratio, γ denotes the growth rate in steady state, and δ the capital depreciation rate. $z_y = R_*^k k_y$, where R_*^k is the steady state rental rate of capital. The resource constraint is subject to an exogenous spending shock ε_t^g which follows an AR(1) process with an iid-normal error term and an iid-normal total factor productivity term[1]:

$$\varepsilon_t^g = \rho^g \varepsilon_{t-1}^g + \eta_t^g + \rho^{ga} \eta_t^a$$

[1]Smets and Wouters (2003, 2007) include the total factor productivity innovation to account for the potential impact of fluctuations in domestic productivity on net exports.

Households optimize utility by choosing between consumption and labor. Consumption dynamics can be described by a standard Euler equation:

$$\hat{c}_t = c_1\hat{c}_{t-1} + (1-c_1)E_t(\hat{c}_{t+1}) + c_2(\hat{l}_t - E_t(\hat{l}_{t+1})) - c_3(\hat{r}_t - E_t(\hat{\pi}_{t+1})) + \varepsilon_t^b \tag{1.2}$$

where

$$c_1 = \frac{\frac{\lambda}{\gamma}}{1+\frac{\lambda}{\gamma}} \qquad c_2 = \frac{(\sigma^c - 1)(\frac{W_*^h L_*}{C_*})}{\sigma^c(1+\frac{\lambda}{\gamma})} \qquad c_3 = \frac{1-\frac{\lambda}{\gamma}}{\sigma^c(1+\frac{\lambda}{\gamma})}$$

The parameter λ captures habit formation, while σ^c denotes the intertemporal consumption substitution elasticity. Current consumption $(\hat{c}_t)$ is based on the weighted average of past and expected future consumption, the expected growth in hours worked, $\hat{l}_t - E_t(\hat{l}_{t+1})$, and the real interest rate, $\hat{r}_t - E_t(\hat{\pi}_{t+1})$, where $\hat{r}_t$ is the nominal interest rate in period t and $\hat{\pi}_t$ the inflation rate. The disturbance term ε_t^b captures the difference between the interest rate and the return on assets received by households and follows a first-order autoregressive process with an iid-normal error term η_t^b.[2].

The investment Euler equation is given by:

$$\hat{i}_t = \frac{1}{1+\beta\gamma^{(1-\sigma^c)}}\hat{i}_{t-1} + \frac{\beta\gamma^{(1-\sigma^c)}}{1+\beta\gamma^{(1-\sigma^c)}}E_t(\hat{i}_{t+1}) + \frac{1}{(\beta\gamma^{(1-\sigma^c)})\gamma^2\varphi}\hat{q}_{t-1} + \varepsilon_t^{qs} \tag{1.3}$$

The parameter φ denotes the elasticity of the capital adjustment cost function at steady state and the parameter β is the household discount factor. A higher elasticity of capital adjustment costs will reduce investment sensitivity, similarly to the consumption Euler equation. The disturbance term ε_t^{qs} follows an AR(1) process with an iid-normal error term, such that $\varepsilon_t^{qs} = \rho^{qs}\varepsilon_{t-1}^{qs} + \eta_t^{qs}$. The real value of capital is given by:

$$\hat{q}_t = \frac{(1-\delta)}{R_*^k + (1-\delta)}E_t(\hat{q}_{t+1}) + \frac{R_*^k}{R_*^k+(1-\delta)}E_t(\hat{r}_{t+1}^k) + \frac{\sigma^c(1+\frac{\lambda}{\gamma})}{1-\frac{\lambda}{\gamma}}\varepsilon_t^b - (\hat{r}_t - E_t(\hat{\pi}_{t+1})) \tag{1.4}$$

where $\hat{r}_t$ is the rental rate of capital for which R_*^k denotes its steady state value. The cap-

[2]I deviate from SW-07 and, as in KMR (2017), a negative shock corresponds to an increase in the required return on assets and a reduction of current consumption. This shock influences the cost and value of capital and investment similarly to the net worth shocks in Bernanke et al. (1999) and Christiano et al. (2005).

ital stock, $\hat{q}_t$, is positively correlated with its expected value in the future. Furthermore, the expected real rental rate on capital, $E_t(\hat{r}^k_{t+1})$, influences the current value of the capital stock positively, and the real interest rate and risk premium disturbances negatively. Capital becomes effective one period after its installation; hence, current capital, $\hat{k}^s_t$, is determined by the level of capital installed in the previous period, $\hat{k}_{t-1}$, and the degree of capital utilization $\hat{z}_t$:

$$\hat{k}^s_t = \hat{k}_{t-1} + \hat{z}_t \tag{1.5}$$

Since cost-minimizing households provide capital services, the degree of capital utilization, $\hat{z}_t$, depends positively on the rental rate of capital $\hat{r}^k_t$:

$$\hat{z}_t = \frac{1-\psi}{\psi}\hat{r}^k_t \tag{1.6}$$

where ψ is the elasticity of the capital utilization adjustment cost function. For $\psi = 0$, the rental rate on capital is constant in equilibrium; for $\psi = 1$, capital utilization is costly to change and therefore remains constant. Capital, $\hat{k}_t$, accumulates depending on investment and its relative efficiency as captured by innovation ε^{qs}_t:

$$\hat{k}_t = \frac{1-\delta}{\gamma}\hat{k}_{t-1} + \frac{\gamma-(1-\delta)}{\gamma}\hat{i}_t + (1-\frac{1-\delta}{\gamma})(\gamma^2\varphi)\varepsilon^{qs}_t \tag{1.7}$$

The aggregate production function is given by:

$$\hat{y}_t = \phi_p\big(\alpha\hat{k}^s_t + (1-\alpha)l_t + \varepsilon^a_t\big) \tag{1.8}$$

Aggregate output is produced by balancing capital, $\hat{k}^s_t$, and labor $\hat{l}_t$. The parameter α represents the share of capital and the parameter $(1+\phi_p)$ corresponds to the share of fixed costs in the production process. Total factor productivity, $\varepsilon^a_t = \rho^a\varepsilon^a_{t-1} + \eta^a_t$, follows an AR(1) process with an iid-normal error term. Price stickiness is introduced according to Calvo (1983), according to which monopolistically competitive intermediate good producers can only slowly adjust their prices to their desired markups. The New-

Keynesian Phillips curve is given by:

$$\hat{\pi}_t = \frac{1}{1+\beta\gamma^{1-\sigma^c}\iota_p}\Big(\beta\gamma^{1-\sigma^c}E_t(\hat{\pi}_{t+1}) + \iota_p\hat{\pi}_{t-1} + \frac{(1-\xi_p)(1-\beta\gamma^{1-\sigma^c}\xi_p)}{\xi_p((\phi_p-1)\epsilon_p+1)}\hat{mc}_t\Big) + \varepsilon_t^p \qquad (1.9)$$

Current inflation, $\hat{\pi}_t$, is positively affected by past and expected inflation, while negatively affected by current price mark-ups. A price mark-up disturbance follows an AR(1) process $\varepsilon_t^p = \rho^p\varepsilon_{t-1}^p + \eta_t^p$, where η_t^p is an iid-normal price mark-up shock.[3] For $\iota_p = 0$, the Philips curve is purely forward looking. A producer's ability to update prices quickly depends on the level of price stickiness, ξ_p, the curvature of the Kimball goods market aggregator, ε_p, and the steady state mark-up.

The marginal cost of labor is the difference between the marginal product of labor and the real wage:

$$\hat{mc}_t = \hat{mpl}_t - \hat{w}_t = \alpha\hat{r}_t^k + (1-\alpha)\hat{w}_t - \varepsilon_t^a \qquad (1.10)$$

According to the assumption that firms try to minimize costs, the capital-labor ratio negatively affects the rental rate of capital and positively impacts the real wage:

$$\hat{r}_t^k = \hat{w}_t - \hat{k}_t^s + \hat{l}_t \qquad (1.11)$$

In monopolistically competitive labor markets, wage mark-ups represent the gap between the marginal rate of substitution between consumption and labor and the real wage:

$$\hat{\mu}_t^w = \hat{w}_t - \hat{mrs}_t = w_t - \Big(\sigma^l\hat{l}_t + \frac{1}{1-\frac{\lambda}{\gamma}}(\hat{c}_t - \frac{\lambda}{\gamma}\hat{c}_{t-1})\Big) \qquad (1.12)$$

where the parameter σ^l corresponds to the labor supply elasticity and λ to the habit parameter in consumption. Similar to the price mark-up shock, the wage mark-up disturbance follows an AR(1) process, $\varepsilon_t^w = \rho^w\varepsilon_{t-1}^w + \eta_t^w$, where η_t^w is an iid-normal error term. Similarly to the goods market, nominal wage stickiness and partial inflation indexation

[3]SW-07 propose an ARMA(1,1) process for the price and wage Phillips curve shocks. Those are not well identified in the euro area data sample. In a previous version of the model for the euro area, Smets and Wouters (2003) (hereafter SW-03) assume the three cost push shocks (ϵ_p, ϵ_q, and ϵ_w) to be iid-normal processes.

lead to a slow adjustment of real wages:

$$\begin{aligned}\hat{w}_t = \frac{1}{(1+\beta\gamma^{1-\sigma^c})}\hat{w}_{t-1} + \frac{\beta\gamma^{1-\sigma^c}}{(1+\beta\gamma^{1-\sigma^c})}(E_t(\hat{w}_{t+1}) + E_t(\hat{\pi}_{t+1})) - \frac{1+\beta\gamma^{1-\sigma^c}\iota_w}{(1+\beta\gamma^{1-\sigma^c})}\hat{\pi}_t \\ + \frac{\iota_w}{(1+\beta\gamma^{1-\sigma^c})}\hat{\pi}_{t-1} - \frac{(1-\xi_w)(1-\beta\gamma^{1-\sigma^c}\xi_w)}{\Big((1+\beta\gamma^{1-\sigma^c})\xi_w\Big)\Big((\phi_w-1)\epsilon_w+1\Big)}\hat{\mu}_t^w + \varepsilon_t^w\end{aligned} \tag{1.13}$$

1.2.2 Implementing the ZLB

As in KMR (2017), monetary policy changes between two regimes. In the first regime, pre-ZLB, monetary policy follows a standard Taylor rule as in SW-07. Once the economy hits the ZLB in $t = T$, the central bank fixes its policy rate at a constant value.[4] At the ZLB, the central bank communicates a lift-off strategy that returns to a Taylor-type policy rule at the later stage $t = d^e + 1$. When the central bank announcements are credible, the expected duration of the ZLB in $t = T$ is given by d^e. After entering the post-ZLB regime in T^*, the central bank reverts to its initial Taylor rule policy, which guarantees a unique and stable solution to the system:

$$\hat{r}_t \equiv \begin{cases} TR, & \text{for } t < T \\ -r, & \text{for } T \leq t < T^* \\ TR, & \text{for } t \geq T^* \end{cases}$$

where the Taylor rule (TR) is defined as the standard feedback rule in SW-07:

$$\hat{r}_t = \rho^m \hat{r}_{t-1} + (1-\rho^R)(\phi_\pi \hat{\pi}_t + \phi_y(\hat{y}_t - \hat{y}_t^f)) + \phi_{\Delta y}(\hat{y}_t - \hat{y}_{t-1}) - (\hat{y}_t^f - \hat{y}_{t-1}^f)) + \varepsilon_t^m \tag{1.14}$$

The parameter ρ^m introduces interest rate smoothing. The nominal interest rate responds to changes in inflation, indicated by parameter ϕ_π, output growth ($\phi_{\Delta y}$), and the output gap (ϕ_y), defined as the deviation of actual output from its potential. Potential output is derived from the output level under a fully flexible economy, i.e., without nominal frictions or mark-up shocks. Monetary policy is subject to a policy shock ε_t^m that follows an AR(1)

[4] Note that the variables are expressed as deviations from steady state. Hence, $r_t = -r$ corresponds to the interest rate level being zero $r_t + r = 0$.

with an iid-normal error term.

1.2.3 Implementing the Yield Curve

Following KMR (2017), I incorporate information from the yield curve into the model economy to help identify the monetary policy stance, and therefore the expected durations at the ZLB. Furthermore, this approach takes into account the consistently negative yields of short- and medium-term (AAA-rated) government bonds in the euro area. As in KMR (2017), and drawing on the expectation hypothesis, which implies that longer maturity bonds reflect agents' expectations of future policy rates, interest rates are set according to:

$$\hat{r}_{j,t} = \frac{1}{j} E_t(\hat{r}_t + \hat{r}_{t+1} + \hat{r}_{t+j-1}) \qquad for\ j = 2,3,...,m \tag{1.15}$$

where $\hat{r}_{j,t}$ denotes the log deviation of the yield from steady state on a j-period bond. The observed yield curve counterpart becomes:

$$r_{j,t} = \hat{r}_{j,t} + r + c_j + \varepsilon_t^{\eta} + \epsilon_{j,t} \qquad for\ \ j = 2,3,...,m \tag{1.16}$$

where r is the steady state of the nominal interest rate. Since c_j is a maturity-specific time-invariant component, $r + c_j$ can be interpreted as the steady state of a yield with j periods to maturity. The time-varying component of the term premium includes a persistent AR(1) shock ε_t^{η} for all observed maturities:

$$\varepsilon_t^{\eta} = \rho^{\eta} \varepsilon_{t-1}^{\eta} + e_{\varepsilon^{\eta},t} \tag{1.17}$$

1.3 Solution Strategy

Standard linear rational expectations (LRE) models can be solved using a number of algorithms, including those proposed by King and Watson (1998, 2002), Anderson and Moore (1985), Binder and Pesaran (1995, 1997), Sims (2002), or Klein (2000). Although the techniques share a similar goal, they differ significantly in terms of accuracy, computational speed, and generality (see e.g., Anderson, 2007). LRE algorithms, however, generally assume a time-invariant structure, which implies that a system's structure remains unchanged over time. Consequently, these standard algorithms cannot accommodate future (un-)anticipated changes in the model structure.

What is more, New Keynesian models with ZLB constraints often face indeterminacy challenges. A prolonged period of near-zero interest rates violates the Taylor principle since interest rates do not sufficiently respond to inflation rate changes (see, for example, Clarida et al. (2000), Kerr and King (1996)). To address these difficulties, Cagliarini and Kulish (2013) propose a rational expectation solution for linear stochastic models with predictable structural variations. Kulish and Pagan (2017) builds on this methodology, by incorporating a time-varying coefficient vector autoregression (VAR) model to formulate the likelihood of structural changes that can be anticipated or unanticipated Using the Kulish and Pagan (2017) approach, KMR (2017) propose a backward induction method for solving models at ZLB that contain both determinate and indeterminate regimes. A key feature of this approach is that it treats the sequence of expected durations at the ZLB as free parameters in estimation. The model may choose the duration sequence that best fits the data, which may result in durations being longer than the underlying policy constraints. As a result, the model accommodates unconventional monetary policy in the form of forward guidance, where the central bank influences public expectations that the policy rate will be lower for longer than implied by the policy rule.

Following KMR (2017), I use the Binder and Pesaran (1995, 1997) algorithm to conveniently compute the time-varying solution at the ZLB. However, since the Binder and Pesaran (1995, 1997) algorithm solves the model iteratively, it becomes computationally expensive. Therefore, following KMR (2017), the time-invariant solutions in the pre- and post-ZLB regimes are obtained using the Sims (2002) algorithm. Nevertheless, for consistency, I present the solution only in Binder and Pesaran (1995, 1997) form. A mathematical representation of both algorithms can be found in the technical appendix.

The model solution comprises three components, as shown in figure 1.1. Before the anticipated structural change occurs at time $t = T$, the model can be expressed in the

Figure 1.1: Monetary Policy Regimes in the Euro Area

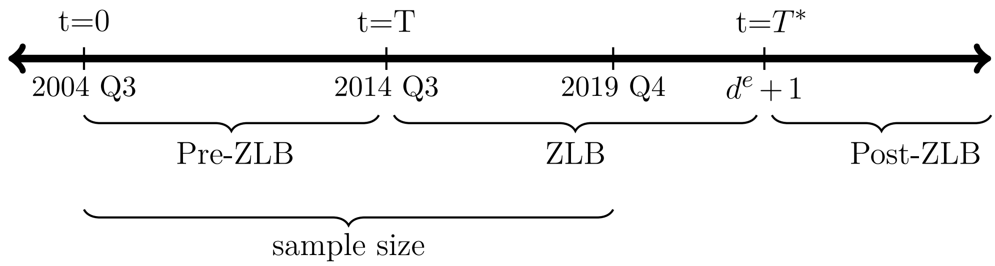

standard Binder and Pesaran (1995, 1997) form:

$$A_0 y_t = C_0 + A_1 y_{t-1} + B_0 E_t y_{t+1} + D_0 \varepsilon_t \tag{1.18}$$

where y_t is the $n \times 1$ state vector and ε_t the $l \times 1$ vector of structural shocks. It follows that the standard rational expectation solution in the pre-ZLB regime is given by:

$$y_t = C + Q y_{t-1} + G \varepsilon_t \tag{1.19}$$

where C, Q, and G are the LRE solution matrices of conformable dimensions.

The structural change in the model, in the form of a fixed interest rate regime, occurs in period $t = T$. The structure is expected to remain in place until $t = d^e + 1 = T^*$ where d^e denotes the expected duration. The canonical form of the model changes to:

$$A_0^* y_t = C_0^* + A_1^* y_{t-1} + B_0^* E_t y_{t+1} + D_0^* \varepsilon_t \tag{1.20}$$

While the interest rate is pegged, the model solution follows a time-varying VAR process:

$$\{C_t\}_{t=1}^{d} + \{Q_t\}_{t=1}^{d} y_{t-1} + \{G_t\}_{t=1}^{d} \varepsilon_t \tag{1.21}$$

The KMR (2017) time-varying solution is based on the assumption that monetary policy will revert to its original Taylor rule in the post-ZLB period. The model solution with anticipated structural changes requires agents to build expectations that a determinate structure will remain in place indefinitely. Consequently, the structural equations in the post-ZLB regime are identical to those in the pre-ZLB regime, and thus, the solution is equivalent to the standard rational expectation solution outlined in equation 1.19. Accordingly, the LRE model solution can be summarized as follows:

$$y_t = \begin{cases} C + Qy_{t-1} + G\varepsilon_t, & \text{for } t < T \\ \{C_t\}_{t=1}^{d} + \{Q_t\}_{t=1}^{d} y_{t-1} + \{G_t\}_{t=1}^{d}\varepsilon_t, & \text{for } T \leq t < T^* \\ C + Qy_{t-1} + G\varepsilon_t, & \text{for } t \geq T^* \end{cases}$$

To obtain the solution matrices C_t, Q_t, and G_t, re-consider the time-varying solution at the ZLB:

$$y_t = C_t + Q_t y_{t-1} + G_t \varepsilon_t \tag{1.22}$$

Assuming no future shocks, $E_t\varepsilon_{t+1} = 0$, implies that the solution in the next period $t+1$ is given by:

$$E_t y_{t+1} = C_{t+1} + Q_{t+1} y_t \tag{1.23}$$

With the method of undetermined coefficients, equations 1.23 and 1.20 imply:

$$(I - B^* Q_{t+1})^{-1}(\Gamma + B^* C_{t+1}) = C_t \tag{1.24}$$

$$(I - B^* Q_{t+1})^{-1} A^* = Q_t \tag{1.25}$$

$$(I - B^* Q_{t+1})^{-1} D^* = G_t \tag{1.26}$$

Equation 1.25 can be transformed to:

$$A^* - Q_t + B^* Q_{t+1} Q_t = 0 \tag{1.27}$$

Equation 1.27 now delivers the solution for Q_t via backward induction. Starting from the first period in the post-ZLB regime, $Q_{d+1} = Q$, a sequence $\{Q_t\}_{t=1}^{d}$ can be chosen under the condition is satisfies the equality in 1.27. Note that the solution only holds if $(I - B_t Q_{t+1})$ is of full rank implying that the post-ZLB regime must be determinate, i.e., satisfies the Taylor principle. In this case, equation 1.27 can be written as:

$$\Lambda_t + F_t C_{t+1} = C_t \tag{1.28}$$

where $\Lambda_t = (I - BQ_{t+1})^{-1}\Gamma$ and $F_t = (I - BQ_{t+1})^{-1}B$. From there, the remaining solution matrices, $\{G_t\}_{t=1}^d$ and $\{C_t\}_{t=1}^d$, can be derived according to:

$$C_t = \Lambda_t + F_t\Lambda_{t+1} + F_t F_{t+1}\Lambda_{t+2} + ... \tag{1.29}$$

Using the KMR (2017) solution method, allows me to simultaneously estimate both the structural parameters (θ) and the expected durations ($\mathbf{d}$) of the ZLB period. In contrast, other solution strategies such as the occasionally-binding constraint algorithms by Guerrieri and Iacoviello (2015) or Jones (2017) do not compute the expected durations as a function of the ZLB constraint. Similarly, regime-switching models, such as the Markov-switching approach by Bianchi (2013), which allow for multiple occurrences of a fixed-interest rate regime, assume constant expected durations. However, these expected durations have shown to be key determinants in assessing monetary policy at the ZLB. For instance, Jones et al. (2022b) combine the strategies of KMR (2017) and Jones (2017) to identify forward guidance shocks in the US and demonstrate that forward guidance shocks can have a more profound impact than conventional monetary policy shocks. Therefore, the key focus of this chapter is the identification of the sequence of expected durations for the euro area and the investigation of their model dynamics.

1.4 Estimating the Model at the ZLB

The model equations are linearized around the steady state and then cast into state-space form before estimating the model with Bayesian estimation techniques. The set of structural parameters and the sequence of expected durations is estimated simultaneously. The likelihood for the data sample is defined as $\mathcal{L}(Z \mid \theta, d)$, where θ denotes the set of structural parameters, Z the data, and d the set of expected durations at the ZLB:

$$p(\theta, d \mid Z) \propto \mathcal{L}(Z \mid, \theta, d) p(\theta) p(d)$$

Using the Metropolis-Hastings algorithm, draws are generated from the posterior proposal of the pre-ZLB sub-sample to get full marginal posterior distributions for each parameter. The proposal is based on the posterior mode obtained by minimizing the negative log posterior of the pre-ZLB sub sample.

1.4.1 Data

The model is estimated using nine observables from the euro area: log difference of real GDP, real consumption, real investment, and real wages, log and demeaned hours worked, log differences of the GDP deflator as the measure for inflation, the main refinancing operations (MRO) rate, and one and five-year maturity bond yields. The first seven observables are constructed as in SW-07 where all real observables are expressed in period-on-period log growth rates. The additional two interest rates correspond to the yield curve augmentation of the model as in KMR (2017). The measurement equation is given as follows:

$$\begin{bmatrix} n^{obs} \end{bmatrix} = \begin{bmatrix} \Delta logGDP_t \\ \Delta logC_t \\ \Delta logI_t \\ \Delta logW \\ logH_t \\ \Delta log\pi_t \\ MRO_t \\ Y_t^4 \\ Y_t^{20} \end{bmatrix} = \begin{bmatrix} \bar{\gamma} \\ \bar{\gamma} \\ \bar{\gamma} \\ \bar{\gamma} \\ \bar{l} \\ \bar{\pi} \\ \bar{r} \\ \bar{r} + c^4 \\ \bar{r} + c^{20} \end{bmatrix} + \begin{bmatrix} y_t - y_{t-1} \\ c_t - c_{t-1} \\ i_t - i_{t-1} \\ w_t - w_{t-1} \\ l_t \\ \pi_t \\ r_t \\ r_t^4 \\ r_t^{20} \end{bmatrix}$$

where $\bar{\gamma}$ denotes the quarterly growth rate to GDP, consumption, investment, and wages. Moreover, $\bar{\pi}$ is the quarterly steady state inflation rate, $\bar{r}$ the steady state interest rate, and $\bar{l}$ the steady state hours worked. c^4 and c^{20} are maturity-specific time-invariant components.

The sample period runs from 2004:Q3 to 2019:Q4.[5] These data are drawn from the *Eurostat* database and the ECB's *Statistical Data Warehouse (SDW)*. These data reflect changes in the composition of the euro area over the time period covered by the sample.[6] A number of outliers have appeared in the investment data series since 2015, including large spikes followed by largely offsetting levels in adjacent quarters. This increase in volatility can be attributed to R&D capitalisation reporting reforms, which include the transfer of intellectual property assets to affiliated entities and redomiciled PLCs, particularly in Ireland. The effects are substantial in national account data, but they have little impact on underlying domestic activity (Avdjiev et al., 2018, Osborne-Kinch et al., 2020). Despite the Central Statistics Office and Ireland's national statistical agency recommending modified indicators, the European Commission is legally bound to adhere to ESA10 reporting standards (Fitzgerald, 2016). In order to eliminate distortions in estimation, I linearly interpolate the investment data to remove the signaling power from the impacted quarters.[7]

[5]The constructed euro bond yield rates for one and five-year maturity bonds are not available before 2004:Q3.

[6]Aside from the 12 member states that were already part of the euro area before the sample period, Slovenia, Cyprus, Malta, Slovakia, Estonia, Latvia, and Lithuania joined the euro area during the sample period. Data with changing composition is available for each observable except hours worked which is only available for a fixed composition of all 19 current member states.

[7]Further discussions of reporting standards for national accounts are given in Lynch and Thage (2017) and Rassier (2017).

Figure 1.2: The Nine Observable Variables

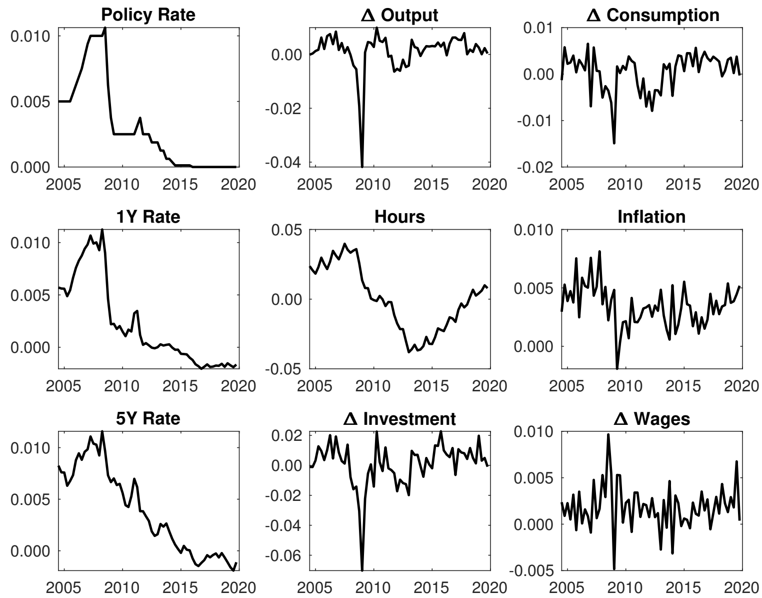

Note: The estimation process involves nine observables: Real GDP, real consumption, real investment, and real wages, hours worked, the GDP deflator as the measure for inflation, the MRO rate, and at 1-year and 5-year rates. The data sample captures the period from 2004:Q3 to 2019:Q4. Source: ECB, Eurostat

The data sample includes both a period in which the MRO rate was strictly zero and a period during which there was an effective lower bound above zero without further movement assumed. In September 2014, the ECB lowered the MRO rate to 0.05% following a 10bp reduction, which at the time was referred to as the effective lower bound. In spite of the ECB's announcement to further reduce the MRO rate by a further 5bp to zero in March 2016, based on the communication provided, I assume that the ZLB constraint effectively binds from 2014-Q3, which is visualized in figure 1.3.

Figure 1.3: The ZLB Constraint in the Euro Area

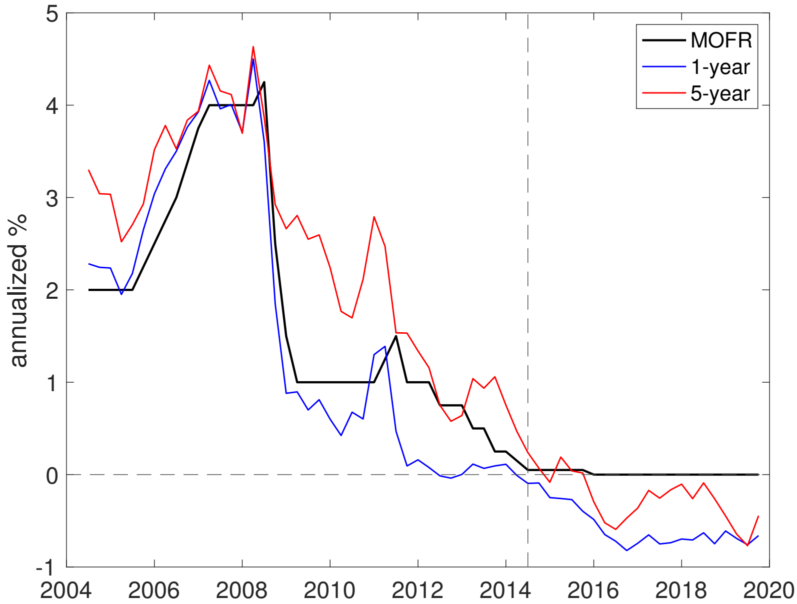

The ZLB constraint binds from 2014Q3. For the first six quarters the lower bound is set at 5bp. From 2016-Q1 the policy rate is strictly zero. In addition to the Main Financing Operatings Rate, the figure plots a constructed series for AAA-rated euro area central government bonds at different maturities: MRO rate (blue), 1-year (orange), 5-year (yellow). Source: ECB SDW.

The euro area yield data is proxied by a constructed data series published by the ECB and includes AAA-rated euro area central government bonds, which are updated every TARGET business day at noon. The ECB estimates zero-coupon yield curves and derives forward and par yield curves. Two additional observables can be obtained from the constructed data, which are zero-coupon par yields for bonds with a maturity of one year and five years.

1.4.2 Prior Structural Parameters $p(\theta)$

The set of priors for the structural parameters are chosen in accordance with SW-03, SW-07 and KMR (2017). I follow KMR (2017) and use a slightly looser prior for the standard deviations of the innovations to capture the high volatility of the sample period, given the GFC and the European Sovereign Debt Crisis. The priors for the standard deviation of the risk premium shock σ_b, the government spending shock σ_g, the monetary policy shock σ_m, and the price mark-up shock σ_p follow an inverse gamma distribution with a mean of 0.2 and a standard deviation of 3. The standard deviation of the productivity shock σ_a, the investment shock σ_q, and the wage mark-up shock follow an inverse gamma distribution with a mean of 0.42 and a standard deviation of 0.29. The priors for all autoregressive coefficients follow a beta distribution with a mean of 0.5 and a standard deviation of 0.2.

Following SW-07, five parameters are fixed in the estimation. The depreciation rate is set at 10% annually ($\delta = 0.025$ on a quarterly basis). The exogenous spending-GDP ratio is fixed at 0.18. The steady state labor market mark-up (λ_w) is set at 1.5, and the Kimball aggregators ε_p (goods market) and ε_w (labor market) are set to 10.

The prior distributions for the remaining parameters are close to the original setting by SW-07 to allow a comparison of the parameter estimates during the ZLB with a baseline estimation. In the pre- and post-ZLB regime the priors for the monetary policy rule parameters are set as in SW-07. The prior for the interest rate smoothing parameter ρ^m follows a beta distribution with a mean of 0.75 and a standard deviation of 0.1. The priors for the reaction parameter to the output gap ϕ_y and to output growth $\phi_{\Delta y}$ follow a normal distribution with a mean of 0.125 and a standard deviation of 0.05. The prior for the response parameter to inflation ϕ_π follows a normal distribution with a mean of 1.5 and a standard deviation of 0.25.

The prior for the parameter associated with the intertemporal elasticity of substitution σ_c follows a normal distribution with mean 1.5 and standard deviation 0.375. The prior for the labor elasticity parameter σ_l follows a normal distribution with a mean of 2 and a standard deviation of 0.5. Besides common boundaries of autoregressive parameters or the Taylor rule parameter for inflation, the lower bound for the labor elasticity parameter is set to 0.5 to ensure a model solution within the determinate parameter space. The prior for consumption habits λ follows a beta distribution with a mean of 0.7 and a standard deviation of 0.1. The prior for the adjustment cost parameter is normally distributed with a mean of 4 and a standard deviation of 1.5. The priors for the Calvo parameters for both prices ξ_p and wages ξ_w are assumed to follow a beta distribution with mean 0.5 and standard deviation 0.1. The degree of indexation to past inflation in the goods ι_p and labor ι_w markets is described by a beta distribution with mean 0.5 and standard deviation 0.15. A summary of prior and posterior distributions can be found in table 1.1.

1.4.3 Prior Expected Durations $p(\mathbf{d})$

The data for the informative prior of the sequence of durations is constructed from the ECB's quarterly Survey of Professional Forecasters (SPF). To my knowledge, this is the first study that utilizes the SPF responses to estimate a sequence of expected durations at the ZLB for the euro area. The survey measure not only aids with the identification of the expected durations but also includes information about agents' expectations of the future path of the policy rate in the estimation process.

Even though the SPF focuses on inflation expectations, it also collects data on real GDP growth, unemployment, and most importantly, the MRO rate for multiple horizons. Participants are professionals affiliated with financial or non-financial institutions within the euro area. The informative prior is subsequently constructed from the following survey question:

Figure 1.4: SPF Questionnaire: Forecasting the Interest Rate

Please report selected other information underlying your forecasts (average over the period):

	2013 Q1	**2013 Q2**	**2013 Q3**	**2013 Q4**	**2014**	**2015**
ECB's interest rate (main refinancing operations)						

Note: Exemplary questionnaire for the 2013 Q1 Survey of Professional Forecasters of euro area macroeconomic variables conducted by the European Central Bank. Source: ECB SPF (2013)

In the survey, agents forecast the future path of the MRO rate over the next four quarters, the average over the next year, and the average over the following year. Forecasters' expectations of liftoff are pinned down by positive non-zero interest rate forecasts, which, in turn, determine the ZLB period's duration. Using these beliefs, I construct a probability distribution for each quarter's expected duration at the ZLB. There are no ambiguities in answers in the first quarter of each year, which includes forecasts for the upcoming 12 quarters respectively. In the remaining quarters, the survey answers may overlap due to the wording of the question. For instance, the survey conducted in 2015-Q2, asks for forecasts for 2015-Q2, 2015-Q3, 2015-Q4, 2016-Q1, 2016, and 2017, thus asking for 2016-Q1 twice. Using 2015 as an example year, table 1.5 visualizes this problem. In order to avoid unequal weighting on the survey answers, if a respondent expects the MRO rate to be zero in 2016-Q1 but believes a non-zero average for the rest of the year, the expected duration will be equally allocated between 2016-Q2, -Q3, and -Q4.

Figure 1.5: Example of Overlapping SPF Responses across Different Quarters

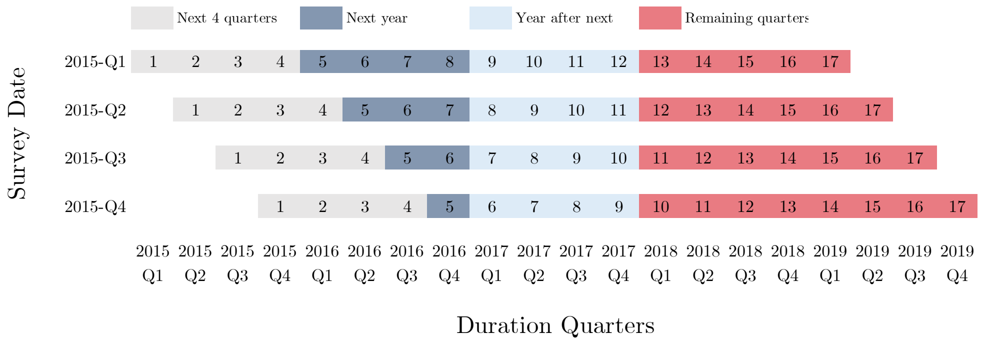

Note: The figure visualizes the overlapping responses in the SPF results and the respective duration quarters.

Because the question is open-ended, there are no point estimates for expected durations beyond the forecasting horizon of the survey. When respondents expect the interest rate to be zero across the entire survey period, there is no indication of when they expect the liftoff to occur. Thus, I introduce an upper bound of 17 quarters for expected durations.[8] When a respondent forecasts a zero MRO rate over the entire survey period, I assign equal probabilities to the following quarters up to a maximum of 17 quarters. Moreover, some respondents to the 2014-Q3 ZLB survey may not have predicted a drop in the MRO rate at quarter end. It is therefore likely that higher interest rate forecasts are not associated with beliefs of a short duration for the ZLB, but with outdated beliefs from the previous quarter. Due to the limited informative power of 2014-Q3, I reuse the responses for 2014-Q4, assuming these are responses for which all respondents have anticipated a fixed interest rate regime. Accordingly, a prior distribution for the expected durations is constructed based on the SPF data and a uniform distribution in which each element is equally weighted.

1.4.4 Posterior Sampler

The sampler for the joint posterior of the structural parameters and the sequence of expected durations of the ZLB is based on the tailored randomized block Metropolis–Hastings algorithm developed by Chib and Ramamurthy (2010). As in KMR (2017),

[8]The MRO rate was strictly zero for 16 periods at the end of the data sample. I vary the upper bound of the estimates to different values and find results are robust to changes.

those are drawn from two separate blocks of the sampler. Instead of updating the entire set of parameters in each draw, the parameters are randomly clustered at every iteration into an arbitrary number of blocks.

Block for the Expected Durations d The block of expected durations uses an independent uniform proposal density. The number of expected durations updated in each draw is randomized from a discrete uniform distribution $[1, l_d]$, where l_d determines the upper bound of durations to be updated. As in KMR (2017), l_d is set equal to two. Those quarters that are selected to be sequentially updated in each draw, are randomized from a discrete uniform distribution $[1, l]$, where l displays the length of the ZLB in the sample ($l = 16$). The corresponding elements are randomly sampled from a discrete uniform distribution $[1, \overline{d}]$, while non-updated parameters remain at their values in d_{j-1}. The maximum admissible duration is given by $\overline{d}$ and is set to 17 quarters, the upper bound limit chosen for the survey point forecasts. The acceptance rate is then calculated according to:

$$\alpha_j^{\mathbf{d}} \equiv \frac{p(\theta_{j-1}, \mathbf{d}_j^{'} \mid Z)}{p(\theta_{j-1}, \mathbf{d}_{j-1} \mid Z)}$$

The proposal is then accepted with probability $min\{\alpha_j^d, 1\}$, setting $\mathbf{d}_j = \mathbf{d}_j^{'}$, or $\mathbf{d}_{j-1}$ otherwise.

Block for the Structural Parameters The block of structural parameters $n_\theta = 40$, and θ the number of parameters updated in each draw is randomized from a discrete uniform distribution $[l_\theta, n_\theta]$. As in KMR (2017), in each draw a minimum of eight structural parameters is updated, so $l_\theta = 8$. The updated parameters in each draw are randomly sampled from a discrete uniform distribution $[1, n_\theta]$. The proposed set of parameters, $\theta_j^{'}$, is constructed from a multivariate Student's t-distribution $\theta_j \sim t(\theta_{j-1}, \Sigma, \nu)$, where ν denotes the degree of freedom and Σ is the scale matrix based on the negative inverse Hessian at the posterior mode of the pre-ZLB sub-sample multiplied by a tuning parameter κ which is set to 0.075 targeting an acceptance ratio between 40% and 50%. The t-distribution is based on the proposal Hessian matrix of the pre-ZLB sub-sample.

Denoting the set of updated parameters in each draw as $\theta_{2,j}$ and those not being updated as $\theta_{1,j}$, the density distribution can then be summarized accordingly:

$$\begin{bmatrix} \theta_{1,j} \\ \theta_{2,j} \end{bmatrix} \sim t\left(\begin{bmatrix} \theta_{1,j-1} \\ \theta_{2,j-1} \end{bmatrix}, \begin{bmatrix} \Sigma_{11} & \Sigma_{12} \\ \Sigma_{21} & \Sigma_{22} \end{bmatrix}, \nu \right)$$

By deviating from the sampler in KMR (2017), the scale matrix Σ is reordered in each draw, such that the updated parameters correspond to the first columns and rows of the scale matrix.

$$\theta_{i,j} \sim t(\theta_{j-1}, \Sigma_i, \nu)$$

The subset of updated parameters, denoted as $\theta_{i,j}$, is determined based on the Cholesky Decomposition of a subset of the scale matrix Σ_i. This technical addition to the sampler ensures that, by construction, the inverted sub-sample of the scale matrix will be again invertible.[9]

Based on Ding (2016) and KMR (2017), the conditional density of the structural parameters is then given by:

$$\theta_{2,j} \mid \theta_{1,j} = \theta_{1,j-1} \sim t\left(\theta_{2,j-1}, \frac{\nu}{\nu + p_1} \Sigma_{22|1}, \nu + p_1 \right)$$

where p_1 is the number of parameters being held constant, and

$$\Sigma_{22|1} \equiv \Sigma_{22} - \Sigma_{21} \Sigma_{11}^{-1} \Sigma_{12}$$

The acceptance ratio for admissible values is calculated according to:

$$\alpha_j^{\theta} \equiv \frac{p(\theta_j, d_j^{'} \mid Z)}{p(\theta_{j-1}, d_j \mid Z)}$$

Subsequently, the proposal is accepted with probability $min\{\alpha_j^{\theta}, 1\}$, setting $\theta_j = \theta_j^{'}$ or θ_{j-1} otherwise.

[9] Even though this holds mathematically without the technical addition, issues may arise due to small numerical inaccuracies throughout the algorithm's code.

1.5 Results

Based on KMR (2017), I jointly estimate the set of structural parameters and expected durations. The posterior mode, used to tailor the proposal density in the sampler, is computed using a sub-sample that ends before the euro area hits the ZLB. A posterior distribution is generated using 500,000 draws with the first half of the draws treated as burn-in for the sampler to converge. Using two parallel chains of 500,000 draws with different starting values, the Brooks, Gelman and Rubin test (Gelman and Rubin, 1992, Brooks and Gelman, 1998) supports convergence of the parameters. The baseline chain starts at the posterior mode, while the second chain starts randomly along the posterior distribution. Results, presented in tables 1.4 and 1.5 in the appendix for Chapter I, do not indicate any non-convergence of parameters.

1.5.1 Structural Parameters

The posterior estimates of the structural parameters are presented in table 1.1. Overall, the results are consistent with those in previous literature, including KMR (2017), SW-03 and, SW-07. It is especially encouraging considering the length of the ZLB period, which makes up a substantial portion of the sample period.

The shock variances are larger than previously estimated by SW-03 and SW-07 for the euro area and the United States respectively. While Smets and Wouters (2005) find substantial differences in shock variance estimates between the euro area and the US, these differences are only partially visible at the ZLB. Comparing the shock process parameters to those estimated by KMR (2017) for the US, the productivity shock innovation σ^a is larger in the euro area, while the preference shock innovation σ^b is quantitatively similar. The price mark-up shock innovation σ^p and the investment shock innovation variance σ^p are estimated to be higher in the euro area. The higher innovation variances are translated into a lower persistence of the shock processes respectively ($\rho^p = 0.27$, $\rho^{qs} = 0.39$) which is also substantially lower than the estimates for the US (KMR (2017) $\rho^p = 0.89$, $\rho^{qs} = 0.70$). Similarly, the monetary policy shock innovation variance is estimated to be larger ($\sigma^m = 0.30$) and the shock process less persistent ($\rho^r = 0.22$) in the euro area. The term

Table 1.1: Posterior Estimates of Structural Parameters

Parameter		**Prior**			**Posterior**				
		Distribution	**Mean**	**Std. dev.**	**Mode**	**Mean**	**Std. dev.**	**10%**	**90%**
Shock Standard Deviations									
Technology	σ^a	IG	0.42	0.29	0.66	0.66	0.05	0.62	0.71
Risk premium	σ^b	IG	0.20	3.00	0.15	0.16	0.01	0.14	0.19
Fiscal	σ^g	IG	0.42	0.29	0.50	0.51	0.03	0.48	0.54
Investment	σ^{qs}	IG	0.42	0.29	0.61	0.6	0.06	0.53	0.66
Monetary	σ^m	IG	0.20	3.00	0.30	0.3	0.01	0.28	0.33
Price mark-up	σ^p	IG	0.20	3.00	0.34	0.35	0.02	0.32	0.38
Wage mark-up	σ^w	IG	0.42	0.29	0.30	0.31	0.01	0.29	0.33
1-year	σ^4	U	1.00	0.58	0.34	0.39	0.1	0.19	0.54
5-year	σ^{20}	U	1.00	0.58	1.09	1.14	0.46	0.85	1.39
Term premium	σ^η	U	2.50	1.44	0.55	0.61	0.16	0.42	0.77
Shock Persistences									
Technology	ρ^a	B	0.50	0.20	0.92	0.87	0.05	0.80	0.94
Risk premium	ρ^b	B	0.50	0.20	0.97	0.96	0.01	0.95	0.97
Fiscal	ρ^g	B	0.50	0.20	0.89	0.9	0.04	0.84	0.95
Fiscal technology	ρ^{ga}	N	0.50	0.20	0.51	0.5	0.08	0.40	0.59
Investment	ρ^{qs}	B	0.50	0.20	0.38	0.39	0.13	0.22	0.58
Monetary	ρ^r	B	0.50	0.20	0.24	0.22	0.08	0.12	0.33
Price mark-up	ρ^p	B	0.50	0.20	0.18	0.27	0.15	0.09	0.47
Wage mark-up	ρ^w	B	0.50	0.20	0.10	0.13	0.07	0.05	0.21
Term premium	ρ^s	B	0.71	0.16	0.97	0.95	0.03	0.92	0.98
Structural Parameters									
Investment Adj. Costs	φ	N	4.00	1.50	5.96	6.12	1.24	4.58	7.77
CRRA	σ^c	N	1.50	0.375	0.94	0.93	0.09	0.81	1.05
Habits	λ	B	0.70	0.10	0.74	0.74	0.05	0.67	0.8
Degree of Wage Stickiness	ξ_w	B	0.50	0.10	0.93	0.93	0.02	0.90	0.95
Elasticity of Labor Supply	σ^l	N	2.00	0.75	1.46	1.51	0.52	0.83	2.16
Degree of Price Stickiness	ξ_p	B	0.50	0.10	0.80	0.77	0.06	0.70	0.84
Indexation Wages	ι_w	B	0.50	0.15	0.39	0.39	0.13	0.22	0.56
Indexation Prices	ι_p	B	0.50	0.15	0.27	0.35	0.15	0.17	0.56
Capacity Utilization	ψ	B	0.50	0.15	0.59	0.62	0.12	0.46	0.77
Fixed Costs	ϕ_p	N	1.25	0.125	1.62	1.63	0.09	1.51	1.74
Monetary Policy: Inflation	ϕ_π	N	1.50	0.25	1.52	1.49	0.22	1.20	1.77
Monetary Policy: Smoothing	ρ_R	B	0.75	0.10	0.87	0.86	0.03	0.82	0.90
Monetary Policy: Output Gap	ϕ_y	N	0.125	0.05	0.05	0.06	0.02	0.04	0.09
Monetary Policy: Output Growth	$\phi_{\Delta y}$	N	0.125	0.05	0.02	0.02	0.02	-0.00	0.05
Constant Inflation	$\bar{\pi}$	G	0.63	0.10	0.51	0.51	0.06	0.43	0.59
Discount Factor	$\beta^{-1}-1$	G	0.25	0.10	0.22	0.2	0.07	0.12	0.29
Constant Labor	$\bar{l}$	N	0.00	2.00	3.71	3.85	0.96	2.59	5.05
Trend Growth	γ	N	0.40	0.10	0.24	0.25	0.03	0.22	0.28
Capital Share	α	N	0.30	0.05	0.26	0.26	0.02	0.23	0.28
Term Premium Constant	c_4	N	1.20	0.25	1.38	1.41	0.23	1.12	1.71
Term Premium Constant	c_{20}	N	2.35	0.25	2.10	2.09	0.21	1.81	2.36

Note: The chain has 500,000 draws, half of which is disregarded as burn-in. Moments are multiplied by 10^{-2}. N= Normal Distribution; IG= Inverse Gamma Distribution; U=Uniform Distribution; B= Beta Distribution; G=Gamma Distribution premium innovation variances are substantially higher (1-year bond $\sigma^4 = 0.39$; 5-year bond $\sigma^{20} = 1.14$) than those estimated by KMR (2017) ($\sigma^{20} = 0.09$). The risk-premium shock persistence ($\rho^b = 0.96$) is in line with findings by KMR (2017) whereas SW-07 find a much lower persistence ($\rho^b = 0.22$).

The posterior mean of the inflation trend parameter ($\bar{\pi}$) implies an annualized inflation target of 2.04% which nearly matches the official target of 2% communicated by the ECB. The posterior mean estimate for the steady state interest rate implies an annual steady state nominal interest rate of 3.78% and an annual steady state real interest rate of 1.74%. Trend growth (γ) is estimated to be around 0.25% on a quarterly basis, which is a bit higher than the average growth rate in the data (0.11%) but in line with estimates of trend growth in other settings.

The relative risk aversion parameter ($\sigma^c = 0.93$) is estimated to be smaller than 1, implying a relatively high inter-temporal elasticity of consumption. While this is substantially lower than estimates by SW-07 for the US ($\sigma^c = 1.38$) or by SW-03 for the euro area ($\sigma^c = 1.61$), more recent studies that include the ZLB period find similarly low estimates (for the US: Jones (2017): $\sigma^c = 0.98$ and KMR (2017): $\sigma^c = 1.05$).[10] Consumption habits are more important ($\lambda = 0.74$) compared to SW-03 and KMR (2017) for the US. The elasticity of labor supply (σ^l) is estimated to be 1.51.[11]

Turning to the Philips curve estimates compared to previous estimates for the euro area (SW-03: $\xi_w = 0.76$), wages are less flexible ($\xi_w = 0.93$) and also less flexible than in the US (KMR (2017): $\xi_w = 0.86$). The degree of price stickiness ($\xi_p = 0.77$) is estimated to be lower than in SW-03 and lower than the degree of wage stickiness. The indexation for past inflation ($\iota_p = 0.35$) and the indexation for wages ($\iota_w = 0.39$) are similar. The share of capital used in the production process (α) is estimated to be 26%. Finally, in the pre- and post-ZLB regimes, the monetary authority responds sufficiently enough to inflation to fulfil the Taylor principle ($\phi_\pi = 1.49$). Reactions to the output gap ($\phi_y = 0.06$) and to output growth ($\phi_{\Delta y} = 0.02$) are small, which is consistent with the idea that the ECB is primarily focused on its inflation target mandate. Interest rates are slightly more

[10] Assuming log utility in consumption (i.e., $\sigma^c = 1$) does not qualitatively and quantitatively affect the remaining structural parameter estimates in the model.

[11] This estimate is substantially higher than the excluded parameter space given a posterior standard deviation of 0.52.

persistent ($\rho^R = 0.86$) than estimated by KMR (2017) for the US ($\rho^R = 0.81$).

1.5.2 Expected Durations

The joint estimation allows me to estimate the duration of the ZLB in each quarter as an independent parameter. The estimates for the sequence of the expected ZLB durations are presented in table 1.2. In the benchmark scenario, the corresponding prior assigns 50% weight to the SPF data and 50% to a uniform distribution.

Table 1.2: Expected Duration Estimates

	Expected Durations per quarter					
	Prior			Posterior		
Quarter	Mean	Mode	Std. Dev.	Mean	Mode	Std. Dev.
2014 Q3	9.89	1	3.93	10.46	12	4.58
2014 Q4	9.89	1	3.93	10.58	14	4.56
2015 Q1	9.17	12	2.73	8.48	9	4.36
2015 Q2	9.46	17	3.63	9.62	11	4.04
2015 Q3	9.06	17	2.94	9.25	10	3.94
2015 Q4	9.45	9	3.01	9.23	9	4.22
2016 Q1	9.34	14	2.88	10.41	12	4.12
2016 Q2	9.21	13	3.16	9.28	11	4.55
2016 Q3	9.57	12	3.29	10.47	13	4.35
2016 Q4	9.75	17	3.50	10.98	14	4.23
2017 Q1	10.81	17	6.21	9.27	13	4.79
2017 Q2	8.71	9	2.25	8.40	10	4.00
2017 Q3	8.33	12	2.58	8.35	9	3.55
2017 Q4	8.00	11	2.49	7.28	7	3.44
2018 Q1	7.69	10	2.14	7.00	8	3.34
2018 Q2	7.44	9	2.02	6.87	5	3.52
2018 Q3	7.47	8	2.42	6.71	6	3.30
2018 Q4	7.23	5	2.06	6.80	5	3.79
2019 Q1	7.23	4	1.67	10.08	4	4.65
2019 Q2	8.38	9	1.90	9.52	7	4.34
2019 Q3	10.03	12	3.77	12.99	17	3.32
2019 Q4	10.73	17	5.38	10.85	13	4.29

Note: The chain has 500,000 draws, half of which is disregarded as burn-in. The prior is constructed by assigning equal weight to a uniform distribution and the survey measure.

The posterior mean estimates for the expected duration exhibit significant movement over the sample period and are influenced by the prior. At the start of the sample period, the ZLB is expected to bind for 2.5 years (10-11 quarters). From 2017 through 2019, the expected durations steadily declined, with the shortest estimate of 6.67 quarters observed in 2018-Q3. However, throughout 2019, the estimates increased sharply, surpassing an expected duration of three years (12.95 quarters) in the third quarter of 2019.

Figure 1.6: Expected Durations of the ZLB

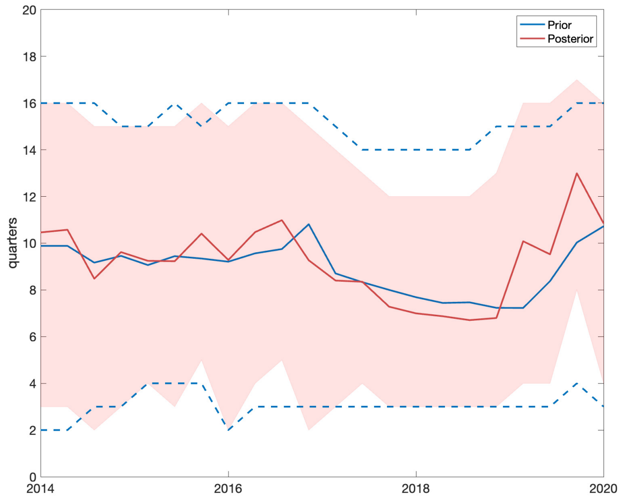

Note: The figure shows the prior (blue line) and posterior mean (red line) and the equal-tailed 80% prior and posterior bands of the expected durations.

Figure 1.6 displays the significant variation in the estimated expected durations over time. Estimates for the euro area consistently show longer durations than those for the US by KMR (2017). US estimates peak around 2012 and then gradually decline thereafter, while euro area estimates exhibit a different pattern. Towards the end of the sample period, expected durations increase, reflecting the euro area's developments that did not suggest an imminent liftoff at the time.

Robustness Exercises I demonstrate the well-identified expected duration estimates and the informative power of the survey data by conducting three robustness exercises. Specifically, I vary the weight of the priors based on the survey, compare the estimates with the market durations implied by the euro area's forward curve, and increase the upper bound limit on the survey measure from 17 to 25 quarters.

Figure 1.7: Expected Durations at Varying Weights

Note: The figure shows the equal-tailed 80% posterior bands and the mean posterior estimates for the expected durations at different prior weights: $\omega = 0$ (uniform distribution), $\omega = 0.5$ (equally split), $\omega = 1$ (solely survey based).

Posterior estimates are based a prior that is constructed either exclusively from a uniform distribution ($\omega = 0$), entirely on the survey data ($\omega = 1$), or equally on both ($\omega = 0.5$).[12] The posterior estimates for a varying survey weight can be found in table 1.3 in the appendix for Chapter I. Across varying survey weights, the expected durations appear robust. Figure 1.7 visualizes the mean posterior estimates for the expected durations for each prior specification. The blue line corresponds to the benchmark case where the prior consists of 50% survey data and 50% uniform distribution.[13] The red line represents the case where the survey data is not taken into account ($\omega = 0$), vice versa the black line corresponds to the case where only the survey data is taken into account ($\omega = 1$).

Despite the uniform distribution predicting a smoother path for the expected durations, a general trend pattern is still evident. During the first half of the sample period, the survey data consistently indicates longer expected durations than what the uniform

[12]When the prior is solely based on a uniform distribution, the starting values of the expected durations for the MCMC algorithm are set to 1 for all quarters.

[13]Although incorporating the survey data makes the likelihood more informative, I follow KMR (2017) and use a prior with equal weights on the survey and a uniform distribution as the benchmark case. This approach ensures that duration outcomes with no weight in the survey are not automatically excluded from the posterior distribution.

distribution implies. The decline in expected durations between 2017 and 2018 appears to be amplified by agents' expectations in the survey, emphasizing the benefit of incorporating subjective information in estimation. Across all exercises, the expected duration peaks towards the end of the sample period. Furthermore, utilizing the survey data in the estimation process enhances the accuracy of the expected duration estimates. When more weight is assigned to the survey, the 80% posterior bands around the mean become narrower, and the standard deviations decrease.[14] This indicates the informative power of the survey data and its significant role in the process of estimating models that capture ZLB periods.

Figure 1.8: Expected Durations implied by a Forward Curve

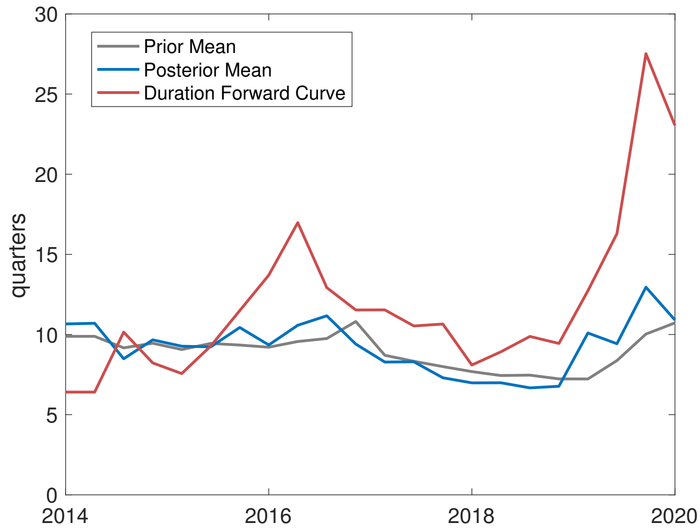

Note: The figure shows the mean prior, the mean posterior estimates for the expected durations at prior weights: $\omega = 0.5$ and the durations implied by the forward curve.

Second, I compare the expected duration estimates with market expectations of the euro area forward curve. Based on the methodology provided by the ECB, I construct the forward curve and the corresponding ZLB duration. The forward rates include a term structure and reflect the different rates at different maturities. The forward rates, therefore, will not only capture market expectations but will also convey forward premium compared to the constructed SPF measure. Since the forward curve incorporates forward premium, the expected durations derived from it, while exhibiting a similar pattern to

[14]The standard deviations for different weights are summarized in table 1.3 in the appendix for Chapter I.

those obtained from the SPF measure, are generally longer over most of the sample period. The forward durations also respond more strongly to the continuous decrease in the MRO rate in 2016, although indicating a comparable decline in the following quarters. Moreover, the market-based measure exhibits a more significant increase in durations towards the end of the sample period, peaking at almost seven years in late 2019.

Finally, I conduct a robustness exercise by varying the upper bounds of the expected duration estimates. Due to the open-ended nature of the SPF question, probabilities must be assigned up to a maximum limit. In the benchmark case, this limit is set to 17 quarters. However, when this limit is increased from 17 to 25 quarters, the duration estimates remain stable, though slightly above the baseline model (refer to the top right plot in Figure 1.9). Nevertheless, it is worth noting that increasing the upper bound also increases the standard deviation of the estimates.

Figure 1.9: Varying the Upper Bound on Expected Durations

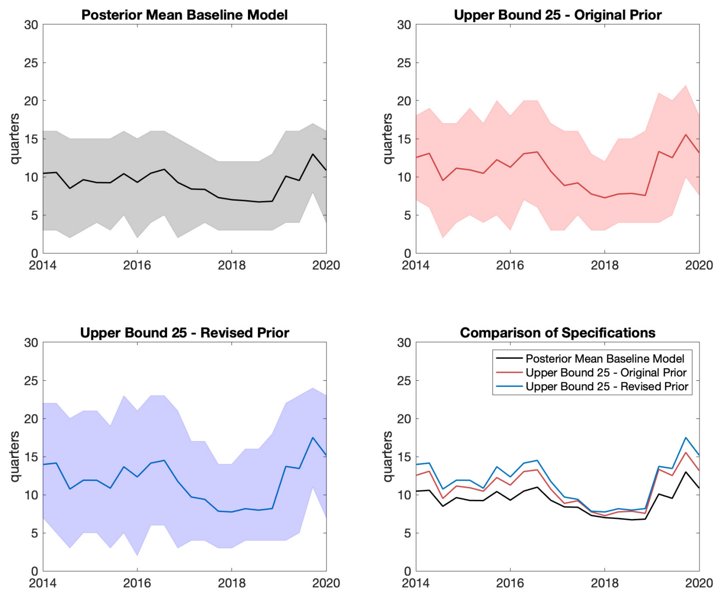

Note: The figure shows the mean prior, the mean posterior estimates for the expected durations for different upper bound specifications.

1.5.3 Fit of the Model

The model produces a relatively accurate prediction of the actual data over the sample period. Specifically, Figure 1.10 plots the actual data series compared to the smoothed one-period ahead forecasts obtained through the Kalman filter at the posterior mean.

Figure 1.10: In-Sample Fit of the Model

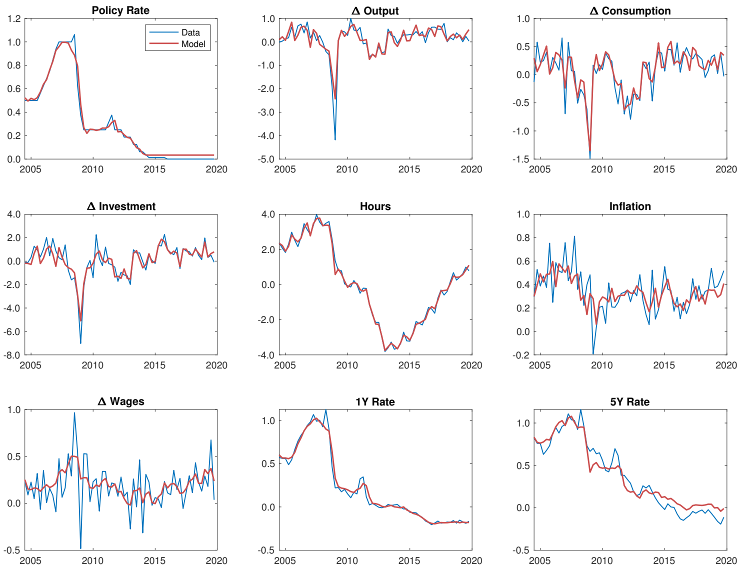

Note: The figure plots the actual data (blue line) as well as the one-period-ahead forecasts obtained from the Kalman smoother (red line), computed using the estimated posterior mean $\hat{\theta}$. See section 1.4.1 for a detailed description of the data sample
.

The model tends to underpredict the effects of the GFC on most real variables. Moreover, the model fails to capture the high volatility observed in real wage growth and inflation. Notably, the model consistently overpredicts yields for the 5-year maturity bond and underpredicts inflation during the ZLB period.

Figure 1.11 shows the posterior bands of the structural shock processes obtained from random draws of the posterior chain. The estimated autoregressive parameters, summarized in table 1.1, suggest that the technology shock (ε^a), preference shock (ε^b), government spending shock (ε^g), and term premium shocks (ε^4 and ε^{20}) are highly persistent. Additionally, the preference shock is estimated to be negative throughout the sample period. The ZLB period is accompanied by a downward trend in the technology shock, government spending shock, and term premium shocks. In line with the euro area's interest rate movements, the latter show a decreasing trend throughout the sample period. The monetary policy shock (ε^m) fluctuates around zero until the ZLB period, during which, by assumption, no shock occurs.[15]

Figure 1.11: Kalman Smoothed Shocks

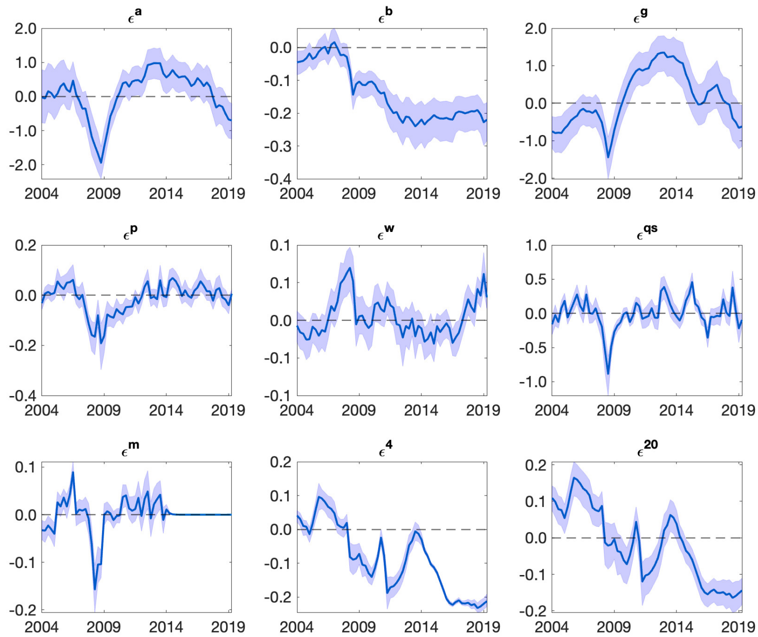

Note: The figure plots a simulated Kalman-smoothed time series for the shock processes: ε_t^a (technology), ε_t^b (risk premium), ε_t^g (exogenous spending), ε_t^p (price mark-up), ε_t^w (wage mark-up), ε_t^{qs} (investment-technology), ε_t^m (monetary policy), ε_t^4 (1Y Term Premium), and ε_t^{20} (5Y Term Premium), using 100 randomized posterior MCMC draws $\hat{\theta}_j$, and the equal-tailed 80% posterior bands.

1.6 Model Dynamics at the ZLB

In LRE models, forward-looking agents incorporate their expectations of the ZLB duration into their decision-making process. The qualitative and quantitative effects of structural shocks will, therefore, depend on the estimated expected durations. It is widely acknowledged that models with a fixed interest rate respond differently to structural shocks, and their effects may seem paradoxical and counterintuitive in comparison to standard New-Keynesian theory (e.g., Werning, 2011, Cochrane, 2017, Diba and Loisel, 2021). This section offers an analysis of the model dynamics for the euro area at ZLB.

[15] As identified by KMR (2017), the risk premium shock appears to be interconnected with potentially expansionary responses of long expected durations. Including a ZLB period in the SW-03, SW-07 model results in a higher persistence of the risk premium shock (Lindé et al., 2016, Kulish et al., 2017). Tightening the prior around the persistence parameter of the shock, and hence forcing the shock to fluctuate around zero, has significant effects on the other structural shocks during the ZLB period.

1.6.1 The Generalized Impulse Response Function Algorithm

Due to the non-linearities at the ZLB, a standard Impulse Response Function (IRF) as it is commonly used to analyze the dynamics in linear models, is not applicable here. A linear impulse response function is defined as the difference between two realizations of a state vector y_{t+n} that are identical until one realization is assumed to be exposed to a shock $\varepsilon_t = \delta$ in period t:

$$IRF(n,\delta,\omega_{t-1}) = E[y_{t+n} \mid \varepsilon_t = \delta,\omega_{t-1}] - E[y_{t+n} \mid \varepsilon_t = 0,\omega_{t-1}]$$

Intuitively, a standard IRF extracts the effects of a single shock of size δ at time t assuming no further future uncertainty, since $\varepsilon_{t+j} = 0$ for $j = 1,2,...T$. In non-linear models, the future shocks are not necessarily zero, which implies that the constructed stochastic process is stationary but the standard IRFs will not converge to zero (Koop et al., 1996). Furthermore, considering a non-linear multivariate model, similar to the linear multivariate case, an IRF will depend on the composition of shocks. To investigate these responses and account for nonlinearities at the ZLB, the dynamics of the model are based on a Generalized Impulse Response Function (GIRF) algorithm similar to the one proposed by Koop et al. (1996). Future shocks are conditioned on only the history and/or shock, and therefore, are averaged out. The subsequent GIRF is an average of what happens given an information set from the present and past based on the conditional expectation on the history ω_{t-1}:

$$GIRF(N,\vartheta,\omega_{t-1}) = E[\tilde{y}_{t+N} \mid \vartheta^j(\varepsilon_t^j = \tilde{\varepsilon}_{t|T}^j),\mathbf{d}_{13},\omega_{t-1}] - E[\tilde{y}_{t+N} \mid \vartheta,\mathbf{d}_{13},\omega_{t-1}]$$

To capture dynamics at the ZLB, the GIRF must cover two regimes, the non-linear ZLB regime and, beyond the estimated duration of the ZLB in any particular quarter, the linear post-ZLB regime (compare figure 1.12). To illustrate the effects of expected durations on the model dynamics, consider the following two scenarios: a duration of 13 quarters and an imminent liftoff after one quarter where the steady state serves as history ω_{t-1} before the respective shock hits the model. Until liftoff, the expected durations decline

Figure 1.12: Timeline of Shock Response Dynamics at the ZLB

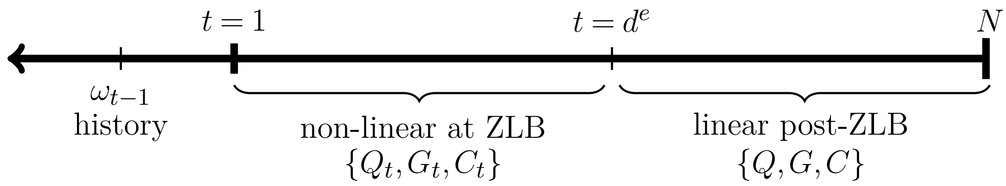

continuously by one period at a time. The responses are then based on random draws from the joint posterior distribution where the duration is estimated to be 13. The shocks ϑ are randomly drawn from the Cholesky-factorized variance-covariance matrix at the respective draw of structural parameters. To model the effects of a particular shock, the random draws of this shock are replaced by a one-standard-deviation shock based on of the smoothed empirical innovation when the interest rate is fixed ($\varepsilon_t^j = \tilde{\varepsilon}_{t|T}^j$).

The GIRF for quarter 2019-Q3 with an estimated duration of $\mathbf{d}_{21}$ is defined as[16]

$$GIRF(N, \vartheta, \omega_{t-1}) = E[\tilde{y}_{t+N} \mid \vartheta^j(\varepsilon_t^j = \tilde{\varepsilon}_{t|T}^j), \mathbf{d}_{21}, \omega_{t-1}] - E[\tilde{y}_{t+N} \mid \vartheta, \mathbf{d}_{21}, \omega_{t-1}]$$

The steps of the algorithm to obtain the GIRFs are as follows:

1. Pick a history ω_{t-1} that corresponds to the state of the model before the respective shock hits. I use the smoothed state in the previous period $\tilde{y}_{20|T}$ (2019-Q2).

2. Take draws from the joint posterior and keep only those draws for which the duration is equal to the mean of the expected durations in 2019-Q3. Randomly choose one draw of structural parameters.

3. For a given horizon ($N = 30$) and a given number of repetitions ($R = 100$), randomly draw $(N+1) \times R$ shocks (ϑ) from the Cholesky-factorized variance-covariance matrix at the respective draw of structural parameters.

4. Construct $\vartheta^j = \vartheta(\varepsilon_t^j = \tilde{\varepsilon}_{t|T}^j)$ by choosing one structural shock and replacing the random draws for this shock by a one-standard-deviation shock based on of the smoothed empirical innovation at the ZLB.

5. Compute the first realization $E[\tilde{y}_{t+N} \mid \vartheta^j, \mathbf{d}_{21}, \omega_{t-1}]$:

[16]Quarter 2019-Q3 displays the 21st quarter of the ZLB period in the data sample.

(a) For $t = 1$: Construct the GIRF for the period in which the chosen shocks hit the economy assuming all other shocks being randomized.

(b) For $t = (2 : \mathbf{d}_{21})$: Iterate on the non-linear regime conditional on ω_{t-1} and ϑ using the solution matrices during the ZLB: $\{Q_t\}_{t=1}^{d_{21}}$, $\{G_t\}_{t=1}^{d_{21}}$, and $\{C_t\}_{t=1}^{d_{21}}$.

(c) For $t = (\mathbf{d}_{21} + 1 : N)$: Iterate on the linear post-ZLB regime conditional on ω_{t-1} and ϑ using the time-invariant solution matrices: Q, G, and C.

6. Compute the second realization $E[\tilde{y}_{t+N} \mid \vartheta, \mathbf{d}_{21}, \omega_{t-1}]$:

(a) For $t = (1 : \mathbf{d}_{21})$: Iterate on the non-linear regime conditional on ω_{t-1} using the solution matrices during the ZLB: $\{Q_t\}_{t=1}^{d_{21}}$, $\{G_t\}_{t=1}^{d_{21}}$, and $\{C_t\}_{t=1}^{d_{21}}$.

(b) For $t = (\mathbf{d}_{21} + 1 : N)$: Iterate on the linear post-ZLB regime conditional on ω_{t-1} using the time-invariant solution matrices Q, G, and C.

7. Repeat steps 4 and 5 ($R = 100$) times, each with a different set of randomized shocks and build the averages:

$$\tilde{y}_{R,t+N}(\vartheta, \omega_{t-1}) = \frac{1}{R}\sum_{i=1}^{R} \tilde{y}_{t+N}^{i}(\vartheta^j, \mathbf{d}_{21}, \omega_{t-1})$$
$$\tilde{y}_{R,t+N}(\omega_{t-1}) = \frac{1}{R}\sum_{i=1}^{R} \tilde{y}_{t+N}^{i}(\mathbf{d}_{21}, \omega_{t-1})$$

8. Take the difference between the two averages $\tilde{y}_{R,t+N}(\vartheta^j, \mathbf{d}_{21}, \omega_{t-1})$ and $\tilde{y}_{R,t+N}(\mathbf{d}_{21}, \omega_{t-1})$.

9. Repeat steps 2 to 8 ($B = 100$) times to allow an accurate estimation of the GIRF random vector.

1.6.2 Structural Shocks with Fixed Interest Rate Periods

Figure 1.13 shows the GIRFs for a positive shock to productivity. The resulting dynamics closely resemble those predicted by standard New-Keynesian theory. The shock directly increases output and reduces the marginal costs of production. Higher levels of income stimulate consumption and investment in the economy. Households adjust their labor-leisure optimization, which decreases hours worked. Additionally, lower marginal costs result in lower inflation. As production becomes more efficient, the rental rate of capital and capacity utilization decrease. At the ZLB, when the central bank is unable to stabilize inflation through expansionary monetary policy, the effects on the real economy are less pronounced. The missing monetary transmission channel is particularly notable for investment and consumption.

Figure 1.13: Generalized Impulse Responses for the Technology Shock

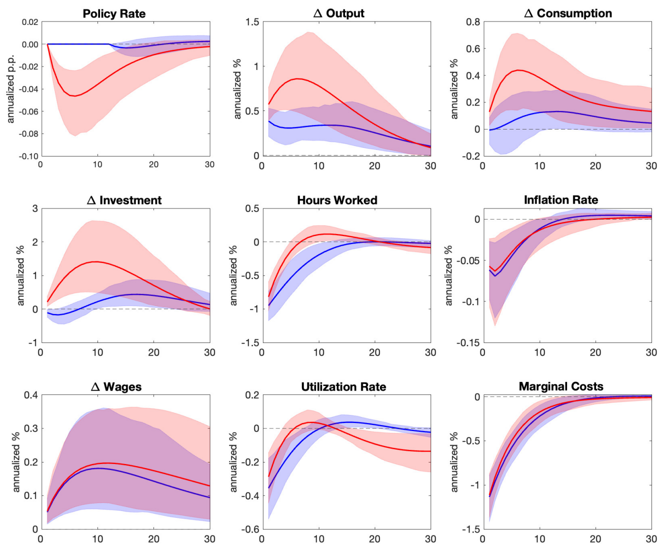

Note: GIRF for a positive technology shock. Blue line: Duration=13 (2019-Q3), Red line: Duration=1

Figure 1.14 plots the GIRFs for a positive exogenous spending shock, such as a government spending shock. Crowding-out effects and overshooting are only visible in the imminent liftoff scenario. This paradox is commonly known as the *fiscal multiplier puzzle*.

According to Christiano et al. (2011), the government-spending multiplier is not only higher at the ZLB, but it also increases with the expected length of the ZLB. In addition, Cochrane (2017) shows that spending multipliers increase exponentially with increasing expected durations. Although the effect on output is similar in both scenarios, this effect is particularly visible for investment. When the policy rate is assumed to be fixed for an extended period, the boost in output combined with falling wages increases hours worked. Contrary to the conventional crowding-out mechanism, investment increases in the absence of interest rate responses. Upon lifting the interest rate peg, the policy rate increases marginally, accelerating the return to steady state. The lack of conventional monetary policy options leaves fiscal policy options as an important policy tool.

Figure 1.14: Generalized Impulse Responses for the Exogenous Spending Shock

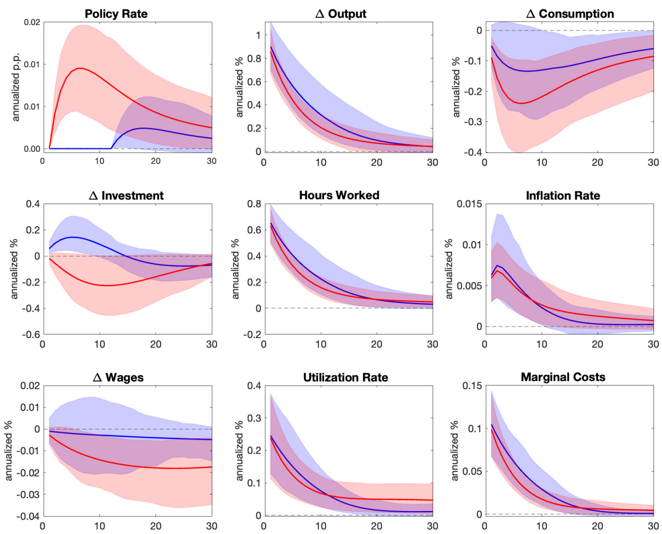

Note: GIRF for a positive exogenous spending shock. Blue line: Duration = 13 quarters, red line: Duration = 1 quarter

Figure 1.15 plots the GIRFs for a supply shock in the form of a wage mark-up shock. In a standard NK-setting, a positive wage mark-up shocks exhibit contractionary effects on the economy. The initial shock increases the real wage and, in turn, raises the real marginal cost and inflation. Higher wages increase the return on capital and capital utilization. When the liftoff is modeled immediately, the central bank responds to rising inflation by increasing the policy rate, which contracts the economy. The real variables (output, investment, and consumption) and hours worked decline. During an interest rate peg, this effect is reversed, resulting in the wage mark-up shock having expansionary effects. If the interest rate is fixed, the central bank is not responding to inflation by raising interest rates, and the shock turns expansionary.

This paradox, also known as the *Paradox of Toil* (Eggertsson, 2010), has a key policy implication that is that lowering firms' marginal costs, for example, by reducing wage mark-ups or the minimum wage, is not stimulatory to the model economy when the nominal interest rate is fixed.

Figure 1.15: Generalized Impulse Responses for the Wage Mark-up Shock

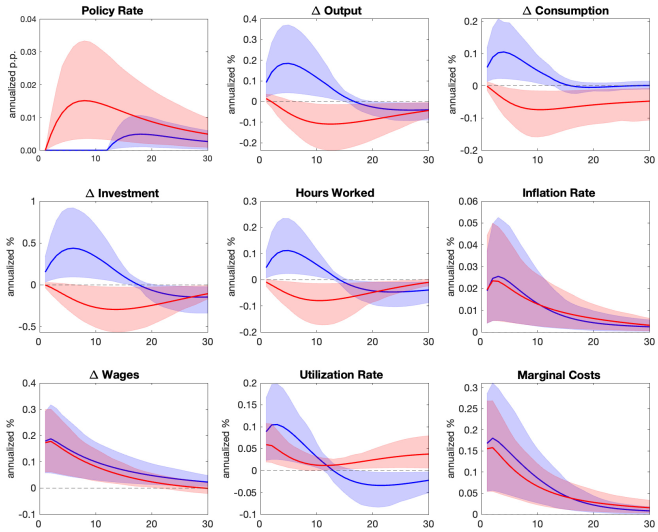

Note: GIRF for a positive wage mark-up shock. Blue line: Duration=13 (2019-Q3), red line: Duration=1

For a positive shock to investment technology, effects on inflation, wages, and marginal costs are small.[17] Surprisingly, the negative effects on consumption are marginally smaller when the liftoff is expected in one quarter.

However, the overall effects are qualitatively and quantitatively similar in both cases. Both scenarios result in rising inflation on impact, while output, consumption, and investment decline. As a response, hours worked and the real wage are decreasing, which triggers a drop in the real marginal costs and subsequently a fall in inflation back to steady state. A price mark-up shock has similar qualitative effects for both scenarios. When expected durations are assumed to be long, the effects of the price mark-up shock are amplified because the central bank is not counteracting rising inflation levels.

Turning to the risk premium shock. As found in KMR (2017) and Jones (2017), this shock interacts with the expected durations in the model. Its strong persistence partially counteracts the potentially significant expansionary effects of long expected durations. As the fixed-interest constraint persists, the response to the shock becomes more pronounced, further highlighting the non-linearities in the model dynamics at the ZLB. The quantitative effects of the shock on the model are considerably affected by the prior assigned to its

[17] The GIRFs for the shock to investment technology, the price mark-up shock , and the risk premium shock are given in the appendix for Chapter I.

persistence ρ^b, and a lower persistence has substantial effects on the remaining structural shocks.

1.7 The Role of Forward Guidance

Since conventional tools at the ZLB have been limited in recent years, central banks have shifted to unconventional monetary policies, including forward guidance. Central banks can use forward guidance to influence expectations about the duration of the ZLB by making credible announcements about the expected future path of the policy rate. Depending on the nature of the expected durations at the ZLB, the implications can be ambiguous. According to Jones (2017), structural shocks affect expected durations in contractionary ways, whereas intentional announcements of forward guidance can have expansionary effects. The ZLB is expected to bind for longer in the first case because the economy deteriorates; this has the same sample implication as traditional contractionary monetary policy shocks. When the central bank extends the duration of the ZLB intentionally and, thereby, stimulates the economy further, this constitutes an expansionary policy shock. Currently, the estimated durations (see table 1.2) for each quarter of the fixed interest rate regime do not reveal their nature. It is not yet known whether the expected length of the ZLB is a result of the underlying policy rule or a deliberate policy decision. In a recent paper, Jones et al. (2022b) build on KMR (2017) and Jones (2017) and propose a method to identify forward guidance shocks during the ZLB and thereby uncover the nature of the expected duration. With their approach, I decompose the expected duration estimates and demonstrate the importance of forward guidance in the euro area.

1.7.1 Decomposition of Expected Durations

Following Jones et al. (2022b), the estimated durations $\mathbf{d}$ corresponds to the actual expected duration. It can, however, differ from the duration implied by the underlying policy rule. In the absence of further shocks, the expected duration $\{\mathbf{d}_t\}_{t=1}^{T}$, is assumed to fall by one quarter in each period t:

$$E_t[\mathbf{d}_{t+1}] = \mathbf{d}_t - 1 \quad \text{for} \quad \mathbf{d}_t > 0 \tag{1.30}$$

It is possible for the actual expected duration $\mathbf{d}_t$ to differ from the expected duration implied by the ZLB constraint and the structural shocks. A central bank can deliberately extend or reduce the expected duration of the ZLB through an intentional communication strategy. In the model, this type of unconventional monetary policy and the resulting deviations correspond to forward guidance. In order to determine the duration implied by forward guidance, I first follow the method of Jones et al. (2022b) and find the duration that corresponds to the underlying policy rule in each period t. This will be referred to as lower bound durations and denoted by $\mathbf{d}_t^{lb}$. With the occasionally binding constraint algorithm of Jones (2017) I identify the lower bound duration in each quarter t using the estimated smoothed state y_{t-1}, the smoothed structural shocks ε_t, and a given fixed interest rate regime.[18] In the absence of further shocks, the lower bound duration is expected to decrease by one quarter every period t:

$$E_t[\mathbf{d}_{t+1}^{lb}] = \mathbf{d}_t^{lb} - 1 \quad \text{for} \quad \mathbf{d}_t^{lb} > 0 \tag{1.31}$$

It is possible, however, to extend the expected durations of the ZLB beyond the constraint and structural shocks by using unconventional monetary policy in the form of forward guidance.[19] The share of the expected durations that cannot be explained by the lower bound duration is referred to as the *forward guidance duration*:

$$\mathbf{d}_t^{fg} \equiv \mathbf{d}_t - \mathbf{d}_t^{lb} \tag{1.32}$$

[18] A detailed description of the algorithm is provided in the technical appendix.

[19] In addition to providing insight into calendar-based forward guidance policies, the duration measure also offers insights into state-contingent forward guidance policies. When the central bank adopts a state-contingent forward guidance strategy based on macroeconomic indicators, the model implies a rational expectation path for each of these indicators. Whenever these expectations differ from those of the occasionally binding constraint, state-contingent forward guidance is equivalent to calendar-based guidance in the model.

In this way, forward guidance shocks capture unexpected changes in the forward guidance duration, $\Delta \mathbf{d}_t^{fg}$, beyond the anticipated one quarter decrease in each period. Consequently, a forward guidance shock in period t is defined as:

$$\varepsilon_t^{fg} = \begin{cases} \mathbf{d}_t^{fg} - \mathbf{d}_{t-1}^{fg}, & \text{if } \mathbf{d}_t^{lb} \geq 1 \\ \mathbf{d}_t^{fg} - \mathbf{d}_{t-1}^{fg} + 1, & \text{if } \mathbf{d}_t^{lb} = 0 \end{cases}$$

1.7.2 Identifying Forward Guidance

Figure 1.16 shows the (rounded) mean expected duration estimates of the ZLB as lower bound durations and forward guidance durations for the euro area based on the posterior estimates of the structural parameters and expected durations.[20]

Figure 1.16: Decomposition of Expected Duration Estimates

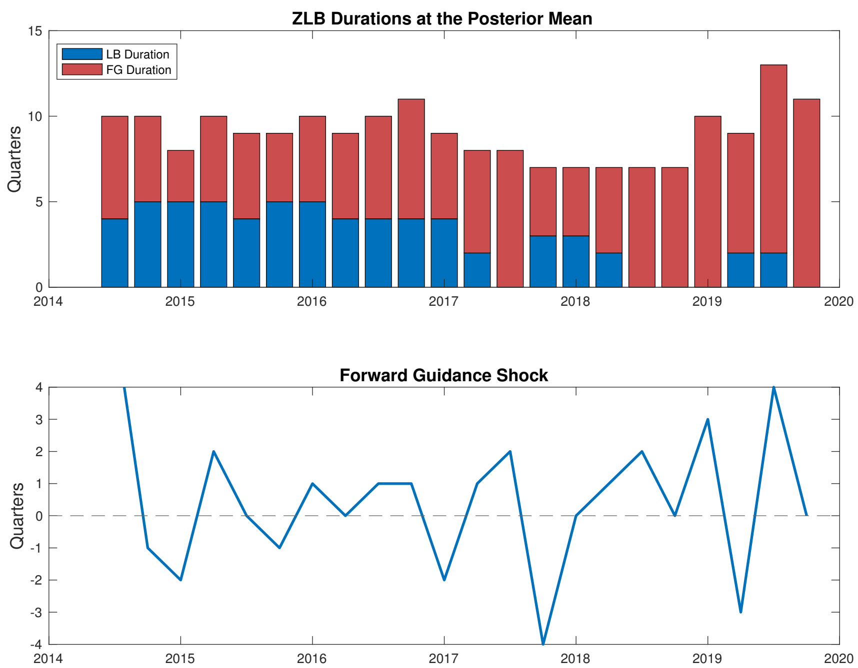

Note: The upper graph shows the decomposition of expected durations into *lower bound duration* and *forward guidance duration*. The lower graph shows the respective forward guidance shock over the sample period.

Approximately half of the total estimated duration, between 4 and 6 quarters, is accounted for by the lower bound duration within the first half of the ZLB period. Con-

[20]Note that, the fixed interest rate at the ZLB, $r_t = r$, changes from 0.05% to 0% in 2016 and hence the steady state value of the interest rate $-r$ as well.

sequently, forward guidance is assumed to account for the other half of the expected durations. Beginning in early 2017, forward guidance takes over and the lower bound durations disappear. Apart from two periods in 2018 and the peak of expected durations towards the end of the sample in 2019, the policy constraint itself is not binding in the second half of the ZLB period. This is supported by the forward guidance shock, depicted in the second graph in figure 1.16. When forward guidance assumes greater importance in the second half of the ZLB period, the forward guidance shock is largely positive. The increase in forward guidance durations, particularly from 2019 onwards, coincides with the ECB's shift to an *enhanced forward guidance* strategy in June 2018.[21]

1.7.3 Forward Guidance Dynamics

A change in the expected duration can have ambiguous effects on the real economy depending on its nature. Falling expected durations due to structural shocks can be expansionary, whereas shorter expected durations due to deliberate policy can be contractionary. In the non-linear model, the following GIRF illustrates the effects of the central bank deliberately reducing expected durations:

$$GIRF(N,\vartheta,\omega_{t-1}) = E[y_{t+N} \mid \vartheta,\mathbf{d},\omega_{t-1}] - E[y_{t+N} \mid \vartheta,\mathbf{d}^{10},\omega_{t-1}] \tag{1.33}$$

where $\mathbf{d}$ is the posterior mean estimate of the expected duration in a particular quarter. The computation follows that in section 1.6, except for a change to the expected duration. Suppose the central bank announces its liftoff after 6 quarters instead of 10 quarters as expected. Hence, consider a four-quarter reduction in the expected duration. This shock is similar to the *Taper Tantrum* exercise in KMR (2017). Since agents expect the policy rate to lift off sooner than they previously anticipated, their expectations about the direction of the policy rate change, and their optimization strategies change accordingly.

Similarly, if the central bank announces to keep the policy rate low for a longer period, the expected path of future interest rates will also be lower. The announcement will have

[21] The ECB's Governing Council adopted a more calendar-based approach by stating that key interest rates will not be increased for at least another year. In previous announcements, it was simply announced that interest rates were staying at their levels for an extended period of time.

Figure 1.17: Forward Guidance Dynamics

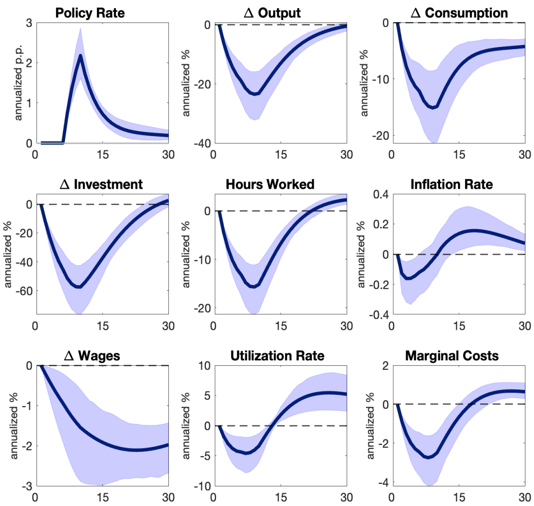

1.17.1 Decrease in d^e by 4 quarters and the equal-tailed 80% posterior interval.

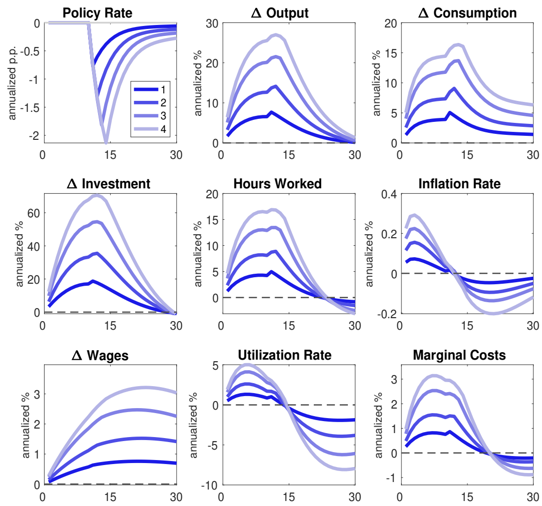

1.17.2 Increase in d^e by 1-4 quarters.

an expansionary effect on the economy, which effects increase the longer the extension is expected. The right panel of figure 1.17 plots the GIRFs for deliberate increases in expected duration by one quarter, two quarters, three quarters, and one year.

As agents expect the lift-off to occur later than expected. As a result, real variables expand on impact, and not when interest rates are raised. If the ZLB duration increases by one quarter, output and consumption increase by roughly 8% and 5%, and investment increases by 18%. An expected four-quarter duration shock, increases output by 27%, consumption by 16%, and investment by nearly 70%. With longer forward guidance extensions, these effects become more pronounced and are non-linear. For instance, increasing the expected duration by two quarters might not necessarily exhibit the same qualitative or quantitative effects as increasing expected duration by four quarters (Del Negro et al., 2012, Campbell et al., 2017). The overprediction of the expansionary effects of forward guidance announcements is a well-known phenomenon called *the forward guidance puzzle.*

Rational agents will base their optimal choices on their expectations about future policy. Thus, the path of endogenous variables, which is determined by backward induction, depends on these beliefs (e.g., Gibbs and McClung, 2023). The fixed interest rate period and expectations of active policy after liftoff create a feedback loop to inflation that leads to the large expansionary effects of real variables. The longer the interest rate is pegged, the stronger these effects become.

1.8 Conclusion

This chapter estimates a DSGE model for the euro area at the zero lower bound (ZLB). Monetary policy switches between a conventional policy regime in the form of a Taylor-type rule and an unconventional policy regime at the ZLB along with forward guidance. By expanding the information set of the model with survey expectations about the expected durations at the ZLB, following Kulish, Morley, and Robinson (2017), the structural parameters and a sequence of expected durations can be jointly estimated. Despite including a policy change for a significant part of the sample period in the well-known model of Smets and Wouters (2007), estimates for the structural parameters are consistent with previous literature. The estimates for the sequence of expected durations at the ZLB are robust against varying priors and financial market expectations in the form of forward curve durations. In addition, putting more weight on the survey measure improves estimation accuracy, reinforcing its significance. Compared to the US results by Kulish et al. (2017), the estimated durations are consistently longer and increase toward the end of the sample period. As a main contribution, this chapter provides a robust estimate of the expected durations at the ZLB in the euro area that can conveniently be incorporated in a wide range of model settings.

It appears that the ZLB's non-linear dynamics are largely determined by its expected length and nature. Furthermore, it is increasingly unconventional policy rather than the structural shocks that determine the duration of the ZLB in the euro area. Forward guidance, thus, extends the duration beyond the underlying policy rule, implying expansionary effects due to increases in expected duration caused by forward guidance announcements. The non-linearities at the ZLB substantially influence the model behavior and emphasize the role of forward guidance. At the ZLB, non-linear dynamics highlight the importance of estimating models with a reasonable measure of expected durations.

1.9 Chapter I Appendix

1.9.1 Additional Information on the Data

Figure 1.18: Investment Outliers

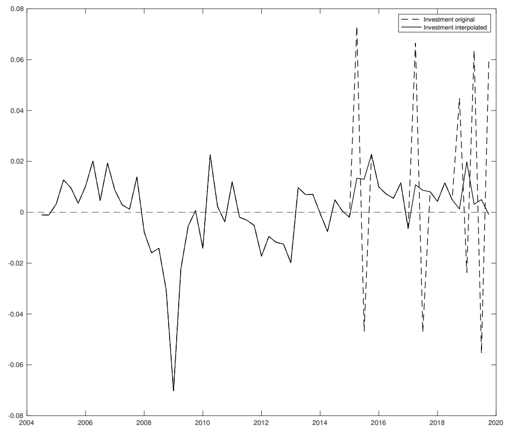

The figure shows the interpolated investment data from 2004:Q3-2019:Q4. Source: Eurostat

1.9.2 Further Results

Table 1.3: Summary of Expected Durations Estimates at Varying Weights

	Prior mean			Posterior mean					
Quarter	$\omega = 0$	$\omega = 0.5$	$\omega = 1$	$\omega = 0$	(std)	$\omega = 0.5$	(std)	$\omega = 1$	(std)
2014 Q3	9	9.89	10.77	10.20	4.63	10.46	4.58	11.27	4.10
2014 Q4	9	9.89	10.77	10.18	4.92	10.58	4.56	11.57	3.98
2015 Q1	9	9.17	9.34	8.34	4.86	8.48	4.36	9.01	4.11
2015 Q2	9	9.46	9.91	9.45	4.90	9.62	4.04	10.06	3.04
2015 Q3	9	9.06	9.13	9.67	4.70	9.25	3.94	9.36	2.89
2015 Q4	9	9.45	9.89	8.97	4.80	9.23	4.22	9.88	3.53
2016 Q1	9	9.34	9.69	10.55	4.94	10.41	4.12	10.77	3.23
2016 Q2	9	9.21	9.42	9.19	4.92	9.28	4.55	9.95	4.05
2016 Q3	9	9.57	10.13	10.49	4.59	10.47	4.35	11.09	3.86
2016 Q4	9	9.75	10.50	10.51	4.75	10.98	4.23	11.78	3.78
2017 Q1	9	10.81	12.62	8.12	4.60	9.27	4.79	11.31	4.36
2017 Q2	9	8.71	8.41	8.46	4.67	8.40	4.00	8.50	3.27
2017 Q3	9	8.33	7.66	8.96	4.51	8.35	3.55	7.93	2.31
2017 Q4	9	8.00	7.00	8.14	4.65	7.28	3.44	6.80	2.24
2018 Q1	9	7.69	6.38	8.36	4.60	7.00	3.34	6.31	1.76
2018 Q2	9	7.44	5.88	8.81	4.64	6.87	3.52	5.71	1.77
2018 Q3	9	7.47	5.93	8.37	4.48	6.71	3.30	5.79	1.45
2018 Q4	9	7.23	5.47	8.91	4.39	6.80	3.79	5.13	1.87
2019 Q1	9	7.23	5.46	12.2	4.10	10.08	4.65	7.20	3.86
2019 Q2	9	8.38	7.75	11.18	4.48	9.52	4.34	8.11	3.47
2019 Q3	9	10.03	11.06	13.35	3.30	12.99	3.32	13.06	3.08
2019 Q4	9	10.73	12.45	9.85	4.67	10.85	4.29	12.34	3.08

Note: The table summarizes the mean posterior estimates and standard deviations for the expected durations at different prior weights: $\omega = 0$ (uniform distribution), $\omega = 0.5$ (equally split), $\omega = 1$ (solely survey based).

Figure 1.19: Prior and Posterior Distributions of Expected Durations

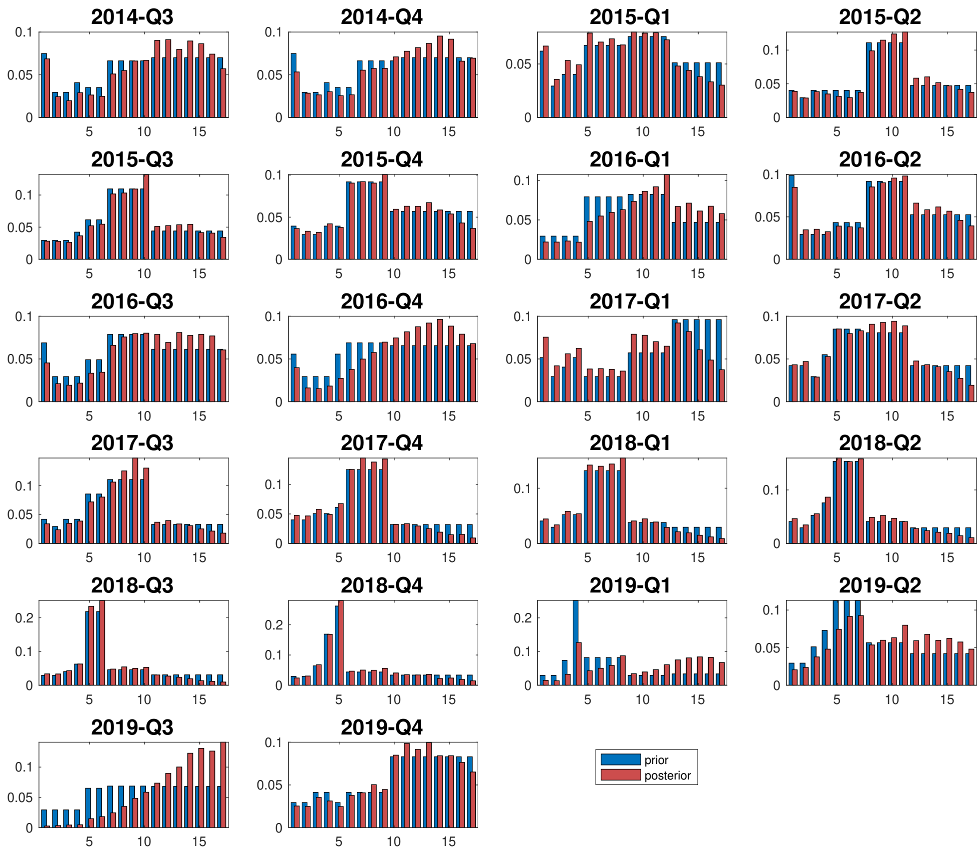

Note: The figure shows the marginal prior and posterior distributions of the expected durations throughout the sample period.

Table 1.4: Convergence Diagnostics Structural Parameters

Parameter		**R - Estimate**
Shock Standard Deviations		
Technology	σ^a	1.003
Risk premium	σ^b	1.010
Fiscal	σ^g	1.003
Investment	σ^{qs}	1.008
Monetary	σ^m	1.003
Price mark-up	σ^p	1.018
Wage mark-up	σ^w	1.008
1-year	σ^4	1.004
5-year	σ^{20}	1.003
Term premium	σ^η	1.034
Shock Persistences		
Technology	ρ^a	1.026
Risk premium	ρ^b	1.012
Fiscal	ρ^g	1.006
Fiscal technology	ρ^{ga}	1.006
Investment	ρ^{qs}	1.004
Monetary	ρ^r	1.009
Price mark-up	ρ^p	1.002
Wage mark-up	ρ^w	1.006
Term premium	ρ^s	1.007
Structural Parameters		
Investment Adj. Costs	φ	1.002
CRRA	σ^c	1.018
Habits	λ	1.001
Degree of Wage Stickiness	ξ_w	1.004
Elasticity of Labor Supply	σ^l	1.018
Degree of Price Stickiness	ξ_p	1.003
Indexation Wages	ι_w	1.006
Indexation Prices	ι_p	1.003
Capacity Utilization	ψ	1.005
Fixed Costs	ϕ_p	1.010
Monetary Policy: Inflation	ϕ_π	1.013
Monetary Policy: Smoothing	ρ_R	1.003
Monetary Policy: Output	ϕ_y	1.005
Monetary Policy: Output Gap	$\phi_{\Delta y}$	1.006
Constant Inflation	$\bar{\pi}$	1.001
Discount Factor	$\beta^{-1}-1$	1.001
Constant Labor	$\bar{l}$	1.002
Trend Growth	γ	1.001
Capital Share	α	1.006
Term Premium Constant	c_4	1.004
Term Premium Constant	c_{20}	1.001

Note: Chains have 500,000 draws, half of which is disregarded as burn-in. Values of R>1.2 indicate non-convergence.

Table 1.5: Convergence Diagnostics Expected Durations

Quarter	R - Estimate
2014 Q3	1.0004
2014 Q4	1.0005
2015 Q1	1.0002
2015 Q2	1.0000
2015 Q3	1.0006
2015 Q4	1.0001
2016 Q1	1.0000
2016 Q2	1.0003
2016 Q3	1.0000
2016 Q4	1.0002
2017 Q1	1.0002
2017 Q2	1.0002
2017 Q3	1.0007
2017 Q4	1.0003
2018 Q1	1.0000
2018 Q2	1.0002
2018 Q3	1.0001
2018 Q4	1.0001
2019 Q1	1.0005
2019 Q2	1.0006
2019 Q3	1.0003
2019 Q4	1.0005

Note: Chains have 500,000 draws, half of which is disregarded as burn-in. Values of R>1.2 indicate non-convergence.

1.9.3 Generalized Impulse Responses

Figure 1.20: Generalized Impulse Responses for the Investment-specific Technology Shock

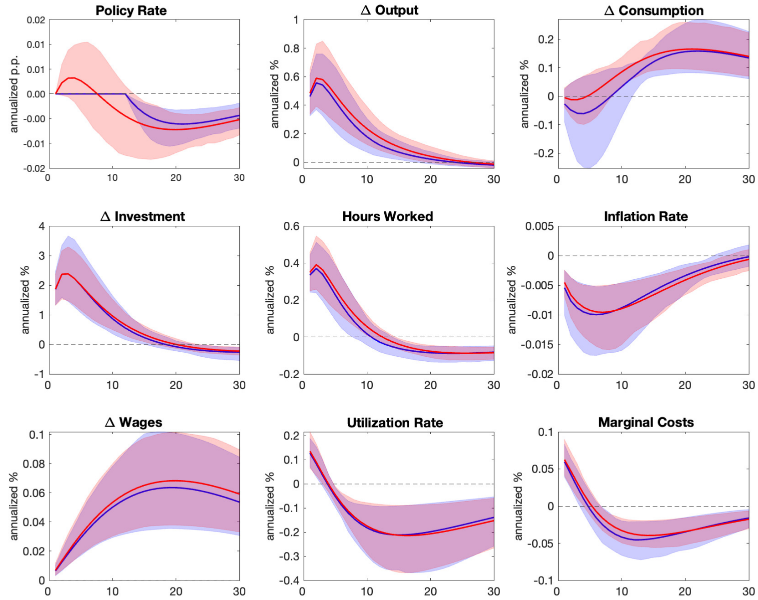

Note: GIRF for a positive investment-specific technology shock. Blue line: Duration=13 (2019-Q3), red line: Duration=1

Figure 1.21: Generalized Impulse Responses for the Price Mark-up Shock

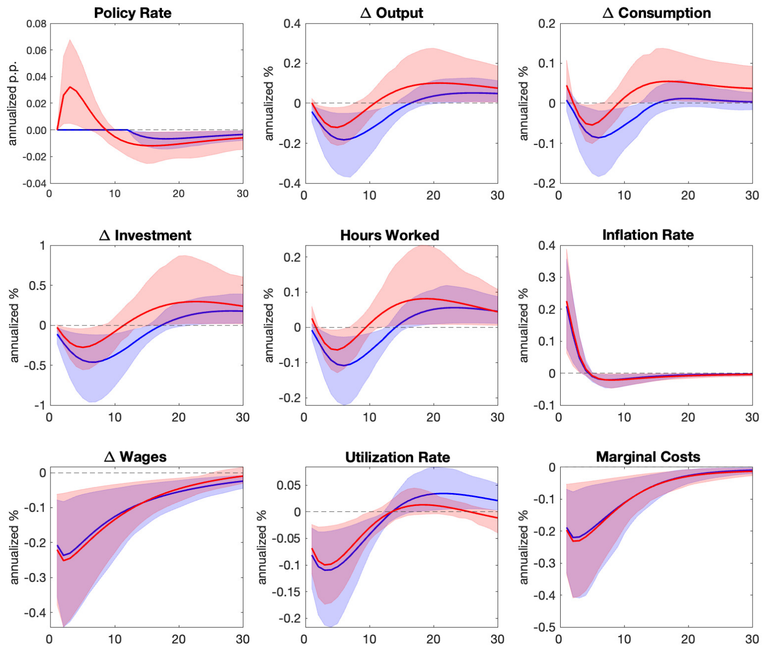

Note: GIRF for a positive price mark-up shock. Blue line: Duration=13 (2019-Q3), red line: Duration=1

Figure 1.22: Generalized Impulse Responses for the Risk Premium Shock

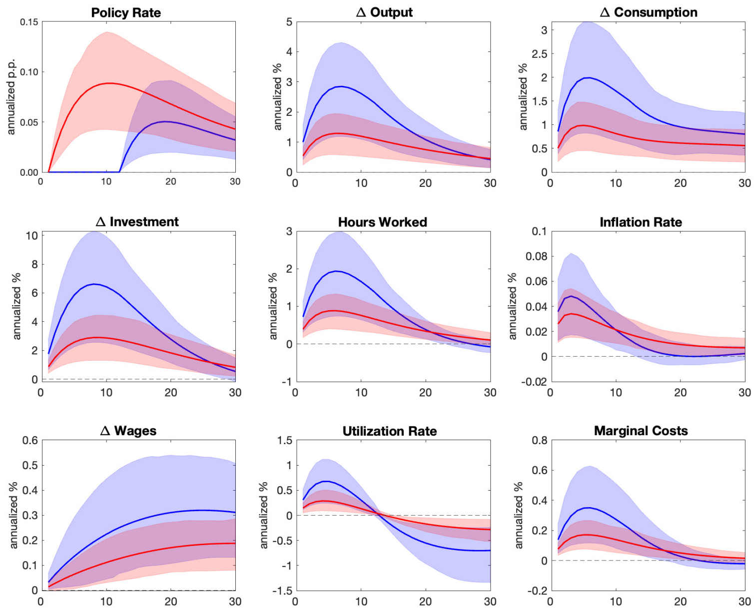

Note: GIRF for a positive risk premium shock. Blue line: Duration=13 (2019-Q3), red line: Duration=1

Chapter 2

The Effectiveness of Forward Guidance under Different Assumptions about the Nature of Liftoff

Abstract

The second chapter of this thesis investigates the impact of liftoff expectations on a structural New-Keynesian model of the euro area at the zero lower bound (ZLB). In particular, I use a sunspot solution to quantify the degree to which the effectiveness of forward guidance depends not only on the anticipated duration of the ZLB regime but also on expectations about the liftoff regime. I consider two possible monetary policy approaches to the liftoff regime: an active response to inflation and a passive response. I find that if the central bank is expected to be passive in responding to inflation following liftoff, forward guidance has relatively weaker effects on the economy, including deflationary pressures. A Bayesian model comparison also shows the sunspot solution to be marginally preferred by the data. These findings have significant implications for the design of monetary policy in a low interest rate environment and suggest that expectations regarding future monetary policy behavior can substantially impact the effectiveness of currently implemented policy measures.

2.1 Introduction

The European Central Bank (ECB) has maintained interest rates at a historically low level for an extended period of time. This type of fixed interest rate regime can constrain the central bank's ability to implement conventional monetary policy tools. As a result, the ECB has turned to unconventional policy measures, such as forward guidance, to influence market expectations and mitigate the impact of the zero lower bound (ZLB) on monetary policy efficacy. This chapter evaluates the effectiveness of unconventional monetary policy tools employed by the ECB during the extended period of low interest rates. In addition to examining how these policy tools affect inflationary and deflationary pressures within the economy, I will also quantify the effectiveness of forward guidance based on expectations about the interest rate path after lifting off from the lower bound.

Forward guidance is a monetary policy tool that involves the central bank making credible statements about the future path of the policy interest rate, which may differ from the path suggested by the underlying policy rule. In economic modeling, expectation formation plays a significant role in understanding unconventional monetary policy dynamics. In a rational expectation setting, agents base their decisions on all available market information. This can make the transmission mechanism of unconventional monetary policy, such as forward guidance, particularly powerful. The effectiveness of forward guidance as an unconventional monetary policy tool has been demonstrated by theoretical models in situations where the ZLB constraints the flexibility of interest rates (Krugman, Dominquez, and Rogoff, 1998, Eggertsson and Woodford, 2003). Nevertheless, the empirical evidence on forward guidance effectiveness remains ambiguous. Filardo and Hofmann (2014) find mixed evidence about the systemic effectiveness of forward guidance, although it can be used to reduce the volatility of near-term expectations. Del Negro, Giannoni, and Patterson (2012) argue that the impact of forward guidance depends on the specific type of guidance being implemented, and Campbell, Evans, Fisher, Justiniano, Calomiris, and Woodford (2012) show that the central bank's communication strategy and private sector expectations determine whether forward guidance is effective.

This chapter focuses not only on forward guidance regarding the duration of the fixed interest rate regime, but also on communication regarding the implementation of the regime following liftoff by the central bank. I demonstrate that in a forward-looking model with price rigidities, the effectiveness of forward guidance depends on both the length of the assumed pegged interest regime and expectations regarding monetary policy in the post-liftoff period. These findings are consistent with observations in real-world environments. While calendar-based forward guidance policies have been generally considered effective in the US (Campbell, Evans, Fisher, Justiniano, Calomiris, and Woodford, 2012, Feroli, Greenlaw, Hooper, Mishkin, and Sufi, 2017), open-ended forward guidance strategies have been less successful in the euro area and Japan despite long-expected durations (Gertler, 2017, Ehrmann, Gaballo, Hoffmann, and Strasser, 2019).

To solve the model at the ZLB, I adopt the backward induction solution strategy with the method of undetermined coefficients, as proposed by Kulish, Morley, and Robinson (2017), hereafter KMR (2017). With this approach, forward guidance can be incorporated into the estimation process by treating the expected durations at the ZLB as free parameters. These durations may exceed the durations indicated by the underlying policy rule, allowing for the adoption of a *lower for longer* policy. To avoid determinacy issues when the interest rate is pegged and does not adequately respond to changes in inflation, the solution strategy proposed by KMR (2017) relies on an active Taylor-rule liftoff regime. This regime is considered determinate if nominal interest rates react adequately to changes in inflation to prevent future inflation from becoming expectational. Consequently, a unique solution is determined by solving the model backwards through the structural equations. This introduces an additional expectation channel into the model.

It may, however, not be altogether unreasonable to deviate from the assumption that monetary policy follows an active Taylor rule upon liftoff. In their seminal work, Clarida, Gali, and Gertler (2000) demonstrate that prior to the Volcker era, monetary policy in the US was characterized by a passive approach towards inflation. Considering these historical occurrences, agents in the euro area may also regard passive policy as a feasible policy alternative after liftoff. Particularly because the long expected forward guidance durations toward the end of the sample period may not indicate that agents expect an immediate return to active policy. To accommodate a passive monetary policy liftoff regime, I deviate from the KMR (2017) solution strategy that relies on an active post-ZLB regime to deliver a unique and stable solution. Following Gibbs and McClung (2023), I generalize the KMR (2017) approach and incorporate a convenient sunspot solution based on Bianchi and Nicolò (2021), which allows for the possibility of an extended period of passive monetary policy after liftoff. This alleviates the restrictive constraints on monetary policy modeling that arise from the determinacy conditions, known as the *Blanchard and Kahn* conditions, that most solution algorithms impose. The simple augmentation expands the possibilities of regimes that can be considered at the ZLB, and importantly, does not interfere with the remaining structural parameters or expected durations.

Using the sunspot augmentation allows for the assumption that the central bank is conveying its intention to either revert to an active monetary policy regime or adopt a passive monetary policy upon liftoff. If the central bank announces its intention to implement an active Taylor-type monetary policy regime upon liftoff, the model exhibits significant expansionary forward guidance effects on the real economy. These effects become more pronounced as the expected durations of the ZLB constraint increase, a phenomenon referred to as *the forward guidance puzzle* (Del Negro, Giannoni, and Patterson, 2012). Conversely, when a central bank announces its intention to implement passive monetary policy upon liftoff, agents will form revised expectations based on the updated expected path of the policy rate. If agents expect that monetary policy will be passive after the end of the fixed interest rate regime, forward guidance is less effective, and the model exhibits deflationary pressures.

This emphasizes the importance of the liftoff regime when modeling the effects of forward guidance. When monetary policy is modeled to be active after the end of the fixed interest rate regime, this leads to an inflation reversal, in which inflation reacts immediately to forward guidance announcements (e.g., Gibbs and McClung, 2023). Under standard New-Keynesian price rigidities, if there is a certain degree of price indexation to lagged inflation, real variables such as output and inflation depend on previous periods (Carlstrom, Fuerst, and Paustian, 2015). The backward induction method creates a feedback loop for inflation that is enhanced by the degree of price stickiness in the model. If monetary policy is anticipated to be passive upon liftoff, the communication may have an effect similar to that of a forward guidance announcement. This may cause a reduction in market expectations of interest rates. Under rational expectations, this may result in a shift or flattening of the yield curve and a decrease in inflation expectations and subsequently a decline in actual inflation.

Finally, coordinating on a sunspot solution in the liftoff regime generates effects similar to introducing history dependence at the ZLB. History dependence has been demonstrated to be an effective way of reducing counterintuitive dynamics in models with fixed interest rate periods (e.g., Cochrane, 2017, Diba and Loisel, 2021, Gibbs and McClung, 2023, Kiley, 2016, among others). This chapter shows that in the sunspot equilibrium, puzzles such as the *fiscal multiplier puzzle* or *the paradox of toil* are alleviated in this model.

The remainder of the chapter is structured as follows. Section 2.2 discusses monetary transmission and expectation channels at the ZLB. Section 2.3 presents the solution strategy for the model. Section 2.4 discusses the estimation methodology. Section 2.5 presents the results. Section 2.6 identifies the role of the liftoff regime in forward guidance effects. Section 2.7 addresses well-known puzzles of New-Keynesian models at the ZLB. Section 2.8 compares the fit of the sunspot model to the benchmark model. Section 2.9 concludes.

2.2 Expectation Formation at the ZLB

In normal times, when the central bank is conducting conventional monetary policy by adjusting the nominal policy rate in response to changing external conditions, agents form their expectations based on the resulting anticipated path of the policy rate. In the context of a rational expectation equilibrium with full market information, this transmission channel becomes an especially powerful mechanism. With traditional monetary policy transmission mechanisms constrained, the expectation formation process at the ZLB is changing. When interest rates are pegged at a certain level, central banks may need to switch from traditional to unconventional monetary policy measures. Among them are forward guidance and general communication by the central bank. In this chapter, I will discuss how to channel expectations at the ZLB by communicating a lift-off monetary policy regime. However, given the close connection between the expected durations, the yield curve, and forward guidance, I will briefly discuss how they can function as unconventional transmission mechanisms for monetary policy when nominal interest rates are pegged.

2.2.1 Expected Durations and the Yield Curve

The yield curve is a commonly used tool for transmitting monetary policy signals to the markets. In normal times, the policy rate influences the level of the yield curve by affecting short- and long-term yields. At the ZLB, the ability to shape the yield curve is constrained when monetary policy is constrained. This results in an atypical transmission of monetary policy through the yield curve.

Although the policy rate has not been adjusted during this time period, it is worth noting that figure 2.1 reveals shifts in the yield curves in the euro area. Since the introduction of the 5bps lower bound, euro area yield curves have declined without corresponding changes in the nominal policy rate. It appears that factors other than the policy rate are influencing yield curve behavior.

Figure 2.1: Yield Curve Developments in the Euro Area over time

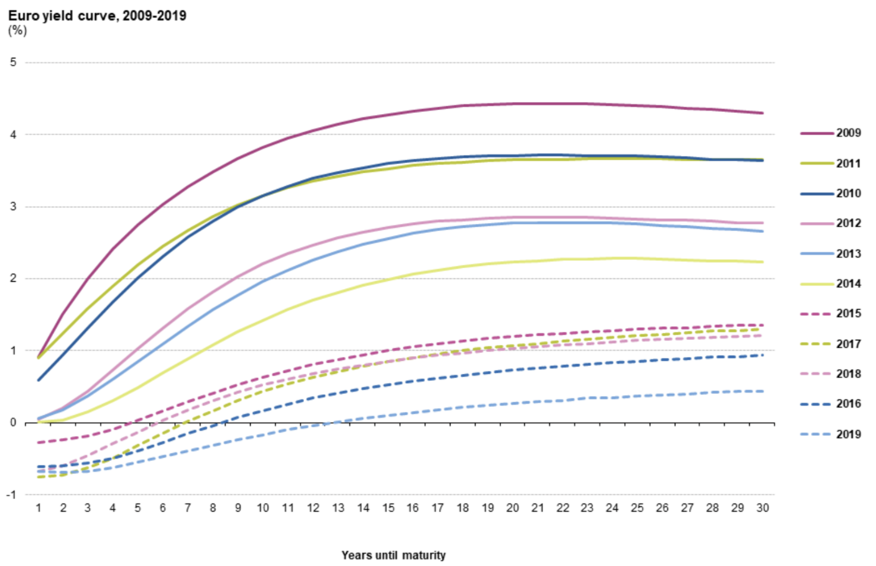

Note: Zero-coupon yield curve spot rate for AAA-rated euro area central government bonds at changing composition. Source: Published by ECB, Eurostat

This may be due to unconventional policies, such as forward guidance announcements, replacing conventional policies and causing a shift in the yield curve. According to Hanson and Stein (2015) and de la Barrera et al. (2017), forward guidance can influence the yield curve through credible announcements about the policy rate's future path if it is delivered credibly. Additionally, forward guidance can lower short-term interest rates, which prompts investors to shift to longer-term maturity investments without changing the interest rate path, ultimately resulting in a reduction in term premiums. Conversely, the yield curve may serve as a reliable indicator of forward guidance announcements and can be used to infer the expected duration of these announcements. From an empirical perspective, using yield curve data in estimation can provide more precise and robust estimates of expected durations, which will be treated as a free parameter in estimation.

In the model, agents make decisions based on how long they expect the interest rate to remain at zero. Central banks can influence these expected durations through unconventional monetary policy at the ZLB. The length of time the constraint is expected to remain in effect can be caused by either structural shocks or deliberate monetary policy actions. It is imperative to distinguish between these two concepts when determining the current stance of monetary policy. If interest rates are expected to remain low for an extended period of time due to the overall state of the economy, the effects are contractionary. Conversely, if the central bank increases expected durations through forward guidance announcements, it results in expansionary monetary policy. Therefore, the nature of the estimates of the expected duration of the fixed interest rate regime also reveals forward guidance in the model.

2.2.2 Forward Guidance

Forward guidance announcements refer to the central bank's communication about the expected future path of the policy rate. Early studies by Eggertsson and Woodford (2003) and Krugman et al. (1998) describe forward guidance as an additional channel of stimulating aggregate demand when the nominal policy rate is pegged. When a central bank communicates credibly that nominal interest rates will remain near zero for an extended period, the effects are similar to those of conventional expansionary monetary policy shocks. A clear communication strategy allows central banks to implement monetary policy more effectively by aligning with market expectations. A *lower-for-longer* policy reduces long-term yields, shifting the yield curve downward, which stimulates the economy and raises inflation. It is also possible, however, that a *lower-for-longer* policy may indicate a more negative economic outlook, which the central bank has more information about.

Campbell et al. (2012) formalize this distinction by distinguishing between *Odyssean* and *Delphic* forward guidance announcements. Delphic forward guidance pertains to monetary policy actions and forecasts of macroeconomic performance aimed at reducing market uncertainty and improving macroeconomic performance. By contrast, Odyssean forward guidance refers to policy commitments that alter agents' expectations about the future and bring the effects of a future policy action forward. Andrade et al. (2019) distinguish between announcements about macroeconomic conditions as Delphic and announcements about monetary policy as Odyssean and find that both shocks can lead to very different outcomes even though both lower the yield curve equally. In normal times, announcements of output or inflation forecasts can be seen as Delphic. When the central bank follows a specific Taylor-rule, forecasts about macroeconomic indicators will then influence expectations about future monetary policy actions.

In my framework, forward guidance at the ZLB is Odyssean in nature, in that it refers to announcements of the future path of the policy rate and not specifically to macroeconomic outcomes. Such forward guidance has been shown to have a significant expansionary effect in standard New-Keynesian models. However, some models tend to overestimate the impact of forward guidance announcements, a phenomenon identified by Del Negro et al. (2012) as the *forward guidance puzzle*. When the expected path of the policy rate is assumed to be fixed, the forward guidance puzzle arises if the response to an announcement about the future path of the policy rate over-predicts the large effects on inflation and output.

A key reason for this puzzle is that the transition from the economy of the future to the economy of today is not entirely smooth (Gibbs and McClung, 2023). When relying on backward induction to solve a linear rational expectation (LRE) model at the ZLB beliefs about monetary policy during and after the ZLB prevail and will be used to iteratively solve the structural equations from the end of the model period (Eggertsson and Woodford (2003) and Gibbs and McClung (2023)). It will take a large response in output and inflation to meet the desired path when the policy rate is pegged. Additionally, this shows a strong connection between forward guidance effects at the ZLB and monetary policy expectations after liftoff, which I will discuss in the next section.

2.2.3 Policy Expectations after Liftoff

An effective way of channeling expectations at the ZLB is to communicate a clear liftoff strategy. As discussed in the previous section, forward-looking models reflect agents' expectations about the future path of nominal interest rates, which affects monetary policy stance today. Therefore, when a central bank communicates a liftoff strategy, agents will adjust their expectations and behavior accordingly. In this chapter, I distinguish between two possible liftoff regimes: *active* and *passive* monetary policy.

Active Monetary Policy Active policy refers to an adjustment of the nominal interest rate by the central bank that exceeds the change in inflation it is responding to. It is a requirement of monetary policy rules to satisfy the *Taylor principle.* Using the *Fisher* equation, consider the relationship between nominal interest rate i_t, real interest rate r_t, and inflation rate π_t:

$$r_t = i_t - E_t(\pi_{t+1}) \tag{2.1}$$

In addition, consider monetary policy as a simplified Taylor rule, in which the central bank only reacts to inflation changes:

$$i_t = i_n + \phi_\pi \pi_t + \phi_y y_t \tag{2.2}$$

where i_n is the steady state level of the nominal interest rate and ϕ_π and ϕ_y are the response parameter to inflation and output respectively. When $\phi_\pi > 1$, a change in inflation triggers an even larger change in the nominal interest rate. It follows from the Fisher Equation that the real interest rate is also increasing. A rising interest rate can discipline inflation dynamics and pin them as a function of real interest rates.

Forward guidance policy has similar effects to conventional monetary policy when agents expect an active monetary policy regime after liftoff. An announcement that interest rates will remain low for an extended period will also delay the start of the active regime. This revised expectation of future policy will influence rational agents' current decisions, leading to an inflation reversal, with inflation rising in response to expansionary forward guidance announcements. During a period when interest rates are fixed, the expected delay of active policy after liftoff creates a feedback loop to inflation that intensifies the inflationary pressures on the economy. These effects are more pronounced the longer the ZLB is expected to remain in effect.

Passive Monetary Policy Passive policy refers to an adjustment of the nominal interest rate by the central bank by less than inflation. Forward-looking agents revise their decision-making process based on this updated information set. The expectation of passive monetary policy in the liftoff regime, which responds only slowly to changes in inflation, lowers market expectations of future interest rate adjustments. This shifts the yield curve downwards as in the active liftoff regime. However, a passive liftoff regime does not imply a feedback loop for inflation since inflation is not reacting on impact to forward guidance announcements. The inflation rate is not affected by these announcements as it reacts only to predetermined variables in the model.

When passive monetary policy is implemented determinacy problems may arise. Although the parameter space is intuitively and theoretically reasonable , the model may not have a unique and stable solution when monetary policy is passive after liftoff. In his proposed policy rule, Taylor (1993) argues that the inflation coefficient must be greater than one to provide a stable and unique solution to the model, a requirement that will become known as *Taylor principle*. If a central bank reacts strongly to inflation, the nominal interest rate will rise faster than inflation, leading to higher real interest rates. Conversely, when the central bank is less aggressive, the nominal interest rate increases less than inflation, resulting in a decrease in the real interest rate. In this case, changes in nominal interest rates cannot pin down inflation as a function of real interest rates. A decreasing interest rate while inflation increases will result in a spiral that leads to an exploding system with no unique solution. When inflation becomes expectational, the number of expectational variables does not match the number of explosive roots, violating *Blanchard and Kahn* conditions. These uniqueness problems, known as indeterminacy, occur if the number of unstable roots (eigenvalues > 1) is smaller than the number of non-predetermined variables. In this case, the forecast errors are not uniquely determined by the fundamental shocks in the model, but rather can be decomposed into a fundamental shock and a sunspot shock component (e.g., Lubik and Schorfheide, 2004). I will describe the implications and a solution strategy for the active and the passive case in the next section.

2.3 Solution Strategy

Traditional LRE solution strategies such as those by Sims (2002) or Binder and Pesaran (1995, 1997) are based on time-invariant structures, which means that a system's structural parameters remain constant over time. As a result, standard algorithms do not necessarily account for future (unanticipated) changes to the model structure. Therefore, I follow KMR (2017) and use the solution method by Cagliarini and Kulish (2013) and Kulish and Pagan (2017) to solve the model at the ZLB. In contrast to recently developed occasionally binding constraint algorithms such as those by Guerrieri and Iacoviello (2015) or Jones (2017), KMR (2017) is unique in that it chooses the sequence of durations that best fits the data, allowing for expected durations that are longer than the policy constraint. Due to this, the model is able to accommodate unconventional policies like forward guidance.

The KMR (2017) solution strategy relies on a determinate liftoff regime to avoid indeterminacy issues when interest rates are fixed and not responding sufficiently to inflation. For a liftoff regime to be determined, nominal interest rates must react enough to changes in inflation to prevent inflation expectations from becoming expectational. Consequently, monetary policy must be active after liftoff in order to obtain a unique and stable model solution. Consequently, the solution method cannot accommodate liftoff regimes that are passive or that do not conform to the Taylor Principle. Thus, following Gibbs and McClung (2023), I generalize KMR (2017) to account for different liftoff regimes such as passive monetary policy after liftoff and use a convenient sunspot solution derived from Bianchi and Nicolò (2021).

LRE models have a unique and stable solution if and only if the number of explosive roots equals the number of forward-looking variables. Indeterminate systems have fewer explosive roots. By using the Bianchi and Nicolò (2021) methodology, the missing explosive roots are augmented by additional autoregressive processes. In an active liftoff regime, the explosive root of the newly introduced autoregressive process is within a unit circle and is therefore not relevant to model dynamics. If monetary policy is passive after liftoff and the model is indeterminate, the sunspot solution produces the missing explosive root, and the solution is the same as in Lubik and Schorfheide (2003) under indeterminacy.

Figure 2.2: Policy after Liftoff

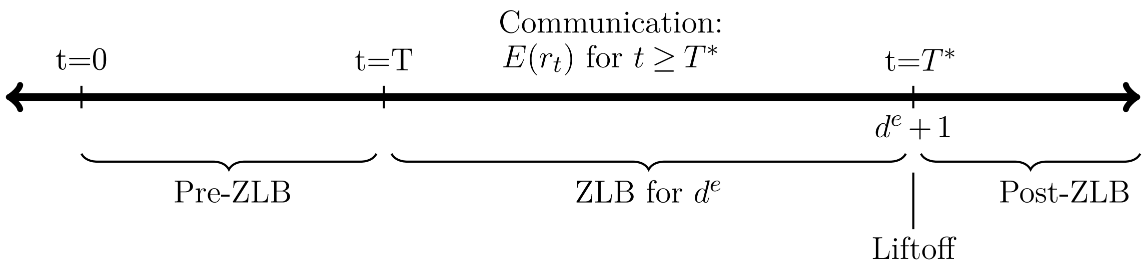

A visualization of the solution steps for the euro area DSGE model with a ZLB period can be seen in figure 2.2. From T to $T-1$, monetary policy follows its standard Taylor-type rule. At T, the central bank switches to a fixed interest rate regime that is expected to last for d^e periods. Because liftoff is not included in the sample period, it is considered an expected future event that occurs in period T^* or after d^e+1 periods. The central bank, however, communicates its liftoff strategy, that can either be active or passive, during the fixed interest rate regime. In addition, the central bank can provide forward guidance to influence the duration d^e. Therefore, deliberate announcements about the future path of the policy rate may delay or advance liftoff.

2.3.1 Time-Invariant Solution

In order to solve the LRE model, I employ the iterative approach proposed in Binder and Pesaran (1995, 1997) and applied in KMR (2017). This method provides a time-invariant solution that is applicable to all determinate monetary policy regimes. The rational expectation model is linearized around a non-stochastic steady state and can be expressed as follows:[1]

$$\underset{n\times n}{A_0}\ \underset{n\times 1}{y_t} = \underset{n\times 1}{C_0} + \underset{n\times n}{A_1}\, y_{t-1} + \underset{n\times n}{B_0}\, E_t y_{t+1} + \underset{n\times l}{D_0}\ \underset{l\times 1}{\varepsilon_t} \tag{2.3}$$

where y_t is the vector of endogenous variables with $k \leq n$ forward-looking variables. The vector of the l exogenous shocks in the model is denoted by ε_t. If all agents have rational expectations under a certain regime, then the only solution is a VAR of the following form:

$$y_t = C + Q y_{t-1} + G\varepsilon_t \tag{2.4}$$

where C, Q, and G are the rational expectation solution matrices of conformable dimensions. When expected future shocks are assumed to be zero, $E_t\varepsilon_{t+1} = 0$, the expected solution to the model in period t will be:

$$E_t y_{t+1} = C + Q y_t \tag{2.5}$$

Consequently, substituting equation 2.4 into equation 2.3 and rearranging terms delivers:

$$A_0 y_t = C + A_1 y_{t-1} + B_0[C + Q y_t + G E_t \varepsilon_{t+1}] + D_0\varepsilon_t \tag{2.6}$$

$$(A_0 - B_0 Q) y_t = C + A_1 y_{t-1} + B_0 C + D_0 \varepsilon_t \tag{2.7}$$

$$y_t = (A_0 - B_0 Q)^{-1}(C + A_1 y_{t-1} + B_0 C + D_0 \varepsilon_t) \tag{2.8}$$

[1] The following derivation of the Binder and Pesaran (1995, 1997) algorithm contains supplementary explanations and notations from Kulish and Pagan (2017), which support the understanding of the mathematical representation.

Rewriting $(A_0 - B_0Q)^{-1}$ as $(I - A_0^{-1}B_0Q)^{-1}A_0^{-1}$ and defining:

$$\Gamma \equiv A_0^{-1}C \qquad\qquad A \equiv A_0^{-1}A_1$$

$$B \equiv A_0^{-1}B_0 \qquad\qquad D \equiv A_0^{-1}D_0$$

Consequently, the system transforms to:

$$y_t = (I - A_0^{-1}B_0Q)^{-1}A_0^{-1}(C + A_1y_{t-1} + B_0C + D_0\varepsilon_t) \tag{2.9}$$

which can be further simplified to:

$$y_t = (I - BQ)^{-1}(\Gamma + BC + Ay_{t-1} - D\varepsilon_t) \tag{2.10}$$

Due to equation 2.10 being equal to equation 2.4, the following conditions can be derived:

$$(I - BQ)^{-1}(\Gamma + BC) = C \tag{2.11}$$

$$(I - BQ)^{-1}A = Q \tag{2.12}$$

$$(I - BQ)^{-1}D = G \tag{2.13}$$

Transforming equation 2.12 determines the solution for Q:

$$A - Q + BQ^2 = 0 \tag{2.14}$$

which can be solved for Q. Next, equation 2.11 can be transformed to:

$$C = \left[(I - (I - BQ)^{-1}B\right]^{-1}(I - BQ)^{-1}\Gamma \tag{2.15}$$

defining $\Lambda = (I - BQ)^{-1}\Gamma$ and $F = (I - BQ)^{-1}B$, equation 2.11 can be expressed as:

$$C = (I - F)^{-1}\Lambda \tag{2.16}$$

Therefore, once the solution for Q is found, C and G can be derived which completes the solution to the model.

2.3.2 Time-Varying Solution

By following KMR (2017), the solution to the model at the ZLB is obtained by a time-varying VAR system that depends on the expected duration of the fixed interest rate regime. In order to determine the solution during the ZLB period, consider the model representation as follows:

$$A_0^* y_t = C_0^* + A_1^* y_{t-1} + B_0^* E_t y_{t+1} + D_0^* \varepsilon_t \tag{2.17}$$

where A_0^*, A_1^*, B_0^*, C_0^*, and D_0^* are identical to the time-invariant case, except that the policy rule is fixed to some value instead of following a Taylor-rule. The solution to this model is the following time-varying VAR that depends on the expected length of the ZLB regime:

$$y_t = C_t + Q_t y_{t-1} + G_t \varepsilon_t \tag{2.18}$$

Assume that expected future shocks in period $t+1$ are zero, hence $E_t \varepsilon_{t=1} = 0$, implying that:

$$E_t y_{t+1} = C_{t+1} + Q_{t+1} y_t \tag{2.19}$$

By substituting equation 2.19 into equation 2.17 and following the same solution steps of the Binder and Pesaran (1995, 1997) algorithm as shown in the previous section, the following conditions can be derived:

$$(I - B^* Q_{t+1})^{-1} (\Gamma + B^* C_{t+1}) = C_t \tag{2.20}$$

$$(I - B^* Q_{t+1})^{-1} A^* = Q_t \tag{2.21}$$

$$(I - B^* Q_{t+1})^{-1} D^* = G_t \tag{2.22}$$

Since Q_t is now time-varying, its solution can be obtained via a backward recursion of equation 2.21:

$$A^* - Q_t + B^* Q_{t+1} Q_t = 0 \tag{2.23}$$

Obtaining the solution requires the following steps. Starting from the solution to the final structure $Q_{d+1} = Q$, choose sequence $\{Q_t\}_{t=T}^{d}$ such that equation 2.23 is satisfied. With this sequence one can determine the sequence $\{G_t\}_{t=T}^{d}$ and $\{C_t\}_{t=T}^{d}$ which completes the solution of the model. Kulish and Pagan (2017) derive the necessary conditions for the existence of a unique and stable final structure Q solution and include the existence and uniqueness of the sequence $\{Q_t\}_{t=T}^{d}$. Consequently, to guarantee a unique and stable solution, the Blanchard and Kahn (1980) conditions must be satisfied, and $(I - B_t Q_{t+1})$ must be of full rank. Equation 2.22 can then be written as:

$$\Lambda_t + F_t C_{t+1} = C_t \tag{2.24}$$

where $\Lambda_t = (I - BQ_{t+1})^{-1}\Gamma$ and $F_t = (I - BQ_{t+1})^{-1}B$. Once Q_t is found, C_t can be solved through a forward recursion of the form:

$$C_t = \Lambda_t + F_t \Lambda_{t+1} + F_t F_{t+1} \Lambda_{t+2} + ... \tag{2.25}$$

Therefore, at the ZLB the temporary solution of the model follows a time-varying VAR model based on the expected duration of the fixed interest rate regime. Kulish and Pagan (2017) and KMR (2017) show that the model has a unique solution when monetary policy is expected to return to its standard Taylor-type rule, or any other rule that satisfies the Taylor principle, in period T^*. Hence, I assume that when the central bank announces an active liftoff regime, the solution of the model will return to that presented in equation 2.4 which will hold in the indefinite future. However, when the central bank announces a passive liftoff regime, the standard KMR (2017) solution strategy cannot deliver a unique solution. In this case, I augment the system with a sunspot process that ensures its uniqueness even if the third regime itself is indeterminate.

2.3.3 The Sunspot Solution under Indeterminacy

One of the first algorithms to compute all indeterminate equilibrium sets was developed by Lubik and Schorfheide (2003). More recently, Farmer et al. (2015) or Bianchi and Nicolò (2021) propose methods of solving LRE model solutions under indeterminacy through sunspot solution techniques. A sunspot solution, proposed by Bianchi and Nicolò (2021) and further used in the ZLB context by Gibbs and McClung (2023), ensures a unique solution for an otherwise indeterminate model when allowing for an extended period of unconventional or passive monetary policy. A sunspot can be used to provide the missing explosive root to ensure a unique and stable solution.

Under indeterminacy, the term $I - BQ$ in equation 2.10 is not invertible and therefore, the solution derived before is not feasible. A LRE model has a unique and stable solution if and only if the number of unstable roots η_f, i.e., eigenvalues are larger than one, is equal to the number of forward-looking variables denoted by k. When the number of unstable roots is smaller than the number of forward-looking variables, $\eta_f < k$, the model has multiple solutions. The degree of indeterminacy is then defined by how many auxiliary equations are needed to guarantee a stable solution $m = k - \eta_f$. To obtain only one solution, I augment the system using a sunspot solution based on Bianchi and Nicolò (2021) and Gibbs and McClung (2023) that provides the necessary m roots:

$$s_t = \begin{pmatrix} \frac{1}{\varrho_1} & 0 & \dots & 0 \\ 0 & \frac{1}{\varrho_2} & \dots & 0 \\ \vdots & 0 & \ddots & \vdots \\ 0 & \dots & 0 & \frac{1}{\varrho_m} \end{pmatrix} s_{t-1} + \begin{pmatrix} x_{1,t} - E_t x_{1,t} \\ x_{2,t} - E_t x_{2,t} \\ \vdots \\ x_{m,t} - E_t x_{m,t} \end{pmatrix} - \begin{pmatrix} \nu_{1,t} \\ \nu_{2,t} \\ \dots \\ \nu_{m,t} \end{pmatrix} \tag{2.26}$$

where s_t is an autoregressive parameter that depends on parameter $\varrho < 1$ and the degrees of indeterminacy m. Sunspot shocks are denoted by$\nu = (\nu_1, \nu_2, ..., \nu_m)'$ and have a standard deviation σ^ν. The vector $x = (x_1 - Etx_1, x_2 - Etx_2, ..., x_m - Etx_m)'$ contains the one-period-ahead forecast error associated with the forward-looking variables that follow the sunspot process. Equation 2.26 is then added to the system given by equation 2.3 which delivers a revised canonical representation of the form:

$$A_0^s y_t^s = C_0^s + A_1^s y_{t-1}^s + B_0^s E_t y_{t+1}^s + D_0^s \varepsilon_t^s \tag{2.27}$$

The sunspot process is adding m additional auxiliary equations to the state vector, $y_t^s \equiv (y_t, x_t, s_t, E_t x_{t+1})$, and m additional exogenous shocks ν_t, such that $\varepsilon_t^s \equiv (\varepsilon_t, \nu_t)$. The sunspot is modelled as a separate block to the original model equations which transforms the solution matrices to:

$$A_0^s = \begin{pmatrix} I_{n-m} & 0_{n-m\times m} & 0_{n-m\times m} & 0_{n-m\times m} \\ 0_{m\times n-m} & I_m & 0_{m\times m} & 0_{m\times m} \\ 0_{m\times n-m} & -I_m & I_m & 0_{m\times m} \\ 0_{m\times n-m} & 0_{m\times m} & 0_{m\times m} & I_m \end{pmatrix} \quad C_0^s = \begin{pmatrix} C_{0y} \\ C_{0x} \\ 0_{m\times 1} \\ 0_{m\times 1} \end{pmatrix}$$

$$A_1^s = \begin{pmatrix} A_{1y} & A_{1yx} & 0_{n-m\times m} & 0_{n-m\times m} \\ A_{1xy} & A_x & 0_{m\times m} & 0_{m\times m} \\ 0_{m\times n-m} & 0_{m\times m} & \varrho_i^{-1} & -I_m \\ 0_{m\times n-m} & 0_{m\times m} & 0_{m\times m} & I_m \end{pmatrix}$$

$$B_0^s = \begin{pmatrix} B_{0y} & B_{0yx} & 0_{n-m\times m} & 0_{n-m\times m} \\ B_{0xy} & B_{0x} & 0_{m\times m} & 0_{m\times m} \\ 0_{m\times n-m} & 0_{m\times m} & 0_{m\times m} & 0_{m\times m} \\ 0_{m\times n-m} & I_m & 0_{m\times m} & 0_{m\times m} \end{pmatrix} \quad D_0^s = \begin{pmatrix} D_{0y} & 0_{m\times m} \\ D_{0x} & 0_{m\times m} \\ 0_{m\times l} & -I_m \\ 0_{m\times l} & 0_{m\times m} \end{pmatrix}$$

When the number of forward-looking variables equals the number of unstable roots, and hence $k = 0$, equation 2.27 is equal to the determinate system given in equation 2.3. However, under indeterminacy when $k > 0$, the solution is a VAR of the form:

$$y_t^s = C^s + Q^s y_{t-1}^s + G^s \varepsilon_t^s \tag{2.28}$$

where C^s, Q^s, and G^s are the solution matrices of conformable dimension in the liftoff regime. Solving this system can be carried out using the same steps as that for the time-invariant solution that is discussed in section 2.3.1.

When expected future shocks are zero, $E_t\varepsilon^s_{t+1} = 0$, and $E_t y^s_{t+1} = C^s + Q^s y^s_t$, substituting equation 2.28 into equation 2.27 and rearranging terms delivers:

$$y^s_t = (A^s_0 - B^s_0 Q^s)^{-1}(C^s + A^s_1 y^s_{t-1} + B^s_0 C^s + D^s_0 \varepsilon^s_t) \tag{2.29}$$

The system can be rewritten such that:

$$y^s_t = (I - B^s Q^s)^{-1}(\Gamma^s + B^s C^s + A^s y^s_{t-1} - D^s \varepsilon^s_t) \tag{2.30}$$

Now, the term $(I - B^s Q^s)$ is invertible and, thus, delivers the solution to an indeterminate liftoff regime which is given by the following three equations:

$$(I - B^s Q^s)^{-1}(\Gamma^s + B^s C^s) = C^s \tag{2.31}$$

$$(I - B^s Q^s)^{-1} A^s = Q^s \tag{2.32}$$

$$(I - B^s Q^s)^{-1} D^s = G^s \tag{2.33}$$

2.3.4 Inflation Sunspot Equilibrium

In the case of passive monetary liftoff regimes, the degree of indeterminacy is one, $m = 1$, therefore it is necessary to add one additional auxiliary equation. Following Gibbs and McClung (2023), I assume that inflation is the forward-looking variable associated with this equilibrium. Therefore, the sunspot process can be described as follows:

$$s_t = \varphi s_{t-1} + (\pi_t - E_{t-1}\pi_t) - \nu_t, \qquad \varphi \equiv \frac{1}{\varrho} \tag{2.34}$$

where φ is a 1×1 matrix, providing a single missing root when monetary policy is modeled actively with $\phi_\pi < 1$. Further, the sunspot is incorporated into all indeterminate systems, the fixed interest rate regime, and the passive policy regime after liftoff. Accordingly, the model's complete solution is as follows:

$$y_t = \begin{cases} C + Qy_{t-1} + G\varepsilon_t, & \text{for } t < T \\ \{C_t^s\}_{t=T}^d + \{Q_t^s\}_{t=T}^d y_{t-1} + \{G_t^s\}_{t=T}^d \varepsilon_t, & \text{for } T \leq t < T^* \\ C^s + Q^s y_{t-1} + G^s \varepsilon_t, & \text{for } T \geq T^* \end{cases}$$

As the solution depends on parameter φ, I choose parameter ϱ such that it guarantees a unique solution if and only if $\phi_\pi \leq 1$. A straightforward way to ensure so, is to set $\varrho \equiv \phi_\pi$.[2]

Table 2.1: Sunspot Solution

Case	Parameter Choice	Unique Solution
$\phi_\pi > 1$	$\frac{1}{\varrho} \equiv \frac{1}{\phi_\pi} < 1$	Sunspot inactive
$\phi_\pi \leq 1$	$\frac{1}{\varrho} \equiv \frac{1}{\phi_\pi} > 1$	Sunspot active

If the sunspot process is augmented to the system of equations, the solution depends on the parameter ϱ. When $\varrho > 1$, the sunspot process is stationary and has no impact as the LRE model solution does not depend on it. In this case, the law of motion for the variables is identical to the solution in the determinate model with active monetary policy. By setting $\varrho < 1$, the sunspot process becomes explosive and thereby provides the necessary unstable root to deliver a unique solution to the system. The Bianchi and Nicolò (2021) solution strategy provides the necessary explosive root under indeterminacy and maps the sunspot shock to forecast errors.

[2]To verify the robustness of this equilibrium, a series of exercises were conducted utilizing different hyperparameters. These exercises have provided support for the selection of this particular equilibrium by producing nearly identical results and dynamics across all estimations.

2.4 Methods

2.4.1 Model

The model is based on SW-07 and their earlier version for the euro area in SW-03, but incorporates adjustments to the monetary policy rule and yield curve as in KMR (2017). I incorporate yield curve information into the model economy to assist in identifying the monetary policy stance and thus expected durations at the ZLB. Households optimize over consumption and labor, which is differentiated by unions that hold some monopoly power over wages. Intermediate goods producers operate under monopolistic competition, whereas final goods producers operate in a perfectly competitive environment and purchase intermediate goods, transform and re-sell them back to households. Sticky prices in the goods and labor market are modeled à la Calvo (1983). A representation of the complete model, sticky and flexible wage economy, and the shock processes can be found in the technical appendix.

Modelling Liftoff As in KMR (2017), monetary policy operates in different regimes over time. In the first regime, pre-ZLB, monetary policy follows a standard Taylor rule as in SW-07. Once the monetary authority enters a ZLB regime in $t = T$, the nominal policy rate is set equal to zero. At the ZLB, the central bank communicates a liftoff strategy including a post-ZLB monetary policy regime from $t = d^e + 1$. Assuming the central bank announcements are credible, the expected duration of the ZLB in $t = T$ is given by d^e. The nature of the post-ZLB regime can be *active* or *passive* depending on the central bank's communication strategy.

Figure 2.3: ZLB in the euro area

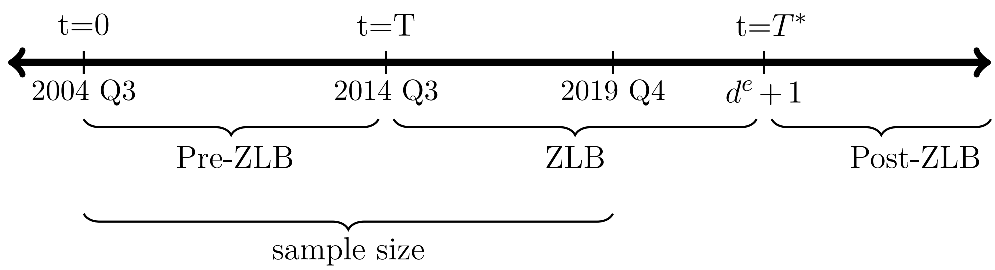

(I) Active Monetary Policy

When the central bank is responding strong enough to changes in inflation to change real interest rates, monetary policy is assumed to be *active*. Specifically, the central bank will communicate to revert to its initial Taylor-type regime after T^*. As shown in Cagliarini and Kulish (2013), the expectation of a final regime that satisfy the Taylor principle is sufficient to guarantee a stable and unique solution to a LRE model. The *active monetary policy* case will serve as the baseline scenario. and as in KMR (2017), the central bank reverts to its initial Taylor rule policy after liftoff:

$$\hat{r}_t \equiv \begin{cases} TR, & \text{for } t < T \\ -r, & \text{for } T \leq t < T^* \\ TR, & \text{for } t \geq T^* \end{cases}$$

where the Taylor rule (TR) is defined as the standard feedback rule in SW-07:

$$\hat{r}_t = \rho_R \hat{r}_{t-1} + \Big(1 - \rho_R\Big)\Big(\phi_\pi \hat{\pi}_t + \phi_y(\hat{y}_t - \hat{y}_t^f)\Big) + \phi_{\Delta y}\Big(\hat{y}_t - \hat{y}_{t-1} - (\hat{y}_t^f - \hat{y}_{t-1}^f)\Big) + \varepsilon_t^m$$

The policy rate adjusts to changes in inflation, denoted by ϕ_π, and changes in the output gap, denoted by ϕ_y. When monetary policy is active, the central bank reacts sufficiently to changes in inflation, such that the parameter ϕ_π is strictly larger than one. The output gap is defined as the difference between model-implied output and potential output, which is the output level that would be sustained in a flexible economy without wage or price stickiness. Furthermore, the policy rate adjusts to changes in the output gap, denoted by $\phi_{\Delta y}$. Finally, the parameter ρ_R determines the degree of interest rate smoothing and ε_t^m denotes a monetary policy shock that follows a first-order autoregressive process with an iid-normal error term.

(II) Passive Monetary Policy

The central bank declares that it will enter a passive monetary policy regime after liftoff and will be less responsive to changes in inflation. This liftoff regime then holds in the indefinite future:

$$\hat{r}_t \equiv \begin{cases} TR, & \text{for } t < T \\ -r, & \text{for } T \leq t < T^* \\ PR, & \text{for } t \geq T^* \end{cases}$$

The Taylor rule (TR) remains the standard feedback rule as defined in SW-07. Monetary policy in the passive post-ZLB regime (PR) continues to follow the feedback rule outlined in SW-07, albeit with updated parameter estimates including a response parameter for inflation which is now strictly smaller than one, $\phi^s_\pi < 1$:

$$\hat{r}_t = \rho^s_R \hat{r}_{t-1} + \left(1 - \rho^s_R\right)\left(\phi^s_\pi \hat{\pi}_t + \phi^s_y(\hat{y}_t - \hat{y}^f_t)\right) + \phi^s_{\Delta y}\left(\hat{y}_t - \hat{y}_{t-1} - (\hat{y}^f_t - \hat{y}^f_{t-1})\right) + \varepsilon^m_t$$

The Yield Curve Similar to KMR (2017), I include yield curve information to form expectations about the future path of the policy rate. The observed yield curve is then given as follows:

$$r_{j,t} = \hat{r}_{j,t} + r + c_j + \eta_t + \varepsilon_{j,t} \qquad for \;\; j = 2, 3, ..., m \tag{2.35}$$

where $\hat{r}_{j,t}$ represents the log deviation of the yield on a j^{th}-period bond from steady state and r is the steady state of the one period nominal interest rate. Since, c_j is a maturity-specific time-invariant component, $r + c_j$ can be interpreted as the steady state of a yield with j periods to maturity. The time-varying component to the term premium includes a persistent AR(1) shock η_t for all observed maturities:

$$\eta_t = \rho^\eta \eta_{t-1} + \varepsilon_{\eta,t} \tag{2.36}$$

2.4.2 Forward Guidance

By estimating the expected durations at the ZLB as free parameters to potentially exceed the underlying policy rule, the KMR (2017) solution strategy accommodates forward guidance. Recall the time-varying solution matrices at the ZLB:

$$y_t = C_t + Q_t y_{t-1} + G_t \varepsilon_t \tag{2.37}$$

The sequences $\{C_t\}_{t=T}^{d}$, $\{Q_t\}_{t=T}^{d}$, and $\{G_t\}_{t=T}^{d}$ are associated by the expected durations of the ZLB in each quarter. In estimation, d is chosen as the sequence that best fits the data which implies that durations can be longer than what is implied by the policy rule. Estimated durations can be divided into two parts: (1) durations arising from structural shocks and from the policy constraint (lower bound durations $\mathbf{d}_t^{lb}$); and (2) durations that result from deliberate policy decisions (forward guidance durations $\mathbf{d}_t^{fg}$):

$$\mathbf{d}_t = \mathbf{d}_t^{lb} + \mathbf{d}_t^{fg} \tag{2.38}$$

Without further shocks or policy announcements, expected durations $\mathbf{d}_t$ will decrease by one quarter every quarter. Therefore, an exogenous change in the expected durations $\mathbf{d}_t$ that exceeds the usual decline of one quarter, stems from forward guidance durations $\mathbf{d}_t^{fg}$.

This feature implies that the model's predicted duration estimates can either originate from structural shocks and the underlying policy rule or from a deliberate announcement of forward guidance. Thus, changes to the estimated expected duration at ZLB may have ambiguous dynamics. Following Jones (2017), an increase in expected durations due to structural shocks is contractionary, whereas an increase due to forward guidance announcements is expansionary. Because of forward-looking models, agents' expectations regarding the future path of nominal interest rates affect the current stance of monetary policy. Agents anticipate that interest rates will remain low for a longer period of time and, therefore, update their beliefs regarding the direction of the policy rate in the future. As such, in theory, forward guidance can serve as a stimulator to aggregate demand when interest rates are assumed to be *lower for longer* (Del Negro et al., 2012, Campbell et al., 2017). On the other hand, deteriorating economic conditions can also result in a *lower for longer* policy, which however, exhibits similar mechanisms to conventional contractionary monetary policy shocks. Whenever a central bank extends its ZLB beyond its policy rule to stimulate the economy, it creates an expansionary policy shock. In addition, the expected path of the future interest rate not only depends on the expected length of the ZLB but also on the monetary policy regime after liftoff.

2.4.3 Data

The model is estimated with Bayesian estimation techniques using nine observables from the euro area: log difference of real GDP, real consumption, real investment, and real wages, log and demeaned hours worked, log differences of the GDP deflator as the measure for inflation, the main refinancing operations (MRO) rate, and 1 and 5-year maturity bond yields. The first seven observables are constructed as in Smets and Wouters (2007). The additional two observables correspond to the yield curve augmentation in the model. The measurement equation is given as follows:

$$\begin{bmatrix} Y_t \end{bmatrix} = \begin{bmatrix} \Delta logGDP_t \\ \Delta logC_t \\ \Delta logI_t \\ \Delta logW \\ logH_t \\ \Delta log\pi_t \\ MRO_t \\ Y_t^4 \\ Y_t^{20} \end{bmatrix} = \begin{bmatrix} \bar{\gamma} \\ \bar{\gamma} \\ \bar{\gamma} \\ \bar{\gamma} \\ \bar{l} \\ \bar{\pi} \\ \bar{r} \\ \bar{r}+c^4 \\ \bar{r}+c^{20} \end{bmatrix} + \begin{bmatrix} y_t - y_{t-1} \\ c_t - c_{t-1} \\ i_t - i_{t-1} \\ w_t - w_{t-1} \\ l_t \\ \pi_t \\ r_t \\ r_t^4 \\ r_t^{20} \end{bmatrix}$$

where $\bar{\gamma}$ denotes the quarterly growth rate to GDP, consumption, investment, and wages. Moreover, $\bar{\pi}$ is the quarterly steady state inflation rate, $\bar{r}$ the steady state interest rate, and $\bar{l}$ the steady state hours worked. All real observables are presented in period-on-period log growth rates. The data used for the Euro area covers the period from $2004-Q3$ to $2019-Q4$. A detailed description of the data used is provided in the Data Appendix.

2.4.4 Priors and Posterior Sampler

The model equations are linearized around the steady state and cast into state-space form. As in KMR (2017), I jointly estimate the two sets of parameters: the structural parameters (θ) and the sequence of expected durations ($\mathbf{d}$). Priors for structural parameters are set according to SW-03, SW-07 and KMR (2017). Due to the inclusion of the Great Financial Crisis and the European Sovereign Debt Crisis in the sample period under consideration, I chose a looser prior for the standard deviations of the innovations. Five parameters are fixed in the estimation procedure, as in SW-07. The depreciation rate is set at 10% annually ($\delta = 0.025$ quarterly). The exogenous spending-GDP ratio is fixed at 0.18. The steady state labor market mark-up (λ_w) is set at 1.5, and the Kimball aggregators ε_p (goods market) and ε_w (labor market) are set at 10.

For the remaining parameters, the prior distribution is close to that set forth by SW-07 to facilitate comparisons with benchmark estimates. In accordance with KMR (2017), some parameters have been truncated not to enter an indeterminate parameter space. To ensure that the model solution falls within the determinate parameter space, I adjust the lower bound for the labor elasticity parameter to 0.5 (KMR (2017): 0.15) along with the common bounds for autoregressive parameters. The priors for the monetary policy rule parameters pre- and post-ZLB are based on those for the standard Taylor rule in SW-03 and SW-07.[3]

Table 2.2: Additionally Estimated Parameters in the Sunspot Model

Parameters	**Distribution**	**Prior**		**Description**
		Mean	**Std.**	
ϕ_π^s	Uniform	[0,1]		Monetary Policy Sunspot: Inflation
ρ_R^s	Beta	0.75	0.10	Monetary Policy Sunspot: Smoothing
ϕ_y^s	Normal	0.125	0.05	Monetary Policy Sunspot: Output Gap
$\phi_{\Delta y}^s$	Normal	0.125	0.05	Monetary Policy Sunspot: Output Growth
σ^ν	Inv Gamma	0.42	0.29	Standard deviation Sunspot

To estimate the model under indeterminacy, when monetary policy is passive, I introduce five additional structural parameters. The proposed Taylor rule in the second regime mimics the Taylor rule in the first regime, except for the inflation reaction parameter ϕ_π^s, which is strictly smaller than one. The prior for $\phi_\pi^s < 1$ follows a uniform distribution over

[3] A summary of all prior and posterior distributions can be found in table 2.3 in section 2.5.

the interval [0,1]. In contrast to Bianchi and Nicolò (2021), who use a uniform distribution over the interval [0,2], the prior used here ensures that the model under indeterminacy, maintains a passive monetary policy regime with an active sunspot process. The priors for the remaining Taylor rule parameters are the same as in the determinate case (compare table 2.2) and the sunspot standard deviation follows an inverse gamma distribution with a mean of 0.42 and a standard deviation of 0.29.[4]

The prior beliefs about the structural parameters $p(\theta)$ and about the expected durations $p(d)$ are updated conditional on the observed data points Z through the likelihood function and result in the joint posterior density $p(\theta, \mathbf{d} \mid Z)$:

$$p(\theta, \mathbf{d} \mid Z) \;\propto\; \mathcal{L}(Z \,|, \theta, \mathbf{d})\, p(\theta)\, p(\mathbf{d})$$

where $\mathcal{L}(Z \,|, \theta, \mathbf{d})$ is the marginal likelihood function of the determinate model. In the sunspot model, the system is augmented by a separate sunspot block s_t. The posterior density $p(\hat{\theta}(\theta, s_t), \mathbf{d} \mid Z)$ in the sunspot model is then given by:

$$p(\hat{\theta}(\theta, s_t), \mathbf{d} \mid Z) \;\propto\; \mathcal{L}(Z \,|, \hat{\theta}(\theta, s_t), \mathbf{d})\, p(\hat{\theta}(\theta, s_t))\, p(\mathbf{d})$$

As in KMR (2017), the sampler for the joint posterior of structural parameters and the sequence of expected durations of the ZLB is based on the tailored randomized block Metropolis–Hastings algorithm developed by Chib and Ramamurthy (2010).

2.5 Results

In this section, I compare the estimation results for the benchmark and the sunspot model. The benchmark model assumes active monetary policy after liftoff, and the sunspot model assumes passive monetary policy. Table 2.3 presents the posterior estimates of the structural parameters of both models.[5]

The sunspot model's structural parameter estimates are broadly in line with those of the

[4]The Taylor rule reaction parameters on output and the output gap are bound to be strictly positive to avoid dual-modal chains.

[5]A comprehensive discussion of the estimation strategy and the results for the benchmark model can be found in Chapter I of this thesis.

Table 2.3: Posterior Estimates of the Benchmark Model and the Sunspot Model

Parameters		**Prior**			**Posterior**					
					Determinate Model			**Sunspot Model**		
		Distribution	**Mean**	**Std. dev.**	**Mode**	**Mean**	**Std. dev.**	**Mode**	**Mean**	**Std. dev.**
Shock Standard Deviations										
Technology	σ^a	IG	0.42	0.29	0.66	0.66	0.05	0.65	0.67	0.04
Risk premium	σ^b	IG	0.20	3.00	0.15	0.16	0.01	0.17	0.18	0.01
Fiscal	σ^g	IG	0.42	0.29	0.50	0.51	0.03	0.50	0.51	0.02
Investment	σ^{qs}	IG	0.42	0.29	0.61	0.60	0.06	0.58	0.59	0.06
Monetary	σ^m	IG	0.20	3.00	0.30	0.30	0.01	0.29	0.30	0.01
Price mark-up	σ^p	IG	0.20	3.00	0.34	0.35	0.02	0.33	0.34	0.02
Wage mark-up	σ^w	IG	0.42	0.29	0.30	0.31	0.01	0.31	0.31	0.01
1-year	σ^4	U	1.00	0.58	0.34	0.39	0.1	0.22	0.35	0.34
5-year	σ^{20}	U	1.00	0.58	1.09	1.14	0.46	0.77	0.91	0.16
Term premium	σ^η	U	2.50	1.44	0.55	0.61	0.16	0.66	0.65	0.09
Sunspot	σ^ν	IG	0.42	0.29	-	-	-	0.37	0.38	0.03
Shock Persistences										
Technology	ρ^a	B	0.50	0.20	0.92	0.87	0.05	0.94	0.86	0.07
Risk premium	ρ^b	B	0.50	0.20	0.97	0.96	0.01	0.95	0.95	0.01
Fiscal	ρ^g	B	0.50	0.20	0.89	0.9	0.04	0.91	0.89	0.05
Fiscal technology	ρ^{ga}	N	0.50	0.20	0.51	0.5	0.08	0.49	0.50	0.07
Investment	ρ^{qs}	B	0.50	0.20	0.38	0.39	0.13	0.40	0.41	0.13
Monetary	ρ^r	B	0.50	0.20	0.24	0.22	0.08	0.23	0.25	0.09
Price mark-up	ρ^p	B	0.50	0.20	0.18	0.27	0.15	0.60	0.52	0.17
Wage mark-up	ρ^w	B	0.50	0.20	0.10	0.13	0.07	0.10	0.15	0.08
Term premium	ρ^s	B	0.71	0.16	0.97	0.95	0.03	0.97	0.95	0.03
Structural Parameters										
Investment Adj. Costs	φ	N	4.00	1.50	5.96	6.12	1.24	6.27	6.31	1.17
CRRA	σ^c	N	1.50	0.375	0.94	0.93	0.09	0.89	0.93	0.08
Habits	λ	B	0.70	0.10	0.74	0.74	0.05	0.77	0.75	0.04
Degree of Wage Stickiness	ξ_w	B	0.50	0.10	0.93	0.93	0.02	0.92	0.92	0.02
Elasticity of Labor Supply	σ^l	N	2.00	0.75	1.46	1.51	0.52	1.58	1.75	0.51
Degree of Price Stickiness	ξ_p	B	0.50	0.10	0.80	0.77	0.06	0.65	0.65	0.08
Indexation Wages	ι_w	B	0.50	0.15	0.39	0.39	0.13	0.35	0.35	0.12
Indexation Prices	ι_p	B	0.50	0.15	0.27	0.35	0.15	0.14	0.15	0.06
Capacity Utilization	ψ	B	0.50	0.15	0.59	0.62	0.12	0.55	0.60	0.12
Fixed Costs	ϕ_p	N	1.25	0.125	1.62	1.63	0.09	1.61	1.59	0.09
Monetary Policy: Inflation	ϕ_π	N	1.50	0.25	1.52	1.49	0.22	1.29	1.38	0.20
Monetary Policy: Smoothing	ρ_R	B	0.75	0.10	0.87	0.86	0.03	0.85	0.84	0.03
Monetary Policy: Output	ϕ_y	N	0.125	0.05	0.05	0.06	0.02	0.05	0.05	0.02
Monetary Policy: Output Gap	$\phi_{\Delta y}$	N	0.125	0.05	0.02	0.02	0.02	0.05	0.04	0.02
Constant Inflation	$\bar{\pi}$	G	0.63	0.10	0.51	0.51	0.06	0.55	0.56	0.06
Discount Factor	$\beta^{-1}-1$	G	0.25	0.10	0.22	0.2	0.07	0.14	0.18	0.07
Constant Labor	$\bar{l}$	N	0.00	2.00	3.71	3.85	0.96	3.78	3.67	0.86
Trend Growth	γ	N	0.40	0.10	0.24	0.25	0.03	0.22	0.22	0.03
Capital Share	α	N	0.30	0.05	0.26	0.26	0.02	0.25	0.26	0.02
Term Premium Constant	c_4	N	1.20	0.25	1.38	1.41	0.23	1.52	1.49	0.20
Term Premium Constant	c_{20}	N	2.35	0.25	2.10	2.09	0.21	2.03	2.02	0.22
Monetary Policy Sunspot: Inflation	ϕ^s_π	U	0	1	-	-	-	0.76	0.56	0.25
Monetary Policy Sunspot: Smoothing	ρ^s_R	B	0.75	0.10	-	-	-	0.74	0.74	0.10
Monetary Policy Sunspot: Output Gap	ϕ^s_y	N	0.125	0.05	-	-	-	0.21	0.21	0.04
Monetary Policy Sunspot: Output Growth	$\phi^s_{\Delta y}$	N	0.125	0.05	-	-	-	0.12	0.10	0.05

Chains have 500,000 draws, half of which is disregarded as burn-in. Moments are multiplied by 10^{-2}.
N= Normal Distribution; IG= Inverse Gamma Distribution; U=Uniform Distribution;
B= Beta Distribution; G=Gamma Distribution

benchmark model. Standard deviations for yield curve shocks are estimated to be lower than those in the benchmark model. Furthermore, differences can be observed for the price Phillips curve. The sunspot model exhibits a greater degree of price mark-up shock persistence than the benchmark model. During the extended period of passive monetary policy, the central bank only reacts sluggishly to inflation shocks, which in turn become more persistent. Furthermore, the price Phillips curve is estimated to be steeper in the sunspot model, with prices becoming more flexible ($\xi_p = 0.65$) than in the determinate model ($\xi_p = 0.77$). Passive monetary policy allows for larger inflation variability, which translates into a decrease in price stickiness. Finally, price indexation in the sunspot model ($\iota_p = 0.15$) is lower than in the benchmark model ($\iota_p = 0.35$).

Turning to the response functions of monetary policy. In the sunspot model, the post-ZLB monetary policy reacts passively to changes in inflation by construction. The mean of the post-liftoff inflation reaction parameter (ϕ_π^s) in the sunspot model is estimated to be 0.56 well below unity. The reduction in inflation response is compensated by reaction parameters for output growth (ϕ_Δ^s) and the output gap (ϕ_y^s). Moreover, the policy inertia in the passive liftoff regime is estimated to be smaller ($\rho_R^s = 0.74$) than in the benchmark model.

The expected duration estimates indicate that even though passive monetary policy is extended, the estimated expected durations of the ZLB period remain stable compared to the benchmark model. The upper plots in Figure 2.4 show the mean posterior estimates of the expected durations for the active and passive policy regimes, along with the corresponding 80% credible intervals and the prior mean, which is derived from a combination of survey measures and a uniform distribution. Generally, the credible intervals for passive liftoff regimes are narrower than those for active liftoff regimes, with a posterior mean that is closer to the prior and less volatile.

In the bottom plot the estimates from the determinate model are compared to those from the sunspot model and shows that agents' expectations regarding monetary policy do not significantly impact inferences about the expected duration of the policy regime. This suggests that even if the central bank engages in a prolonged period of passive monetary policy, the expected durations of ZLB regimes are unlikely to exhibit significant variability.

Figure 2.4: Expected Durations with Passive Policy after Liftoff

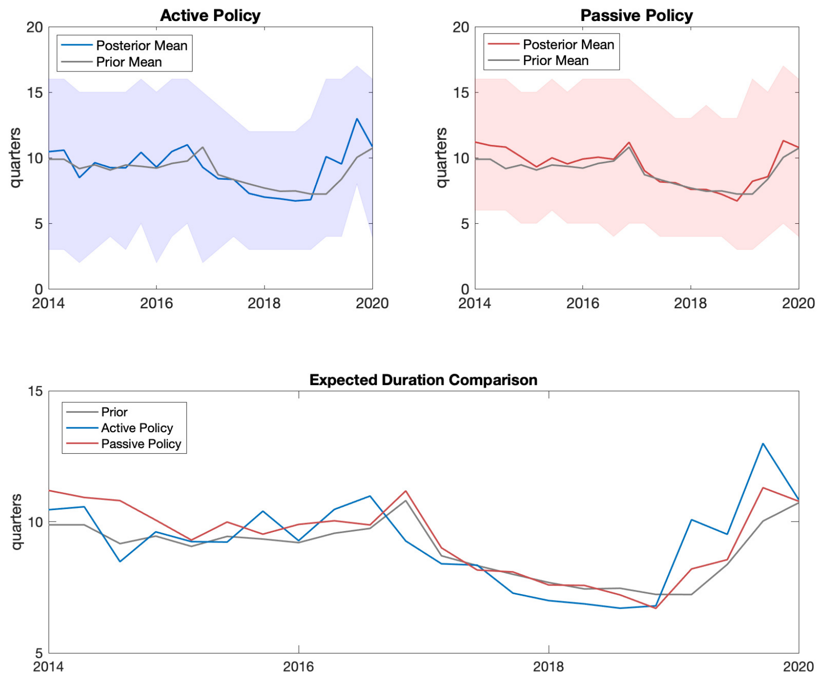

Note: The figure shows the mean prior, the mean posterior estimates for the active policy model and the durations when monetary is expected to be passive after liftoff at prior weights: $\omega = 0.5$

Turning to the the smoothed shock estimates presented in figure 2.9 in the appendix for Chapter II. It can be observed that the sunspot model exhibits a higher volatility for the mark-up shocks. This is not unexpected, as output and inflation are both forward-looking variables and are therefore linked to monetary policy. Intuitively, forward guidance reduces uncertainty and helps form expectations about future inflation. By reducing the inflation reaction parameter, the central bank is also allowing for more volatility in future inflation. When inflation is allowed to fluctuate, prices become less rigid, shifting the Phillips curve. This results in more pronounced fluctuations in mark-up shocks, and a higher degree of variability in the inflation and output levels.

2.6 Forward Guidance and Liftoff Expectations

Assuming that the central bank is not expected to return to an active monetary policy regime after liftoff, forward-looking agents update their beliefs about the future stance of monetary policy. The revised expectations significantly affect the effectiveness of current unconventional monetary policy. When agents expect the central bank to commit to passive monetary policy for an extended or indefinite horizon, the expansionary effects of forward guidance are less pronounced.

To demonstrate the different model dynamics, I simulate forward guidance announcements of one, two, three, and four additional quarters for the determinate model and the sunspot model. To analyze the forward guidance announcements in a regime-switching environment, I use the following generalized impulse response functions (GIRF) based on Koop et al. (1996):

$$GIRF(N, \vartheta, \omega_{t-1}) = E[y_{t+N} \mid \vartheta, \mathbf{d}, \omega_{t-1}] - E[y_{t+N} \mid \vartheta, \mathbf{d}^{10}, \omega_{t-1}] \tag{2.39}$$

The future shocks considered in this analysis are conditioned only on the model's steady state and are averaged out over time. Figure 2.5 compares the GIRFs for a deliberate increase in expected durations ($\mathbf{d}$). I simulate forward guidance shocks of one, two, three, and four quarters for the determinate model (left-hand plot) and the sunspot model (right-hand plot).

Figure 2.5: Forward Guidance Announcements under Different Liftoff Scenarios

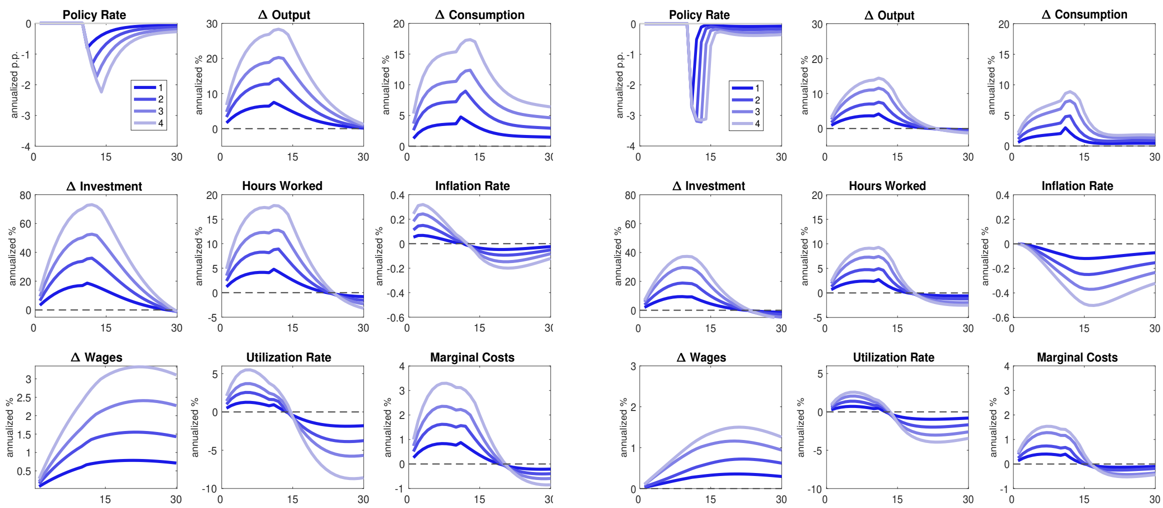

2.5.1 1-4 quarter increase in expected durations d with an active liftoff regime.

2.5.2 1-4 quarter increase in expected durations d with a passive liftoff regime.

A four-quarter increase in expected durations triggers an approximately 28% increase in output and a 70% increase in investment in the determinate model. In the sunspot model, the same increase results in a jump in output by close to 14% and a 35% increase in investment. Furthermore, while forward guidance inflates the economy when the central bank communicates a return to normalized monetary policy, it exhibits deflationary pressures otherwise.

2.6.1 Liftoff as Expectation Channel

Empirical evidence regarding the effectiveness of forward guidance in different settings has yielded inconclusive results. While theory predicts a strong efficacy of forward guidance (e.g., Krugman et al., 1998, Eggertsson and Woodford, 2003), empirical findings have been less consistent (e.g., Moessner et al., 2017, Filardo and Hofmann, 2014). Addressing this disconnect, Del Negro et al. (2012) and Campbell et al. (2012) emphasize the role of the type of forward guidance announcements, central bank communication, and the formation of private expectations in determining the effectiveness of forward guidance. Furthermore, the latter show that the effectiveness of forward guidance can be influenced by expectations regarding non-disclosed future economic conditions, which may not necessarily align with economic theory.[6]

By applying this logic to monetary policy expectations after liftoff, agents may assume that the central bank's commitment to the future regime is Delphic in nature, meaning that the central bank's undisclosed expectations about economic conditions do not seem promising. This explanation might not be sufficient, however, since effects on the real economy, except for inflation, are still consistent with an expansionary shock. However, it is worth noting that a passive monetary policy stance in the liftoff regime may lead to a decrease in market expectations for future interest rates. This can have a similar effect to forward guidance announcements, by prolonging the expected duration of lower rates and decreasing the term premium. As a result, this may manifest as a shift or flattening of the yield curve, decreasing expectations of future inflation, thus reducing actual inflation. Therefore, it is possible that expectations of a return to a passive monetary policy regime account for the relatively muted empirical effects of forward guidance in practice.

[6] Campbell et al. (2012) demonstrate that while news of monetary tightening raises interest rates, inflation forecasts also increase, whereas unemployment forecasts decrease.

2.6.2 Inflation Feedback Loop and the Phillips Curve

Another explanation may be the inflation feedback loop that is only prominent in a model with active policy after liftoff. In contrast, the coordination on a sunspot solution in the liftoff regime exhibits similar effects to introducing history dependence at the ZLB.

In the inflation-sunspot equilibrium, inflation expectations are no longer purely forward-looking in response to forward guidance announcements but are rather pre-determined (see Gibbs and McClung, 2023). Several papers have shown that introducing history dependence can anchor expectations at the ZLB and eliminates the New-Keynesian puzzles. Cochrane (2017) demonstrates that equilibrium selection at the ZLB can mitigate these puzzles, particularly those, which involve expectations of active fiscal policy and passive monetary policy. Alternatively, Kiley (2016) and Carlstrom, Fuerst, and Paustian (2015) show that sticky information models can resolve these paradoxes. Other papers, such as Diba and Loisel (2021), Gibbs and McClung (2023), and Cole (2018), propose the use of policy frameworks such as inflation targeting, price targeting, or endogenizing bank reserves as potential solutions to these challenges

The inflation-sunspot solution, while not incorporating history-dependent policy, can lead to similar effects by predetermining inflation expectations at the ZLB. Kiley (2016) shows that under a pegged interest rate regime, forward guidance effects are amplified by increased price flexibility and a steeper Phillips curve; the *paradox of volatility*. Furthermore, a forward guidance announcement leads to an inflation reversal when monetary policy is modeled actively in the liftoff regime, jumping on impact, and then turning negative, known as the *reversal puzzle*. Carlstrom et al. (2015) offer an explanation for this puzzle by showing that if there is a degree of inflation indexation, the relationship between lagged inflation and current inflation becomes endogenous at the ZLB. They demonstrate that in a model with inflation indexation, future inflation depends on past inflation, and past inflation depends on future inflation, resulting in a feedback loop that can amplify inflation fluctuations and create difficulty for policymakers.

This feedback loop is present in the model when monetary policy is active upon liftoff and it is amplified by the degree of price stickiness, as argued by Carlstrom et al. (2015).

In contrast, implementing passive monetary policy upon liftoff, can result in inflation outcomes that are not affected by forward guidance, therefore breaking the feedback loop.

Figure 2.6: Philips Curve Effects under Different Liftoff Scenarios

Active monetary policy after liftoff — Passive monetary policy after liftoff

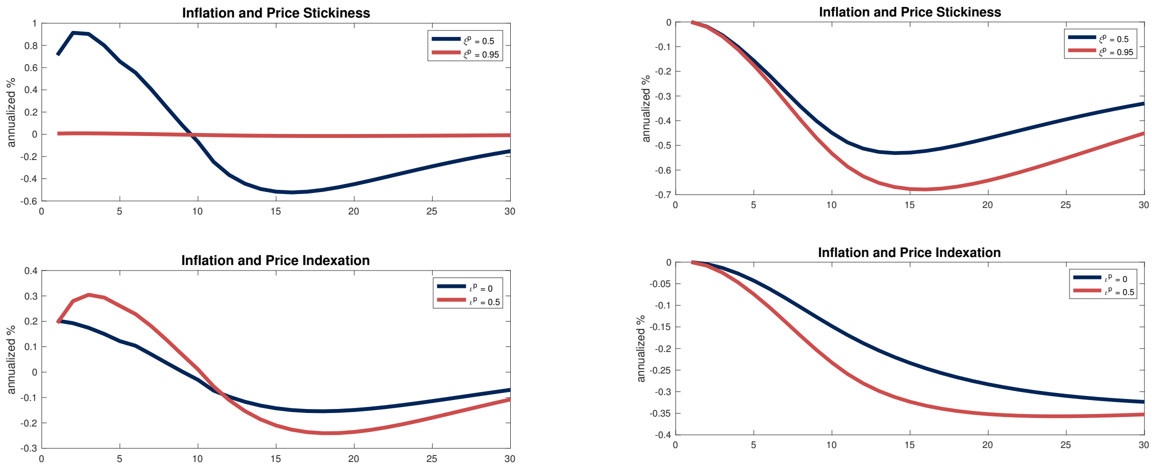

Note: The figure shows inflation responses to a 5-quarter increase in expected durations at different Phillips curve parameter values (price stickiness ξ_p and price indexation ι_p).

Figure 2.6 demonstrates that under passive monetary policy, inflation dynamics are less affected by price stickiness. The sunspot model also reveals that higher degrees of flexibility are associated with lower inflation responses. Central banks may respond less forcefully to inflation changes, allowing for more variability in price setting, and may be viewed as less committed to managing inflation as a result. This is supported by the estimation results, which confirm that the indeterminate model exhibits a steeper Phillips curve.

As agents incorporate these newly formed inflation expectations into their decision-making, forward guidance announcements become less expansionary. This highlights the significance of central bank signaling and communication in setting inflation expectations, particularly in the context of passive monetary policy.

2.6.3 Communication of the Central Bank

The results presented in this chapter suggest that the communication strategy employed by the central bank around what they will do in the liftoff period, as well as the type of forward guidance used, plays a crucial role in determining its effectiveness.

Forward guidance in this model appears to be more powerful when the central bank communicates its intention to return to an active monetary policy stance following liftoff. This finding is consistent with the varying experiences of different central banks with forward guidance, as well as the idea that implementing a clear communication strategy is essential for forward guidance to be effective.

While in the US calendar-based forward guidance was generally effective (Campbell et al., 2012, Feroli et al., 2017), forward guidance had only limited success in inflating the economy in Japan or the euro area despite having long expected durations at the ZLB. Gertler (2017) argues that, for Japan, the absence of an inflation target might explain why individuals have adaptive rather than rational expectations. However, this is not applicable in the euro area. Instead, ECB policy focused on an upper-bound asymmetric inflation target that might have prevented inflation expectations from rising. In addition, central banks in the euro area and Japan relied on an open-ended forward guidance strategy that does not clearly communicate a potential liftoff strategy. When comparing different types of forward guidance, Ehrmann et al. (2019) find that open-ended forward guidance increases uncertainty and maintains market responsiveness rather than reducing it.

The sunspot solution provides a theoretical basis for the distinction between passive and active monetary policy in relation to forward guidance effectiveness in this model. Based on these results, it is evident that a clear liftoff strategy is essential for the effective implementation of monetary policy at the ZLB in forward-looking models. A *lower for longer* policy may not be as effective in stimulating the economy when agents expect monetary policy to become less active in the future. The sunspot model appears to match the empirical experience of the relatively muted effects of forward guidance on inflating the economy, compared to what theory predicts in the determinate case. Overall, the results suggest that the interaction between forward guidance and agents' expectations about future monetary policy must be considered when evaluating the effectiveness of forward guidance at the ZLB and emphasize the importance of clear communication from the central bank in shaping expectations about future monetary policy actions.

2.7 Addressing New-Keynesian Puzzles at the ZLB

Similar to the absence of inflation feedback loop dynamics after forward guidance announcements, the sunspot equilibrium also mitigates other well-known puzzles at the ZLB. The coordination on a sunspot solution in the liftoff regime exhibits similar effects as introducing history dependence at the ZLB. History dependence was found to be an effective way of reducing counterintuitive dynamics in models with fixed interest rate periods (e.g., Cochrane, 2017, Diba and Loisel, 2021, Gibbs and McClung, 2023, Kiley, 2016, among others).

Among these puzzles is the *fiscal multiplier puzzle*. In the benchmark model, the fiscal spending multiplier, particularly on investment, becomes larger at the ZLB, the longer the constraint is expected to bind (e.g., Christiano et al., 2011, Cochrane, 2017). As output increases and wages fall, hours worked increase when the policy rate is fixed for an extended period. Investment increases when interest rates do not respond. Lifting the interest rate peg increases the policy rate marginally, accelerating a return to steady state.

Figure 2.7: Exogenous Spending Shock Dynamics under different Liftoff Regimes

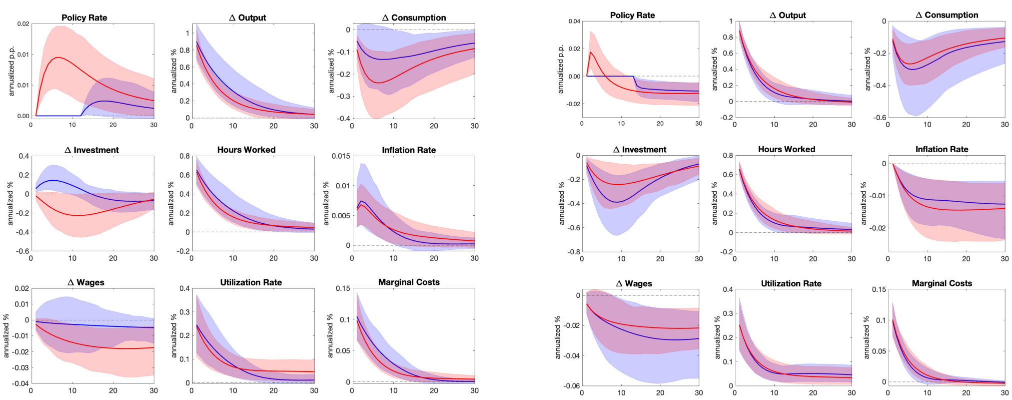

Note: GIRF for a positive spending shock in the Benchmark model (left panel) and the sunspot model (right panel). Blue line: initial duration=13, Red line: initial duration=1.

For two scenarios with different expected durations of the ZLB constraint, figure 2.7 shows a comparison of the impulse responses to a positive one-standard deviation exogenous spending shock in the benchmark model and the sunspot model. Investment increases when the interest rate remains fixed for an extended period of time in the benchmark model. While both models produce an approximately similar reaction to output following an exogenous spending shock, the sunspot model does not generate an increase in investment when the policy rate is fixed. Additionally, in the sunspot model, inflation does not rise on impact, but instead exhibits deflationary pressures on the economy. Inflation and investment responses differ significantly between the benchmark model and the sunspot model, emphasizing how agents' expectations about the duration and liftoff from the ZLB can influence monetary policy effectiveness.

In line with other papers in the literature, the sunspot model exhibits less expansionary effects to an exogenous spending shock, mitigating the fiscal multiplier puzzle. Modeling history dependence has shown to be an effective method of reducing counterintuitive puzzles at the ZLB. For example, Hills and Nakata (2018) demonstrate that including a lagged shadow policy rate in the interest rate feedback rule decreases the government spending multiplier at the ZLB. Kiley (2016) shows that the fiscal multiplier is smaller at the ZLB when considering a sticky information model, and Cochrane (2017) argues that the multiplier can also be small in an alternative backward-stable equilibrium. Finally, Cochrane (2017) and McClung (2021) show that active fiscal policy and passive monetary policy after liftoff can resolve puzzles at the ZLB. While the inflation-sunspot solution does not introduce history-dependent policy, it exhibits these effects by predetermining inflation expectations at the ZLB. Inflation expectations are no longer purely forward-looking in response to forward guidance announcements, but are predetermined (e.g., Gibbs and McClung, 2023). As a result, forward guidance announcements do not have a direct impact on inflation, and the economy is not experiencing inflationary pressures.

Similar dynamics can be observed for a wage mark-up shock. In the benchmark model the supply shock is subject to the *Paradox of Toil* (Eggertsson, 2010). A positive wage-mark-up shock increases real wages and raises inflation. If liftoff is modeled immediately, interest rates rise and the economy contracts. In contrast, when the interest rate is pegged

Figure 2.8: Wage Mark-up Shock Dynamics under different Liftoff Regimes

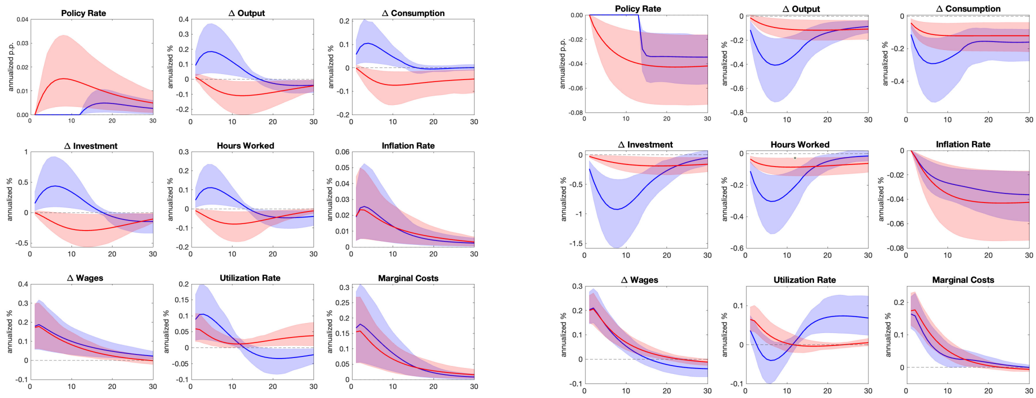

Note: GIRF for a positive wage mark-up shock in the Benchmark model (left panel) and the sunspot model (right panel). Blue line: initial duration=13, Red line: initial duration=1

the central bank cannot raise interest rates, which leads to expansionary shocks. As a result, the sunspot model exhibits contractionary effects in both scenarios. However, the effects are stronger when the ZLB is expected to bind for a longer period. Inflation does not increase on impact, but rather decreases gradually in response to other economic factors. Although shock effects may intensify with the expected length of the ZLB constraint, the sunspot model eliminates the reversal responses that occur in the benchmark model when the interest rate is fixed. The results are consistent with those of Gibbs and McClung (2023), who formally show how the sunspot solution alleviates New-Keynesian puzzles at the ZLB.

2.8 VAR Comparison

In this section, I conduct a performance comparison between the benchmark model and the sunspot model using the same dataset. To assess the goodness-of-fit of each model, I calculate the log of the marginal data density (MDD) using the modified harmonic mean estimator proposed by Geweke (1999). By comparing the MDD of the two models, it is possible to determine which model provides a better fit to the data. Starting from Bayes' Identity it follows that:

$$p(\theta \mid y) = \frac{p(y \mid \theta)p(\theta)}{p(y)}$$

where $p(\theta \mid y)$ is the probability density function (pdf) for θ conditional on the observations y or the posterior density. $p(y)$ is the marginal likelihood or data density, $p(y \mid \theta)$ is the likelihood function for the model, and $p(\theta)$ is the marginal pdf for θ, commonly referred to as the prior density. Rearranging delivers the marginal data density (MDD):

$$\frac{1}{p(y)} = \frac{1}{p(y \mid \theta)p(\theta)} p(\theta \mid y)$$

Multiplying both sides by a pdf $f(\theta)$ and integrating over θ delivers the modified harmonic mean estimator:

$$p(y) = \left[\frac{1}{G}\sum_{g=1}^{G} \frac{f(\theta)}{p(Y \mid \theta)p(\theta)}\right]^{-1}$$

Geweke (1999) then proposes to set $f(\theta)$ to be an approximation to the posterior density, but to truncate its tails at some value τ. I initially set τ equal to 0.9 and later reduce it to 0.5. The log-MDD marginally supports the sunspot model indicating a slightly better fit respective to the benchmark model in both cases. To further check for robustness, the root

Table 2.4: Model Comparison

	Benchmark Model	Sunspot Model
RMSE	0.0247	0.0155
MDD ($\tau = 0.9$)	2122.8	2125.5
MDD ($\tau = 0.5$)	2122.5	2125.5

mean squared error (RMSE) for the point prediction in each model is also calculated. This additional metric provides insight into their relative performance and helps to substantiate or refute any conclusions drawn from the comparison of the log MDD. The point prediction is the mean of the corresponding predictive distribution, where $\hat{y}_{t+1|t}$ denotes the one-step-ahead forecast value for the state vector. The RMSE for the point prediction is then calculated according to:

$$\text{RMSE}(\hat{y}_{t+1|t}, y_t) = \sqrt{\frac{1}{T-1}\sum_{t=1}^{T-1}(y_t - \hat{y}_{t+1|t})^2}$$

According to the results obtained, the sunspot model appears to perform marginally better, as indicated by a smaller RMSE. The RMSE is commonly used to measure forecast accuracy, where a smaller RMSE indicates a lower forecast error. Thus, the sunspot model has a smaller RMSE than the benchmark model, which implies that it provides a marginally better forecast.

2.9 Conclusion

In this chapter, I investigate the role that expectations about the monetary policy trajectory play in shaping the dynamics of forward guidance when interest rates are constrained by the zero lower bound (ZLB). For that, I extend the approach of Kulish et al. (2017) by following Gibbs and McClung (2023) and introducing a sunspot solution, as proposed by Bianchi and Nicolò (2021), which accounts for the possibility that the central bank does not follow its original Taylor rule upon liftoff but implements passive monetary policy. In this case, the central bank reacts only sluggishly to changes in inflation. I find that this sunspot solution does not significantly impact the estimates of structural parameters or the expected duration of the ZLB period. However, it reduces forward guidance effects on real variables such as output or investment. In particular, when agents expect a passive monetary policy regime upon liftoff, an increase in the expected duration of the ZLB period in the sunspot model can significantly dampen the expansionary effects on the real economy and even lead to deflationary pressures in a forward-looking model.

These results emphasize the importance of considering the liftoff regime when modeling the effects of forward guidance. A rational expectation model that incorporates New-Keynesian features results in a reversal of inflation once monetary policy has been actively modeled after liftoff (Carlstrom et al., 2015, Gibbs and McClung, 2023). This feedback loop for inflation is further amplified by the degree of price stickiness. Similarly, if monetary policy is expected to be passive following liftoff, communicating this expectation can have similar results to forward guidance announcements, resulting in lower expected interest rates in the market and a flattening of the yield curve. This, in turn, can reduce inflation expectations and lead to lower inflation.

Finally, the coordination on a sunspot solution in the liftoff regime exhibits similar effects as introducing history dependence at the ZLB. History dependence has been demonstrated to be an effective method of reducing counterintuitive dynamics in models with fixed interest rate periods (e.g., Cochrane, 2017, Diba and Loisel, 2021, Gibbs and McClung, 2023, Kiley, 2016, among others). I demonstrate that in this model, puzzles such as the fiscal multiplier puzzle and the paradox of toil are mitigated in a sunspot equilibrium.

2.10 Chapter II Appendix

Figure 2.9: Kalman Smoothed Structural Shock Comparison

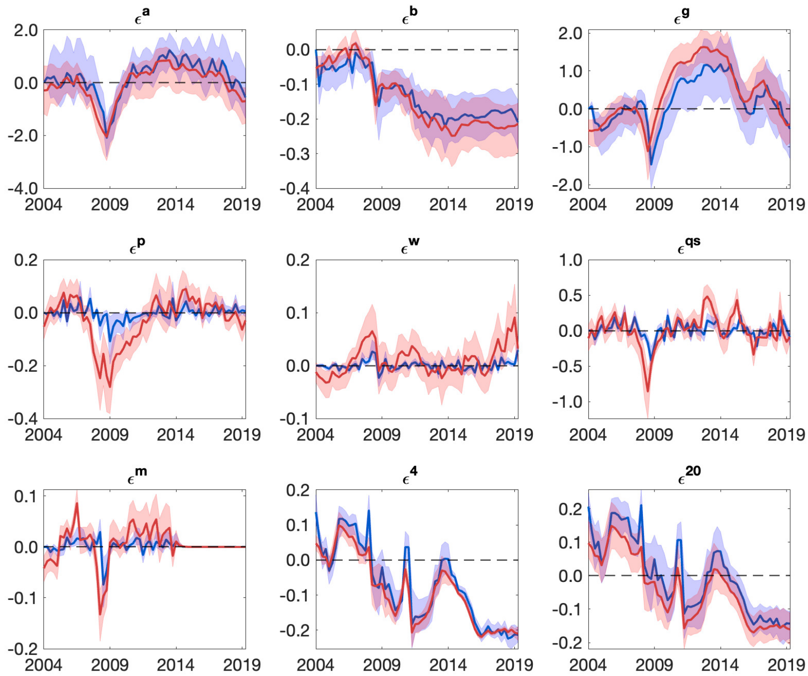

Note: The figure plots a simulated Kalman-smoothed time series for the shock processes for the determinate (blue) and the sunspot model (red): ε_t^a (technology), ε_t^b (risk premium), ε_t^g (exogenous spending), ε_t^p (price mark-up), ε_t^w (wage mark-up), ε_t^{qs} (investment-technology), ε_t^m (monetary policy), ε_t^4 (1Y Term Premium), and ε_t^{20} (5Y Term Premium), using 100 randomized posterior MCMC draws $th\hat{e}ta_j$, and the equal-tailed 80% posterior bands.

Table 2.5: Estimated Expected Durations for the Benchmark and the Sunspot Model

	Prior		Posterior					
			Active Liftoff Regime			Passive Liftoff Regime		
Quarter	Mean	Std. Dev.	Mean	Mode	Std. Dev.	Mean	Mode	Std. Dev.
2014 Q3	9.89	10.77	10.46	12	4.58	11.20	8	3.72
2014 Q4	9.89	10.77	10.58	14	4.56	10.93	7	3.84
2015 Q1	9.17	9.34	8.48	9	4.36	10.81	9	3.47
2015 Q2	9.46	9.91	9.62	11	4.04	10.07	8	3.53
2015 Q3	9.06	9.13	9.25	10	3.94	9.30	8	3.62
2015 Q4	9.45	9.89	9.23	9	4.22	9.99	8	3.65
2016 Q1	9.34	9.69	10.41	12	4.12	9.53	6	3.86
2016 Q2	9.21	9.42	9.28	11	4.55	9.90	8	3.74
2016 Q3	9.57	10.13	10.47	13	4.35	10.04	7	4.11
2016 Q4	9.75	10.50	10.98	14	4.23	9.88	6	4.53
2017 Q1	10.81	12.62	9.27	13	4.79	11.18	13	4.01
2017 Q2	8.71	8.41	8.40	10	4.00	9.01	6	3.72
2017 Q3	8.33	7.66	8.35	9	3.55	8.16	5	3.69
2017 Q4	8.00	7.00	7.28	7	3.44	8.09	6	3.40
2018 Q1	7.69	6.38	7.00	8	3.34	7.59	5	3.50
2018 Q2	7.44	5.88	6.87	5	3.52	7.58	6	3.69
2018 Q3	7.47	5.93	6.71	6	3.30	7.21	5	3.56
2018 Q4	7.23	5.47	6.80	5	3.79	6.70	5	3.75
2019 Q1	7.23	5.46	10.08	4	4.65	8.20	4	4.96
2019 Q2	8.38	7.75	9.52	7	4.34	8.56	5	4.33
2019 Q3	10.03	11.06	12.99	17	3.32	11.30	15	4.54
2019 Q4	10.73	12.45	10.85	13	4.29	10.79	14	4.34

Note: The table summarizes the mean posterior estimates and standard deviations for the expected durations for the active liftoff and passive liftoff models.

Chapter 3

A Time-Series Approach to Estimating DSGE Models with Covid-19 Data

Abstract

This chapter proposes a time-series approach to handling extreme data outliers such as those observed during the Covid-19 pandemic when estimating Dynamic Stochastic General Equilibrium (DSGE) models. Without changing the structural equations of a model, three adjustments can be made to the estimation procedure: A time-varying variance-covariance matrix to capture changes in shock variances, an ARMA(1,1) correction for TFP shock innovations, and a Kalman filter measurement correction for consumption data. Results show robust estimates for structural parameters for a standard DSGE model of the euro area. Because the Covid-19 pandemic occurred at a time when the zero lower bound was in effect, this estimation approach also provides insight into the expansionary monetary policy stance during the pandemic, including in terms of a structural shadow rate measure.

3.1 Introduction

The Covid-19 pandemic has had a significant impact on the euro area, resulting in a contraction that exceeds the effects of both the Great Financial Crisis and the Sovereign Debt Crisis. Unlike these earlier crises, the Covid-19 contraction was primarily caused by supply and demand restrictions, such as lockdowns and social health measures, rather than structural issues. The Covid-19 shock led to a sudden but temporary decline in real variables such as output, consumption, and investment, followed by a rapid rebound. GDP decreased approximately twice as much as it did during the GFC, while investment decreased three times as much. In contrast to the U-shaped recovery that followed the GFC, the economy experienced an immediate recovery in 2020-Q3, giving the shock a V-shaped appearance.

Given the unprecedented nature of the pandemic, questions arise regarding the validity of Covid-19 data for inferring economic models or whether the extreme volatility in the data distorts parameter estimates. In fact, the latter has been indicated for the US by Schorfheide and Song (2021), Lenza and Primiceri (2022) and Carriero, Clark, Marcellino, and Mertens (2021) and for the euro area by Bobeica and Hartwig (2021) and Morley, Rodriguez Palenzuela, Sun, and Wong (2022). Therefore, it is important to select the appropriate setting when making inferences from data periods with extreme heteroskedasticity, such as during Covid-19.

The literature on time-varying macroeconomic shock volatility is extensive in the context of Vector Autoregression (VAR) (e.g., Jacquier, Polson, and Rossi, 2002, Cogley and Sargent, 2005, Clark and Ravazzolo, 2015, Carriero, Clark, and Marcellino, 2016) and Dynamic Stochastic General Equilibrium (DSGE) Models (e.g., Justiniano and Primiceri, 2008, Fernández-Villaverde and Rubio-Ramírez, 2007). As such, it is important to compare where this study fits within recent developments in volatility modeling strategies for large outliers such as Covid-19. Unlike most periods with high volatility, which occur continuously over time, the Covid-19 shock period is characterized by its transitory nature, occurring only in selected quarters without a transition period. As a result, traditional models such as stochastic volatility models, Markov switching models, and conditional heteroskedasticity models, including (G)ARCH models, may not be well-suited to capturing these large volatility changes with low persistence. Furthermore, the volatility increase can be accurately attributed to a specific time period, making the estimation of the additional variance relatively straightforward.

Over the past two years, some literature has emerged describing how to handle large Covid-19 outliers within VAR models. Among the methods to address the extreme outliers is to exclude all Covid-19 observations from estimation and consider them uninformative. Schorfheide and Song (2021) show that omitting the recent data from estimation delivers a fair forecasting performance in a mixed-frequency VAR except for 2020-Q2. Nevertheless, this may understate the degree of forecast uncertainty in future applications. Addressing the latter, Carriero et al. (2021) find that a stochastic volatility model with Student's t-distributed shock innovations and allowing for outliers prevents a persistent increase in volatility when estimating single-frequency Bayesian vector autoregression (BVAR).

The approach used in this chapter is closely related to that in Lenza and Primiceri (2022) and Morley et al. (2022) for VAR models and is thereby aiming to extend the literature on estimating Covid-19 outliers in VAR models to structural DSGE models. Lenza and Primiceri (2022) re-scale the shock innovation-covariances to capture the increased volatility during the Covid-19 months by estimating scaling factors for each month of the pandemic that decay over time. Morley et al. (2022) build on the Lenza and Primiceri (2022) approach and estimate quarterly scaling factors for the covariance matrix of a large BVAR for the euro area without the volatility decay, finding that the data variation post 2020-Q3 appears to be close to its original level.

Similarly, I propose a simple time series approach that does not require a change of the structural equations in the model to accommodate the extreme outliers in estimation. Building on Lenza and Primiceri (2022) and Morley et al. (2022), but allowing for heterogeneity in the change in shock volatility, the approach entails three adjustments to an otherwise standard DSGE model estimation: A time-varying variance-covariance matrix, an autoregressive moving average (ARMA) correction for total factor productivity (TFP) shock innovations, and a measurement correction for consumption data in the Kalman filter.

The transitory change in shock volatility is modeled using a time-varying shock innovation-covariance matrix that estimates heterogeneous additive shock variance terms across the Covid-19 shock quarters. As in Lenza and Primiceri (2022), this effectively reduces the weight on the Covid-19 outliers in estimation and delivers robust structural parameter estimates compared to those in the pre-Covid sample. Similar to Morley et al. (2022), I do not model a decay in additive shock volatility for quarterly data, finding that in the euro area, volatility in the data after 2020-Q3 appears to be close to pre-pandemic levels.

In addition, the TFP shock and the TFP component in the exogenous spending shock follow an autoregressive moving average (ARMA) process in 2020-Q2 and 2020-Q3 in order to reduce the persistence of the negative TFP shock innovations in 2020-Q1 and 2020-Q2 and to allow for a negative autocorrelation during the Covid-19 period. Intuitively, this correction includes agents' perception of the nature of the shock in the model. Lowering the persistence of TFP shock innovations assumes that agents were aware of the transitory nature of economic developments at the time and knew that productivity would recover quickly once social health measures and lockdowns were lifted.

The Moving Average (MA) correction delivers sensible model outcomes in response to monetary policy reactions. The monetary policy response to the pandemic in the euro area was constrained by the ZLB. While the Federal Reserve lowered interest rates immediately, the European Central Bank had no such options since the policy rate was already at its effective lower bound since 2014. To understand the monetary policy stance in the euro area at the time, I construct a structural shadow rate based on Jones, Kulish, and Morley (2022a). In contrast to other interest rate rule equivalents that use yield curve information (e.g., Black, 1995, Krippner, 2013, Wu and Xia, 2016), the Jones et al. (2022a) approach explicitly models the effects of unconventional monetary policy during a fixed-interest rate regime. The estimated structural shadow rate follows a similar trend as the term structure rate by Wu and Xia (2016) but implies less expansionary policy at any given point in time. While both measures react expansionary to unconventional policies, such as the implementation of the Asset-Purchasing Program (APP) in early 2015, the effects of the structural shadow rate measure are less pronounced and quantitatively closer to the recent measure of De Rezende and Ristiniemi (2023). The monetary policy stance of the structural shadow rate during the Covid-19 pandemic appears to be more expansionary than the Wu and Xia (2016) measure compared to the respective pre-pandemic levels. The negative TFP shock innovations result in a substantial overshoot of the shadow rate when MA-correction is not applied. The shadow rate forecasts a smoother rebound quarter when the persistence of shock innovations is reduced. Instead of interpreting the rebound effect as an expansionary effect, agents understood it was simply the result of lockdown and health measure easing, causing the shadow rate to return to its pre-pandemic level. Excluding data temporarily from the measurement equation is a similar but simpler approach compared to adding large measurement errors.

Finally, I exclude consumption data from the Kalman filter during the Covid-19 pandemic and in subsequent quarters as a final adjustment. A large drop in consumption during the pandemic was accompanied by higher volatility in the following quarters, due to social health measures, lockdowns, and social distancing. These fluctuations pose a challenge to the model, as it does not accurately reflect consumption behavior during these times. Therefore, it cannot provide information about the structural parameters influencing consumption behavior. The increased volatility during the pandemic and the following months distorts the estimates of the consumption Euler equation, such as habit formation and intertemporal substitution elasticity, and is in direct contrast to traditional consumption theory, which suggests households prefer a smooth path of consumption (e.g., Friedman, 1957, Modigliani and Brumberg, 1954). Therefore, I add a measurement correction for consumption data in the Kalman filter due to the lack of informative power regarding economic decision-making.

I demonstrate the approach on handling Covid-19 outliers by estimating the well-known medium-scale DSGE model of Smets and Wouters (2003, 2007) for the euro area from 2004-Q3 to 2021-Q4. There are two challenges with the estimation strategy of the model during the sample period. The ECB implemented a fixed interest rate regime throughout the sample period from 2014 onwards. Furthermore, conventional monetary policy was severely constrained when the Covid-19 shock hit the economy, with interest rates fixed at the zero lower bound (ZLB). To incorporate the ZLB, I follow the time-varying solution strategy of Kulish, Morley, and Robinson (2017) (hereafter KMR (2017)). Their approach simultaneously estimates the set of structural parameters and a sequence of expected durations that indicate how long the ZLB is expected to be in place.[1]

The expected duration estimates for the ZLB constraint remain quite long during the Covid-19 pandemic. Compared to the pre-Covid-19 period, forward guidance dynamics are similar, but overall lower, now accounting for just under half of the estimated durations initially and expanding throughout the ZLB period. Lower bound durations change based on how structural shocks are transmitted. Since Covid-19 quarters were volatile, the usual drivers of expected durations might not appear as negative. The three adjustments are straightforward methods for estimating DSGE models with Covid-19 data, which deliver reasonable results both for structural parameter estimates and implied model responses. However, as the additive shock variances estimated during the Covid-19 shock may not be sufficiently identified to measure the increase in volatility quantitatively, they serve primarily as controls for the extreme heteroskedasticity. As each variance is based on one observation only, identification becomes increasingly challenging when additional variances are estimated for each shock and quarter. The identification of these estimates can be improved by introducing scaling factors that are common to all shocks similar to Lenza and Primiceri (2022). This approach, however, neglects the degree of heterogeneity in shock responses or timing that seems to be present in my model. Nevertheless, I re-estimate the model with common scaling factors to test the sensitivity of the results.

The remainder of this chapter is structured as follows. In section 3.2, stylized facts about the Covid-19 pandemic in the euro area are presented, including details regarding the economic contraction and the monetary policy response. Section 3.3 discusses the estimation methodology for incorporating Covid-19 outliers at the ZLB. Section 3.4 outlines an application for the euro area and presents the estimation results including a VAR analysis of the model. Section 3.5 discusses a trade-off between the identification of Covid-19 shock variances and shock heterogeneity. Section 3.6 assesses the stance of monetary policy in a structural shadow system. Section 3.7 concludes.

[1] The first and second chapters of this thesis provide a detailed description of how a DSGE model can be estimated when interest rates are temporarily fixed at the ZLB.

3.2 Stylized Facts

3.2.1 Contraction of Economic Activity

The Covid-19 pandemic caused an unprecedented level of economic volatility in the euro area. Unlike previous recessions such as the GFC or the Sovereign Debt Crisis, the Covid-19 recession was not caused by structural problems within the economy, but rather by temporary responses to the pandemic and intentional policy measures designed to minimize public health risks. Social health measures, such as lockdowns and work restrictions, resulted in a decline in the economy across all sectors. These measures set the Covid-19 shock apart and give it a unique dynamic.

The Covid-19 shock hit the economy in the first quarter of 2020. Figures 3.1 and 3.2 display the significant decline in output, consumption, and investment during the onset of the pandemic and the subsequent quarters. In 2020-Q2, output fell by approximately 10%, more than double what it contracted during the GFC. As a result of its volatile nature, investment fell even more than output, approximately three times more than it did during the GFC.

Figure 3.1: Contractionary Effects on Output

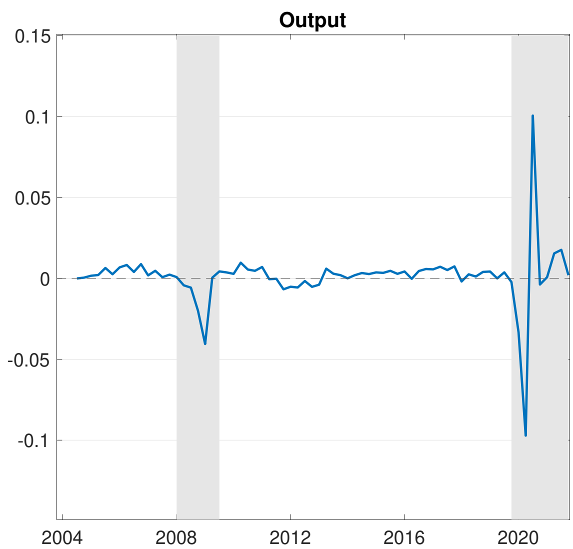

Note: Output data is expressed in period-on-period log growth rates. The sample period runs from 2004:Q3 to 2021:Q4. *Source: Eurostat*

In contrast to the U-shaped recovery path following the GFC, real variables show an immediate rebound effect in 2020-Q3, giving the shock a V-shaped appearance. This can largely be attributed to the shock's nature and the fact that it was not caused by structural issues. Instead, it was caused by intentional supply and demand constraints such as lockdowns and social distancing. In the immediate aftermath of lifting the measures, the economy began to rebound, resulting in a significant economic recovery.

Figure 3.2: Contractionary Effects on Consumption and Investment

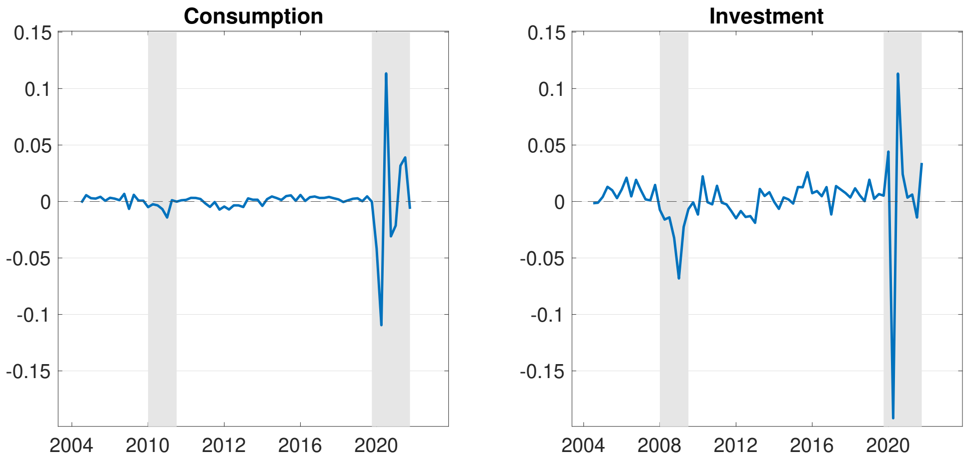

Note: Consumption and investment data is expressed in period-on-period log growth rates. The sample period runs from 2004:Q3 to 2021:Q4. *Source: Eurostat*

Consumption data have been more volatile than they would be under normal economic conditions. In contrast to traditional consumption theories such as the permanent income hypothesis (Friedman, 1957) or the life-cycle hypothesis (Modigliani and Brumberg, 1954), that suggest that households choose a smooth path of consumption, the Covid-19 shock resulted in a fall in consumption by approximately 10%. While consumption did not significantly decrease during the GFC, it became increasingly volatile during the initial Covid shock and subsequent quarters due to social health measures and lockdowns. Although the following lockdowns did not have the same impact as the first lockdowns in 2020-Q2, consumption remained highly volatile throughout the period.

As for nominal variables, both prices and wages have become significantly more volatile as a result of the Covid-19 pandemic. Figure 3.3 shows that inflation dropped during the lockdown period, possibly due to a general economic slowdown. While wages initially increased during the lockdown period, as indicated by the labor cost index in the right panel of Figure 3.3, they subsequently declined. The labor cost index measures the total cost of hiring workers on an hourly basis. During the pandemic, many fiscal governments in the euro area enacted wage programs that maintained equal pay rates despite a reduction in hours worked and labor productivity. This led to an increase in labor costs per hour.

Figure 3.3: Effects on Prices in the Economy during the Pandemic

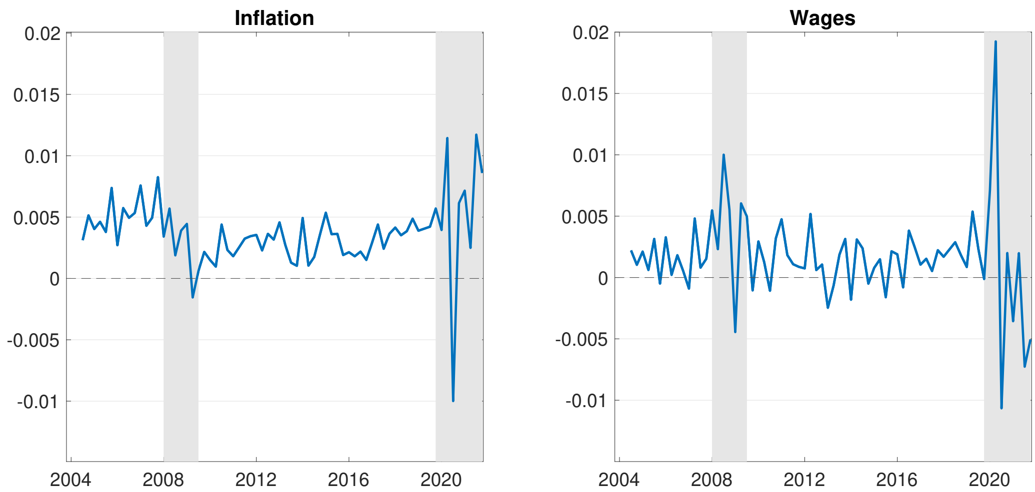

Note: Inflation is measured by the GDP deflator and wages are past on the wage index with base year 2010. *Source: Eurostat*

The Covid-19 pandemic had a severe impact on both the demand and supply sides of the economy, affecting nearly all sectors simultaneously. Despite the presence of extreme outliers in the data, the structural equations of the model will remain unchanged in estimation. The following sections provide a detailed explanation of the steps involved in the estimation process, including how these extreme outliers will be addressed.

3.2.2 Monetary Policy Reaction

In the immediate aftermath of the Covid-19 shock, the ECB was severely limited in its conventional monetary policy instruments. The policy rate had already been at or close to zero since 2014, thereby limiting the institution's ability to implement interest rate cuts as a response to the decline in economic activity.

Figure 3.4 displays the policy rate and the yields of AAA-rated central government bonds over one and five years. Each of these rates declined significantly during the GFC but remained stable during the Covid-19 pandemic. Therefore, the Covid-19 shock was the euro area's first recession that was not cushioned by conventional expansionary monetary policy, but instead relied on unconventional monetary policy methods.

Figure 3.4: Monetary Policy in the Euro Area during the Pandemic

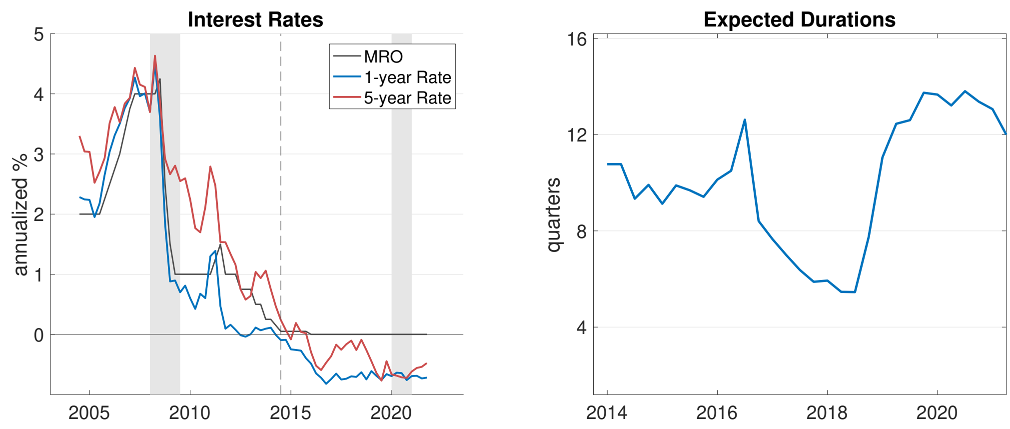

Note: Panel on the left shows the main operating finance rate and the 1-year and 5-year maturity bonds of triple A rated countries in the euro area. The right panel shows the prior mean of the sequence of expected durations constructed from the Survey of Professional Forecasters. *Source: ECB*

To obtain a full understanding of the stance of monetary policy, it is necessary to take into account the use of unconventional policies. Using a survey measure that provides estimates of the expected durations at the ZLB, professional forecasters are asked to provide an accurate date of liftoff from the lower bound. It is not only possible to see a change in these expected durations based on economic circumstances, but it is also possible for these changes to be the result of deliberate monetary policy actions, which can serve as an indicator of the stance of monetary policy.

According to the survey responses shown in figure 3.4, the expected durations were increasing after 2019 and the lower bound was expected to prevail throughout the Covid-19 pandemic. While survey responses indicated a less expansionary stance of monetary policy throughout 2017 and the beginning of 2018, expectations increased sharply in mid-2018. Forecasters predicted that the fixed-interest rate regime would remain in place for over three more years during this pandemic. This is the highest level since the implementation of the fixed-interest rate regime in 2014.[2]

Using the professional forecaster survey information as an informative prior, I estimate the sequence of expected durations along with structural parameters in the model. This approach allows me to evaluate the monetary policy stance throughout the pandemic.

[2] A top-coding limit of 17 quarters has been imposed on the survey question due to its open-ended nature, thus expectations for periods beyond this limit are not captured in this measure.

3.3 Estimating a DSGE Model with Covid-19 Data

To enhance the robustness of a DSGE model estimation subject to the extreme outliers caused by the Covid-19 pandemic, I propose three adjustments to an otherwise standard DSGE model estimation. In the spirit of Lenza and Primiceri (2022), I introduce a time-varying shock innovation-covariance matrix that captures extreme heteroskedasticity in shock variances. To reduce the persistence of negative TFP innovations in 2020-Q1 and 2020-Q2, I propose an Autoregressive Moving Average (ARMA(1,1)) process for the respective shocks. In addition, I adjust the Kalman filter to account for extreme outliers in consumption data that may not be indicative of other behavioral responses at other times and therefore may not be informative regarding the structural parameters associated with consumption patterns.

Let the linearized structural equations with n variables and l structural shocks be given by:

$$\underset{n\times 1}{y_t} = \underset{n\times 1}{C_0} + \underset{n\times n}{A_1}\, y_{t-1} + \underset{n\times n}{B_0}\, E_t y_{t+1} + \underset{n\times l}{D_0}\; \underset{l\times 1}{e_t} \tag{3.1}$$

with the reduced form being:

$$y_t = C + Qy_{t-1} + Ge_t \tag{3.2}$$

where C, Q, and G are the linear rational expectations solution matrices.

3.3.1 Large Changes in Shock Volatility

To account for transitory changes in shock variances during the pandemic, I introduce additive variance terms for Covid-19 shock periods into the shock innovation-covariance matrix. Initially, all shock processes follow a first-order autoregressive process with an iid-normal error term:

$$\varepsilon_t = \rho\varepsilon_{t-1} + \eta_t$$

where $\eta_t \sim iid(0,\sigma^2)$ with $E(\eta_t'\eta_t) = \Omega_t$ and $E(\eta_t'\eta_{t-j}) = 0$, $\forall j > 0$. The data volatility is absorbed by additive variance terms that are estimated for the Covid-19 pandemic quarters. Instead of scaling factors that are common to all shocks as in Lenza and Primiceri (2022), individual standard deviations are estimated for each shock innovation and quarter. Following Morley et al. (2022), no decay for the additional quarterly shock variances is estimated.[3] I take this approach to address not only the extreme heteroskedasticity in shock volatility but also its heterogeneity across the structural shocks. For each quarter of the Covid-19 shock, 2020-Q1, 2020-Q2, and 2020-Q3, an additional shock innovation variance term $\sigma_{i,j}^2$ is estimated:

$$\sigma_{i,t}^2 = \sigma_i^2 + D_{t,j}\sigma_{i,j}^2$$

where $D_{t,j} = [0,1]$ is a dummy-vector that indicates periods, $j = [2020 - Q1, -Q2, -Q3]$, with higher volatility. The subscript i identifies each of the shocks in the system $i = [a, b, g, qs, p, w]$. When $D_{t,j} = 0$, the variance-covariance matrix is identical to the one from the pre-Covid-19 sample.[4] When $D_{t,j} = 1$, an additional shock variance parameter is estimated to reflect the increased volatility during this period.

$$\sigma_{i,t}^2 = \sigma_i^2 + \begin{cases} 0, & \text{if } D_{t,j} = 0 \\ \sigma_{i,j}^2, & \text{if } D_{t,j} = 1 \end{cases}$$

where j denotes the quarters in which additional shock variances are estimated. Because of the transitory nature of the shock, these additional variances are not persistent and have no effect on future periods. To capture these effects, Ω_t^{covid} becomes a time-varying

[3]Including shock variances for the post-Covid-19 era does not significantly affect estimates of structural parameters. However, some observables, foremost consumption, exhibit increased volatility until the end of the extended sample period in 2021-Q1. This is addressed by a measurement correction in the Kalman filter, further described in more detail in section 3.3.3.

[4]During the entire pandemic period, monetary policy was at the ZLB, so no additional shock variances are estimated for monetary policy or yield curve shocks. By construction, the monetary policy shock is zero at the ZLB, and therefore also the yield curve shocks exhibit no additional volatility in this period.

shock innovation-covariance matrix:

$$\Omega_t^{covid} = \begin{pmatrix} \sigma_1^2 + D_{t,j}\sigma_{1,j}^2 & 0 & \dots & 0 \\ 0 & \sigma_2^2 + D_{t,j}\sigma_{2,j}^2 & \dots & 0 \\ \vdots & 0 & \ddots & \vdots \\ 0 & \dots & 0 & \sigma_l^2 + D_{t,j}\sigma_{l,j}^2 \end{pmatrix}$$

Each of the additional shock variances is estimated using a prior that follows an inverse gamma distribution with a mean of 1 and a standard deviation of 2.

3.3.2 ARMA (1,1) correction

Besides the temporary change in the shock innovation-covariance matrix, I propose an Autoregressive Moving Average (ARMA) process for the TFP shock innovations affecting the technology shock and the exogenous spending shock. This accounts for the transitory nature of real activity dynamics during the pandemic.[5] The exogenous spending shock comprises net exports, which are influenced by domestic TFP fluctuations and hence are affected by TFP shock innovations. Both shocks, the TFP shock (ε_t^a) and the exogenous spending shock (ε_t^g), follow first-order autoregressive processes with heteroskedastic TFP innovation terms:

$$\varepsilon_t^a = \rho^a \varepsilon_{t-1}^a + \eta_t^a$$
$$\varepsilon_t^g = \rho^g \varepsilon_{t-1}^g + \eta_t^g + \rho^{ga}\eta_t^a$$

where $\eta_t^a \sim \mathcal{N}(0, \sigma_{a,t}^2)$. Restricting ρ^a and ρ^g to be smaller than one guarantees that the process is stationary and that the consequences of the shock innovation η_t^a die out eventually. The Covid-19 pandemic, however, is characterized by a very low shock persistence in the sense of a large contraction followed by an immediate rebound before returning more to its usual dynamics. Estimating the technology Covid-19 shock using an AR(1) process alone does not capture this rapid rebound effect. To address this issue, I propose

[5] In a preliminary analysis I considered an ARMA correction for all structural shocks in the model, the technology shock appears to absorb most of the unusual dynamics around the Covid-19 pandemic. For most other shocks, the additional MA parameter is not well-identified and significantly lowers the shock persistence.

modeling a Moving Average (MA) term for the TFP shock innovations in 2020-Q2 and 2020-Q3:

$$\varepsilon_t^a = \begin{cases} \rho^a \varepsilon_{t-1}^a + \eta_t^a - \theta^a \eta_{t-1}^a, & \text{if } t\text{=2020-Q2 or } t\text{=2020-Q3} \\ \rho^a \varepsilon_{t-1}^a + \eta_t^a, & \text{for all other } t \end{cases}$$

In case of the exogenous spending shock, the MA component is adjusted by the parameter that indicates how important the TFP shock innovation is to the shock process ρ^{ga}:

$$\varepsilon_t^g = \begin{cases} \rho^g \varepsilon_{t-1}^g + \eta_t^g + \rho^{ga} \eta_t^a - \theta^a \rho^{ga} \eta_{t-1}^a, & \text{if } t\text{=2020-Q2 or } t\text{=2020-Q3} \\ \rho^g \varepsilon_{t-1}^g + \eta_t^g + \rho^{ga} \eta_t^a, & \text{for all other } t \end{cases}$$

The MA dynamics cause the effects of the pandemic from 2020-Q1 and 2020-Q2 to be less persistent compared to other shock innovations that follow autoregressive dynamics. The newly introduced parameter θ^a is restricted to be between zero and one, which induces a temporary negative autocorrelation into the series. The larger θ^a is estimated, the greater the reduction in the persistent effects of the shock innovations and the stronger the negative autocorrelation. This way, the addition of the MA term can account for the unusual V-shaped dynamics of the Covid-19 pandemic.

3.3.3 Measurement Correction in the Kalman Filter

Unlike the GFC when consumption declined slightly, the implementation of social health measures, lockdowns, and social distancing measures caused a significant drop in consumption during the Covid-19 pandemic, with higher volatility in the following quarters. As shown in figure 3.2, consumption fell by approximately 10% during the pandemic, in contrast to only a 2% decline during the GFC. Although subsequent lockdowns and social restrictions in 2021 did not generate a response similar to the first lockdown in 2020-Q2, consumption volatility remained considerably higher than any other period in the sample.

The structural model has difficulties accommodating these prolonged large fluctuations. The observed consumption data does not accurately reflect the behavioral responses in other periods and therefore does not provide informative insights into the structural parameters that are associated with consumption behavior. It is likely that the Euler equation, which usually describes consumption behavior in the model, does not adequately capture the complexity of consumption behavior during the Covid-19 period due to policy restrictions that are not explicitly incorporated into the model. As opposed to the traditional consumption theory that suggests that households choose a smooth path of consumption (e.g., Friedman, 1957, Modigliani and Brumberg, 1954), the increased volatility during the pandemic and the months following distorts consumption Euler equation estimates, such as habit formation and intertemporal substitution elasticity.[6] Thus, along with shock adjustments, consumption observations will also be dropped from the Kalman filter throughout the post-Covid-19 sample period.

Recall the standard reduced-form solution of the VAR:

$$y_t = C + Qy_{t-1} + Ge_t \tag{3.3}$$

The measurement equation is then given by:

$$z_t = Hy_t + \nu_t \tag{3.4}$$

where a $n^{obs} \times n$ matrix links the observables (n^{obs}) to the state variables, y_t and ν_t represent the vector of measurement errors ($\nu_t \sim \mathcal{N}(0, \mathcal{V})$) which is assigned a variance of zero in estimation. By introducing an auxiliary $(n^{obs} - p_t) \times n$ matrix $\mathcal{C}$ to reduce the number of observables to p_t in the Kalman filter, $\check{z}_t \equiv \mathcal{C}z_t$, $\check{H} \equiv \mathcal{C}H$, and $\check{\nu}_t \equiv \mathcal{C}\nu_t$. p_t is time-varying in the sense that the number of observables that are excluded from estimation changes throughout the sample period. This changes the measurement equation during the Covid-shock to:

$$\check{z}_t = \check{H}y_t + \check{\nu}_t \tag{3.5}$$

[6]Estimation experiments indicated a significantly smaller parameter for consumption habits and the elasticity of intertemporal substitution both of which interact with the forward guidance dynamics in the model.

where the $(n^{obs}-2)\times n$ matrix $\mathcal{C}$ reduces the number of observables to seven, $\check{z}_t \equiv \mathcal{C} z_t$, $\check{H} \equiv \mathcal{C} H$, and $\check{\nu}_t \equiv \mathcal{C} \nu_t$.

Denoting forecasts with '$\sim$', and given the forecast of the variables, $\tilde{y}_{t|t-1}$, and its variance-covariance matrix of the prediction error, $\Sigma_{t|t-1}$, the forecast of the observables is $\tilde{\check{z}}_{t|t-1} = \check{H}\tilde{y}_{t|t-1}$, and their forecast error is $u_t \equiv \check{z}_t - \tilde{\check{z}}_{t|t-1} = \check{H}(y_t - \tilde{y}_{t|t-1}) + \check{\nu}_t$, with variance-covariance matrix $\check{F}_t \equiv \check{H}\Sigma_{t|t-1}\check{H}^{'} + WCW^{'}$. The time-varying variance-covariance matrix Ω_t^{covid} is defined as:

$$\Omega_t^{covid} = \begin{pmatrix} \sigma_1^2 + D_{t,j}\sigma_{1j}^2 & 0 & \dots & 0 \\ 0 & \sigma_2^2 + D_{t,j}\sigma_{2j}^2 & \dots & 0 \\ \vdots & 0 & \ddots & \vdots \\ 0 & \dots & 0 & \sigma_{lj}^2 + D_{t,j}\sigma_{lj}^2 \end{pmatrix} \tag{3.6}$$

3.4 Application to a DSGE Model for the Euro Area

3.4.1 The Medium-Scale DSGE Model

This chapter uses the medium-scale DSGE model by Smets and Wouters (2007) and its earlier euro area version, Smets and Wouters (2003), with adjustments to monetary policy based on KMR (2017) to account for the fixed-interest rate regime in the data sample. The model features standard New-Keynesian properties, and all variables are log-linearized around the steady state balanced growth path. By choosing the optimal level of labor and consumption, households maximize their utility. Intermediate firms are subject to monopolistic competition, whereas final goods producers are fully competitive. Prices and wages are indexed to account for inflation persistence. Nominal frictions are included by a Calvo price component in the Phillips curve. Furthermore, monetary policy operates in two regimes. Monetary policy follows a Taylor-type rule in normal times that is based on inflation, output growth, and the output gap, where potential output is defined as the output level under a fully flexible economy. At the ZLB, conventional monetary policy in inactive and the nominal interest rate is fixed. A representation of the complete model, including the sticky and flexible wage economies, and the shock processes can be found in the technical appendix.

3.4.2 VAR Solution

The model incorporates an anticipated structural change in the form of a fixed interest rate regime. When the policy rate follows a Taylor-type policy rule the solution to the model can be expressed in the following state-space form:

$$y_t = C_0 + A_1 y_{t-1} + B_0 E_t y_{t+1} + D_0 e_t \tag{3.7}$$

where y_t is the $n \times 1$ vector of model variables and e_t the $l \times 1$ of structural shocks. C_0, A_1, B_0, and D_0 are matrices of conformable dimension. The reduced form solution of this system is:

$$y_t = C + Q y_{t-1} + G e_t \tag{3.8}$$

where C, Q, and G are the linear rational expectation solution matrices.

When the policy rate is zero at the ZLB, the state-space model becomes:

$$y_t = \bar{C}_0 + \bar{A}_1 y_{t-1} + \bar{B}_0 E_t y_{t+1} + \bar{D}_0 e_t \tag{3.9}$$

As shown in Kulish and Pagan (2017) and KMR (2017), the reduced form solution is then a time-varying VAR of the form:

$$y_t = C_t + Q_t y_{t-1} + G_t e_t \tag{3.10}$$

The solution matrices C_t, Q_t, and G_t are denoted as sequences based on the duration of the ZLB in each quarter. Thus, variability over time is consistent with the expected duration of the ZLB regime. Since the data sample ends before liftoff, the model is expected to return to the time-invariant solution (equation 3.7) after liftoff. For instance, if the ZLB is expected to last for d periods before the model reverts to its original Taylor rule regime, the time-varying solution is described by the sequences $\{Q_t\}_{t=1}^{d}$, $\{G_t\}_{t=1}^{d}$, and

$\{C_t\}_{t=1}^{d}$. In addition, in the Covid-19 rebound quarter in 2020-Q3, the solution matrices incorporate the temporary ARMA correction of the technology shock.

In estimation, the model chooses a sequence of expected durations d that best fits the data. This is not necessarily the same duration as implied by the underlying policy rule and the structural shocks of the model. Following Jones et al. (2022b), the estimated duration is the combination of two different types of expected durations.

$$d_t = d_t^{lb} + d_t^{fg} \tag{3.11}$$

The first type, henceforth called *lower bound duration* d_t^{lb}, is the duration that results from the policy rule itself when a contractionary shock occurs. In the absence of further shocks, this duration is expected to decrease by one each quarter. Second, there are *forward guidance durations*, d_t^{fg}, which are used to capture forward guidance announcements. Both types have different effects on the model economy. Lower bound durations predict a contraction, and an increase would have a negative effect. Forward guidance durations, however, imply a reduction in interest rates, which would have an expansionary effect on the economy. Although the conventional monetary policy response remained unchanged during the Covid-19 pandemic, a sudden change in the expected duration of the ZLB may reflect a shift in the monetary policy stance.

3.4.3 Estimation

The model is estimated with Bayesian estimation techniques using nine quarterly data series for the euro area. Seven observables follow Smets and Wouters (2007): log differences of real output, real consumption and real investment, real wages, demeaned log hours worked, log differences of the GDP deflator, and the MRO rate. The remaining two observables are constructed euro area yields with one-year and five-year maturity, which are used, following KMR (2017), to include information about the term structure of interest rates in the model. Due to data availability, the sample period starts in 2004-Q3 and includes the Covid pandemic up until 2021-Q4. The additional standard deviations are estimated for each shock with the exception of the monetary policy and the yield curve shocks, given that there was no conventional monetary policy reaction during the Covid-19 pandemic. Each additional shock variance is estimated using a prior that follows an inverse gamma distribution with a mean of 1 and a standard deviation of 2.

Following KMR (2017), I jointly estimate the set of structural parameters and a set of expected durations. The model is estimated using Bayesian estimation techniques. The likelihood is defined as $\mathcal{L}(Z \mid \theta, d)$, where θ denotes the structural parameters, Z the data, and d the sequence of expected durations:

$$p(\theta, d \mid Z) \propto \mathcal{L}(Z \mid \theta, d) p(\theta) p(d)$$

A Metropolis-Hastings algorithm is used to generate draws from a posterior proposal distribution, which is a multivariate Student's t-distribution with its scale matrix chosen using the inverse of the Hessian matrix at the mode of the pre-ZLB period. A detailed description of the sampler is given in the appendix.

The priors for the structural parameters are given in table 3.1 and follow Smets and Wouters (2007) and KMR (2017). The prior for the expected durations is constructed using point forecasts of the MRO rate from the ECB's survey of professional forecasters and a uniform distribution. The upper limit of the probability distribution is set at 17 quarters.[7] The second quarter in 2020, the most contractionary quarter of the Covid-19 pandemic, is the only quarter in which the upper bound is consistently hit in the MCMC draws. Increasing the limit to 100 quarters reveals that the expected durations increase to around 10 years. However, increasing the upper limit comes with a loss of identification for the remaining quarters. Therefore, the expected durations should be seen as an indication for an exceptionally large contractionary shock rather than a precise estimate of how long the ZLB was expected to bind in this particular quarter.

3.4.4 Results

Structural Parameters and Shocks Drawing on the modifications outlined above, the model is estimated over the sample period from 2004-Q3 to 2021-Q4. Despite the large

[7] On a closer discussion of this upper limit refers to Chapters I and II of this thesis.

Table 3.1: Posterior Estimates of the Benchmark Model and the Covid-19 Model

Parameters		**Prior**			**Posterior**			**Posterior**		
					Pre-Covid Model			**Covid Model**		
		Distribution	**Mean**	**Std. dev.**	**Mode**	**Mean**	**Std. dev.**	Mode	**Mean**	**Std. dev.**
Shock Standard Deviations										
Technology	σ^a	IG	0.42	0.29	0.66	0.66	0.05	0.67	0.67	0.21
Risk premium	σ^b	IG	0.20	3.00	0.15	0.16	0.01	0.16	0.16	0.08
Fiscal	σ^g	IG	0.42	0.29	0.50	0.51	0.03	0.58	0.59	0.20
Investment	σ^{qs}	IG	0.42	0.29	0.61	0.60	0.06	0.63	0.65	0.25
Monetary	σ^m	IG	0.20	3.00	0.30	0.30	0.01	0.29	0.30	0.11
Price mark-up	σ^p	IG	0.20	3.00	0.34	0.35	0.02	0.41	0.41	0.14
Wage mark-up	σ^w	IG	0.42	0.29	0.30	0.31	0.01	0.32	0.33	0.11
1-year	σ^4	U	1.00	0.58	0.34	0.39	0.10	0.35	0.39	0.31
5-year	σ^{20}	U	1.00	0.58	1.09	1.14	0.46	1.13	1.12	0.65
Term Premium	σ^η	U	2.50	1.44	0.55	0.61	0.16	0.48	0.53	0.37
Shock Persistences										
Technology	ρ^a	B	0.50	0.20	0.92	0.87	0.05	0.85	0.87	0.05
Risk premium	ρ^b	B	0.50	0.20	0.97	0.96	0.01	0.96	0.96	0.01
Fiscal	ρ^g	B	0.50	0.20	0.89	0.90	0.04	0.86	0.86	0.05
Fiscal technology	ρ^{ga}	N	0.50	0.20	0.51	0.50	0.08	0.53	0.55	0.10
Investment	ρ^{qs}	B	0.50	0.20	0.38	0.39	0.13	0.34	0.37	0.09
Monetary	ρ^r	B	0.50	0.20	0.24	0.22	0.08	0.21	0.21	0.08
Price mark-up	ρ^p	B	0.50	0.20	0.18	0.27	0.15	0.10	0.24	0.15
Wage mark-up	ρ^w	B	0.50	0.20	0.10	0.13	0.07	0.03	0.06	0.03
Term premium	ρ^s	B	0.71	0.16	0.97	0.95	0.03	0.98	0.96	0.02
Structural Parameters										
Investment Adj. Costs	φ	N	4.00	1.50	5.96	6.12	1.24	6.15	6.25	1.33
CRRA	σ^c	N	1.50	0.375	0.94	0.93	0.09	0.91	0.90	0.10
Habits	λ	B	0.70	0.10	0.74	0.74	0.05	0.76	0.73	0.06
Degree of Wage Stickiness	ξ_w	B	0.50	0.10	0.93	0.93	0.02	0.93	0.93	0.01
Elasticity of Labor Supply	σ^l	N	2.00	0.75	1.46	1.51	0.52	1.72	1.70	0.49
Degree of Price Stickiness	ξ_p	B	0.50	0.10	0.80	0.77	0.06	0.69	0.70	0.06
Indexation Wages	ι_w	B	0.50	0.15	0.39	0.39	0.13	0.15	0.18	0.07
Indexation Prices	ι_p	B	0.50	0.15	0.27	0.35	0.15	0.22	0.27	0.12
Capacity Utilization	ψ	B	0.50	0.15	0.59	0.62	0.12	0.62	0.63	0.12
Fixed Costs	ϕ_p	N	1.25	0.125	1.62	1.63	0.09	1.57	1.60	0.11
Monetary Policy: Inflation	ϕ_π	N	1.50	0.25	1.52	1.49	0.22	1.40	1.50	0.24
Monetary Policy: Smoothing	ρ_R	B	0.75	0.10	0.87	0.86	0.03	0.87	0.87	0.03
Monetary Policy: Output Gap	ϕ_y	N	0.125	0.05	0.05	0.06	0.02	0.07	0.08	0.03
Monetary Policy: Output Growth	$\phi_{\Delta y}$	N	0.125	0.05	0.02	0.02	0.02	0.03	0.04	0.02
Constant Inflation	$\bar{\pi}$	G	0.63	0.10	0.51	0.51	0.06	0.48	0.50	0.06
Discount Factor	$\beta^{-1}-1$	G	0.25	0.10	0.22	0.2	0.07	0.24	0.24	0.08
Constant Labor	$\bar{l}$	N	0.00	2.00	3.71	3.85	0.96	3.23	2.91	0.87
Trend Growth	γ	N	0.40	0.10	0.24	0.25	0.03	0.20	0.20	0.02
Capital Share	α	N	0.30	0.05	0.26	0.26	0.02	0.22	0.21	0.03
Term Premium Constant	c_4	N	1.20	0.25	1.38	1.41	0.23	1.45	1.47	0.20
Term Premium Constant	c_{20}	N	2.35	0.25	2.10	2.09	0.21	2.08	2.02	0.19

Chains have 500,000 draws, half of which is disregarded as burn-in. Moments are multiplied by 10^{-2}.
N= Normal Distribution; IG= Inverse Gamma Distribution; U=Uniform Distribution; B= Beta Distribution; G=Gamma Distribution

increase in volatility in the Covid-19 data, most structural parameter estimates remain stable compared to the pre-Covid-19 sample.[8]

The introduction of additional variance terms effectively absorbs most of the elevated volatility in the data, resulting in the estimation of shock standard deviations that are almost identical to those obtained from the pre-Covid-19 sample. The only exceptions are the exogenous spending shock (ε^g) and the price mark-up shock (ε^p), for which the standard deviation is marginally higher. Notably, there are also differences in the estimates of the wage Phillips curve, which indicate a lower wage indexation (ι^w) and reduced persistence of the wage mark-up shock (ρ^w).

When the consumption data is removed from the Kalman filter during the Covid-19

[8]A comprehensive discussion of the estimation strategy and the results for the benchmark model can be found in Chapter I of this thesis.

period, the resulting estimates for the consumption Euler equation parameters are nearly identical. Conversely, the habit formation parameter, which represents the backward-looking component of the Euler equation, decreases substantially when consumption data are included. This, in turn, causes the constant risk aversion parameter (σ^c) to decrease considerably, suggesting a shift in preferences during the pandemic. The model estimates appear to be distorted by changes in agent behavior during the pandemic and hence do not accurately reflect typical consumption preferences.

Table 3.2: Additional Covid Parameters to the Smets and Wouters (2003, 2007)Model

Additional Covid Parameters		**Prior**			**Posterior**		
		Distribution	**Mean**	**Std. dev.**	**Mode**	**Mean**	**Std. dev.**
Shock Standard Deviations 2020-Q1							
Technology	σ^{a1}	IG	1	2	1.06	1.28	0.90
Risk premium	σ^{b1}	IG	1	2	0.54	0.73	0.59
Fiscal	σ^{g1}	IG	1	2	0.71	1.47	1.27
Investment	σ^{q1}	IG	1	2	0.66	1.17	1.01
Price mark-up	σ^{p1}	IG	1	2	0.55	0.77	0.65
Wage mark-up	σ^{w1}	IG	1	2	0.63	0.80	0.75
Shock Standard Deviations 2020-Q2							
Technology	σ^{a2}	IG	1	2	2.36	2.10	1.10
Risk premium	σ^{b2}	IG	1	2	0.54	0.76	0.61
Fiscal	σ^{g2}	IG	1	2	0.63	1.11	1.09
Investment	σ^{q2}	IG	1	2	0.75	1.48	1.25
Price mark-up	σ^{p2}	IG	1	2	0.62	0.86	0.86
Wage mark-up	σ^{w2}	IG	1	2	0.87	1.09	0.73
Shock Standard Deviations 2020-Q3							
Technology	σ^{a3}	IG	1	2	0.62	0.84	0.69
Risk premium	σ^{b3}	IG	1	2	0.56	0.77	0.64
Fiscal	σ^{g3}	IG	1	2	1.52	1.59	1.06
Investment	σ^{q3}	IG	1	2	1.76	1.95	1.31
Price mark-up	σ^{p3}	IG	1	2	0.89	1.13	0.96
Wage mark-up	σ^{w3}	IG	1	2	0.91	1.10	0.82
ARMA Correction							
MA Parameter technology	θ^a	B	0.71	0.16	0.74	0.72	0.10

Chain has 500,000 draws, with the first half discarded as a burn-in.
IG= Inverse Gamma Distribution; B= Beta Distribution

The posterior mean of the MA parameter for the technology shock (θ^a) is estimated to be 0.72, which is smaller than the autoregressive parameter of the technology shock. In the exogenous spending shock process, the MA parameter is adjusted by the parameter ρ^{ga} and is thereby also reducing the signal from prior TFP shock innovations. Consequently, the TFP shock innovation persistence from 2020-Q1 and 2020-Q2 is significantly reduced, although not entirely eliminated.

Moving on to the additional variance terms in the Covid-19 sample, which are displayed in table 3.2, it is worth noting that these estimates are intended to control for heteroskedasticity, rather than to precisely estimate the variances themselves. However, they do confirm the substantial increase in volatility observed throughout the Covid-19 period.[9] Considering that each estimate is based on data that is only available for one quarter, the high uncertainty about of these estimates is not surprising.

Figure 3.5: Kalman Smoothed Structural Shocks during the Pandemic

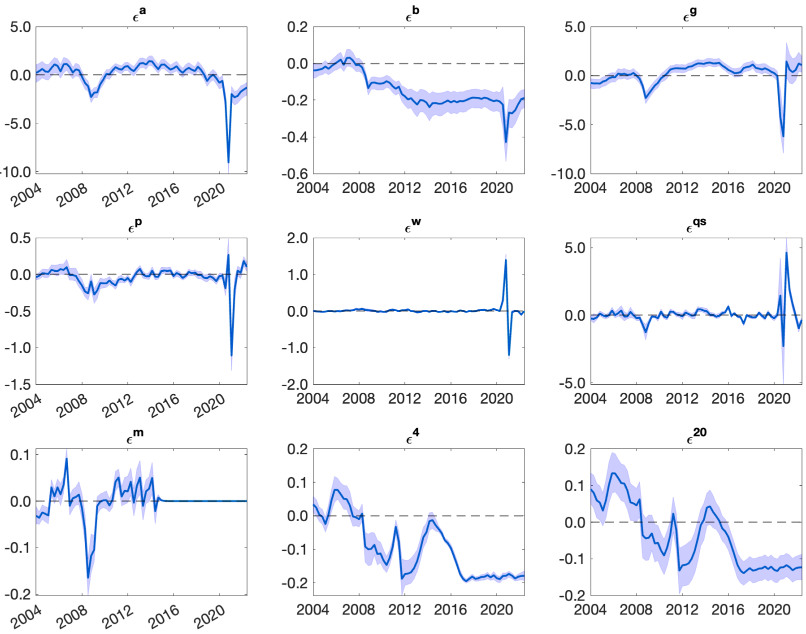

Note: The figure plots a simulated Kalman-smoothed time series for the shock processes over the Covid-19 period: ε_t^a (technology), ε_t^b (risk premium), ε_t^g (exogenous spending), ε_t^p (price mark-up), ε_t^w (wage mark-up), ε_t^{qs} (investment), ε_t^m (monetary policy), ε_t^4 (1Y Term Premium), and ε_t^{20} (5Y Term Premium), using 100 randomized posterior MCMC draws $\hat{\theta}_j$, and the equal-tailed 80% posterior bands.

Figure 3.5 displays a smoothed series of structural shocks to visualize how the pandemic impacted the model. The volatility of all shocks increased significantly during the Covid-19 shock quarters. Specifically, in the first two quarters of 2020, the technology shock had a strong negative impact before quickly returning to pre-Covid levels. The Phillips curve shocks follow inflation and wages data movements and exhibit large and V-shaped fluctuations. Additionally, the investment-specific technology shock is characterized by a strong rebound effect. By construction, the monetary policy shock is strictly zero at the ZLB, which translates into very small movements in the yield curve shocks.

[9] As an independent exercise, I estimated scaling factors that are common to all shocks, similar to Lenza and Primiceri (2022) and found scaling factors between three and five. Estimates for other parameters were quantitatively similar to those obtained using additive variance terms. However, I make the additive variance approach the baseline because the scaling factors do not allow for what appears to be some degree of heterogeneity in how much shock volatilities change. A more detailed discussion on this is given in section 3.5

Monetary Policy during the Covid Pandemic At the onset of the Covid-19 pandemic, monetary policy was already constrained by the ZLB. Consequently, the contractionary shock could not be mitigated through an interest rate response, resulting in little movement in yields across different maturities. However, the model's estimated expected duration can provide valuable insights into the stance of monetary policy during the pandemic. These estimates not only shed light on agents' expectations about the expected duration of the ZLB constraint but also convey information on deliberate monetary policy actions.

Figure 3.6 depicts the marginal prior and posterior distributions of the expected durations throughout the pandemic. Despite the similarity of the prior distributions between 2019-Q4 and 2020-Q3, there has been a significant shift toward longer duration estimates. Before the Covid-19 pandemic, the posterior distribution of the expected duration for 2019-Q4 placed the majority of the mass at around two and a half to three years. During and after the pandemic, the expected duration distributions displayed a left tail with a mass skewed toward longer durations. Specifically, during the Covid quarters, the posterior distribution showed the mass at over four years. This suggests that the data supported longer duration estimates as the pandemic progressed.

Due to the large fluctuations in the data, estimated durations remain high until the end of the sample period. Moreover, from late 2018 to the end of 2021, the posterior mean estimates exceed the prior means consistently, as depicted by the lower left panel of figure 3.7. Forward guidance durations are determined by separating the expected duration estimates by source, as described in 3.4.2. The results of this decomposition are shown in the upper panel of figure 3.7. For most of the sample period, monetary policy was expansionary, and forward guidance appears to have contributed significantly to expected duration estimates.

Consistent with the pre-Covid-19 sample in chapters 1 and 2, the expected duration estimates are top-coded by an upper bound of 17 quarters. When using different upper bound limits in the analysis, the estimate for 2020-Q2 shows a significant increase, but this comes at the cost of accurately identifying the remaining durations.[10]

[10] The higher the upper bound, the weaker the other durations are identified. As a result, long durations in all periods of the ZLB have been given more prior weight.

Figure 3.6: Posterior Distribution for the Expected Duration Estimates

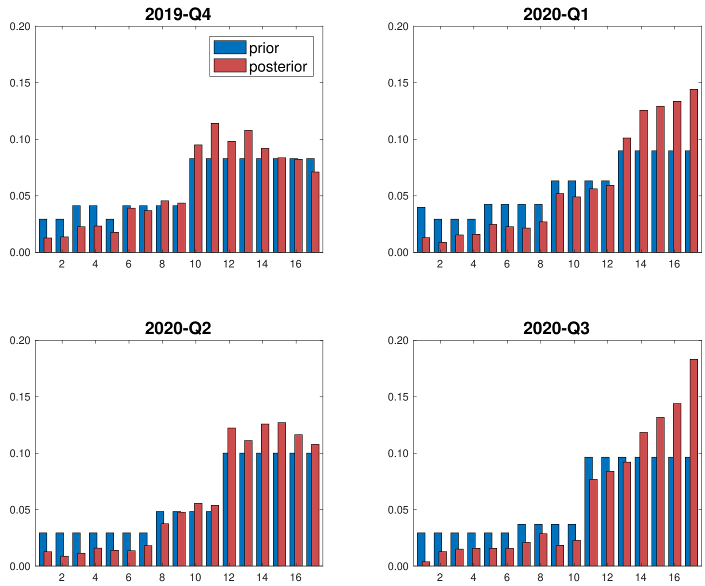

Note: The figure plots the prior and posterior distribution of the duration estimates from 2019-Q4 to 2020-Q3. The prior is constructed as an equally weighted combination of the distribution implied by the SPF data and a uniform distribution over all possible durations.

During the Covid-19 shock, duration estimates remain high, while forward guidance shocks show visible higher volatility. The forward guidance dynamics are similar but overall lower when estimated using data from the pre-Covid-19 period, accounting for just below half of the estimated durations initially and expanding throughout the ZLB period. The level shift in the lower bound duration reflects how differently the structural shocks transmitted through the economy. The large volatility in the Covid-19 quarters might not make the usual drivers of the expected durations appear as negative as before.

The lower bound and forward guidance durations are qualitatively similar to those of the pre-Covid-19 sample. Except for the large contraction in 2020-Q2, forward guidance remains the main driver behind durations throughout the Covid-19 pandemic. The lower bound duration in this quarter exceeds the estimated parameter, indicating a negative trend in forward guidance for the coming quarter. The long durations in the following quarters may have been the result of a deliberate monetary policy, which was abandoned earlier than anticipated in mid-2022 when interest rates were announced to increase for the first time in almost a decade at the ZLB. Moreover, the durations seem to be influenced by inflation throughout the Covid-19 period. The lower bound durations are determined by

Figure 3.7: Decomposition of Duration Estimates during the Pandemic

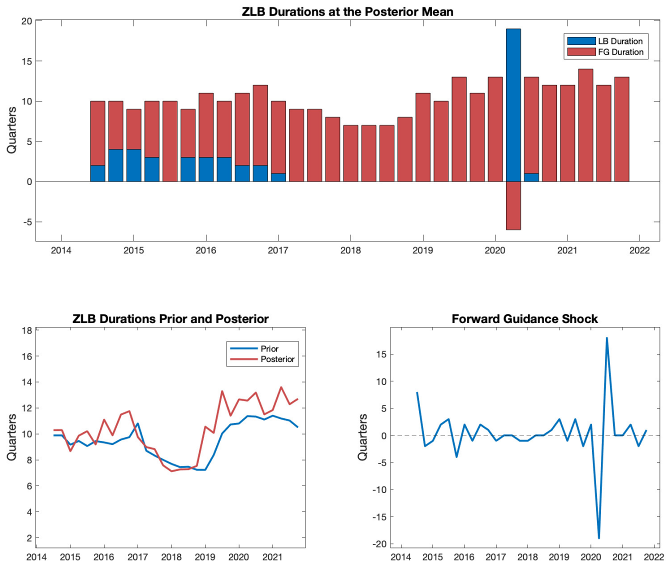

Note: The upper graph shows the decomposition of expected durations into *lower bound duration* and *forward guidance duration* during the entire sample period. The lower right graph shows the respective forward guidance shock. The lower left graph plots the expected duration estimates against the prior with as survey weight of 50%.

the underlying policy rule responses that are constrained at the ZLB. However, according to the policy rule estimates, most of the policy function reaction is due to inflation rather than output growth or the output gap. Since inflation picked up soon after the onset of the pandemic, the underlying policy rule might not have been constrained even if the output gap remained negative.

Historical Shock Decomposition After demonstrating the robustness of the model estimates when including the Covid-19 sample period, this section focuses on analyzing the properties of the VAR model. Specifically, a historical shock decomposition is used to identify the shocks that drive the real variables in the model during the pandemic. This provides a better understanding of the impact of different types of shocks on the observable endogenous variables throughout the sample period.

Figure 3.8 shows the historical contribution of each shock to changes in output and inflation levels over the sample period. The main drivers of output are the TFP shock and demand shocks, which include the risk premium shock, the investment-specific technology shock, and exogenous spending shock. In the pre-ZLB period, monetary policy had a countercyclical impact on output, suggesting that some form of stabilization policy was in

Figure 3.8: Historical Shock Decomposition for Output and Inflation

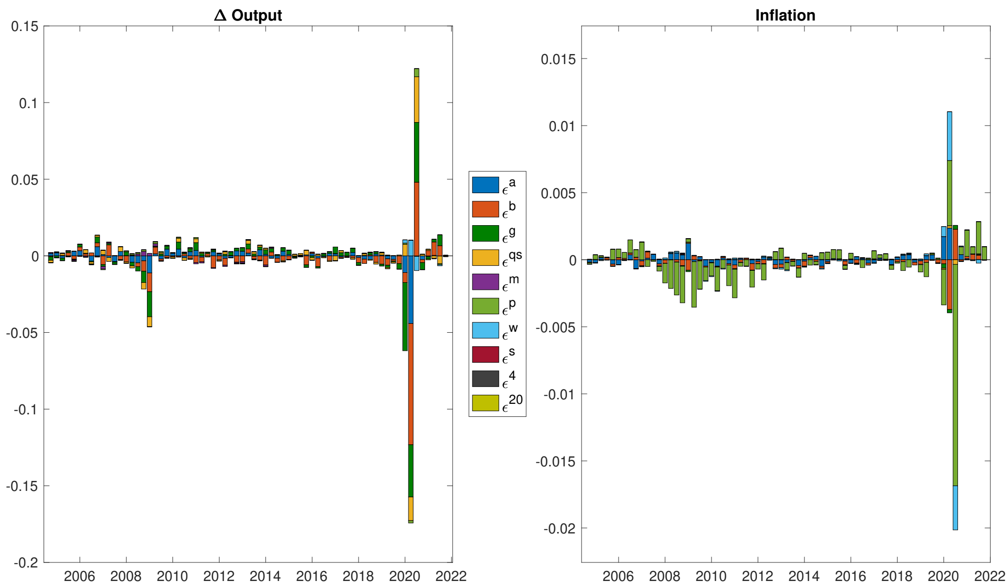

Note: This figure depicts the historical contribution of each shock to output and inflation over the sample period. ε_t^a (TFP), ε_t^b (risk premium), ε_t^g (exogenous spending), ε_t^p (price mark-up), ε_t^w (wage mark-up), qs_t (investment-technology), ε_t^m (monetary policy), ε_t^4 (1Y Term Premium), and ε_t^{20} (5Y Term Premium). As in Smets and Wouters (2003, 2007), the demand shocks include the risk premium, investment-specific technology, and exogenous spending shocks. Trend growth is estimated at 0.8 percent and mean inflation is estimated at 2 percent.

place. Although the usual drivers of output remain similar during the pandemic, the MA correction of TFP shock innovations' persistence significantly reduced their contribution to output recovery.

Inflation in the model is primarily driven by price mark-up shock. It appears that TFP shocks and risk premium shocks are more prominent during economic recessions, such as during the GFC or the Covid-19 pandemic. Even before the ZLB period, monetary policy had limited impact on inflation developments in the model.[11] During the pandemic, some of the variation in inflation is explained by wage mark-up shocks.

Figure 3.9 illustrates the historical contribution of each shock to hours worked and changes in the wage index over the sample period. The wage index is mainly driven by mark-up shocks, while hours worked are influenced by both demand and supply shocks. The risk premium shock and the total factor productivity shock account for the majority of the variation in hours worked, with the former having a pro-cyclical impact and the latter having a counter-cyclical impact. The relationship between productivity shocks and

[11] By construction, the conventional monetary policy shock cannot affect any developments during the ZLB period.

Figure 3.9: Historical Shock Decomposition for Hours Worked and Wages

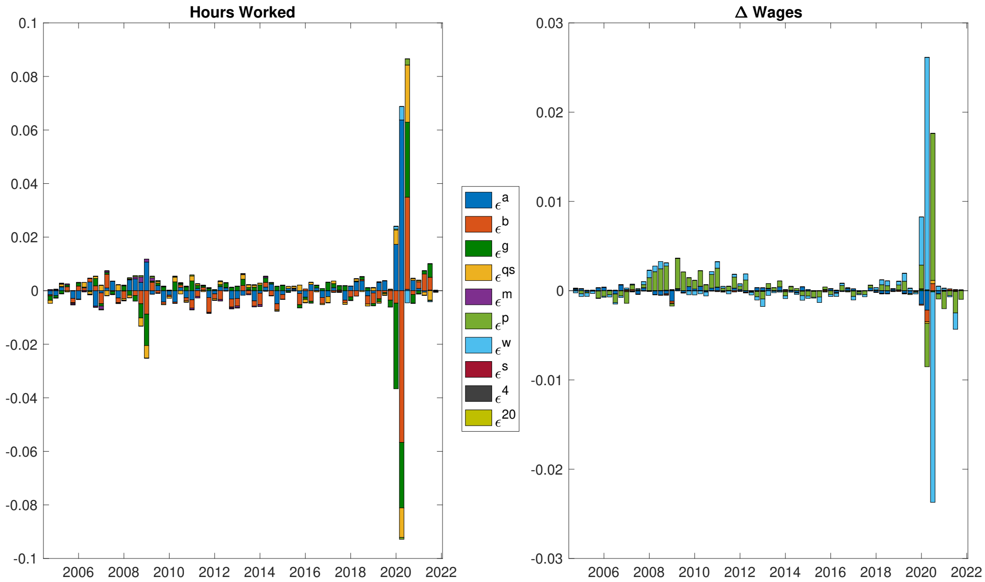

Note: This figure depicts the historical contribution of each shock to hours worked and wages over the sample period. ε_t^a (TFP), ε_t^b (risk premium), ε_t^g (exogenous spending), ε_t^p (price mark-up), ε_t^w (wage mark-up), qs_t (investment-technology), ε_t^m (monetary policy), ε_t^4 (1Y Term Premium), and ε_t^{20} (5Y Term Premium). As in Smets and Wouters (2003, 2007), the demand shocks include the risk premium, investment-specific technology, and exogenous spending shocks. Trend growth is estimated at 0.8 percent and mean inflation is estimated at 2 percent.

hours worked has been discussed extensively in the literature. As discussed in Gali (1999) and confirmed for this model in Smets and Wouters (2007), a positive productivity shock in the model leads to a significant reduction in hours worked. Confirming the results in Francis and Ramey (2005), Smets and Wouters (2007) explain the negative impact of productivity on hours worked by the degree of habit persistence and the significance of capital adjustment costs in the model. Thus, during the Covid-19 pandemic, the negative TFP shock innovations contributed positively to hours worked.

The historical shock decompositions for consumption and investment (figure 3.17) and the one-year and five-year maturity bonds (figure 3.18) can be found in the appendix for Chapter III. The risk premium shock appears to be the main driver of consumption, whereas monetary policy shocks also had an impact on consumption before reaching the ZLB. During the pandemic, consumption data were excluded from the Kalman filter, and the model predicts a more moderate decline in consumption mainly driven by the risk premium shock. Throughout the sample period, investment was primarily influenced by demand shocks, particularly the risk premium and the investment-specific technology shocks.

In the period leading up to the ZLB, both bond yields were influenced by a variety of shocks. Monetary policy had a stronger effect on short-term rates. At the ZLB, the one-year rate was largely driven by term premium shocks and remained negative throughout the fixed-interest rate period. In contrast, the five-year rate was more volatile and affected by term premium shocks and demand shocks. The five-year rate also exhibited a larger response to the pandemic than the one-year rate.

3.5 The Trade-off between Heterogeneity and Identification of Shock Variances

So far, the additive shock variances have been included to control for heteroskedasticity during the Covid-19 quarters, rather than to quantify the increase in variances. However, the identification of these additional variances is increasingly difficult, as each variance is based on only one observation in the data. Figure 3.10 visualizes the identification challenges by plotting the prior and posterior distributions for the Covid-19 parameters associated with the total factor productivity shock.

Figure 3.10: Posterior Distribution for the Covid-19 Shock Parameters

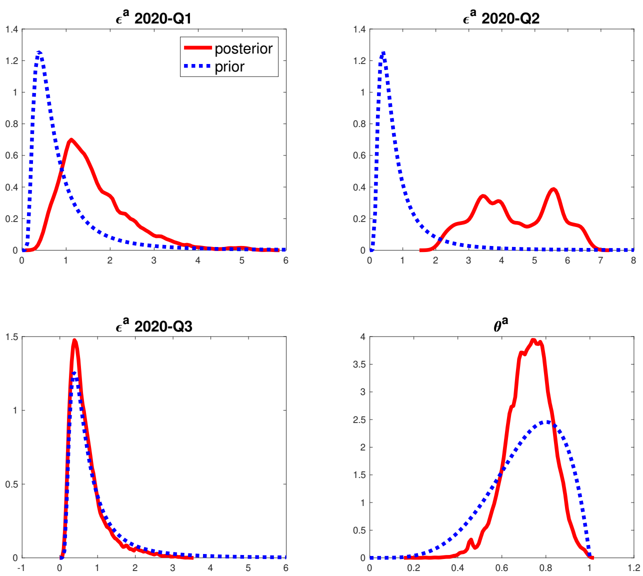

Note: The figure plots prior and posterior distributions for the Covid parameters associated with the total factor productivity shock.

The posterior distribution of the additive shock variance term of the TFP shock for 2020-Q2 is relatively flat and bimodal, suggesting possible identification difficulties. Nevertheless, the mass of the posterior distribution indicates a large increase in data volatility during this quarter. To improve the identification of the estimates, it is possible to estimate scaling factors or additive variance terms that are common to all shocks or all quarters. However, these approaches overlook the possibility of heterogeneous shock responses in the model.

This section demonstrates that the shock responses to the Covid-19 pandemic were heterogeneous in the model. Moreover, as a robustness exercise, I re-estimate the model using the common scale factor approach by Lenza and Primiceri (2022) and demonstrate that despite the identification challenges in the benchmark approach, the results are similar. Therefore, it is important to control for heteroskedasticity to obtain robust estimates during the Covid-19 pandemic, but the loss of identification does not interfere with the dynamics of the model when controlling for heterogeneity.

3.5.1 Heterogeneous Shock Responses to Covid-19

Examining the shock responses to the Covid-19 pandemic individually, reveals that they were heterogeneous, not just in magnitude, but also in timing. Figure 3.11 visualizes the increased volatility relative to the benchmark case, which is normalized to one. The TFP shock saw the greatest increase in volatility during the second quarter of 2020, with a variance that was approximately 3.5 times larger than the benchmark. This increase was particularly pronounced during the contractionary quarters of 2020-Q1 and 2020-Q2, where the shock responses were stronger than during the rebound quarter in 2020-Q3.[12] On the demand side, the exogenous spending shock, and the investment-specific technology shock both exhibit strong rebound effects, whereas the risk preference shock and the mark-up shocks exhibit similarly alleviated responses in all three quarters.

It appears that the demand shocks in the model, particularly the investment-specific technology shock and the exogenous spending shock, are characterized by a strong rebound effect. In the case of supply-driven shocks, such as the mark-up shocks and the TFP shock,

[12]Note for the TFP shock process, shock innovation persistence has been reduced which lowers the overall magnitude of the shock response.

Figure 3.11: Heterogeneity among Shock Variances

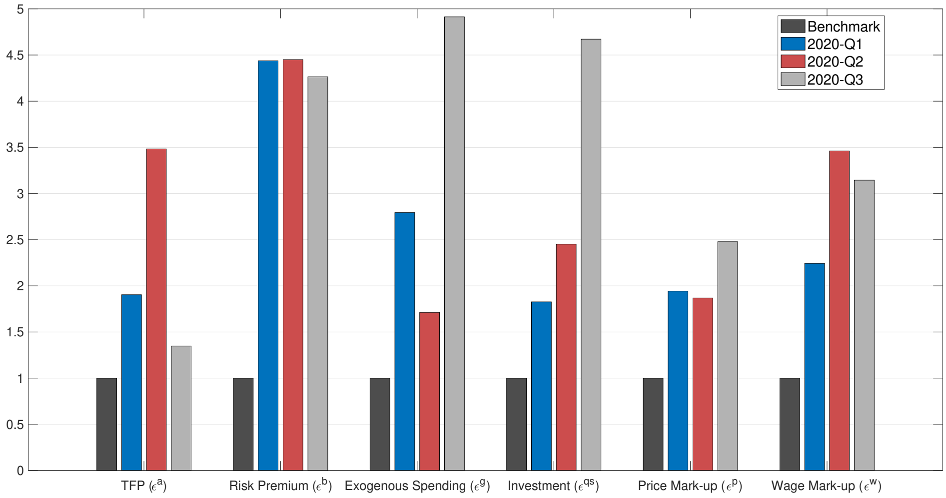

Note: The figure compares the increase in shock volatility for each shock and quarter relative to the posterior mean of the benchmark variance. The Benchmark variance is normalized to one.

the contractionary shock quarters 2020-Q1 and Q2 were equally or more important than the rebound quarter.

3.5.2 Estimating Scaling Factors

While the scaling factors are better identified, they neglect the degree of heterogeneity in shock responses that is visible across the Covid-19 shock quarters.

Identification can be improved by estimating scaling factors that are common to all shocks. In Lenza and Primiceri (2022), the entire shock innovation-covariance matrix is rescaled, and the Covid-19 observations are given less weight. Although common scaling factors are better identified, they do not capture the heterogeneity in shock responses. Nonetheless, to assess the robustness of the results, I re-estimate the model using common scaling factors for all shocks based on Lenza and Primiceri (2022).

Reverting to the benchmark model, in which all shock processes are modeled as first-order autoregressive processes with iid-normal errors implies that:

$$\varepsilon_t = \rho \varepsilon_{t-1} + \eta_t \tag{3.12}$$

where $\eta_t \sim iid(0,\sigma^2)$ with $E(\eta_t'\eta_t) = \Omega_t$ and $E(\eta_t'\eta_{t-j}) = 0$, $\forall j > 0$. During the Covid-19 quarters, the shock innovation covariance matrix is up scaled by common scaling factors s_t:

$$\sigma_{j,t}^2 = (s_t\sigma_j)^2 \tag{3.13}$$

where $s_t = 1$ except for the three quarters that were affected by the Covid-19 shock; 2020-Q1, 2020-Q2, and 2020-Q3. The shock innovation-covariance matrix of the structural shocks, Ω_t, becomes time-varying and transforms to:

$$\Omega_t = \begin{pmatrix} (s_t\sigma_1)^2 & 0 & \dots & 0 \\ 0 & (s_t\sigma_2)^2 & \dots & 0 \\ \vdots & 0 & \ddots & \vdots \\ 0 & \dots & 0 & (s_t\sigma_l)^2 \end{pmatrix} \tag{3.14}$$

Each scaling factor is estimated with a prior that follows a normal distribution with a mean of 2 and a standard deviation of 1.

Table 3.3: Variance Scaling Factors for Covid-19

Additional Covid Parameters		**Prior**			**Posterior**		
		Distribution	**Mean**	**Std. dev.**	**Mode**	**Mean**	**Std. dev.**
Scaling Factor 2020-Q1	s_1	N	2	1	3.14	3.34	0.61
Scaling Factor 2020-Q2	s_2	N	2	1	5.14	5.26	0.59
Scaling Factor 2020-Q3	s_3	N	2	1	4.70	4.71	0.59
MA Parameter technology	θ^a	B	0.71	0.16	0.76	0.70	0.15

Chains have 500,000 draws, half of which is disregarded as burn-in.
N= Normal Distribution; B= Beta Distribution

The estimated scaling factors, presented in table 3.3, range between three and five. The largest scaling factor is estimated for the contractionary shock quarter in 2020-Q2, while the estimates for 2020-Q1 and the rebound quarter in 2020-Q3 are somewhat smaller. Figure 3.12 indicates that the common scaling factors are well identified, and the data assign significant weight to larger scaling factors than the prior suggests.

However, the approach does not account for what appears to be a certain degree of shock heterogeneity in this model. Specifically, the responses of demand shocks during 2020-Q2 and 2020-Q3 appear to be overestimated. In the model with scaling factors, the volatility increase in 2020-Q2 is estimated to be more than five times the benchmark standard deviation. When considering shock heterogeneity, the volatility increase for demand shocks, such as exogenous expenditures and the investment-specific technology shock, is approximately twice the volatility in the benchmark scenario. Furthermore, the scaling factor in the third quarter is estimated to be lower than the additional variances estimated when accounting for heterogeneity, which translates into a slightly higher benchmark volatility for these shocks.

Figure 3.12: Prior and Posterior Distribution of the Scaling Factors

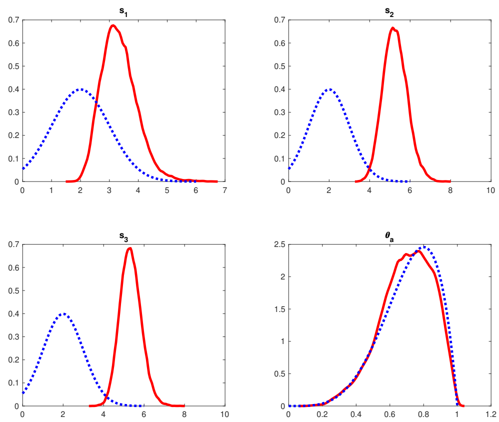

Note: The figure plots prior and posterior distributions for the scaling factors and the MA parameter in the Covid-19 model.

The estimates for the structural parameters and the expected are quantitatively similar to those obtained using additive variance terms. The results support the use of Covid-19 data in DSGE model estimations. Although both approaches produce similar results, I choose the additive variance approach as the baseline. The scaling factors do not account for what appears to be a considerable degree of heterogeneity in my model in how much shock volatilities change.

3.6 A Structural Shadow Rate during the Pandemic

While analyzing the expected durations at the ZLB can offer some insight into the stance of monetary policy during the pandemic, it can still be challenging to fully determine the monetary policy stance during this time. Factors such as unconventional policy measures may complicate the interpretation of the policy stance.

Policy rates typically reflect what a central bank seeks to accomplish in normal times. The ECB, unlike many central banks around the world, including the Federal Reserve Bank, could not employ conventional means of conducting expansionary monetary policy at this time. Ahead of the Covid-19 pandemic, the euro area policy rate had already reached its effective lower bound, and short-term and long-term government bond yields showed little variation.

During the Covid-19 pandemic, examining shadow rates may provide insight into the extent to which monetary policy has been expansionary. Shadow rates refer to alternative paths of interest rates that do not adhere to the ZLB and can be used to determine the equivalent of a fixed interest-rate regime. In recent years, various methods have been developed to calculate shadow rates. For instance, Black (1995) uses yield curve information to explain negative shadow rates, Krippner (2013) applies a ZLB framework based on non-negative forward rates from bonds to measure the stance of monetary policy in Japan, and Wu and Xia (2016) use a term-structure model to construct an unconstrained policy rate for the US and the euro area. These methods, however, rely solely on interest rate term structures and cannot differentiate between unconventional monetary policy measures and structural economic shocks. In contrast, De Rezende and Ristiniemi (2023) construct a shadow rate for the euro area that employs a term structure model and directly accounts for unconventional monetary policy actions without imposing a binding ZLB constraint. However, their shadow rate measure is not based on a structural model. Addressing the latter, Jones et al. (2022a) argue that to fully understand the stance of monetary policy, it is necessary to determine whether the duration of fixed interest rates is due to underlying shocks in the model or the result of deliberate monetary policy measures.

The euro area's situation in 2018 provides a useful example of why this distinction matters. At the time, the economic conditions had improved to the point where the actual policy constraint no longer applied. Instead, unconventional monetary policies were the sole driver of the ZLB at the time.

The estimates for expected durations had shortened, indicating a less expansionary stance of monetary policy during these quarters. The shadow rate estimate from the structural shadow rate approach of Jones et al. (2022a) reflects the net effects of both the

ZLB constraint and unconventional policy measures. Therefore, I expect that this shadow rate estimate is less expansionary than a term-structure shadow rate measure, which only considers the impact of the ZLB constraint.

The Jones et al. (2022a) shadow rate measure is based on the underlying structural model. By augmenting the vector of estimated structural shocks with alternative shocks that replicate the data outcomes under a ZLB regime in a *shadow* Taylor-rule regime, a structural shadow rate measure can be derived. While Jones et al. (2022a) construct a shadow rate for the US during the pandemic, they do so without including the Covid-19 data in estimation. In contrast, I use the proposed time-series approach to estimate the model for the extended euro area sample and estimate both the structural shocks and the sequence of expected durations during the Covid-19 pandemic.

3.6.1 Constructing the Structural Shadow Rate

The Jones et al. (2022a) structural measure for the shadow rate is based on a hypothetical scenario in which an unconstrained Taylor-rule regime would produce outcomes similar to those observed in a fixed-interest rate regime without the ZLB constraint. This allows the shadow rate measure to capture the effects of both the structural shocks and unconventional monetary policy measures on interest rate decisions.

Recall the time-invariant reduced form solution of the model when monetary policy is not constrained:

$$y_t = C + Qy_{t-1} + Ge_t \tag{3.15}$$

This solution corresponds to the monetary policy regime in which the central bank follows a standard Taylor-type rule. Furthermore, recall the time-varying reduced form solution for the fixed-interest rate regime:

$$y_t = C_t + Q_t y_{t-1} + G_t e_t \tag{3.16}$$

Since, by definition, the monetary shock is set to zero at the ZLB, the vector of structural shocks has to be augmented by a policy shock ε^*_{rt} in the shadow system. The shock is chosen so that the *shadow* system with the determinate rational expectation solution matrices in equation 3.15 matches some of the outcomes of the data in the time-varying ZLB solution in equation 3.16:

$$y_t^* = C + Qy_{t-1}^* + Ge_t^* \tag{3.17}$$

The method of calculating a structural shadow rate has the advantage of considering both economic conditions and unconventional monetary policy measures, which may have either expansionary or contractionary effects. This allows for a more comprehensive understanding of the stance of monetary policy and the factors influencing it. The structural shadow rate can be derived from the estimated policy rate in the shadow system, which is based on a hypothetical scenario in which an unconstrained Taylor-rule regime would produce outcomes similar to those observed in a fixed-interest rate regime. This approach enables the capture of the effects of both the structural shocks and deliberate monetary policy actions on interest rate decisions.

When the ZLB constraint is expected to bind, a shadow monetary policy shock is chosen to minimize the distance between selected variables in the shadow system and the same variables in the constrained system under a set of structural shocks e_t. Formally, denote ξ to be a vector of the targeted variables with $\Delta_t = \xi(y_t - y_t^*)$ denoting the difference between the observed targeted variables and the same variables that evolve in the shadow system. The shadow monetary policy shock ε_{rt}^* is chosen for each period to solve:

$$\min_{\varepsilon_{rt}^*} \Delta_t' W \Delta_t$$

The diagonal elements of W are inverses of the variances of the targeted variables, reflecting the volatility of those variables. Through this weighting scheme, data are effectively standardized, and, as a result, each variable is assigned equal weights. The shadow rate i_t^* is then constructed by applying the unconstrained policy rule to the shadow rate shock that satisfies the minimization problem.

3.6.2 The Structural Shadow Rate Estimate

The shadow rate measure for the euro area using the model from Smets and Wouters (2003, 2007) is calculated as described previously. However, unlike Jones et al. (2022a), who consider all observables, I focus on a subset of observables to account for developments during the Covid-19 pandemic. This allows for a more specific analysis of the implications of the pandemic on monetary policy.[13]

Figure 3.13: Structural Shadow Rate for the Euro Area

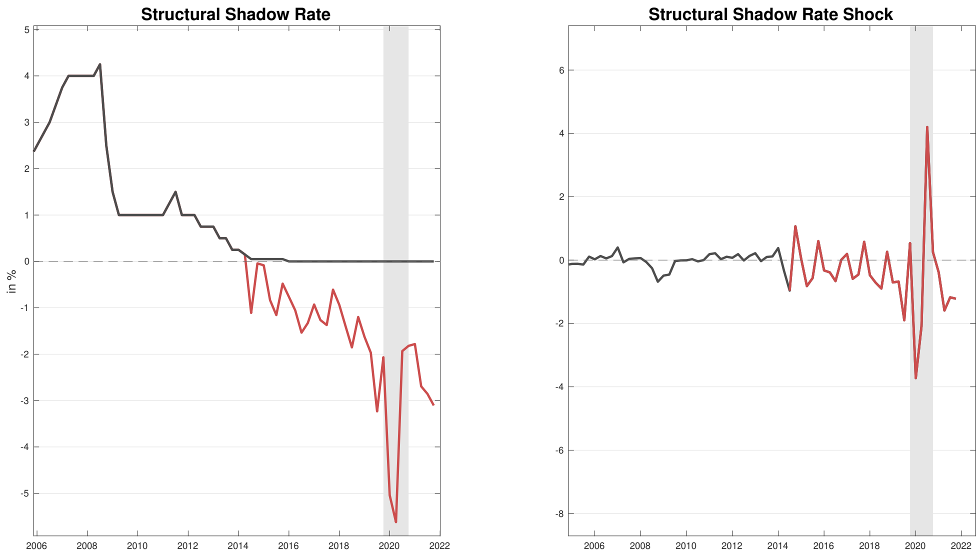

Note: The figure plots the estimated structural shadow rate measure for the euro area at the posterior mean during the ZLB (left panel) and the shadow rate shock (right panel).

Figure 3.13 depicts the estimated structural shadow rate and the shadow rate shock at the posterior mean. Throughout the ZLB period, the constructed shadow rate has consistently been lower than the MRO rate. In the period between 2014 and 2016, the structural rate fluctuates between 0% and -1%. The introduction of the asset purchasing program in 2015 and the further decrease of the MRO rate in early 2016 translate into expansionary policy and lead to a decrease in the shadow rate to approximately -1.5%. The estimated shadow rate indicates an expansionary stance of monetary policy compared to the policy response throughout the sample period, and peaks during the Covid-19

[13]Based on the results presented in this chapter, inflation and output are the most relevant variables for monetary policy. Nevertheless, the results are robust even when other combinations of targeted observables are taken into account, except for consumption, which is excluded from estimation during this period, and investment, which has been intertwined with consumption.

pandemic when the shadow rate decreased to almost -6%. In general, shadow rate shocks are negative during the ZLB period, but they exhibit exceptional volatility during the pandemic.

Figure 3.14: A Comparison of Different Shadow Rate Measures for the Euro Area

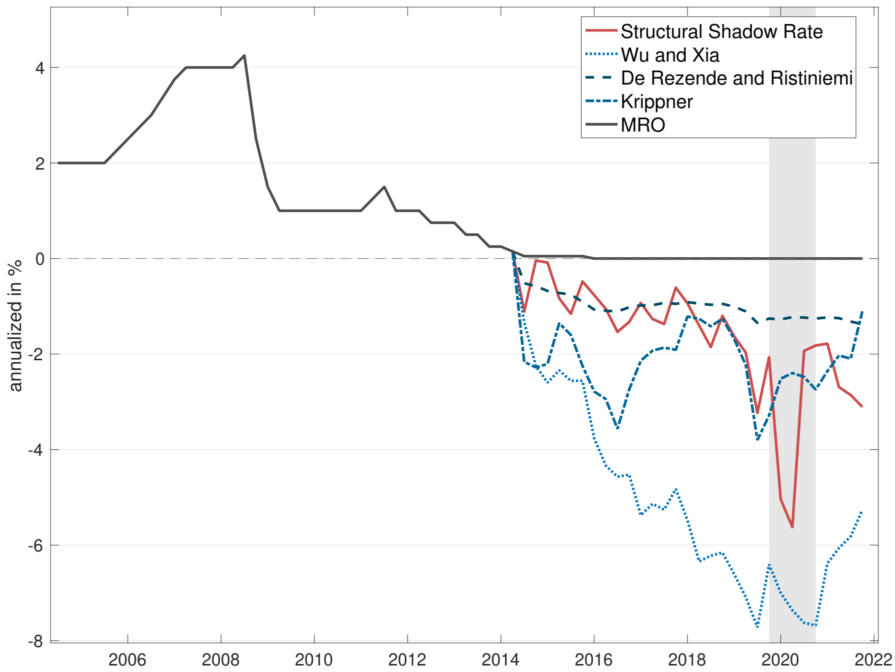

Note: This figure shows the MRO rate (solid grey line) and different shadow rate measures. The solid red line corresponds to the structural shadow rate measure calculated in this study. The dotted blue line plots the Wu and Xia (2016) shadow rate. The dashed blue line corresponds to the De Rezende and Ristiniemi (2023) shadow rate with two pricing factors and the dotted-dashed line plots the Krippner (2015) shadow rate.

Figure 3.14 shows a comparison between the structural shadow rate and shadow rates developed by Wu and Xia (2016), Krippner (2015), and De Rezende and Ristiniemi (2023). The estimated structural shadow rate follows a similar trend to the term-structure rate by Wu and Xia (2016) but is less negative at any given period. At the onset of the ZLB period in 2014, the two measures were nearly identical, but the structural shadow rate rose above the Wu and Xia (2016) measure and had pronounced fluctuations that appear to be closely linked to forward guidance announcements. The Wu and Xia (2016) measure reacts strongly to the announcement of the ECB to start with an Asset Purchasing Program (APP) in early 2015. In contrast, the Krippner (2015) measure predicts a tightening of monetary policy in the following months (for a discussion see, e.g., Elbourne et al., 2018).

The structural shadow rate measure still views this announcement as expansionary, but the effects are less pronounced and quantitatively closer to the recent shadow rates of De Rezende and Ristiniemi (2023) and Krippner (2015). All four measures react contractionary to announcements to reduce and eventually end the APP in 2017 and 2018, before turning expansionary to a worsening economic outlook in 2019.

Each of these measures displays a different pattern as the Covid-19 pandemic unfolded. The De Rezende and Ristiniemi (2023) shadow rate measure remains stable around -1% with little movement throughout the pandemic period. The Krippner (2015) shadow rate measure reacts contractionary at the onset of the pandemic before slightly falling in the subsequent quarters. The Wu and Xia (2016) measure has consistently been around -6% to -8% since 2017 and reacts only marginally but expansionary to the Covid-19 shock. The shadow rate measures of Krippner (2015) and De Rezende and Ristiniemi (2023) show no visible movement. In contrast, the structural measure constructed in this chapter shows a noticeable decline that almost closes the gap between the two measures, peaking at close to -6% in 2020-Q2. In the Covid-19 pandemic, economic uncertainty may have contributed to the large drop. In the ECB's Survey of Professional Forecasters, expected duration reports increased, suggesting that agents expected the ZLB to bind for a longer period of time during the onset of the pandemic. It was understood by rational agents at that time that once social health restrictions were lifted, temporary policy measures would likely be rolled back and the monetary policy stance would return to pre-pandemic levels, as indicated by the immediate rebound in the structural shadow rate. During the second period of lockdowns in 2021, the structural measure becomes once again expansionary, whereas the Wu and Xia (2016) and the Krippner (2015) measures continue to have an increasing trend.

Similar to the sensitivity observed in term structure shadow rate models to changes in the estimation procedure as discussed in Krippner (2020), the measurement of the structural shadow rate may exhibit sensitivity to the underlying structural model. However, as highlighted by Jones et al. (2022a), the approach has the potential to be robust across different model specifications due to incorporating expected durations based not only on survey data but also estimates of the structural shocks and the model-implied monetary policy rule.

3.6.3 The Role of the MA Parameter for TFP Shock Innovations

When estimating the model with the Covid-19 sample period, the moving average (MA) correction for TFP shock innovations reduces their persistence effectively. The MA coefficient, θ^a, is estimated with a mean of 0.72, which is lower than the persistence parameter of the technology shock ($\rho^a = 0.87$). Similarly, when the MA coefficient is combined with the parameter in the exogenous spending shock that indicates the relevance of TFP shock innovations for the shock, the MA coefficient is once again smaller than the autoregressive coefficient for the exogenous spending shock. This indicates that the persistence of TFP shock innovations in 2020-Q1 and 2020-Q2 has been significantly reduced, but not entirely offset. By setting the MA coefficient equal to the autoregressive coefficient, it would prevent any persistent effects of TFP shock innovation in 2020-Q1 and 2020-Q2.

Figure 3.15: Structural Shadow Rate without ARMA correction

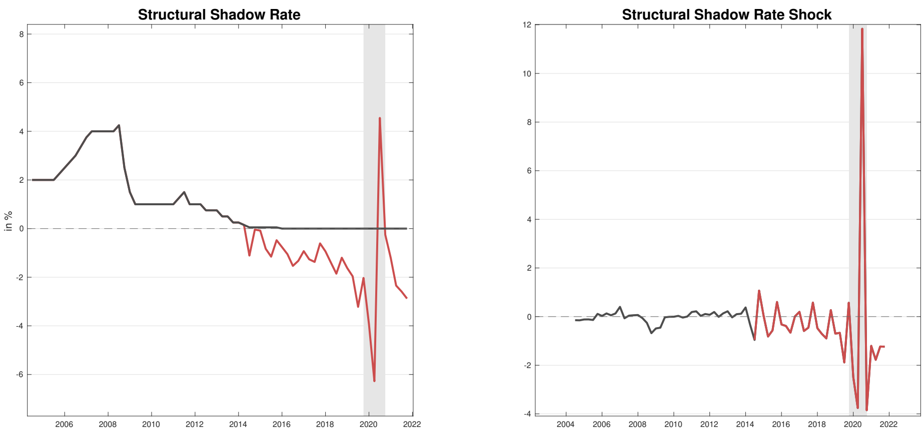

Note: The figure plots the estimated structural shadow rate measure for the euro area at the posterior mean during the ZLB (left panel) and the shadow rate shock (right panel) when the MA parameter θ^a is set to zero.

Without the MA dynamics in the shock processes, the highly negative shock innovations observed in the first half of 2020 would have persistent effects, as illustrated in Figure 3.15. As a result, the rebound effect would be considered a highly positive shock to the economy, for which the model implies not only a liftoff but also a policy rate exceeding four percent. The shadow rate displayed similar behavior before and during the Covid-19 shock, as in the model with MA correction, although it showed a more pronounced downward movement in 2020-Q2.

The persistence of TFP shock innovations over the course of the Covid-19 pandemic may indicate that the constraint is expected to bind for a longer period, resulting in a long duration of the lower bound. As a result, the spike in the shadow rate can be attributed to the sudden disappearance of lower bound durations in the quarter following the rebound. Although long lower bound durations are still estimated with the MA parameter included the spike in the shadow rate has been eliminated.

The decline in TFP shock innovations appears to indicate that agents expected the loss of productivity to be transitory and expected an immediate recovery as soon as the lockdowns and social health measures had been lifted. As a result, the shadow rate projects a much smoother path during the rebound quarter. Rather than interpreting the rebound effect as an expansionary impact on the economy, agents understood it to be simply a result of lockdown easing, which resulted in the shadow rate returning to its pre-pandemic level.

3.7 Conclusion

The Covid-19 pandemic has been the largest contractionary shock to hit the euro area in recent history, including both the Great Financial Crisis and the Sovereign Debt Crisis. The large additional variation in the Covid-19 data and its low persistence presents challenges for the estimation of DSGE models and can distort structural parameter and expected duration estimates.

This chapter aims to extend the literature on estimating Covid-19 outliers in VAR models (e.g., Lenza and Primiceri, 2022, Carriero et al., 2021, Schorfheide and Song, 2021) to structural DSGE models. For this, I propose a time-series approach to deal with the extreme data outliers observed during the Covid-19 pandemic. My approach, in the spirit of Lenza and Primiceri (2022) for VAR models, makes three adjustments to the standard estimation procedure without modifying the structural equations of the model. I introduce a time-varying shock innovation-covariance matrix that captures the extreme heteroskedasticity in the shock variances, an Autoregressive Moving Average

(ARMA) correction to lower the persistence of effects of total factor productivity shock innovations during the pandemic, and a measurement correction for consumption data using the Kalman filter. The latter is required as the measured consumption data does not reflect the behavioral responses during previous periods and, therefore, is not informative about structural parameters related to consumption behavior. The adjustments to the estimation procedure are straightforward to implement and do not require an adjustment to the structural equations of the model.

Results yield similar structural parameter estimates to the original Smets and Wouters (2003, 2007) estimation results and to those for the pre-Covid-19 sample presented in Chapter I and Chapter II of this thesis.

In addition, the framework allows for an assessment of monetary policy during the Covid-19 pandemic despite being at the ZLB at the time. Overall, while incorporating Covid-19 data delivers robust parameter estimates compared to the pre-Covid-19 sample, it implies somewhat longer forward guidance durations. In early 2020, the estimates of the expected durations indicate an expansionary stance of monetary policy throughout the Covid-19 pandemic quarters. This is confirmed by the construction of a structural shadow rate measure based on the approach in Jones et al. (2022a). This measure is based on the underlying structural model and so incorporates the developments of structural shocks in the economy but also accounts for unconventional monetary policy actions. Compared to other shadow rate measures, such as Krippner (2013), Wu and Xia (2016), and De Rezende and Ristiniemi (2023), the structural shadow rate indicates a fully expansionary stance of monetary policy despite the lack of movement in the yield curve.

3.8 Chapter III Appendix

Figure 3.16: Prior and Posterior Distributions for the Additive Shock Variances

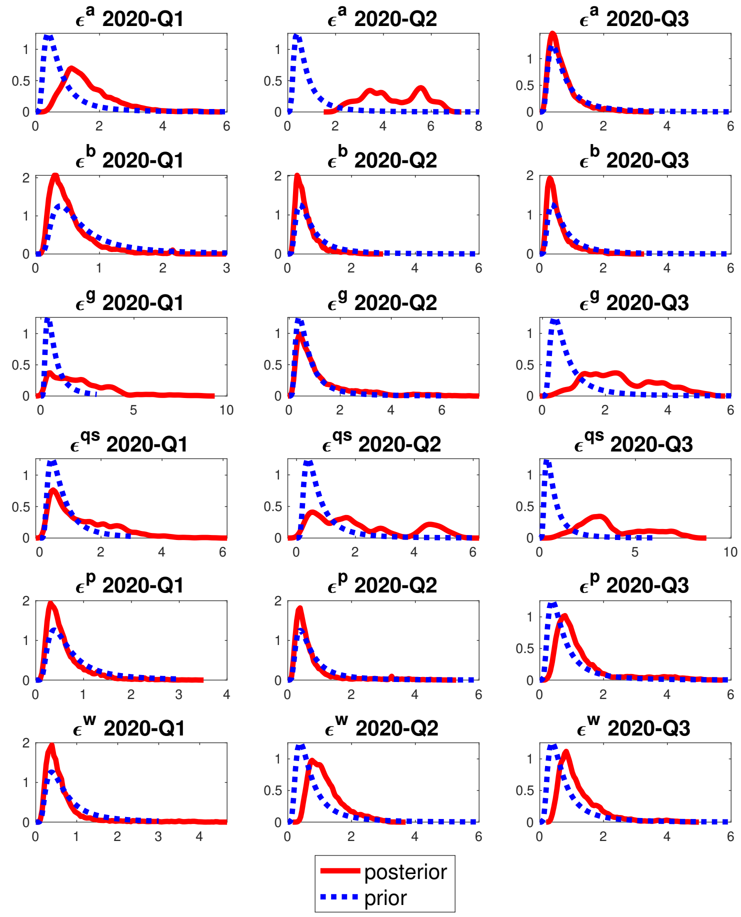

Note: This figure depicts the prior and posterior distributions of each shock over the sample period. ε_t^a (TFP), ε_t^b (risk premium), ε_t^g (exogenous spending), ε_t^p (price mark-up), ε_t^w (wage mark-up), qs_t (investment-technology), ε_t^m (monetary policy), ε_t^4 (1Y Term Premium), and ε_t^{20} (5Y Term Premium). As in Smets and Wouters (2003, 2007), the demand shocks include the risk premium, investment-specific technology, and exogenous spending shocks.

Figure 3.17: Historical Shock Decomposition for Consumption and Investment

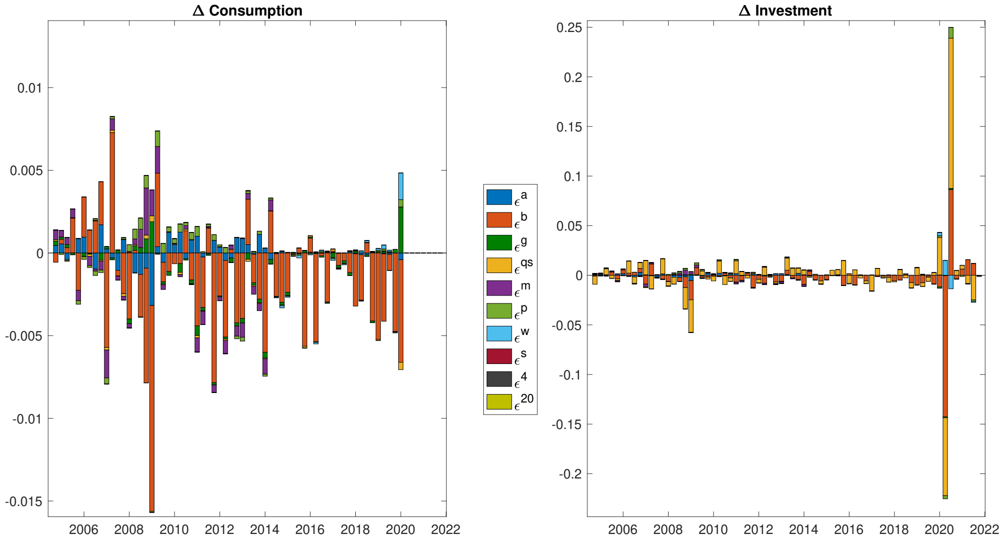

Note: This figure depicts the historical contribution of each shock to consumption and investment over the sample period. ε_t^a (TFP), ε_t^b (risk premium), ε_t^g (exogenous spending), ε_t^p (price mark-up), ε_t^w (wage mark-up), qs_t (investment-technology), ε_t^m (monetary policy), ε_t^4 (1Y Term Premium), and ε_t^{20} (5Y Term Premium). As in Smets and Wouters (2003, 2007), the demand shocks include the risk premium, investment-specific technology, and exogenous spending shocks. Trend growth is estimated at 0.8 percent and mean inflation is estimated at 2 percent.

Figure 3.18: Historical Shock Decomposition for the 1Y Rate and the 5Y Rate

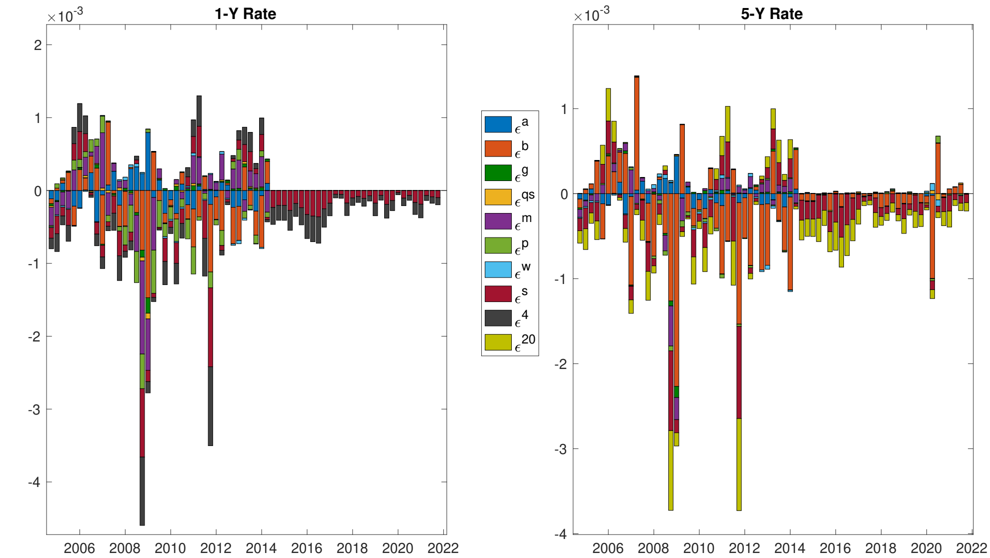

Note: This figure depicts the historical contribution of each shock to the 1Y rate and the 5Y rate over the sample period. ε_t^a (TFP), ε_t^b (risk premium), ε_t^g (exogenous spending), ε_t^p (price mark-up), ε_t^w (wage mark-up), qs_t (investment-technology), ε_t^m (monetary policy), ε_t^4 (1Y Term Premium), and ε_t^{20} (5Y Term Premium). As in Smets and Wouters (2003, 2007), the demand shocks include the risk premium, investment-specific technology, and exogenous spending shocks. Trend growth is estimated at 0.8 percent and mean inflation is estimated at 2 percent.

Figure 3.19: Prior and Posterior Distribution for the Expected Duration Estimates

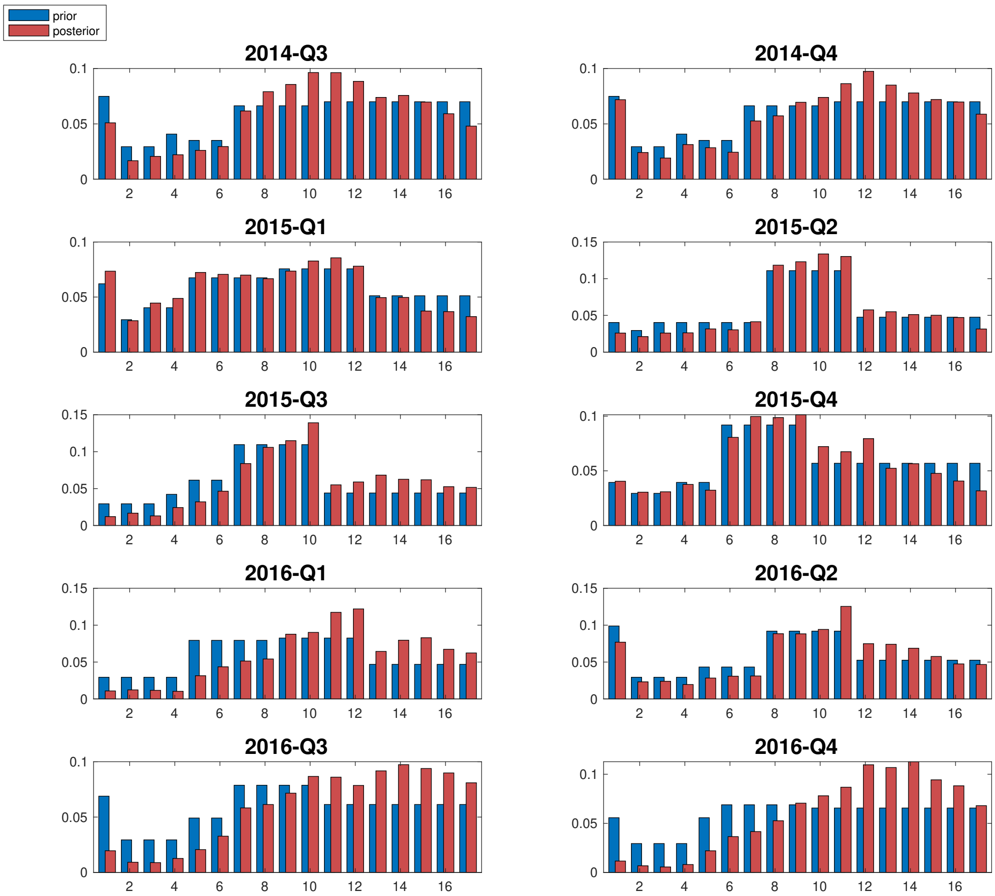

Note: The figure plots the prior and posterior distribution of the duration estimates from 2014-Q3 to 2016-Q4. The prior is constructed as an equally weighted combination of the distribution implied by the SPF data and a uniform distribution over all possible durations.

Figure 3.20: Prior and Posterior Distribution for the Expected Duration Estimates

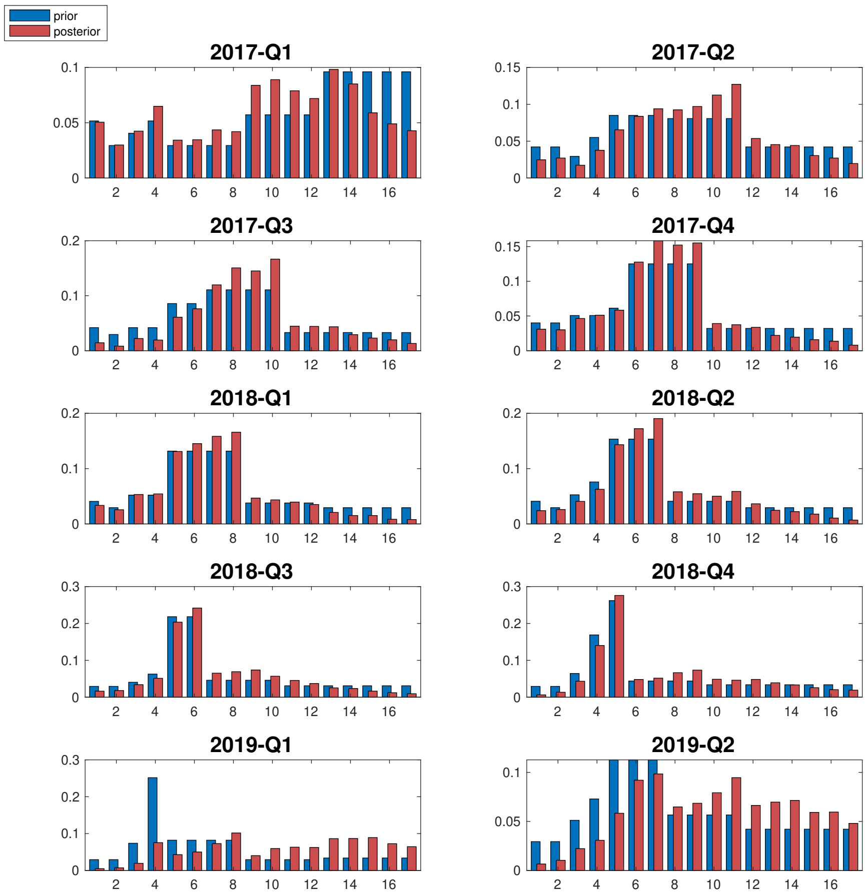

Note: The figure plots the prior and posterior distribution of the duration estimates from 2017-Q1 to 2019-Q2. The prior is constructed as an equally weighted combination of the distribution implied by the SPF data and a uniform distribution over all possible durations.

Figure 3.21: Prior and Posterior Distribution for the Expected Duration Estimates

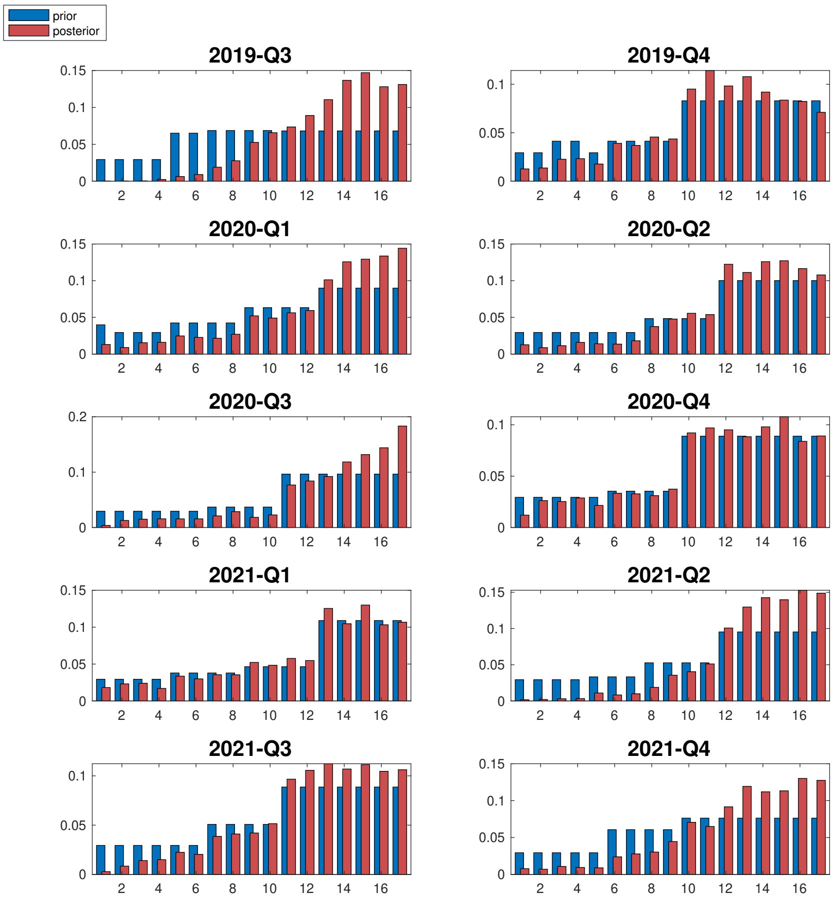

Note: The figure plots the prior and posterior distribution of the duration estimates from 2019-Q3 to 2021-Q4. The prior is constructed as an equally weighted combination of the distribution implied by the SPF data and a uniform distribution over all possible durations.

Concluding Chapter

The three chapters of this thesis explore the transmission of monetary policy during unconventional times. Chapter I estimates a medium-sized DSGE model for the euro area when interest rates are constrained at the zero lower bound (ZLB). Results indicate that agents' expectations regarding how long the interest rate will remain at zero play a significant role in the model's non-linear dynamics. The framework provides an additional channel for unconventional monetary policy in the form of forward guidance when the expected duration of the ZLB constraint exceeds what is implied by the underlying rule.

Chapter II investigates the role of liftoff expectations in mitigating the effects of forward guidance dynamics, finding that a passive monetary policy regime upon liftoff can significantly dampen the expansionary effects on the real economy, even causing deflationary pressures.

Finally, Chapter III aims to extend the literature on estimating the extreme Covid-19 outliers in VAR models to structural DSGE models. I propose a time-series approach that adjusts the estimation procedure to deal with the extreme data outliers observed during the Covid-19 pandemic. This approach can be used to assess monetary policy during the Covid-19 pandemic even though interest rates were constrained at the ZLB during this time.

Appendix A

Technical Appendix

A.1 Additional Information on the Data

$$
\begin{bmatrix} n^{obs} \end{bmatrix} = \begin{bmatrix} \Delta logGDP_t \\ \Delta logC_t \\ \Delta logI_t \\ \Delta logW \\ logH_t \\ \Delta log\pi_t \\ MRO_t \\ Y_t^4 \\ Y_t^{20} \end{bmatrix} = \begin{bmatrix} \bar{\gamma} \\ \bar{\gamma} \\ \bar{\gamma} \\ \bar{\gamma} \\ \bar{l} \\ \bar{\pi} \\ \bar{r} \\ \bar{r}+c^4 \\ \bar{r}+c^{20} \end{bmatrix} + \begin{bmatrix} y_t - y_{t-1} \\ c_t - c_{t-1} \\ i_t - i_{t-1} \\ w_t - w_{t-1} \\ l_t \\ \pi_t \\ r_t \\ r_t^4 \\ r_t^{20} \end{bmatrix}
$$

where $\bar{\gamma}$ denotes the quarterly growth rate to GDP, consumption, investment, and wages. Moreover, $\bar{\pi}$ is the quarterly steady state inflation rate, $\bar{r}$ the steady state interest rate, and $\bar{l}$ the steady state hours worked. c^4 and c^{20} are maturity-specific time-invariant components.

Figure A.1: Observable Variables

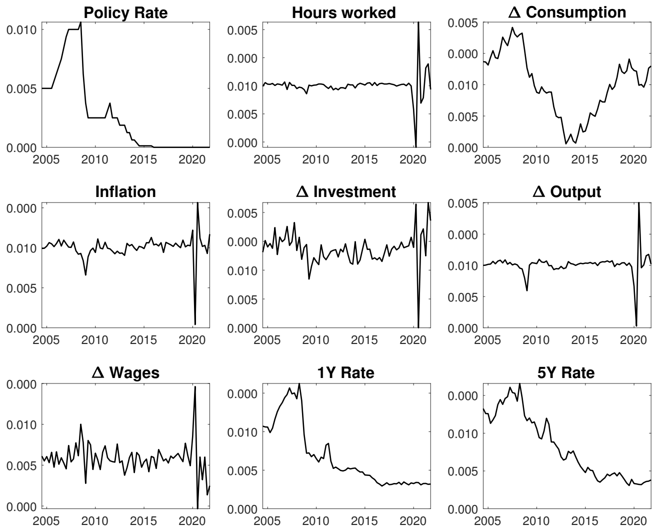

Note: The figure plots the nine observables for the Covid-19 sample: Real GDP, real consumption, real investment, and real wages, hours worked, the GDP deflator as the measure for inflation, the MRO rate, and at 1-year and 5-year rates. The data sample captures the period from 2004:Q3 to 2021:Q4. The benchmark and the sunspot model are sub-samples of the Covid-19 sample that captures the period from 2004:Q3 to 2019:Q4 Source: ECB, Eurostat

Figure A.2: Interest Rate and Yield Curve Developments in the Euro Area

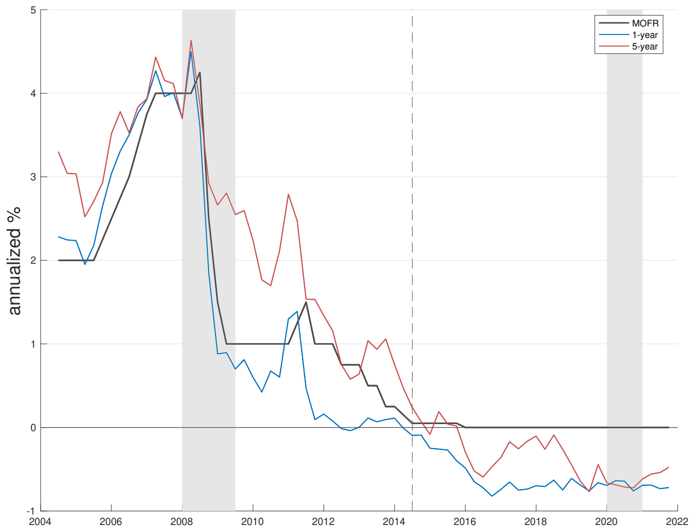

Note: The figure plots the main operating financing rate and AAA-rated euro area central government bonds at different maturities: MRO rate (black line), 1-year (blue line), 5-year (red line). Source: ECB SDW.

A.2 The Model

A.2.1 Sticky Price Economy

Consumption Euler Equation:

$$\hat{c}_t = \frac{\frac{\lambda}{\gamma}}{1+\frac{\lambda}{\gamma}}\hat{c}_{t-1} + \frac{1}{1+\frac{\lambda}{\gamma}}E_t(\hat{c}_{t+1}) + \frac{(\sigma^c-1)(\frac{W_*^h L_*}{C_*})}{\sigma^c(1+\frac{\lambda}{\gamma})}(\hat{l}_t - E_t(\hat{l}_{t+1})) - \frac{1-\frac{\lambda}{\gamma}}{\sigma^c(1+\frac{\lambda}{\gamma})}(\hat{r}_t - E_t(\hat{\pi}_{t+1})) + \varepsilon_t^b \tag{A.1}$$

Resource constraint:

$$\hat{y}_t = c_y\hat{c}_t + i_y\hat{i}_t + z_y\hat{z}_t + \varepsilon_t^g \tag{A.2}$$

Investment decision:

$$\hat{i}_t = \frac{1}{1+\beta\gamma^{(1-\sigma^c)}}\hat{i}_{t-1} + \frac{\beta\gamma^{(1-\sigma^c)}}{1+\beta\gamma^{(1-\sigma^c)}}E_t(\hat{i}_{t+1}) + \frac{1}{(\beta\gamma^{(1-\sigma^c)})\gamma^2\varphi}\hat{q}_{t-1} + \varepsilon_t^{qs} \tag{A.3}$$

$$\hat{q}_t = \frac{(1-\delta)}{R_*^k+(1-\delta)}E_t(\hat{q}_{t+1}) + \frac{R_*^k}{R_*^k+(1-\delta)}E_t(\hat{r}_{t+1}^k) + \frac{\sigma^c(1+\frac{\lambda}{\gamma})}{1-\frac{\lambda}{\gamma}}\varepsilon_t^b - (\hat{r}_t - E_t(\hat{\pi}_{t+1})) \tag{A.4}$$

Capital accumulation:

$$\hat{k}_t = \frac{1-\delta}{\gamma}\hat{k}_{t-1} + \frac{\gamma-(1-\delta)}{\gamma}\hat{i}_t + (1-\frac{1-\delta}{\gamma})(\gamma^2\varphi)\varepsilon_t^{qs} \tag{A.5}$$

Production Function:

$$\hat{y}_t = \phi_p\left(\alpha\hat{k}_t^s + (1-\alpha)l_t + \varepsilon_t^a\right) \tag{A.6}$$

$$\hat{k}_t^s = \hat{k}_{t-1} + \hat{z}_t \tag{A.7}$$

Factor prices:

$$\hat{z}_t = \frac{1-\psi}{\psi}\hat{r}_t^k \tag{A.8}$$

$$\hat{mc}_t = \hat{mpl}_t - \hat{w}_t = \alpha \hat{r}^k_t + (1-\alpha)\hat{w}_t - \varepsilon^a_t \tag{A.9}$$

$$\hat{r}^k_t = \hat{w}_t - \hat{k}^s_t + \hat{l}_t \tag{A.10}$$

$$\hat{\mu}^w_t = \hat{w}_t - \hat{mrs}_t = w_t - \big(\sigma^l \hat{l}_t + \frac{1}{1-\frac{\lambda}{\gamma}}(\hat{c}_t - \frac{\lambda}{\gamma}\hat{c}_{t-1})\big) \tag{A.11}$$

Price and Wage Philips Curve:

$$\hat{\pi}_t = \frac{1}{1+\beta\gamma^{1-\sigma^c}\iota_p}\big(\beta\gamma^{1-\sigma^c}E_t(\hat{\pi}_{t+1}) + \iota_p\hat{\pi}_{t-1} + \frac{(1-\xi_p)(1-\beta\gamma^{1-\sigma^c}\xi_p)}{\xi_p((\phi_p-1)\epsilon_p+1)}\hat{mc}_t\big) + \varepsilon^p_t \tag{A.12}$$

$$\begin{aligned}\hat{w}_t = &\frac{1}{(1+\beta\gamma^{1-\sigma^c})}\hat{w}_{t-1} + \frac{\beta\gamma^{1-\sigma^c}}{(1+\beta\gamma^{1-\sigma^c})}(E_t(\hat{w}_{t+1}) + E_t(\hat{\pi}_{t+1})) - \frac{1+\beta\gamma^{1-\sigma^c}\iota_w}{(1+\beta\gamma^{1-\sigma^c})}\hat{\pi}_t \\ &+ \frac{\iota_w}{(1+\beta\gamma^{1-\sigma^c})}\hat{\pi}_{t-1} - \frac{(1-\xi_w)(1-\beta\gamma^{1-\sigma^c}\xi_w)}{\big((1+\beta\gamma^{1-\sigma^c})\xi_w\big)\big((\phi_w-1)\epsilon_w+1\big)}\hat{\mu}^w_t + \varepsilon^w_t\end{aligned} \tag{A.13}$$

A.2.2 Flexible Price Economy

$$\hat{c}^f_t = \frac{\frac{\lambda}{\gamma}}{1+\frac{\lambda}{\gamma}}\hat{c}^f_{t-1} + \frac{1}{1+\frac{\lambda}{\gamma}}E_t(\hat{c}^f_{t+1}) + \frac{(\sigma^c-1)(\frac{W^h_* L_*}{C_*})}{\sigma^c(1+\frac{\lambda}{\gamma})}(\hat{l}^f_t - E_t(\hat{l}^f_{t+1})) - \frac{1-\frac{\lambda}{\gamma}}{\sigma^c(1+\frac{\lambda}{\gamma})}\hat{rr}^f_t + \varepsilon^b_t \tag{A.14}$$

$$\hat{y}^f_t = c_y\hat{c}^f_t + i_y\hat{i}^f_t + z_y\hat{z}^f_t + \varepsilon^g_t \tag{A.15}$$

$$\hat{i}^f_t = \frac{1}{1+\beta\gamma^{(1-\sigma^c)}}\hat{i}^f_{t-1} + \frac{\beta\gamma^{(1-\sigma^c)}}{1+\beta\gamma^{(1-\sigma^c)}}E_t(\hat{i}^f_{t+1}) + \frac{1}{(\beta\gamma^{(1-\sigma^c)})\gamma^2\varphi}\hat{q}^f_{t-1} + \varepsilon^{qs}_t \tag{A.16}$$

$$\hat{q}_t^f = \frac{(1-\delta)}{R_*^k + (1-\delta)} E_t(\hat{q}_{t+1}^f) + \frac{R_*^k}{R_*^k + (1-\delta)} E_t(\hat{r}k_{t+1}^f) + \frac{\sigma^c(1+\frac{\lambda}{\gamma})}{1-\frac{\lambda}{\gamma}} \varepsilon_t^b - \hat{r}r_t^f \tag{A.17}$$

$$\hat{k}_t^f = \frac{1-\delta}{\gamma} \hat{k}_{t-1}^f + \frac{\gamma-(1-\delta)}{\gamma} \hat{i}_t^f + (1 - \frac{1-\delta}{\gamma})(\gamma^2\varphi)\varepsilon_t^{qs} \tag{A.18}$$

$$\hat{y}_t^f = \phi_p \Big(\alpha \hat{k}_t^{sf} + (1-\alpha) l_t^f + \varepsilon_t^a \Big) \tag{A.19}$$

$$\hat{k}_t^{sf} = \hat{k}_{t-1}^f + \hat{z}_t^f \tag{A.20}$$

$$\hat{z}_t^f = \frac{1-\psi}{\psi} \hat{r}_t^{kf} \tag{A.21}$$

$$0 = \alpha \hat{r}_t^{kf} + (1-\alpha)\hat{w}_t^f - \varepsilon_t^a \tag{A.22}$$

$$\hat{r}_t^{kf} = \hat{w}_t^f - \hat{k}_t^{sf} + \hat{l}_t^f \tag{A.23}$$

$$\hat{w}_t^f = \sigma^l \hat{l}_t^f + \frac{1}{1-\frac{\lambda}{\gamma}} \hat{c}_t^f - \frac{\frac{\lambda}{\gamma}}{1-\frac{\lambda}{\gamma}} \hat{c}_{t-1}^f \tag{A.24}$$

A.2.3 Taylor Rule and Yield Curve

$$\hat{r}_t \equiv \begin{cases} TR, & \text{for } t < T \\ -r, & \text{for } T \leq t < T^* \\ TR, & \text{for } T \geq T^* \end{cases}$$

where TR:

$$\hat{r}_t = \rho_R \hat{r}_{t-1} + (1-\rho_R)(\phi_\pi \hat{\pi}_t + \phi_y(\hat{y}_t - \hat{y}_t^f)) + \phi_{\Delta y}[(\hat{y}_t - \hat{y}_{t-1}) - (\hat{y}_t^f - \hat{y}_{t-1}^f)] + \varepsilon_t^m \quad \text{(A.25)}$$

Yield Curve:

$$r_{j,t} = \hat{r}_{j,t} + r + c_j + \eta_t + \varepsilon_{j,t} \qquad for \;\; j = 2,3,...,m \quad \text{(A.26)}$$

A.2.4 Structural Shocks

Technology Shock:

$$\varepsilon_t^a = \rho^a \varepsilon_{t-1}^a + \eta_t^a \quad \text{(A.27)}$$

Household Preference Shock:

$$\varepsilon_t^b = \rho^b \varepsilon_{t-1}^b + \eta_t^b \quad \text{(A.28)}$$

Government Spending Shock:

$$\varepsilon_t^g = \rho^g \varepsilon_{t-1}^g + \eta_t^g + \rho^{ga} \eta_t^a \quad \text{(A.29)}$$

Monetary Policy Shock:

$$\varepsilon_t^m = \rho^m \varepsilon_{t-1}^m + \eta_t^m \quad \text{(A.30)}$$

Investment Technology Shock:

$$\varepsilon_t^{qs} = \rho^{qs} \varepsilon_{t-1}^{qs} + \eta_t^{qs} \quad \text{(A.31)}$$

Price mark-up Shock[1]

$$\varepsilon_t^p = \rho^p \varepsilon_{t-1}^p + \eta_t^p \tag{A.32}$$

Wage Mark-up Shock:

$$\varepsilon_t^w = \rho^w \varepsilon_{t-1}^w + \eta_t^w \tag{A.33}$$

Yield Curve Shock[2]

$$\eta_t = \rho^\eta \eta_{t-1} + \varepsilon_{\eta,t} \tag{A.34}$$

[1]Smets and Wouters (2007) propose an ARMA(1,1) process for the price and wage Phillips curve shocks. These are not well identified for the European data sample. In a previous version of the model for the euro area, Smets and Wouters (2003) assume the three cost pushed shocks (ϵ_p, ϵ_q, and ϵ_w) to be iid-normal processes.

[2]Furthermore, I examine shocks specific to maturity periods of 4 quarters and 20 quarters.

A.3 Solution Strategy

A.3.1 Time-Invariant solution

The model can be cast into state-space form following Binder and Pesaran (1995, 1997). A rational expectation model that is linearized around a non-stochastic steady state can be cast in the following form:[3]

$$A_0 y_t = C_0 + A_1 y_{t-1} + B_0 E_t y_{t+1} + D_0 \varepsilon_t \tag{A.35}$$

where y_t is a $nx1$ vector of endogenous variables with $k \leq n$ forward-looking (non-predetermined) variables and ε_t is a $lx1$ vector of exogenous shocks. The dimensions of the remaining matrices of the system can be summarized as:

$$\begin{array}{cc} A_0 & n \times n \\ C & n \times 1 \\ A_1 & n \times n \\ B_0 & n \times n \\ D_0 & n \times l \end{array}$$

Given that all agents form rational expectations under a known regime, the unique solution is a VAR of the following form:

$$y_t = C + Q y_{t-1} + G \varepsilon_t \tag{A.36}$$

where C, Q, and G are conformable matrices. Given $E_t \varepsilon_{t+1} = 0$, and $E_t y_{t+1} = C + Q y_t$, substituting equation A.36 into equation A.35 and rearranging terms subsequently

[3] The following derivation of the Binder and Pesaran (1995, 1997) algorithm contains supplementary explanations and notations form Kulish and Pagan (2017), which support the understanding of the mathematical representation.

delivers:

$$A_0 y_t = C + A_1 y_{t-1} + B_0[C + Q y_t + G E_t \varepsilon_{t+1}] + D_0 \varepsilon_t \tag{A.37}$$

$$(A_0 - B_0 Q) y_t = C + A_1 y_{t-1} + B_0 C + D_0 \varepsilon_t \tag{A.38}$$

$$y_t = (A_0 - B_0 Q)^{-1}(C + A_1 y_{t-1} + B_0 C + D_0 \varepsilon_t) \tag{A.39}$$

Re-writing $(A_0 - B_0 Q)^{-1} = (I - A_0^{-1} B_0 Q)^{-1} A_0^{-1}$ and defining $\Gamma \equiv A_0^{-1} C, A \equiv A_0^{-1} A_1, B \equiv A_0^{-1} B_0$, and $D \equiv A_0^{-1} D_0$ the system becomes:

$$y_t = (I - A_0^{-1} B_0 Q)^{-1} A_0^{-1}(C + A_1 y_{t-1} + B_0 C + D_0 \varepsilon_t) \tag{A.40}$$

$$y_t = (I - BQ)^{-1}(\Gamma + BC + A y_{t-1} - D \varepsilon_t) \tag{A.41}$$

Equation A.41 has to be equal to equation A.36, which implies that:

$$(I - BQ)^{-1}(\Gamma + BC) = C \tag{A.42}$$

$$(I - BQ)^{-1} A = Q \tag{A.43}$$

$$(I - BQ)^{-1} D = G \tag{A.44}$$

Equation A.43 determines Q by implying that:

$$A - Q + BQ^2 = 0 \tag{A.45}$$

Furthermore, by showing that equation A.42 can be transformed to:

$$C = \left[(I - (I - BQ)^{-1} B\right]^{-1} (I - BQ)^{-1} \Gamma \tag{A.46}$$

where $\Lambda = (I - BQ)^{-1} \Gamma$ and $F = (I - BQ)^{-1} B$, the equation becomes:

$$C = (I - F)^{-1} \Lambda \tag{A.47}$$

Once Q is found, it is possible to determine C and G, and thereby the solution of the model.

A.3.2 Time-Varying solution

To derive the solution during the ZLB period, re-consider the time-varying VAR solution for the LRE model:

$$y_t = C_t + Q_t y_{t-1} + G_t \varepsilon_t \tag{A.48}$$

Assuming $E_t \varepsilon_{t=1} = 0$ implies that in period $t+1$:

$$E_t y_{t+1} = C_{t+1} + Q_{t+1} y_t \tag{A.49}$$

By using equation A.49 and the canonical form of the structural equations during the ZLB (equation A.48), the following conditions can be derived for the time-varying regime:

$$(I - B^* Q_{t+1})^{-1}(\Gamma + B^* C_{t+1}) = C_t \tag{A.50}$$

$$(I - B^* Q_{t+1})^{-1} A^* = Q_t \tag{A.51}$$

$$(I - B^* Q_{t+1})^{-1} D^* = G_t \tag{A.52}$$

Equation A.51 implies that the solution for Q_t involves a backward recursion:

$$A^* - Q_t + B^* Q_{t+1} Q_t = 0 \tag{A.53}$$

Starting from the solution to the final structure $Q_{d+1} = Q$, choose sequence $\{Q_t\}_{t=T}^{T+d}$ such that equation A.53 is satisfied. With this sequence we can determine sequence $\{G_t\}_{t=T}^{T+d}$ and $\{C_t\}_{t=T}^{T+d}$ which completes the solution of the model. Kulish and Pagan (2017) derive the necessary conditions for the existence of a unique and stable final structure Q solution and include the existence and uniqueness of the sequence $\{Q_t\}_{t=T}^{T+d}$. Consequently, to guarantee a unique and stable solution $(I - B_t Q_{t+1})$ must be invertible and therefore of full rank. Equation A.53 can be written as:

$$\Lambda_t + F_t C_{t+1} = C_t \tag{A.54}$$

where $\Lambda_t = (I - BQ_{t+1})^{-1}\Gamma$ and $F_t = (I - BQ_{t+1})^{-1}B$. After deriving Q_t, C_t can be solved through a forward recursion of the form:

$$C_t = \Lambda_t + F_t\Lambda_{t+1} + F_t F_{t+1}\Lambda_{t+2} + ... \tag{A.55}$$

At the ZLB, $t = T, ..., T^* - 1$, the solution to the system is a time-varying VAR, which depends on the anticipated changes to the structure.

A.3.3 The Sunspot Solution under Indeterminacy

Under indeterminacy, $I - BQ$ is not invertible and therefore, the solution derived before is not feasible. The sunspot solution follows Bianchi and Nicolò (2021) and Gibbs and McClung (2023) and provides auxiliary equations to make the matrix singular.

A LRE model has a unique and stable solution if and only if the number of unstable roots η_f, eigenvalues that are larger than one, is equal to the number of forward-looking variables. Recall that k denotes the number of forward-looking variables in the system. When the number of unstable eigenvalues is smaller than the number of forward-looking variables, the model solution is indeterminate ($\eta_f < k$). The degree of indeterminacy is then defined by how many auxiliary equations are needed to guarantee a stable solution $m = k - \eta_f$. As in Gibbs and McClung (2023), I use the sunspot solution proposed by Bianchi and Nicolò (2021):

$$s_t = \begin{pmatrix} \frac{1}{\varrho_1} & 0 & \dots & 0 \\ 0 & \frac{1}{\varrho_2} & \dots & 0 \\ \vdots & 0 & \ddots & \vdots \\ 0 & \dots & 0 & \frac{1}{\varrho_m} \end{pmatrix} s_{t-1} + \begin{pmatrix} x_{1,t} - E_t x_{1,t} \\ x_{2,t} - E_t x_{2,t} \\ \vdots \\ x_{m,t} - E_t x_{m,t} \end{pmatrix} - \begin{pmatrix} \nu_{1,t} \\ \nu_{2,t} \\ \dots \\ \nu_{m,t} \end{pmatrix} \tag{A.56}$$

where s_t is an autoregressive parameter dependent on parameter $\varrho < 1$ and the degrees of indeterminacy m. $\nu = (\nu_1, \nu_2, ..., \nu_m)'$ is a sunspot shock with standard deviation σ^ν and $x = (x_1, x_2, ..., x_m)'$ is a one-period ahead forecast error associated with the forward-looking variable that follow the sunspot process.

Equation A.56 is added to the determinate system (equation A.35) which delivers a revised canonical form:

$$A_0^s y_t^s = C_0^s + A_1^s y_{t-1}^s + B_0^s E_t y_{t+1}^s + D_0^s \varepsilon_t^s \tag{A.57}$$

The sunspot is adding m additional auxiliary equations to the system, such that $y_t^s \equiv (y_t, x_t, s_t, E_t x_{t+1})$ and one additional exogenous shock ν_t, such that $\varepsilon_t^s \equiv (\varepsilon_t, \nu_t)$, and the solution matrices become:

$$A_0^s = \begin{pmatrix} I_{n-m} & 0_{n-m\times m} & 0_{n-m\times m} & 0_{n-m\times m} \\ 0_{m\times n-m} & I_m & 0_{m\times m} & 0_{m\times m} \\ 0_{m\times n-m} & -I_m & I_m & 0_{m\times m} \\ 0_{m\times n-m} & 0_{m\times m} & 0_{m\times m} & I_m \end{pmatrix} \quad C_0^s = \begin{pmatrix} C_{0y} \\ C_{0x} \\ 0_{m\times 1} \\ 0_{m\times 1} \end{pmatrix}$$

$$A_1^s = \begin{pmatrix} A_{1y} & A_{1yx} & 0_{n-m\times m} & 0_{n-m\times m} \\ A_{1xy} & A_x & 0_{m\times m} & 0_{m\times m} \\ 0_{m\times n-m} & 0_{m\times m} & \varrho_i^{-1} & -I_m \\ 0_{m\times n-m} & 0_{m\times m} & 0_{m\times m} & I_m \end{pmatrix}$$

$$B_0^s = \begin{pmatrix} B_{0y} & B_{0yx} & 0_{n-m\times m} & 0_{n-m\times m} \\ B_{0xy} & B_x & 0_{m\times m} & 0_{m\times m} \\ 0_{m\times n-m} & 0_{m\times m} & 0_{m\times m} & 0_{m\times m} \\ 0_{m\times n-m} & I_m & 0_{m\times m} & 0_{m\times m} \end{pmatrix} \quad D_0^s = \begin{pmatrix} D_{0y} & 0_{m\times m} \\ D_{0x} & 0_{m\times m} \\ 0_{m\times l} & -I_m \\ 0_{m\times l} & 0_{m\times m} \end{pmatrix}$$

When $k = 0$, equation A.56 is equal to the determinate system (equation A.35). When $k > 0$, the solution is a VAR of the form:

$$y_t^s = C^s + Q^s y_{t-1}^s + G^s \varepsilon_t^s \tag{A.58}$$

where C^s, Q^s, and G^s are of conformable dimension.

Given $E_t \varepsilon^s_{t+1} = 0$, and $E_t y^s_{t+1} = C^s + Q^s y^s_t$, substituting equation A.58 into equation A.57 and rearranging terms subsequently delivers:

$$y^s_t = (A^s_0 - B^s_0 Q^s)^{-1}(C^s + A^s_1 y^s_{t-1} + B^s_0 C^s + D^s_0 \varepsilon^s_t) \tag{A.59}$$

Rewriting the system delivers:

$$y^s_t = (I - B^s Q^s)^{-1}(\Gamma^s + B^s C^s + A^s y^s_{t-1} - D^s \varepsilon^s_t) \tag{A.60}$$

Which implies:

$$(I - B^s Q^s)^{-1}(\Gamma^s + B^s C^s) = C^s \tag{A.61}$$

$$(I - B^s Q^s)^{-1} A^s = Q^s \tag{A.62}$$

$$(I - B^s Q^s)^{-1} D^s = G^s \tag{A.63}$$

A.3.4 Inflation Sunspot Equilibrium

The degree of indeterminacy in a passive monetary policy regime is $m = 1$, hence, the one additional auxiliary equation needs to be augmented to the system. As in Gibbs and McClung (2023), the respective forward-looking variable that is associated with this equilibrium will be inflation.

$$s_t = \varphi s_{t-1} + (\pi_t - E_{t-1}\pi_t) - \nu_t, \qquad \varphi \equiv \frac{1}{\varrho_1} \tag{A.64}$$

In the case considered here φ is a 1×1 matrix, providing a single missing root in case of indeterminacy when $\phi^s_\pi < 1$. If the root is provided depends on the parameter ϱ. By setting $\varrho < 1$, the sunspot solution provides the necessary explosive root to guarantee a unique and stable solution to the system. For $\varrho > 1$, the sunspot has no impact as the LRE model solution does not depend on it.

The canonical form of the LRE model becomes:

$$y_t = \begin{cases} C + Qy_{t-1} + G\varepsilon_t, & \text{for } t < T \\ \{C_t\}_{t=T}^{T+d} + \{Q_t\}_{t=T}^{T+d} y_{t-1} + \{G_t\}_{t=T}^{T+d} \varepsilon_t, & \text{for } T \leq t < T^* \\ C^s + Q^s y_{t-1} + G^s \varepsilon_t, & \text{for } T \geq T^* \end{cases}$$

where in the third regime allows for a longer period of unconventional monetary policy where the central bank reacts passively to changes in inflation $\phi_\pi^s < 1$:

$$\hat{r}_t = \rho_R^s \hat{r}_{t-1} + (1-\rho_R^s)(\phi_\pi^s \hat{\pi}_t + \phi_y^s(\hat{y}_t - \hat{y}_t^f)) + \phi_{\Delta y}^s(\hat{y}_t - \hat{y}_{t-1}) - (\hat{y}_t^f - \hat{y}_{t-1}^f)) + \varepsilon_t^r$$

A.4 Posterior Sampler

The sampler for the joint posterior of structural parameters and the sequence of expected durations of the ZLB is based on the tailored randomized block Metropolis–Hastings algorithm developed by Chib and Ramamurthy (2010). As in KMR (2017), those are drawn from two separate blocks of the sampler. Instead of updating the entire set of parameters in each draw, the parameters are randomly clustered at every iteration into an arbitrary number of blocks.

Durations Block d

For this block, I use an independent uniform proposal density. The number of expected durations updated in each draw is randomized from a discrete uniform distribution $[1, l_d]$, where l_d determines the upper bound of durations to be updated. I set l_d to 2, as in KMR (2017). The particular quarters that are updated in each draw sequentially are randomized from a discrete uniform distribution $[1, l]$, where l displays the length of the ZLB in the sample ($l = 16$). The corresponding elements are randomly sampled from a discrete uniform distribution $[1, \overline{d}]$, while the non-updated parameters remain at the values in d_{j-1}, where $\overline{d}$ is the maximum admissible duration, which I set to 17 quarters. The acceptance rate is calculated according to:

$$\alpha_j^{\mathbf{d}} \equiv \frac{p(\theta_{j-1}, \mathbf{d}_j^{'} \mid Z)}{p(\theta_{j-1}, \mathbf{d}_{j-1} \mid Z)}$$

The proposal is then accepted with probability $min\{\alpha_j^d, 1\}$, setting $\mathbf{d}_j = \mathbf{d}_j^{'}$, or $\mathbf{d}_{j-1}$ otherwise.

Structural Parameters Block

The block of structural parameters $n_\theta = 42$, and θ the number of parameters updated in each draw is randomized from a discrete uniform distribution $[l_\theta, n_\theta]$, where l_θ determines the lower bound of parameters to be updated. I set l_θ to 8, as in KMR (2017). Then, I randomly sample which parameters to update from a discrete uniform distribution $[1, n_\theta]$. The proposed $\theta_j^{'}$ is constructed from a multivariate Student's t-distribution $\theta_j \sim t(\theta_{j-1}, \Sigma, \nu)$, where ν denotes the degree of freedom and Σ is the scale matrix based on the negative inverse Hessian at the posterior mode of the pre-ZLB sub-sample, multiplied by a tuning parameter κ which is set to 0.075 to ensure an acceptance ratio between 40% and 50%. Denoting the set of updated parameters in each draw as $\theta_{2,j}$ and those being held constant as $\theta_{1,j}$, the density can then be written as:

$$\begin{bmatrix} \theta_{1,j} \\ \theta_{2,j} \end{bmatrix} \sim t\left(\begin{bmatrix} \theta_{1,j-1} \\ \theta_{2,j-1} \end{bmatrix}, \begin{bmatrix} \Sigma_{11} & \Sigma_{12} \\ \Sigma_{21} & \Sigma_{22} \end{bmatrix}, \nu \right)$$

Deviating from KMR (2017), in each draw Σ is reordered, such that the updated parameters correspond to the first columns and rows of the scale matrix.

$$\theta_{i,j} \sim t(\theta_{j-1}, \Sigma_i, \nu)$$

The subset of updated parameters $\theta_{i,j}$ is then based on the Cholesky Decomposition of this subset of the scale matrix Σ_i. This technical addition to the sampler ensures that by construction the inverted sub-sample of the scale matrix will be invertible as well.[4] The conditional density, based on Ding (2016) and KMR (2017), is defined as:

$$\theta_{2,j} \mid \theta_{1,j} = \theta_{1,j-1} \sim t\left(\theta_{2,j-1}, \frac{\nu}{\nu + p_1} \Sigma_{22|1}, \nu + p_1\right)$$

where p_1 is the number of parameters being held constant, and

$$\Sigma_{22|1} \equiv \Sigma_{22} - \Sigma_{21}\Sigma_{11}^{-1}\Sigma_{12}$$

The acceptance ratio for admissible values is calculated according to:[5]

$$\alpha_j^\theta \equiv \frac{p(\theta_j, d_j^{'} \mid Z)}{p(\theta_{j-1}, d_j \mid Z)}$$

[4]In spite of the fact that this is always true mathematically, small numerical inaccuracies in the sampler code may lead to this error.

[5]Note, for inadmissible values α_j^θ is set to 0.

Subsequently, the proposal is accepted with probability $min\{\alpha_j^{\theta}, 1\}$, setting $\theta_j = \theta_j^{'}$ or θ_{j-1} otherwise.

A.5 The Kalman Filter

The Kalman filter to construct the likelihood function follows closely the approach of KMR (2017). Before the ZLB hits the economy, the model variables follow a standard reduced-form solution:

$$y_t = C + Qy_{t-1} + G\varepsilon_t \tag{A.65}$$

This implies the following measurement equation, in which a $n^{obs} \times n$ matrix links the nine observables (n^{obs}) to the state variables, y_t and ν_t represent the vector of measurement errors ($\nu_t \sim \mathcal{N}(0, \mathcal{V})$):

$$z_t = Hy_t + \nu_t \tag{A.66}$$

The model follows a time-varying reduced form solution during the ZLB:

$$y_t = C_t + Q_t y_{t-1} + G_t \varepsilon_t \tag{A.67}$$

The ZLB eliminates any variation in the data which would result in singularity in the Kalman filter. Hence, following the approach of KMR (2017), the observable for the policy interest rate is dropped during the ZLB. The measurement equation at the ZLB is therefore:

$$\bar{z}_t = \bar{H}y_t + \bar{\nu}_t \tag{A.68}$$

By introducing an auxiliary $(n^{obs} - 1) \times n$ matrix $\mathcal{W}$ to reduce the number of observables to eight in the Kalman filter, I define $\bar{z}_t \equiv \mathcal{W}z_t$, $\bar{H} \equiv \mathcal{W}H$, and $\bar{\nu}_t \equiv \mathcal{W}\nu_t$.

The measurement equations (A.66, A.68) and the two model reduced-form solutions (A.65, A.67) build the state-space model for which the Kalman filter can be applied and hence, the likelihood function is constructed. Denoting forecasts with '$\sim$', and given the forecast of the variables $\tilde{y}_{t|t-1}$ and its variance-covariance matrix of the prediction error

$\Sigma_{t|t-1}$, the forecast of the observables is $\tilde{\bar{z}}_{t|t-1} = \bar{H}\tilde{y}_{t|t-1}$, and their forecast error is $u_t \equiv \bar{z}_t - \tilde{\bar{z}}_{t|t-1} = \bar{H}(y_t - \tilde{y}_{t|t-1}) + \bar{\nu}_t$, with variance-covariance matrix $\bar{F}_t \equiv \bar{H}\Sigma_{t|t-1}\bar{H}^{'} + WVW^{'}$. The variables of the model are then given by:

$$\tilde{y}_{t|t} = \tilde{y}_{t|t-1} + \Sigma_{t|t-1}\bar{H}^{'}\bar{F}_t^{-1}u_t$$

which implies the forecast value of the model variables:

$$\tilde{y}_{t+1|t} = C_{t+1} + Q_{t+1}y_t + \bar{K}_t u_t$$

and with the Kalman gain matrix $\bar{K}_t \equiv Q_{t+1}\Sigma_{t|t-1}\bar{H}^{'}\bar{F}_t^{-1}$. The recursion for the mean squared error matrix $\Sigma_{t|t-1}$ is given by:

$$\Sigma_{t+1|t} = G_{t+1}\Omega G_{t+1}^{'} + Q_{t+1}(\Sigma_{t|t-1} - \Sigma_{t|t-1}\bar{H}^{'}\bar{F}_t^{-1}\bar{H}\Sigma_{t|t-1})Q_{t+1}^{'}$$

And the log-likelihood function for the ZLB period is:

$$\bar{\mathcal{L}} = -\Big(\frac{n^{obs}L}{2}\Big)ln(2\pi) - \frac{1}{2}\sum_t ln \mid \bar{F}_t \mid - \frac{1}{2}\sum_t u_t^{'}\bar{F}_t^{-1}u_t$$

where L represents the number of quarters of the sub-sample after entering the ZLB.

The Kalman Filter during the Covid-19 Pandemic

Recall the standard reduced-form solution of the VAR:

$$y_t = C + Qy_{t-1} + Ge_t \tag{A.69}$$

The measurement equation is then given by:

$$z_t = Hy_t + \nu_t \tag{A.70}$$

where a $n^{obs} \times n$ matrix links the observables (n^{obs}) to the state variables, y_t and ν_t represent the vector of measurement errors ($\nu_t \sim \mathcal{N}(0, \mathcal{V})$). By introducing an auxiliary

$(n^{obs}-2)\times n$ matrix $\mathcal{C}$ to reduce the number of observables to p_t in the Kalman filter, $\check{z}_t \equiv \mathcal{C}z_t$, $\check{H}\equiv \mathcal{C}H$, and $\check{\nu}_t \equiv \mathcal{C}\nu_t$. This changes the measurement equation during the Covid-19 pandemic to:

$$\check{z}_t = \check{H}y_t + \check{\nu}_t \tag{A.71}$$

where the $(n^{obs}-2)\times n$ matrix $\mathcal{C}$ reduces the number of observables to seven, $\check{z}_t \equiv \mathcal{C}z_t$, $\check{H}\equiv \mathcal{C}H$, and $\check{\nu}_t \equiv \mathcal{C}\nu_t$.

Denoting forecasts with '$\sim$', and given the forecast of the variables, $\tilde{y}_{t|t-1}$, and its variance-covariance matrix of the prediction error, $\Sigma_{t|t-1}$, the forecast of the observables is $\tilde{\check{z}}_{t|t-1} = \check{H}\tilde{y}_{t|t-1}$, and their forecast error is $u_t \equiv \check{z}_t - \tilde{\check{z}}_{t|t-1} = \check{H}(y_t - \tilde{y}_{t|t-1}) + \check{\nu}_t$, with variance-covariance matrix $\check{F}_t \equiv \check{H}\Sigma_{t|t-1}\check{H}^{'} + WCW^{'}$. The time-varying variance-covariance matrix Ω_t^{covid} is defined as:

$$\Omega_t = \begin{pmatrix} \sigma_1^2 + D_t\sigma_{1,j}^2 & 0 & \dots & 0 \\ 0 & \sigma_2^2 + D_t\sigma_{2,j}^2 & \dots & 0 \\ \vdots & 0 & \ddots & \vdots \\ 0 & \dots & 0 & \sigma_l^2 + D_t\sigma_{l,j}^2 \end{pmatrix}$$

A.6 The Kalman Smoother

The Kalman smoother equations follow Hamilton (1994, pp. 394-397).

$$\tilde{y}_{t|T} = \tilde{y}_{t|t} + J_t(\tilde{y}_{t+1|T} - \tilde{y}_{t+1|t}) \tag{A.72}$$

The steps of the Kalman smoother are as follows. After calculating the Kalman filter according to section A.5, the sequences $\{\tilde{y}_{t|t}\}_{t=1}^T$, $\{\tilde{y}_{t+1|t}\}_{t=1}^T$ and $\{\Sigma_{t|t}\}_{t=1}^T$ are known. The smoothed estimate for time T is denoted as $\tilde{y}_{T|T}$ and is given by the last entry in $\{\tilde{y}_{t|t}\}_{t=1}^T$. Defining J_t as:

$$J_t = \Sigma_{t|t}Q_t'\Sigma_{t+1|t}^{-1} \tag{A.73}$$

Recursively, from $t = T : 1$ using equation A.72 delivers the full set of smoothed estimates. The smoothed estimate $\tilde{y}_{T|T}$ imply the mean square error (MSE):

$$\Sigma_{t|T} = \Sigma_{t|t} + J_t(\Sigma_{t+1|T} - \Sigma_{t+1|t})J_t' \tag{A.74}$$

A.7 Convergence Diagnostics

The Brooks, Gelman and Rubin test (Gelman and Rubin (1992) and Brooks and Gelman (1998)) compares M different chains $(\psi_1^m, \psi_2^m, ..., \psi_N^m)$ with different starting points. For each chain, the posterior mean is calculated according to:

$$\hat{\mu} = \frac{1}{N}\sum_i^N \psi_i^m$$

Let $\hat{\mu} = \bar{\psi}...$, the between-sequence variance B/n and the within variance W can be derived:

$$\frac{B}{n} = \frac{1}{m-1}\sum_{j=1}^m (\bar{\psi}_j. - \bar{\psi}..)^2$$

$$W = \frac{1}{m(n-1)}\sum_{j=1}^m \sum_{t=1}^n (\bar{\psi}_{jt} - \bar{\psi}_j.)^2$$

With this in hand, the weighted average variance σ^2 can be calculated:

$$\hat{\sigma}_+^2 = \frac{n-1}{n}W + \frac{B}{n}$$

Considering the sampling variability of $\hat{\mu}$ implies a pooled posterior variance estimate

$$\hat{V} = \hat{\sigma}_+^2 + \frac{B}{mn}$$

Finally, convergence is assessed by comparing the variance ratio between the pooled and within-chain inferences:

$$R = \frac{\hat{V}}{\sigma^2}$$

The scale reduction factor, $\sqrt{R}$, is unknown and hence must be estimated which is called the potential scale reduction factor (PSRF).

$$\hat{R} = \frac{\hat{V}}{W} = \frac{m+1}{m}\frac{\hat{\sigma}_+^2}{W}\frac{n-1}{mn}$$

The chains have converged, if the PSFR is close to 1. A common reference point for convergence is $\hat{R} < 1.2$.

A.8 Generalized Impulse Response Functions

The GIRF with an estimated duration of $\mathbf{d} = 13$ is defined as:

$$GIRF(N, \vartheta, \omega_{t-1}) = E[\tilde{y}_{t+N} \mid \vartheta^j(\varepsilon_t^j = \tilde{\varepsilon}_{t|T}^j), \mathbf{d}_{13}, \omega_{t-1}] - E[\tilde{y}_{t+N} \mid \vartheta, \mathbf{d}_{13}, \omega_{t-1}]$$

The steps of the algorithm to obtain the GIRFs are as follows:

1. Pick a history ω_{t-1} that corresponds to the steady state of the model before the respective shock hits.

2. Take draws from the joint posterior and keep only those draws for which the duration is equal to the chosen expected duration. Randomly choose one draw of structural parameters.

3. For a given horizon ($N = 30$) and a given number of repetitions ($R = 100$), randomly draw $(N+1) \times R$ shocks (ϑ) from the Cholesky-factorized variance-covariance matrix at the respective draw of structural parameters.

4. Construct $\vartheta^j = \vartheta(\varepsilon_t^j = \tilde{\varepsilon}_{t|T}^j)$ by choosing one structural shock and replacing the random draws for this shock by the standard deviation of the smoothed empirical innovation at the ZLB.

5. Compute the first realization $E[\tilde{y}_{t+N} \mid \vartheta^j, \mathbf{d}_{13}, \omega_{t-1}]$:

   (a) For $t = 1$: Construct the GIRF for the period in which the chosen shocks hit the economy assuming all other shocks being randomized.

(b) For $t = (2 : \mathbf{d}_{13})$: Iterate on the non-linear regime conditional on ω_{t-1} and ϑ using the solution matrices during the fixed-interest regime: $\{Q_t\}_{t=1}^{d_{13}}$, $\{G_t\}_{t=1}^{d_{13}}$, and $\{C_t\}_{t=1}^{d_{13}}$.

(c) For $t = (\mathbf{d}_{13} + 1 : N)$: Iterate on the linear post-fixed interest regime conditional on ω_{t-1} and ϑ using the time-invariant solution matrices: Q, G, and C.

6. Compute the second realization $E[\tilde{y}_{t+N} \mid \vartheta, \mathbf{d}_{13}, \omega_{t-1}]$:

   (a) For $t = (1 : \mathbf{d}_{13})$: Iterate on the non-linear regime conditional on ω_{t-1} using the solution matrices during the fixed-interest regime: $\{Q_t\}_{t=1}^{d_{13}}$, $\{G_t\}_{t=1}^{d_{13}}$, and $\{C_t\}_{t=1}^{d_{13}}$.

   (b) For $t = (\mathbf{d}_{13} + 1 : N)$: Iterate on the linear post-fixed interest regime conditional on ω_{t-1} using the time-invariant solution matrices Q, G, and C.

7. Repeat steps 4 and 5 ($R = 100$) times, each with a different set of randomized shocks and build the averages:

$$\tilde{y}_{R,t+N}(\vartheta, \omega_{t-1}) = \frac{1}{R}\sum_{i=1}^{R} \tilde{y}^i_{t+N}(\vartheta^j, \mathbf{d}_{13}, \omega_{t-1})$$
$$\tilde{y}_{R,t+N}(\omega_{t-1}) = \frac{1}{R}\sum_{i=1}^{R} \tilde{y}^i_{t+N}(\mathbf{d}_{13}, \omega_{t-1})$$

8. Take the difference between the two averages $\tilde{y}_{R,t+N}(\vartheta^j, \mathbf{d}_{13}, \omega_{t-1})$ and $\tilde{y}_{R,t+N}(\mathbf{d}_{13}, \omega_{t-1})$.

9. Repeat steps 2 to 8 ($B = 100$) times to allow an accurate estimation of the GIRF random vector.

Figure A.3: Generalized Impulse Response Function Algorithm

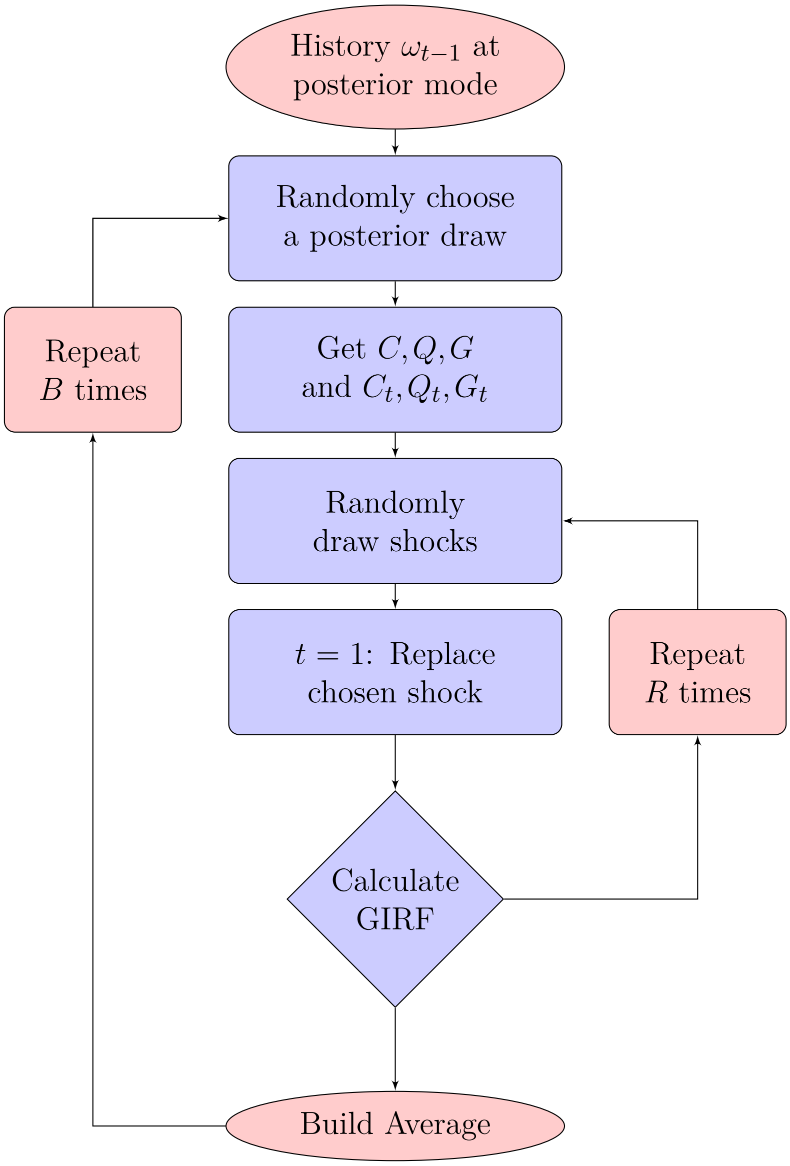

A.9 Solution Algorithms

Sims (2002) Sims (2002) presents a solution algorithm for LRE models and derives conditions that ensure the existence and uniqueness of a stable solution[6]. The Sims (2002) solution is a generalized version of the method derived by Blanchard and Kahn (1980). A distinctive difference is that the Sims (2002) method includes singular Γ_0 cases. While other papers like King and Watson (1998, 2002), Anderson and Moore (1985), or Klein (2000) consider this as well, the Sims (2002) algorithm determines endogenously

[6]The following derivation of the Sims (2002) algorithm contains supplementary explanations and notations form Cagliarini and Kulish (2013), Lubik and Schorfheide (2003), and Bianchi and Nicolò (2021), which support the understanding of the mathematical representation.

the linear combination of variables and does not require to separate endogenous variables into predetermined and non-predetermined variables. Following Sims (2002) the structural equations of a LRE model can be cast in the form:

$$\Gamma_0 y_t = C + \Gamma_1 y_{t-1} + \psi \varepsilon_t + \Pi \eta_t \tag{A.75}$$

where C is a vector of constants, y_t is an $n \times 1$ vector of endogenous state and jump variables, with no loss of generality ε_t is a $l \times 1$ vector of exogenous random disturbances, and η_t is a $k \times 1$ vector of one period ahead forecast errors, satisfying $E_{t-1}[\eta_t] = 0$ for all t. The dimensions of the remaining matrices of the system can be summarized as:

$$\begin{array}{cc} C & nx1 \\ \Gamma_0 & nxn \\ \Gamma_1 & nxn \\ \Psi & nxl \\ \Pi & nxk \end{array}$$

The canonical form, in particular the matrices Γ_0 and Γ_1 can be decomposed through a Generalized Schur Decomposition (see Lubik and Schorfheide (2003)). By using the unitary matrices Q and Z, and the upper-triangular matrices Λ and Ω, Γ_0 and Γ_1 can be expressed as:

$$Q' \Lambda Z' = \Gamma_0$$
$$Q' \Omega Z' = \Gamma_1$$

Such that:

$$Q' \Lambda Z' y_t = C + Q' \Omega Z' y_{t-1} + \psi \varepsilon_t + \Pi \eta_t \tag{A.76}$$

Substituting $w_t \equiv Z' y_t$ and multiplying by Q delivers:

$$\Lambda w_t = \Omega w_{t-1} + QC + Q\Psi\varepsilon_t + Q\Pi\eta_t \tag{A.77}$$

Although the QZ decomposition is not unique, the set of generalized eigenvalues (the collection of values for the ratios of diagonal elements of Λ and Ω usually are. Therefore, Sims (2002) algorithm orders the generalized eigenvalues in absolute value in an increasing order. The resulting system can be partitioned into a set of non-explosive components, whose generalized eigenvalues are smaller than one and where the sub-vector $w_{1,t}$ is of dimension $0 \leq m \leq n$; and into a set of explosive eigenvalues $(w_{2,t})$ whose generalized eigenvalues are larger than one:

$$\mid \omega_{jj}/\lambda_{jj} \mid \geq \mid \omega_{ii}/\lambda_{ii} \mid \qquad for \quad jj \geq ii$$

Then equation A.77 can be rewritten as follows:

$$\begin{pmatrix} \Lambda_{11} & \Lambda_{12} \\ 0 & \Lambda_{22} \end{pmatrix} \begin{pmatrix} w_{1,t} \\ w_{2,t} \end{pmatrix} = \begin{pmatrix} \Omega_{11} & \Omega_{12} \\ 0 & \Omega_{22} \end{pmatrix} \begin{pmatrix} w_{1,t-1} \\ w_{2,t-1} \end{pmatrix} + \begin{pmatrix} Q_1 \\ Q_2 \end{pmatrix} (C + \psi\varepsilon_t + \Pi\eta_t) \tag{A.78}$$

where the first block contains the set of equations for which $\mid \omega_{jj}/\lambda_{jj} \mid < 1$ (non-explosive) and the second block equations for which $\mid \omega_{jj}/\lambda_{jj} \mid > 1$ (explosive) Equation A.78 can be broken down into:

$$\Lambda_{11} w_{1,t} + \Lambda_{12} w_{2,t} = \Omega_{11} w_{1,t-1} + \Omega_{12} w_{2,t-1} + Q_1(C + \psi\varepsilon_t + \Pi\eta_t)$$

$$\Lambda_{22} w_{2,t} = \Omega_{22} w_{2,t-1} + Q_2(C + \psi\varepsilon_t + \Pi\eta_t) \tag{A.79}$$

This can be transformed to:

$$w_{2,t} = \Lambda_{22}^{-1} \Omega_{22} w_{2,t-1} + \Lambda_{22}^{-1} Q_2(C + \Psi_{\varepsilon_t} + \Pi\eta_t) \tag{A.80}$$

Solving Forward When defining $M \equiv \Omega_{22}^{-1}\Lambda_{22}$ and $x_{2,t} \equiv Q_2(C + \Psi_{\varepsilon_t} + \Pi\eta_t)$, equation A.79 can be solved forwards[7]

$$\begin{aligned} w_{2,t} &= Mw_{2,t+1} - \Omega_{22}^{-1}x_{2,t+1} \\ &= M^2 w_{2,t+2} - M\Omega_{22}^{-1}x_{2,t+2} - \Omega_{22}^{-1}x_{2,t+1} \\ &= -\sum_{s=1}^{\infty} M^{s-1}\Omega_{22}^{-1}x_{2,t+s} \end{aligned} \tag{A.81}$$

The last equality in equation A.81 implies that $lim_{s\to\infty}M^s w_{2,t+s} = 0$. When replacing M and $x_{2,t}$ with their original definitions, $w_{2,t}$ can be expressed as:

$$w_{2,t} = (\Lambda_{22} - \Omega_{22})^{-1}Q_2C - \sum_{s=1}^{\infty} M^{s-1}\Omega_{22}^{-1}Q_2(\Psi\varepsilon_{t+s} + \Pi\eta_{t+s}) \tag{A.82}$$

Taking expectations conditional on time t does not change the left-hand side of equation A.82, which delivers[8]

$$w_{2,t} = (\Lambda_{22} - \Omega_{22})^{-1}Q_2C - E_t\sum_{s=1}^{\infty} M^{s-1}\Omega_{22}^{-1}Q_2\Psi\varepsilon_{t+s} \tag{A.83}$$

Taking expectations conditional on time $t+1$ gives:

$$w_{2,t} = (\Lambda_{22} - \Omega_{22})^{-1}Q_2C - E_{t+1}\sum_{s=1}^{\infty} M^{s-1}\Omega_{22}^{-1}Q_2\Psi\varepsilon_{t+s} - \Omega_{22}^{-1}Q_2\Pi\eta_{t+1} \tag{A.84}$$

Equality between equations A.83 and A.84 holds if and only if:

$$\begin{aligned} \Omega_{22}^{-1}Q_2\Pi\eta_{t+1} &= E_t\Big(\sum_{s=1}^{\infty} M^{s-1}\Omega_{22}^{-1}Q_2\Psi\varepsilon_{t+s}\Big) - E_{t+1}\Big(\sum_{s=1}^{\infty} M^{s-1}\Omega_{22}^{-1}Q_2\Psi\varepsilon_{t+s}\Big) \\ Q_2\Pi\eta_{t+1} &= \sum_{s=1}^{\infty}\Omega_{22}M^{s-1}\Omega_{22}^{-1}Q_2\Psi(E_t\varepsilon_{t+s} - E_{t+1}\varepsilon_{t+s}) \end{aligned} \tag{A.85}$$

In the case that $E_t\varepsilon_{t+i} = 0$ for $i \geq 1$, equation A.85 becomes:

$$Q_2\Pi\eta_{t+1} = -Q_2\Psi\varepsilon_{t+1} \tag{A.86}$$

[7]Pre multiplying equation A.79 by Ω_{22}^{-1} delivers $\Omega_{22}^{-1}\Lambda_{22}w_{2,t} = \Omega_{22}^{-1}\Omega_{22}w_{2,t-1} + \Omega_{22}^{-1}Q_2(\Psi\varepsilon_t + \Pi\eta_t)$. Then substitute for M and $x_{2,t}$.

[8]Note that $E_t\eta_{t+s} = 0$ for $s \geq 1$.

Existence and Uniqueness Assuming $E_t \varepsilon_{t+i} = 0$ and C=0, the equation for $w_{2,t}$ can then be expressed as:

$$w_{2,t} = \Lambda_{22}^{-1}\Omega_{22}w_{2,t-1} + \Lambda_{22}^{-1}Q_2(\Pi\eta_t + \Psi\varepsilon_t) \tag{A.87}$$

From equation A.87 it follows that for a non-explosive (bounded) solution it has to hold that, first:

$$w_{2,0} = 0 \tag{A.88}$$

and second, the endogenous forecast errors η_t need to be able to offset the impact of the innovations ε_t on $w_{2,t}$:

$$Q_2\Psi\varepsilon_t + Q_2\Pi\eta_t = 0 \tag{A.89}$$

$$\eta_t = -\Psi^{-1}\Pi\varepsilon_t \tag{A.90}$$

This delivers the block of stable equations:

$$w_{1,t} = \Lambda_{11}^{-1}\Omega_{11}w_{1,t-1} + \Lambda_{11}^{-1}Q_1(C + \Pi\eta_t + \Psi\varepsilon_t) \tag{A.91}$$

Sims (2002) derives that existence problems arise if the shocks matrix η cannot adjust to offset exogenous disturbances. The existence of a stable solution requires that the number of explosive roots cannot be larger than the dimension of η.

Since $Q_2\Pi$ is of $m \times k$ dimension, this requires that $m \leq k$. In practice, this often referred to the notion that there are existence problems if the number of unstable eigenvalues exceeds the number of non-predetermined variables. The necessary and sufficient condition for a solution to exist is that the column space of $Q_2\Psi$ needs to be contained in the space of $Q_2\Pi$:

$$span\Big(\{\Omega_{22}M^{s-1}\Omega{-}1_{22}Q2\Psi\}_{s=1}^{m}\Big) \subseteq span(Q_2\Pi) \tag{A.92}$$

Existence of a stable solution does not necessarily imply that this solution is unique. The vector of endogenous forecast errors η_t does not necessarily have to be unique and generalization allows that even for $k < m$ there might be the possibility of linearly dependent rows in $Q_2\Pi$ (Lubik and Schorfheide, 2003). In this case, it is not possible to determine the value of $Q1\Pi\eta_t$, which is needed to solve the LRE model. In a unique solution, the number of explosive roots (eigenvalues outside the unit circle) must be equal to the number of forward-looking variables. Hence, existence and uniqueness require that $m = k$. For a solution to be unique it is necessary and sufficient if the row space of $Q1\Pi$ be contained in $Q_2\Pi$. Therefore, it exists a matrix Φ such that:

$$Q_1\Pi = \Phi Q_2\Pi \tag{A.93}$$

Pre-multiplying equation A.78 by $[I - \Phi]$ delivers a new set of equations without a notion of η_t:

$$\begin{aligned}\begin{pmatrix} I - \Phi \end{pmatrix}\begin{pmatrix} \Lambda_{11} & \Lambda_{12} \\ 0 & \Lambda_{22} \end{pmatrix}\begin{pmatrix} w_{1,t} \\ w_{2,t} \end{pmatrix} &= \begin{pmatrix} I - \Phi \end{pmatrix}\begin{pmatrix} \Omega_{11} & \Omega_{12} \\ 0 & \Omega_{22} \end{pmatrix}\begin{pmatrix} w_{1,t-1} \\ w_{2,t-1} \end{pmatrix} \\ &+ \begin{pmatrix} Q_1 \\ Q_2 \end{pmatrix}(C + \psi\varepsilon_t + \Pi\eta_t)\end{aligned} \tag{A.94}$$

This delivers:

$$\begin{aligned}\begin{pmatrix} \Lambda_{11}\Lambda_{12} - \Phi\Lambda_{22} \end{pmatrix}\begin{pmatrix} w_{1,t} \\ w_{2,t} \end{pmatrix} &= \begin{pmatrix} \Omega_{11}\Omega_{12} - \Phi\Omega_{22} \end{pmatrix}\begin{pmatrix} w_{1,t-1} \\ w_{2,t-1} \end{pmatrix} + (Q_1\Psi - \Phi Q_2\Psi)C \\ &+ (Q_1\Psi - \Phi Q_2\Psi)\varepsilon_t + (Q_1\Pi - \Phi Q_2\Pi)\eta_t\end{aligned} \tag{A.95}$$

In a unique solution $Q_1\Pi = \Phi Q_2\Pi$, so the last term drops out:

$$\begin{pmatrix}\Lambda_{11}\Lambda_{12} - \Phi\Lambda_{22}\end{pmatrix}\begin{pmatrix} w_{1,t} \\ w_{2,t}\end{pmatrix} = \begin{pmatrix}\Omega_{11}\Omega_{12} - \Phi\Omega_{22}\end{pmatrix}\begin{pmatrix} w_{1,t-1} \\ w_{2,t-1}\end{pmatrix} + (Q_1\Psi - \Phi Q2\Psi)C + (Q_1\Psi - \Phi Q_2\Psi)\varepsilon_t \tag{A.96}$$

Considering the possibility of linearly dependent rows in $Q_2\Pi$ it is useful to work with a singular value decomposition:

$$Q_2\Pi = UDV' = U_1 D_{11} V_1'$$

where U and V are orthogonal matrices and D_{11} is a diagonal matrix. The pseudo inverse of $Q_2\Pi$ is then given by:

$$Q_2\Pi^{+} = V_1 D_{11}^{-1} U_1'$$

It follows:

$$\Phi = Q_1\Pi(V_1 D_{11}^{-1} U_1')$$

Determinate Solution Matrices Combining equation A.83 and equation A.96 delivers the system in terms of w_t:

$$\begin{aligned}\begin{pmatrix}\Lambda_{11} & \Lambda_{12} - \Phi\Lambda_{22} \\ 0 & I\end{pmatrix}\begin{pmatrix} w_{1,t} \\ w_{2,t}\end{pmatrix} = &\begin{pmatrix}\Omega_{11} & \Omega_{12} - \Phi\Omega_{22} \\ 0 & 0\end{pmatrix}\begin{pmatrix} w_{1,t-1} \\ w_{2,t-1}\end{pmatrix} \\ &+ \begin{pmatrix} Q_1 - \Phi Q_2 \\ 0 \end{pmatrix}\psi C + \begin{pmatrix} 0 \\ (\Lambda_{22} - \Omega_{22})^{-1} Q_2 \end{pmatrix} C \\ &+ \begin{pmatrix} Q_1 - \Phi Q_2 \\ 0 \end{pmatrix}\psi\varepsilon_t - E_t\begin{pmatrix} 0 \\ \sum_{s=1}^{\infty} M^{s-1}\Omega_{22}^{-1} Q_2 \Psi \varepsilon_{t+s}\end{pmatrix}\end{aligned} \tag{A.97}$$

Given the inverse of a partitioned matrix:

$$\begin{pmatrix} \Lambda_{11} & \Lambda_{12}-\Phi\Lambda_{22} \\ 0 & I \end{pmatrix}^{-1} = \begin{pmatrix} \Lambda_{11}^{-1} & -\Lambda_{11}^{-1}(\Lambda_{12}-\Phi\Lambda_{22}) \\ 0 & I \end{pmatrix} \tag{A.98}$$

It holds:

$$\begin{aligned} \begin{pmatrix} w_{1,t} \\ w_{2,t} \end{pmatrix} = & \begin{pmatrix} \Lambda_{11}^{-1} & -\Lambda_{11}^{-1}(\Lambda_{12}-\Phi\Lambda_{22}) \\ 0 & I \end{pmatrix} \begin{pmatrix} \Omega_{11} & \Omega_{12}-\Phi\Omega_{22} \\ 0 & 0 \end{pmatrix} \begin{pmatrix} w_{1,t-1} \\ w_{2,t-1} \end{pmatrix} \\ & + \begin{pmatrix} \Lambda_{11}^{-1} & -\Lambda_{11}^{-1}(\Lambda_{12}-\Phi\Lambda_{22}) \\ 0 & I \end{pmatrix} \begin{pmatrix} Q_1-\Phi Q_2 \\ 0 \end{pmatrix} \psi C \\ & + \begin{pmatrix} \Lambda_{11}^{-1} & -\Lambda_{11}^{-1}(\Lambda_{12}-\Phi\Lambda_{22}) \\ 0 & I \end{pmatrix} \begin{pmatrix} 0 \\ (\Lambda_{22}-\Omega_{22})^{-1}Q_2 \end{pmatrix} C \\ & + \begin{pmatrix} \Lambda_{11}^{-1} & -\Lambda_{11}^{-1}(\Lambda_{12}-\Phi\Lambda_{22}) \\ 0 & I \end{pmatrix} \begin{pmatrix} Q_1-\Phi Q_2 \\ 0 \end{pmatrix} \psi \varepsilon_t \\ & - \begin{pmatrix} \Lambda_{11}^{-1} & -\Lambda_{11}^{-1}(\Lambda_{12}-\Phi\Lambda_{22}) \\ 0 & I \end{pmatrix} \begin{pmatrix} 0 \\ \sum_{s=1}^{\infty} M^{s-1}\Omega_{22}^{-1}Q_2\Psi \end{pmatrix} E_t\varepsilon_{t+s} \end{aligned} \tag{A.99}$$

Assuming that $E_t\varepsilon_{t+i}=0$ and re-substituting w_t ($\equiv Z'y_t$) yields:

$$\begin{aligned} \begin{pmatrix} Z_1' \\ Z_2' \end{pmatrix} y_t = & \begin{pmatrix} \Lambda_{11}^{-1} & -\Lambda_{11}^{-1}(\Lambda_{12}-\Phi\Lambda_{22}) \\ 0 & I \end{pmatrix} \begin{pmatrix} \Omega_{11} & \Omega_{12}-\Phi\Omega_{22} \\ 0 & 0 \end{pmatrix} \begin{pmatrix} Z_1' \\ Z_2' \end{pmatrix} y_{t-1} \\ & + \begin{pmatrix} \Lambda_{11}^{-1} & -\Lambda_{11}^{-1}(\Lambda_{12}-\Phi\Lambda_{22}) \\ 0 & I \end{pmatrix} \begin{pmatrix} Q_1-\Phi Q_2 \\ 0 \end{pmatrix} \psi C \\ & + \begin{pmatrix} \Lambda_{11}^{-1} & -\Lambda_{11}^{-1}(\Lambda_{12}-\Phi\Lambda_{22}) \\ 0 & I \end{pmatrix} \begin{pmatrix} 0 \\ (\Lambda_{22}-\Omega_{22})^{-1}Q_2 \end{pmatrix} C \\ & + \begin{pmatrix} \Lambda_{11}^{-1} & -\Lambda_{11}^{-1}(\Lambda_{12}-\Phi\Lambda_{22}) \\ 0 & I \end{pmatrix} \begin{pmatrix} Q_1-\Phi Q_2 \\ 0 \end{pmatrix} \psi \varepsilon_t \end{aligned} \tag{A.100}$$

Multiply by Z:

$$
\begin{aligned}
y_t = & Z \begin{pmatrix} \Lambda_{11}^{-1} & -\Lambda_{11}^{-1}(\Lambda_{12} - \Phi\Lambda_{22}) \\ 0 & I \end{pmatrix} \begin{pmatrix} \Omega_{11} & \Omega_{12} - \Phi\Omega_{22} \\ 0 & 0 \end{pmatrix} Z' y_{t-1} \\
& + Z \begin{pmatrix} \Lambda_{11}^{-1} & -\Lambda_{11}^{-1}(\Lambda_{12} - \Phi\Lambda_{22}) \\ 0 & I \end{pmatrix} \begin{pmatrix} Q_1 - \Phi Q_2 \\ 0 \end{pmatrix} \psi C \\
& + Z \begin{pmatrix} \Lambda_{11}^{-1} & -\Lambda_{11}^{-1}(\Lambda_{12} - \Phi\Lambda_{22}) \\ 0 & I \end{pmatrix} \begin{pmatrix} 0 \\ (\Lambda_{22} - \Omega_{22})^{-1} Q_2 \end{pmatrix} C \\
& + Z \begin{pmatrix} \Lambda_{11}^{-1} & -\Lambda_{11}^{-1}(\Lambda_{12} - \Phi\Lambda_{22}) \\ 0 & I \end{pmatrix} \begin{pmatrix} Q_1 - \Phi Q_2 \\ 0 \end{pmatrix} \psi \varepsilon_t
\end{aligned} \tag{A.101}
$$

The reduced-form of the LRE model becomes:

$$
y_t = S_0 + S_1 y_{t-1} + S_2 \varepsilon_t \tag{A.102}
$$

where

$$
H \equiv Z \begin{pmatrix} \Lambda_{11}^{-1} & -\Lambda_{11}^{-1}(\Lambda_{12} - \Phi\Lambda_{22}) \\ 0 & I \end{pmatrix}
$$

$$
S_0 = H \begin{pmatrix} Q_1 - \Phi Q_2 \\ (\Lambda_{22} - \Omega_{22})^{-1} Q_2 \end{pmatrix} C
$$

$$
S_1 = H \begin{pmatrix} \Omega_{11} & \Omega_{12} - \Phi\Omega_{22} \\ 0 & 0 \end{pmatrix} Z'
$$

$$
S_2 = H \begin{pmatrix} Q_1 - \Phi Q_2 \\ 0 \end{pmatrix} \psi
$$

Indeterminate Solution Matrices

Binder and Pesaran (1995, 1997) Binder and Pesaran (1995, 1997) describe an iterative method to solve LRE models. A rational expectation model that is linearized around a non-stochastic steady state can be cast in the following form[9]

$$A_0 y_t = C_0 + A_1 y_{t-1} + B_0 E_t y_{t+1} + D_0 \varepsilon_t \tag{A.103}$$

where y_t is a $nx1$ vector and ε_t is a $lx1$ vector. The dimensions of the remaining matrices of the system can be summarized as:

A_0	$n \times n$
C	$n \times 1$
A_1	$n \times n$
B_0	$n \times n$
D_0	$n \times l$

Given that all agents form rational expectations under a known regime, the unique solution (if it exists) is a VAR of the following form:

$$y_t = C + Q y_{t-1} + G \varepsilon_t \tag{A.104}$$

where C, Q, and G are conformable matrices. Given $E_t \varepsilon_{t+1} = 0$, and $E_t y_{t+1} = C + Q y_t$, substituting equation A.104 into equation A.103 and rearranging terms subsequently delivers:

$$A_0 y_t = C + A_1 y_{t-1} + B_0 [C + Q y_t + G E_t \varepsilon_{t+1}] + D_0 \varepsilon_t \tag{A.105}$$

$$(A_0 - B_0 Q) y_t = C + A_1 y_{t-1} + B_0 C + D_0 \varepsilon_t \tag{A.106}$$

[9]The following derivation of the Binder and Pesaran (1995, 1997) algorithm contains supplementary explanations and notations form Kulish and Pagan (2017), which support the understanding of the mathematical representation.

$$y_t = (A_0 - B_0 Q)^{-1}(C + A_1 y_{t-1} + B_0 C + D_0 \varepsilon_t) \tag{A.107}$$

Rewriting $(A_0 - B_0 Q)^{-1} = (I - A_0^{-1} B_0 Q)^{-1} A_0^{-1}$ and defining $\Gamma \equiv A_0^{-1} C, A \equiv A_0^{-1} A_1, B \equiv A_0^{-1} B_0$, and $D \equiv A_0^{-1} D_0$ the system becomes:

$$y_t = (I - A_0^{-1} B_0 Q)^{-1} A_0^{-1}(C + A_1 y_{t-1} + B_0 C + D_0 \varepsilon_t) \tag{A.108}$$

$$y_t = (I - BQ)^{-1}(\Gamma + BC + A y_{t-1} - D\varepsilon_t) \tag{A.109}$$

Equation A.109 has to be equal to equation A.104, which implies that:

$$(I - BQ)^{-1}(\Gamma + BC) = C \tag{A.110}$$

$$(I - BQ)^{-1} A = Q \tag{A.111}$$

$$(I - BQ)^{-1} D = G \tag{A.112}$$

Equation A.111 determines Q by implying that:

$$A - Q + BQ^2 = 0 \tag{A.113}$$

Furthermore, by showing that equation A.110 can be transformed to:

$$C = \left[(I - (I - BQ)^{-1} B\right]^{-1} (I - BQ)^{-1} \Gamma \tag{A.114}$$

where $\Lambda = (I - BQ)^{-1}\Gamma$ and $F = (I - BQ)^{-1} B$, equation A.110 can be expressed as:

$$C = (I - F)^{-1} \Lambda \tag{A.115}$$

Hence, once Q is found, it is possible to determine C and G, and thereby the solution of the model.

A.10 ZLB Algorithm by Jones (2017)

This section presents the steps of the ZLB algorithm as presented in Jones (2017) which is used to find the lower bound durations. The model is linearized around its steady state and brought into the Binder and Pesaran (1995, 1997) form. From that the same solution method is used to obtain the well-known reduced form:

$$y_t = C + Qy_{t-1} + G\varepsilon_t \tag{A.116}$$

The steps of the algorithm can be summarized as follows:

1. For each period t:

   (a) Solve for the path $\{y_\tau\}_{\tau=t}^{T}$ using the reduced form and assuming no future uncertainty $\{w_\tau\}_{\tau=t+1}^{T} = 0$, so that $y_t = C + Qy_{t-1} + G\varepsilon_t$, and $y_{t+1} = C + Qy_t$, until $y_T = C + Qy_{T-1}$. This step gives a path for $r_t^k = \{r_\tau\}_{\tau=t}^{T}$.

   (b) Examine the path $r_t^k = \{r_\tau\}_{\tau=t}^{T}$. If $r_t^k \geq 0$, then the ZLB does not bind, and move to step (2). If $r_t^k \leq 0$, then move to step (1c). That is:

      - If $r_\tau \geq 0$ for all $t \leq \tau < T$, accept $\{y_\tau\}_{\tau=t}^{T}$. The path of the nominal interest rate does not violate the ZLB today or in future.
      - If $r_\tau < 0$ for any $t \leq \tau < T$, move to step (1c).

   (c) Update the path of $\{r_\tau\}_{\tau=t}^{T}$ for the ZLB. Denote by t^* the first time period where $r_t^k < 0$, and set the nominal interest rate in that period to zero. This changes the anticipated structure of the economy.

      Computing the new path $\{r_\tau\}_{\tau=t}^{T}$ under the structural change involves computing $\{y_\tau\}_{\tau=t}^{t^*}$ and $\{y_\tau\}_{\tau=t^*+1}^{T}$. At t^*, $E_{t^*}[y_{t^*+1}]$ is computed using the reduced form solution and $\varepsilon_{t^*+1} = 0$. This expresses y_{t^*} as a function of y_{t^*-1}. Proceeding in this way with the correct structural matrices, compute the path $r_t^{k+1} = \{r_\tau\}_{\tau=t}^{T}$.

      A convenient way to compute the new path $r_t^{k+1} = \{r_\tau\}_{\tau=t}^{T}$ is to form the time varying matrices $\{C_\tau, Q_\tau, G_\tau\}_{\tau=t}^{T}$ with the final set of reduced form matrices for the recursion being the non-ZLB matrices C, Q, G. The time-varying matrices are then used to compute the path $\{y_\tau\}_{\tau=t}^{t^*}$ by calculating $y_t = C_\tau + Q_\tau y_{\tau-1} + G_\tau \varepsilon_t$. Iterate on steps 2 and 3 until convergence of r_t^{k+1} and r_t^k.

2. Increment t. The initial vector of variables becomes y_t, which was solved for in step 1. Draw a new vector of unanticipated shocks w_{t+1} and return to step 1. The algorithm yields a set of time-varying structural matrices:

$$y_t = C_t + Q_t y_{t-1} + G_t \varepsilon_t \tag{A.117}$$

from which we get the path $\{y_\tau\}_{\tau=t}^{\infty}$ where the nominal interest rate is subject to the ZLB. Furthermore, if the ZLB does bind under the sequence of exogenous variables, the algorithm produces, at each period t, a sequence of expected durations of the ZLB.

Bibliography

G. Anderson and G. Moore. A linear algebraic procedure for solving linear perfect foresight models. *Economics letters*, 17(3):247–252, 1985.

G. S. Anderson. Solving linear rational expectations models: A horse race. *Computational Economics*, 31(2):95–113, sep 2007. doi: 10.1007/s10614-007-9108-0.

P. Andrade, G. Gaballo, E. Mengus, and B. Mojon. Forward guidance and heterogeneous beliefs. *American Economic Journal: Macroeconomics*, 11(3):1–29, 2019.

S. Avdjiev, M. Everett, P. R. Lane, and H. S. Shin. Tracking the international footprints of global firms. *BIS Quarterly Review, March*, 2018.

L. Baele, G. Bekaert, S. Cho, K. Inghelbrecht, and A. Moreno. Macroeconomic regimes. *Journal of Monetary Economics*, 70:51–71, 2015.

B. S. Bernanke, M. Gertler, and S. Gilchrist. The financial accelerator in a quantitative business cycle framework. In *Handbook of Macroeconomics*, volume 1, pages 1341–1393. Elsevier, 1999.

F. Bianchi. Regime switches, agents' beliefs, and post-world war ii us macroeconomic dynamics. *Review of Economic Studies*, 80(2):463–490, 2013.

F. Bianchi and G. Nicolò. A generalized approach to indeterminacy in linear rational expectations models. *Quantitative Economics*, 12(3):843–868, 2021.

M. Binder and M. H. Pesaran. Multivariate rational expectations models and macroeconometric modelling: A review and some new results. *Handbook of applied econometrics*, 1:139–187, 1995.

M. Binder and M. H. Pesaran. Multivariate linear rational expectations models: characterization of the nature of the solutions and their fully recursive computation. *Econometric Theory*, pages 877–888, 1997.

F. Black. Interest rates as options. *the Journal of Finance*, 50(5):1371–1376, 1995.

O. J. Blanchard and C. M. Kahn. The solution of linear difference models under rational expectations. *Econometrica: Journal of the Econometric Society*, pages 1305–1311, 1980.

E. Bobeica and B. Hartwig. The covid-19 shock and challenges for time series models. Technical report, ECB Working Paper, 2021.

S. Brooks and A. Gelman. General methods for monitoring convergence of iterative simulations. *Journal of Computational and Graphical Statistics*, 7(4):434–455, 1998.

A. Cagliarini and M. Kulish. Solving linear rational expectations models with predictable structural changes. *Review of Economics and Statistics*, 95(1):328–336, 2013.

G. A. Calvo. Staggered prices in a utility-maximizing framework. *Journal of Monetary Economics*, 12(3):383–398, 1983.

J. R. Campbell, C. L. Evans, J. D. Fisher, A. Justiniano, C. W. Calomiris, and M. Woodford. Macroeconomic effects of federal reserve forward guidance [with comments and discussion]. *Brookings papers on economic activity*, pages 1–80, 2012.

J. R. Campbell, J. D. Fisher, A. Justiniano, and L. Melosi. Forward guidance and macroeconomic outcomes since the financial crisis. *NBER Macroeconomics Annual*, 31(1):283–357, 2017.

C. T. Carlstrom, T. S. Fuerst, and M. Paustian. Inflation and output in new keynesian models with a transient interest rate peg. *Journal of Monetary Economics*, 76:230–243, 2015.

A. Carriero, T. E. Clark, and M. Marcellino. Common drifting volatility in large bayesian vars. *Journal of Business & Economic Statistics*, 34(3):375–390, 2016.

A. Carriero, T. E. Clark, M. Marcellino, and E. Mertens. Addressing covid-19 outliers in bvars with stochastic volatility. *The Review of Economics and Statistics*, pages 1–38, 2021.

S. Chib and S. Ramamurthy. Tailored randomized block mcmc methods with application to dsge models. *Journal of Econometrics*, 155(1):19–38, 2010.

L. Christiano, M. Eichenbaum, and S. Rebelo. When is the government spending multiplier large? *Journal of Political Economy*, 119(1):78–121, 2011.

L. J. Christiano, M. Eichenbaum, and C. L. Evans. Nominal rigidities and the dynamic effects of a shock to monetary policy. *Journal of Political Economy*, 113(1):1–45, 2005.

R. Clarida, J. Gali, and M. Gertler. Monetary policy rules and macroeconomic stability: evidence and some theory. *The Quarterly Journal of Economics*, 115(1):147–180, 2000.

T. E. Clark and F. Ravazzolo. Macroeconomic forecasting performance under alternative specifications of time-varying volatility. *Journal of Applied Econometrics*, 30(4):551–575, 2015.

J. H. Cochrane. The new-keynesian liquidity trap. *Journal of Monetary Economics*, 92:47–63, 2017.

T. Cogley and T. J. Sargent. Drifts and volatilities: monetary policies and outcomes in the post wwii us. *Review of Economic dynamics*, 8(2):262–302, 2005.

S. J. Cole. The effectiveness of central bank forward guidance under inflation and price-level targeting. *Journal of Macroeconomics*, 55:146–161, 2018.

M. de la Barrera, J. Falath, D. Henricot, and J.-A. Vaglio. The impact of forward guidance on inflation expectations: Evidence from the ecb, 2017.

R. B. De Rezende and A. Ristiniemi. A shadow rate without a lower bound constraint. *Journal of Banking & Finance*, 146:106686, 2023.

M. Del Negro and S. Eusepi. Fitting observed inflation expectations. *Journal of Economic Dynamics and control*, 35(12):2105–2131, 2011.

M. Del Negro, M. P. Giannoni, and C. Patterson. The forward guidance puzzle. FRB of New York Staff Report, 2012.

B. Diba and O. Loisel. Pegging the interest rate on bank reserves: a resolution of new keynesian puzzles and paradoxes. *Journal of Monetary Economics*, 118:230–244, 2021.

P. Ding. On the conditional distribution of the multivariate t distribution. *The American Statistician*, 70(3):293–295, 2016.

ECB SPF. Survey of professional forecasters (spf), 2013.

G. Eggertsson. The paradox of toil. FRB of New York Staff Report, 2010.

G. Eggertsson and M. Woodford. Zero bound on interest rates and optimal monetary policy. *Brookings Papers on Economic Activity*, 2003(1):139–233, 2003.

M. Ehrmann, G. Gaballo, P. Hoffmann, and G. Strasser. Can more public information raise uncertainty? the international evidence on forward guidance. *Journal of Monetary Economics*, 108:93–112, 2019.

A. Elbourne, K. Ji, and S. Duijndam. The effects of unconventional monetary policy in the euro area. Technical report, CPB Netherlands Bureau for Economic Policy Analysis, 2018.

R. E. Farmer, V. Khramov, and G. Nicolò. Solving and estimating indeterminate dsge models. *Journal of Economic Dynamics and Control*, 54:17–36, 2015.

J. Fernández-Villaverde and J. F. Rubio-Ramírez. Estimating macroeconomic models: A likelihood approach. *The Review of Economic Studies*, 74(4):1059–1087, 2007.

J. Fernández-Villaverde, G. Gordon, P. Guerrón-Quintana, and J. F. Rubio-Ramirez. Nonlinear adventures at the zero lower bound. *Journal of Economic Dynamics and Control*, 57:182–204, 2015.

M. Feroli, D. Greenlaw, P. Hooper, F. S. Mishkin, and A. Sufi. Language after liftoff: Fed communication away from the zero lower bound. *Research in Economics*, 71(3):452–490, 2017.

A. Filardo and B. Hofmann. Forward guidance at the zero lower bound. *BIS Quarterly Review*, 2014.

J. Fitzgerald. Problems with the irish national accounts and possible solutions. mimeo, 2016.

N. Francis and V. A. Ramey. Is the technology-driven real business cycle hypothesis dead? shocks and aggregate fluctuations revisited. *Journal of Monetary Economics*, 52(8):1379–1399, 2005.

M. Friedman. *A Theory of the Consumption Function*. Princeton University Press, 1957. ISBN 0-691-04182-2.

J. Gali. Technology, employment, and the business cycle: do technology shocks explain aggregate fluctuations? *American Economic Review*, 89(1):249–271, 1999.

A. Gelman and D. B. Rubin. Inference from iterative simulation using multiple sequences. *Statistical Science*, 7(4):457–472, 1992.

M. Gertler. Rethinking the power of forward guidance: Lessons from japan keynote speech by mark gertler. *Monetary and Economic Studies*, 35:39–58, 2017.

J. Geweke. Using simulation methods for bayesian econometric models: inference, development, and communication. *Econometric Reviews*, 18(1):1–73, 1999.

C. Gibbs and N. McClung. Does my model predict a forward guidance puzzle? *Review of Economic Dynamics*, 2023.

L. Guerrieri and M. Iacoviello. Occbin: A toolkit for solving dynamic models with occasionally binding constraints easily. *Journal of Monetary Economics*, 70:22–38, 2015.

J. D. Hamilton. *Time series analysis*. Princeton university press, 1994.

S. G. Hanson and J. C. Stein. Monetary policy and long-term real rates. *Journal of Financial Economics*, 115:429–448, 2015.

T. S. Hills and T. Nakata. Fiscal multipliers at the zero lower bound: the role of policy inertia. *Journal of Money, Credit and Banking*, 50(1):155–172, 2018.

E. Jacquier, N. G. Polson, and P. E. Rossi. Bayesian analysis of stochastic volatility models. *Journal of Business & Economic Statistics*, 20(1):69–87, 2002.

C. Jones. Unanticipated shocks and forward guidance at the zero lower bound. NYU Working Paper, 2017.

C. Jones, M. Kulish, and J. Morley. A structural measure of the shadow federal funds rate. Technical Report 61/2022, CAMA Working Paper, Oct. 2022a.

C. Jones, M. Kulish, and D. M. Rees. International spillovers of forward guidance shocks. *Journal of Applied Econometrics*, 37(1):131–160, 2022b.

A. Justiniano and G. E. Primiceri. The time-varying volatility of macroeconomic fluctuations. *American Economic Review*, 98(3):604–41, 2008.

W. Kerr and R. G. King. Limits on interest rate rules in the is model. *FRB Richmond Economic Quarterly*, 82(2):47–76, 1996.

M. T. Kiley. Policy paradoxes in the new keynesian model. *Review of Economic Dynamics*, 21: 1–15, 2016.

R. G. King and M. W. Watson. The solution of singular linear difference systems under rational expectations. *International Economic Review*, pages 1015–1026, 1998.

R. G. King and M. W. Watson. System reduction and solution algorithms for singular linear difference systems under rational expectations. *Computational Economics*, 20(1-2):57–86, 2002.

P. Klein. Using the generalized schur form to solve a multivariate linear rational expectations model. *Journal of Economic Dynamics and Control*, 24(10):1405–1423, 2000.

G. Koop, M. H. Pesaran, and S. M. Potter. Impulse response analysis in nonlinear multivariate models. *Journal of Econometrics*, 74(1):119–147, 1996.

L. Krippner. Measuring the stance of monetary policy in zero lower bound environments. *Economics Letters*, 118(1):135–138, 2013.

L. Krippner. *Zero lower bound term structure modeling: A practitioner's guide*. Springer, 2015.

L. Krippner. A note of caution on shadow rate estimates. *Journal of Money, Credit and Banking*, 52(4):951–962, 2020.

P. R. Krugman, K. M. Dominquez, and K. Rogoff. It's baaack: Japan's slump and the return of the liquidity trap. *Brookings Papers on Economic Activity*, 1998(2):137–205, 1998.

M. Kulish and A. Pagan. Estimation and solution of models with expectations and structural changes. *Journal of Applied Econometrics*, 32(2):255–274, 2017.

M. Kulish, J. Morley, and T. Robinson. Estimating dsge models with zero interest rate policy. *Journal of Monetary Economics*, 88:35–49, 2017.

M. Lenza and G. E. Primiceri. How to estimate a vector autoregression after march 2020. *Journal of Applied Econometrics*, 2022.

J. Lindé, F. Smets, and R. Wouters. Challenges for central banks' macro models. In *Handbook of macroeconomics*, volume 2, pages 2185–2262. Elsevier, 2016.

T. A. Lubik and F. Schorfheide. Computing sunspot equilibria in linear rational expectations models. *Journal of Economic Dynamics and Control*, 28(2):273–285, 2003.

T. A. Lubik and F. Schorfheide. Testing for indeterminacy: An application to us monetary policy. *American Economic Review*, 94(1):190–217, 2004.

R. E. Lucas. Econometric policy evaluation: A critique. In *Carnegie-Rochester conference series on public policy*, volume 1, pages 19–46. Elsevier Science Publishers, 1976.

R. Lynch and B. Thage. Maintaining the national accounts as official statistics. *Review of Income and Wealth*, 63:S411–S436, 2017.

C. F. Manski. Measuring expectations. *Econometrica*, 72(5):1329–1376, 2004.

N. McClung. The power of forward guidance and the fiscal theory of the price level. *International Journal of Central Banking*, 17(71):1–57, 2021.

F. Modigliani and R. Brumberg. Utility analysis and the consumption function: An interpretation of cross-section data. *Franco Modigliani*, 1(1):388–436, 1954.

R. Moessner, D.-J. Jansen, and J. de Haan. Communication about future policy rates in theory and practice: A survey. *Journal of Economic Surveys*, 31(3):678–711, 2017.

J. Morley, D. Rodriguez Palenzuela, Y. Sun, and B. Wong. Estimating the euro area output gap using multivariate information and addressing the covid-19 pandemic. Technical report, European Central Bank, 2022.

T. Müller, K. Christoffel, F. Mazelis, and C. Montes-Galdón. Disciplining expectations and the forward guidance puzzle. *Journal of Economic Dynamics and Control*, 137:104336, 2022.

J. Osborne-Kinch, C. Mehigan, and M. Woods. Understanding the presence of mnes in ireland as an end user. *IFC Bulletins chapters*, 52, 2020.

D. G. Rassier. Improving the sna treatment of multinational enterprises. *Review of Income and Wealth*, 63:S287–S320, 2017.

F. Schorfheide and D. Song. Real-time forecasting with a (standard) mixed-frequency var during a pandemic. Technical report, National Bureau of Economic Research, 2021.

C. A. Sims. Solving linear rational expectations models. *Computational Economics*, 20(1-2): 1–20, 2002.

F. Smets and R. Wouters. An estimated dynamic stochastic general equilibrium model of the euro area. *Journal of the European Economic Association*, 1(5):1123–1, 2003.

F. Smets and R. Wouters. Comparing shocks and frictions in us and euro area business cycles: a bayesian dsge approach. *Journal of Applied Econometrics*, 20(2):161–183, 2005.

F. Smets and R. Wouters. Shocks and frictions in us business cycles: A bayesian dsge approach. *American Economic Review*, 97(3):586–606, 2007.

L. Svensson. The zero bound in an open economy: A foolproof way of escaping from a liquidity trap. Technical report, Stockholm University, Institute for International Economic Studies, 2000.

J. B. Taylor. Discretion versus policy rules in practice. In *Carnegie-Rochester Conference Series on Public Policy*, volume 39, pages 195–214, 1993.

I. Werning. Managing a liquidity trap: Monetary and fiscal policy. Technical report, National Bureau of Economic Research, 2011.

J. C. Wu and F. D. Xia. Measuring the macroeconomic impact of monetary policy at the zero lower bound. *Journal of Money, Credit and Banking*, 48(2-3):253–291, 2016.